PROGRAM OF THE CONFERENCE

Wednesday, September 21

13.00 *Registration*
13.30 *Opening*
13.40 I. Karachentsev
14.30 A. Maeder
15.20 *Coffee Break*
15.50 Y. V. Dumin
16.40 G. Feulner
17.30 M. Křížek

Thursday, September 22

9.00 P. Kroupa
9.50 M. Nowakovski
10.40 *Coffee Break*
11.10 L. Makarova
11.40 D. Makarov
12.10 *Lunch Break*
14.00 I. Goldman
14.30 I. V. Sokolov
15.00 *Coffee Break*
15.30 K. A. Tomilin
16.00 I. N. Taganov
16.50 Y. V. Baryshev

Friday, September 23

9.00 A. Mészáros
9.30 R. P. Nigam
10.00 A. D. A. M. Spallicci
10.30 *Coffee Break*
11.00 A. B. Balakin
11.30 A. Zaiats
12.00 *Lunch Break*
14.00 V. A. Popov
14.30 B. Mishra
15.00 M. Křížek
15.30 Discussion

Saturday, September 24

9.00 – 12.00 Excursion to the astronomical and cosmological sights of Prague

Statue of Atlas supporting the Universe on his back

ISBN 978-80-85823-66-0

COSMOLOGY ON SMALL SCALES 2016

Proceedings of the International Conference

Cosmology on Small Scales 2016

Local Hubble Expansion and Selected Controversies in Cosmology

Prague, September 21–24, 2016

Edited by
Michal Křížek and Yurii V. Dumin

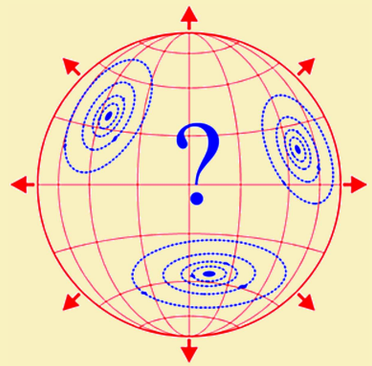

Institute of Mathematics
Czech Academy of Sciences

Proceedings of the International Conference

COSMOLOGY ON SMALL SCALES 2016

Local Hubble Expansion and Selected Controversies in Cosmology

Prague, September 21–24, 2016

Edited by
Michal Křížek and Yurii V. Dumin

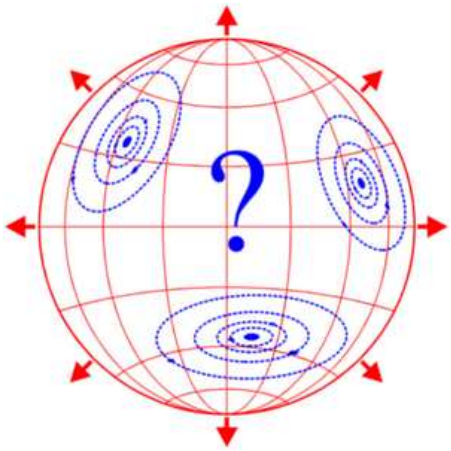

Institute of Mathematics
Czech Academy of Sciences
Prague 2016

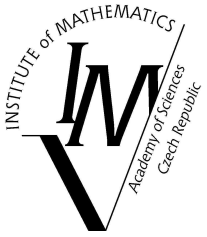

ISBN 978-80-85823-66-0
Institute of Mathematics
Czech Academy of Sciences
Prague 2016
LaTeX typesetting prepared by Hana Bílková
Printed by TIGRIS Company, Zlín

Dedicated to Emmy Noether

CONTENTS

Alternative cosmological theories

PREFACE

All truth passes through three stages:
First, it is ridiculed.
Second, it is violently opposed.
Third, it is accepted as self-evident.

Arthur Schopenhauer

The problem of cosmological expansion on small scales (e.g., inside planetary systems) has a long history, dating back to the papers (McVittie, 1932, 1933), and quite many researchers dealt with this topic in the subsequent few decades. Although most of them concluded that the Hubble expansion should be strongly suppressed at small distances, there is no commonly-established criterion for such suppression at present. Moreover, some of the widely-used theoretical arguments against the local Hubble expansion contradict each other.

On the other hand, there is more and more evidence that a few long-standing problems in planetology and celestial mechanics (e.g., the faint young Sun paradox, the lunar tidal catastrophe, and some other puzzles in the dynamics and evolution of the Solar system) could be well resolved by taking into account local cosmological influences. Lastly, the presence of Hubble expansion in the Local group of galaxies at the scale 1–2 Mpc (i.e., an order of magnitude less than assumed before) became commonly recognized in the last couple decades.

Unfortunately, the subject of local Hubble expansion remains strongly underrepresented at astronomical meetings. In fact, the only exception that we know was the international conference "Problems of Practical Cosmology", which was held in Saint-Petersburg (Russia) eight years ago, on June 23–27, 2008 (for details see `http://ppc08.astro.spbu.ru/index.html`). One of its sessions was specifically devoted to the problems of local cosmology and entitled "The Earth, the Solar system, and stellar systems for cosmology". Unfortunately, the tradition of these conferences has not been continued until the present time.

So, it is timely to gather specialists from different disciplines, ranging from planetology to galaxy evolution, to discuss the problem of local cosmological influences from various points of view, both theoretical and observational. To bring more light into this topic we decided to organize the international conference *Cosmology on Small Scales 2016: Local Hubble Expansion and Selected Controversies in Cosmology*. It was held at the Institute of Mathematics of the Czech Academy of Sciences in Žitná 25, Prague 1, from 21 to 24 September 2016 (see `http://css2016.math.cas.cz`).

The Scientific Committee consisted of

Prof. Yurij Baryshev (St. Petersburg University, Russia)
Prof. Igor Karachentsev (Special Astrophysical Observatory of RAS, Russia)
Prof. Jaroslav Klokočník (Astronomical Institute of CAS, Czech Republic)
Prof. Sergei Kopeikin (University of Missouri, USA)
Prof. André Maeder (Geneva Observatory, Switzerland)
Assoc. Prof. Attila Mészáros (Charles University, Czech Republic)
Eng. Vladimír Novotný (Cosmological Section of CAS, Czech Republic)
Prof. Marek Nowakowski (Universidad de los Andes, Colombia)
Prof. Lawrence Somer (The Catholic University of America, USA)
Prof. Weijia Zhang (Oxford University, Great Britain)

Local Organizing Committee consisted of

Prof. Michal Křížek — Chair (Czech Academy of Sciences, Czech Republic)
Dr. Yurii Dumin — Vice-Chair (Russian Academy of Sciences, Russia)
Assoc. Prof. Tomáš Vejchodský (Czech Academy of Sciences, Czech Republic)
Hana Bílková (Institute of Computer Science of CAS, Czech Republic)

The present book of Proceedings includes only a fraction of the reports that were presented at the meeting. Some other authors preferred to not submit their reports for publication, because the corresponding results are already available in the literature. This book is organized as follows: the first part contains the contributions immediately related to the problem of local Hubble expansion. The second part involves a number of works in a wider cosmological context, particularly, discussing the relevant controversies. Finally, there is a contribution devoted to an alternative theory of Hubble expansion, but the Program Committee is not responsible for its scientific content.

We are deeply grateful to all authors for their contributions and the support of RVO 67985840 (Institute of Mathematics of the Czech Academy of Sciences). Out sincere thanks go also to all active members of the Cosmological Section of the Czech Astronomical Society for their continual help. Finally, we are indebted to Caroline Griffis Krizek and Lawrence Somer for proofreading, Hana Bílková for technical assistance in the final typesetting, and Tomáš Vejchodský fot his helpful cooperation. The Proceedings can be downloaded from the website:

`http://users.math.cas.cz/~krizek/list.html`

Michal Křížek and Yurii V. Dumin

Conference *Cosmology on Small Scales 2016*
Michal Křížek and Yurii Dumin (Eds.)
Institute of Mathematics CAS, Prague

TWO FUNDAMENTAL COSMOLOGICAL LAWS OF THE LOCAL UNIVERSE

Yurij V. Baryshev

Astronomical Department of the Saint Petersburg State University
Universitetskij pr. 28, Staryj Peterhoff, St. Petersburg, 198504, Russia
yubaryshev@mail.ru

Abstract: The Local Universe is the most detail studied part of the observable region of space with the radius R about 100 Mpc. There are two empirical fundamental cosmological laws directly established from observations in the Local Universe independently from cosmological theory: first, the Hubble-Humason-Sandage linear redshift-distance law and second, Carpenter-Karachentsev-de Vaucouleurs density-radius power-law. Review of modern state of these empirical laws and their cosmological significance is given. Possible theoretical interpretations of the surprising coexistence of both laws at the spatial scales from 1 Mpc to 100 Mpc are discussed. Comparison of the standard space-expansion explanation of the cosmological redshift with possible global gravitational redshift model is given.

Keywords: Cosmology, Local Universe, redshift law, density law

PACS: 98.80.-k

1. Introduction

Cosmology as a physical science is based on observations, experiments and theoretical interpretations. Hubble 1937 [22] put forwarded "The Observational Approach to Cosmology". It was developed later by Sandage 1995a [41] who used the term "Practical Cosmology" to denote the observational study of "our sample of the Universe", which delivers possibilities for testing alternative initial hypotheses and main predictions of cosmological models.

Cosmology deals with a number of empirical facts among which one hopes to find fundamental laws. This process is complicated by great limitations and even under the paradigmatic grip of any current standard cosmology. One should distinguish between two kinds of cosmological laws:

- directly measured empirical laws,
- logically inferred theoretical laws.

The empirical laws are directly measured relations between observable quantities, which should be corrected for known selection and distortion effects. The logically inferred theoretical laws (theoretical interpretations) are made on the basis of an accepted cosmological model, e.g. the standard or an alternative cosmological model. Theoretical derivations utilize modern theoretical physics and even its possible extensions, which can be tested by observations.

During one hundred years of intensive investigations of the Local Universe (which can be defined as region of space with radius R about 100 Mpc) two especially important cosmological empirical laws were unveiled (see reviews in [7], [5], [8]):

- the cosmological linear redshift-distance law $cz = HR$,
- the power-law correlation of galaxy clustering $\Gamma(r) \propto r^{-\gamma}$.

Here R is the distance to a galaxy, H is the Hubble constant, r is the radius of test spheres around each galaxy, $\Gamma(r)$ is the complete correlation function (the conditional density) and γ is the power-law exponent.

The empirical laws, being based on repeatable observations, are independent of existing or future cosmological models. However, the derived theoretical laws are valid only in the frame of a specific cosmological model. Good examples are the empirical Hubble linear redshift-distance ($z \propto R$) law and the derived theoretical space-expansion velocity-distance ($V_{\rm sp-exp} \propto R$) law within the Friedmann model.

An analysis of both empirical cosmological facts and theoretical initial assumptions together with main logical inference in the frame of the standard and several alternative cosmological models is presented in our book Baryshev & Teerikorpi 2012 [7]. Below I concentrate on the significance for cosmology the redshift-radius and density-radius empirical cosmological laws.

2. Hubble–Humason–Sandage linear redshift-distance law

The linear relation between cosmological redshift and distance to galaxies was first established by Hubble 1929 [21] using distance estimations for 30 galaxies at very small scales $1 \div 10$ Mpc, corresponding to redshifts $z < 0.003$ or spectroscopic radial velocities $v_{\rm rad} < 1000$ km/s.

The extension of the linearity of the redshift-distance relation up to redshifts about $z < 0.05$ or scales about 150 Mpc was done by Hubble & Humason 1931 [23]. They emphasized that *The interpretation of red-shift as actual velocity, however, does not command the same confidence, and the term "velocity" will be used for the present in the sense of "apparent" velocity, without prejudice as to its ultimate significance.*

Many years of detail studies of the linearity of the redshift-distance law was performed by Sandage at the Palomar 5 m Hale telescope. Sandage developed a special program for 5 m telescope to discriminate between selected world models [39]. One of the last paper of Sandage's team, devoted to analysis of the observed redshift-distance relation, demonstrated linearity of $z(R)$ law in the interval of redshifts $0.001 \div 0.1$, see [43].

Hence for the Local Universe we have observationally established the linear redshift-distance Hubble–Humason–Sandage (HHS) law in the form:

$$z = \frac{H_{\rm loc} R}{c} = \frac{V_{\rm app}}{c}\,, \tag{1}$$

where c is the speed of light, $H_{\rm loc}$ is the value of the Hubble constant measured in the Local Universe, R is the measured distance to a galaxy, $V_{\rm app} = H_{\rm loc} \times R$ is the apparent radial velocity which corresponds measured shift of spectral lines z:

$$z = \frac{\lambda_{\rm obs} - \lambda_{\rm emit}}{\lambda_{\rm emit}}\,, \tag{2}$$

where $\lambda_{\rm obs}$ is the observed photon wavelength at the telescope and $\lambda_{\rm emit}$ is the wavelength of photon emitted at distance R. The HHS law (1) is also frequently called the Hubble law of redshifts. Note that here z is the cosmological part of the observed shift of spectral lines after corrections for the Solar system motions and averaging over peculiar velocities of galaxies.

The cosmological redshift is a universal physical phenomenon which does not depend on the wavelength of a photon. A very important cosmological question is about the minimal scale where the HHS law is true. Resent studies by Ekholm et al. 2001 [14], Karachentsev et al. 2003 [28], and Karachentsev et al. 2013 [29] demonstrated that according to modern data on 869 galaxy distances in the Local Volume the linear Hubble law well established at small scales $1 \div 10\,$Mpc. Remarkably, this is exactly the same interval of scales where Hubble 1929 [21] discovered the redshift-distance law with only 30 galaxies.

In Fig. 1 apparent radial velocity-distance relation $V_{\rm app} = cz = H_{\rm loc} R$ for 156 Local Volume galaxies is shown from [28]. The value of the local Hubble constant is $H_{\rm loc} = 72 \pm 3\,$km/sec/Mpc, which is consistent with recent estimations from different Local Universe surveys.

3. Carpenter–Karachentsev–de Vaucouleurs density-radius power-law

The rich history of discovery and acute discussions around the density-radius relation for the spatial galaxy distribution in the Local Universe is presented in [5], [6], [7], [45], and [47].

Carpenter 1938 [9] was the first who obtained from observations of galaxy systems of different sizes an approximate power-law relation between the number of galaxies N in a cluster and the size r of the clusters in the form $N(r) \propto r^{1.5}$.

Karachentsev 1966, 1968 [26], [27] added an important aspect to Carpenters result. He estimated average properties of 143 systems from binary galaxies to superclusters and found evidence that both luminous and total (virial) mass densities are decreasing with increasing size of a system. This showed for the first time that the massradius behavior of the dark matter is also a power law, but the exponent can be different than for the luminous matter.

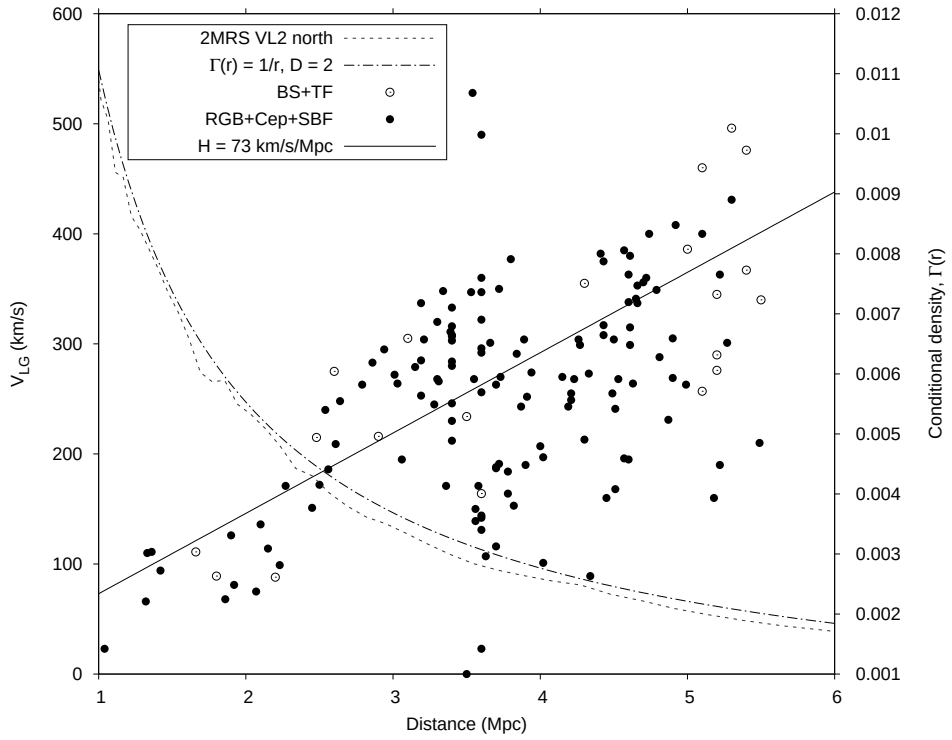

Figure 1: Apparent radial velocity-distance relation $V_{\rm app} = cz = H_{\rm loc}R$ for 156 Local Volume galaxies is shown in [28]. Also the density-radius relation $\Gamma(r) \propto r^{-\gamma}$ from [48] is shown dy thin lines for VL2N sample from 2MRS survey [25] and for power-law density-radius relation for exponent $\gamma = 1$.

De Vaucouleurs 1970, 1971 [10], [11] summarized his own and many others works in studies of galaxy systems from pairs to superclusters, including clustering of Abel's rich galaxy clusters [1], [2]. Based on all available data de Vaucouleurs made the decisive step in recognizing the cosmological significance of the clustering of galaxies as the universal observational power-law density-radius relation [10]. He considered this fundamental cosmological law as the case for a hierarchical cosmology.

Since that time the Carpenter–Karachentsev–de Vaucouleurs (CKdeV) density-radius empirical cosmological law was discovered and presented in the form

$$\rho(r) = \rho_0 \, (r/r_0)^{-\gamma}, \tag{3}$$

where $\rho(r)$ is the mass density within a spherical volume of radius r and ρ_0 and r_0 are the density and radius at the lower cutoff of the structure. The available at that time galaxy data led to the power-law exponent $\gamma = 1.7$.

Intriguingly, at international astronomical conferences, the Great Debate on the existence of very large scale structures in the observed galaxy universe was originated. An acute discussion between homogeneity defenders and inhomogeneity observers (see reviews [6], [7]) is actually ongoing nowadays, though modern data demonstrate

the existence of galaxy structures with sizes up to 400–1000 Mpc (see e.g. [44]). The reason of the hot debates is that in the frame of the standard cosmological model the homogeneous matter distribution is the basic mathematical assumption for the derivation of linear Hubble law of redshifts [35], [7].

In fact, to understand the observed CKdeV density-radius relation one needs to develop a new mathematical and physical concepts which include discrete fractal stochastic structures. This was done by Mandelbrot 1977 [33] in his theory of fractals, which opens a new perspective for description of complex discrete physical systems with properties very different from continuous fluid flows. Fractal approach to the analysis of the distribution of galaxies was first used in [33], [38] and developed in [46], [18], [47]. For a detailed review of the history and prospects of the fractal approach to the study of the large-scale distribution of galaxies see [6], [7].

One of the most fundamental statistical properties of the general space distribution of galaxies, which includes complex observed structures (filaments, voids, shells, and walls), is the fractal dimension of the global structure as a whole. According to [18], the fractal dimension D of a stochastic fractal point process in 3-dimensional space can be inferred from the complete correlation function (conditional density) $\Gamma(r)$, which has the power-law:

$$\Gamma(r) = \frac{\langle n(\vec{r}_1) n(\vec{r}_2)\rangle}{\langle n(r)\rangle} = k\, r^{-\gamma} = k\, r^{-(3-D)}, \tag{4}$$

where $n(\vec{r}_i)$, is the particle number density inside volume dV_i around point i with the coordinates $\vec{r}_i$, $r = |\vec{r}_{12}| = |\vec{r}_1 - \vec{r}_2|$, the vector of the distance between points 1 and 2, and $\langle x\rangle$, the ensemble average of x. The second and third equalities are written for isotropic stationary processes, where D is the fractal dimension and $\gamma = 3 - D$ is called the co-dimension of the fractal. The physical dimension of the $\Gamma(r)$ is $1/\mathrm{cm}^3$ and it is calculated under the condition of all occupied points, this is why it is called the *conditional density*.

The power-law character of the conditional density (4) is the principal explanation of the CKdeV density-radius law (3). A more detailed analysis will include transition from number density $n(r)$ to mass density $\rho(r)$, which should also take into account the luminous and dark matter. Fortunately, conditional density analysis of the real galaxy catalogues shows that it is sufficient for describing the spatial galaxy distribution as a good first approximation.

The statistical estimate of the complete correlation function $\Gamma(r)$ (conditional density) for the galaxy sample considered is defined as (see [18]):

$$\Gamma(r) = \frac{1}{N_c(r)} \sum_{i=1}^{N_c(r)} \frac{N_i(r)}{V(r)}\,, \tag{5}$$

where $N_i(r)$ is the number of points inside spherical volume $V(r)$ around i-th point and $N_c(r)$ is the number of centers of test spheres, i.e., the number of points about which this volume is circumscribed. It is important to bear in mind that averaging

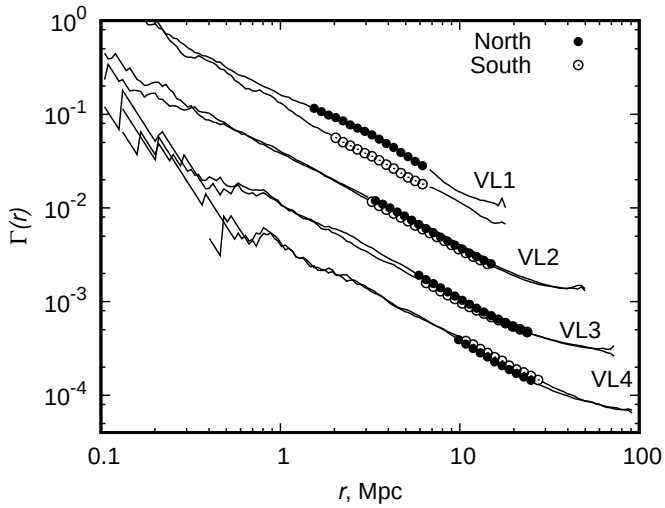

Figure 2: Conditional density for Volume Limited samples of 2MRS galaxies in the Local Universe [48]. The large dots mark the conditional density values where the most reliable slope estimation is possible. The slope $\gamma = 1.0 \pm 0.1$ for all VL samples.

has to be performed without going beyond the considered sample volume, and this restriction has important effect on the value of the greatest available scale lengths. This condition strongly restricts the scale-lengths accessible for the analysis of galaxy correlations, because, strictly speaking, in order to reliably compute the conditional density on some selected scale, we must analyze much greater spherical region, where all test spheres are completely embedded.

For large galaxy redshift surveys the conditional density $\Gamma(r)$ is a directly determined quantity, which characterizes the spatial, kinematical, and dynamical state of the Local Universe. It can be estimated from the power-law slope γ (co-dimension of the fractal) of the complete correlation function $\Gamma(r)$ without invoking any a priori assumptions about the evolution of non-baryonic dark matter and its association with baryonic matter (galaxies) or the form of the distribution of peculiar velocities of galaxies.

Note that the complete correlation function $\Gamma(r)$ has an important advantage over reduced correlation function $\xi(r)$ (Peebles's two-point correlation function) in that the computation of conditional density requires no assumption about the homogeneity of spatial galaxy distribution within analyzed galaxy sample.

Fig. 2 shows the conditional density calculations [48] for the largest complete all-sky galaxy redshift survey 2MRS of the Local Universe [25]. The observed global space distribution of 2MRS galaxies can be described by the power-law complete correlation function of the form $\Gamma(r) = kr^{-\gamma}$ with a slope of $\gamma \approx 1$ over a wide interval of scale-lengths spanning from 0.1 Mpc to 100 Mpc. The deeper all-sky volume limited sample is used (from VL1 to VL4), the larger is the maximum scale-length, where the density power-law can be reliably estimated. The shift of the power-law maxi-

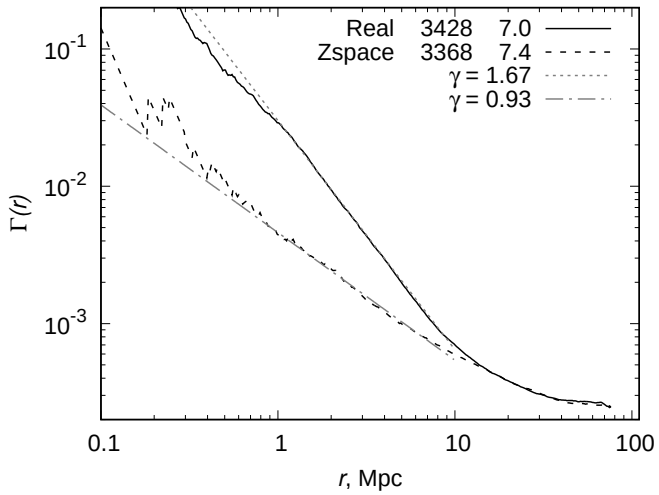

Figure 3: Conditional density of Millennium mock galaxy catalog in a sample similar to S1VL2 as a function of scale length in real and z space [48]. The slopes are estimated in the $1 < r < 10$ Mpc interval. After scales about 30 Mpc the mock galaxy distribution becomes homogeneous.

mum scale-length is consistent with the stochastic fractal model having the fractal dimension $D = 3 - \gamma \approx 2$ in the whole interval of analyzed scales from 0.1 Mpc up to 100 Mpc.

In the frame of the LCDM theory of large scale structure formation there are two important predictions:

- the galaxy Local Universe is homogeneous after scales about 30 Mpc;
- due to galaxy peculiar velocities there is very large difference between slopes of conditional density calculated for redshift-based distances and real distances independent on z.

According to [48], Fig. 3 shows results of the conditional density calculations for the Millennium galaxy catalog (in a sample similar to S1VL2 2MRS) as a function of scale length in real and z space. The predicted slopes are very different for z- and r-space. Also over scales of 30 Mpc the galaxy distribution becomes homogeneous.

So for future testing of the nature of the Local Universe galaxy distribution there are two possibilities — first, to get more deep all-sky galaxy redshift surveys (at least up to 500 Mpc) and second, to compare conditional densities measured for redshift and real space: $\Gamma(r_z) \Longleftrightarrow \Gamma(r_{\rm real})$. Hence, very important observational test of the large scale structure origin in the Local Universe is the direct measurements of the peculiar velocities of galaxies. This will require further development of redshift-independent methods for determining galaxy distances and performing

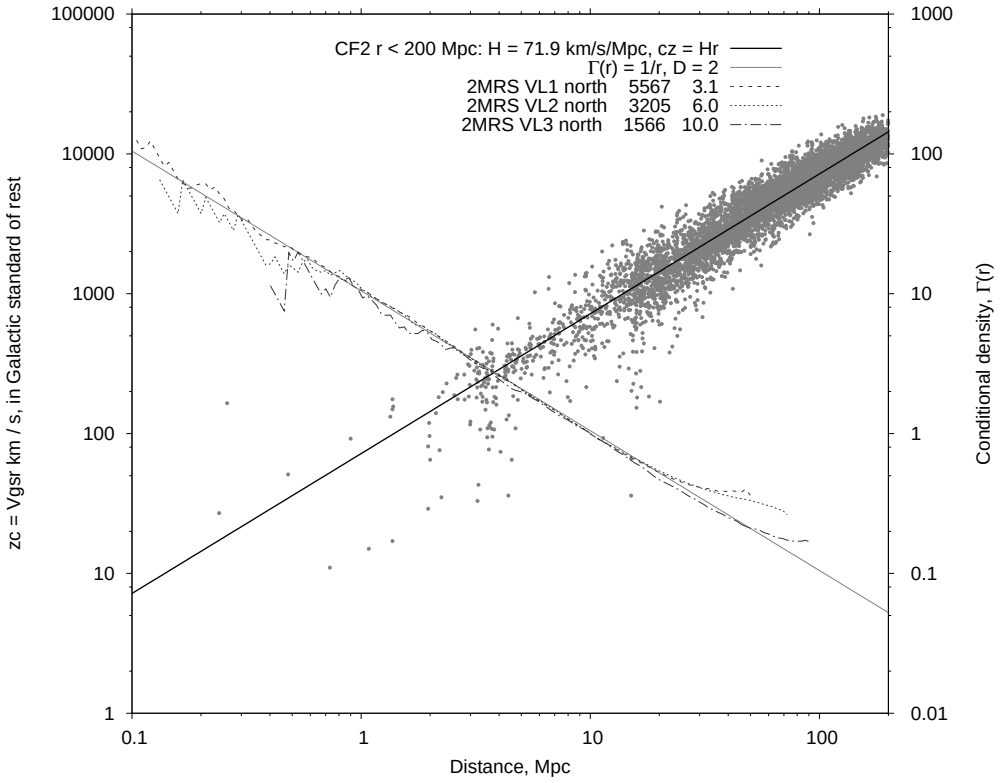

Figure 4: Demonstration of the Hubble–de Vaucouleurs paradox in the Local Universe. The Hubble-Humason-Sandage linear redshift law $cz = H_{\rm loc}R$ and the fractal Carpenter–Karachentsev–de Vaucouleurs density law $\Gamma(r) = kr^{-\gamma}$ with $\gamma \approx 1$ coexist at the same length-scale interval $0.1 \div 100\,$Mpc. While in the frame of the SCM *the linear redshift-distance relation is the strict consequence of homogeneity* [36].

time consuming observational programs aimed to measurement of such distances, like Cosmic Flows surveys [49].

Note that stochastic fractal structures naturally arise in physics as a result of the dynamical evolution of complex systems. Physical fractals are discrete stochastic systems characterized by power-law correlation functions. In particular, fractal structures arise in turbulent flows and in deterministic chaos of nonlinear dynamic systems. Phase transitions and thermodynamics of self-gravitating systems are also characterized by the formation of fractal structures [12], [13], [37]. However, many important aspects of these studies so far remain undiscovered.

4. Physical interpretations of the relation between redshift and density laws

Here I consider two possibilities for explanation of the surprising coincidence of the observed spatial scales, where two empirical cosmological laws simultaneously exit (see Fig. 4).

In the frame of the Friedmann model of the Standard Cosmological Model (SCM) there is a deep paradox between Hubble–Humason–Sandage linear redshift-distance law and Carpenter–Karachentsev–de Vaucouleurs density-radius power-law. This observational Hubble–de Vaucouleurs (HdeV) paradox exists due to the very basis of SCM, which explains the linear HHS law as a strict mathematical consequence of the homogeneity of the matter distribution (see [36], [35], [4]).

For a solution of HdeV paradox within SCM one should assume a large amount of homogeneously distributed non-baryonic dark matter and dark energy. The dominance of homogeneous dark substance density over the usual baryonic matter (galaxies) must start from scales where the linear HHS redshift-distance law already exists. There are also several conceptual problems with interpretation of space-expansion in SCM [4], [17], [20], [19].

Another solution of HdeV paradox can be obtained in the frame of the Fractal Cosmological Model (FCM) [3], presented at the International conference *Problems of Practical Cosmology 2008*. In the frame of the FCM the space-geometry is static flat Minkowski space-time, the gravitational interaction is described within Feynman's field gravity approach [15], [16], [7], and the matter is a dynamically evolving usual baryonic substance.

The spatial distribution of galaxies in the Local Universe is the stochastic fractal structure with fractal dimension $D \approx 2$ and the cosmological redshift is the new gravitational global effect due to the whole mass within the sphere having radius equal to the distance between the source and the observer. For fractal dimension $D = 2$ the mass of the sphere of radius r grows as $M(r) \propto r^D \propto r^2$. Hence, the gravitational potential is $\varphi \propto M/r \propto r^1$ and the cosmological global gravitational redshift is the linear function of distance $z_{gl-gr} \propto r$. This means that the surprising coincidence of length scales for both HHS and CKdeV cosmological laws now is a natural prediction of the fractal cosmological model.

So an important task of Practical Cosmology is to observationally distinct between expanding and static spaces, i.e., to establish the nature of the observed cosmological redshift. Note, that in the classical papers, Hubble 1929 [21] and Hubble & Humason 1931 [23] emphasized that the cosmological part of the measured redshift should be called *apparent radial velocity* and actually can present the *de Sitter effect of "slowing down of atomic vibrations"* — which is actually a kind of the global gravitational effect. During all his life Hubble insisted on the necessity of the observational verification of the nature of the cosmological redshift and suggested several tests together with Tolman [24].

Intriguingly, up to now, after 85 years of observational cosmology there is no crucial experiment which directly measures the real increasing distance with time. In Sandage's List of 23 Astronomical Problems for the 1995–2025 years [42] the first problem of the Practical Cosmology is to test *Is the expansion real?*

The usually considered tests of space expansion

- Tolman's surface brightness $(1 + z)^4$ test;

- Time dilation with SN Ia $t(z) = t(0)(1 + z)$;
- CMBR temperature $T(z) = T(0)(1 + z)$

cannot distinct between space expansion redshift and global gravitational redshift mechanisms.

The crucial test of cosmological space expansion should measure the real increasing distances with time. Nowadays there are at least two proposals for such crucial tests of the expansion of the Universe:

- Sandage's $z(t)$ test;
- Kopeikin's $\Delta\nu/\nu$ test in the Solar system.

It is important to note that on the verge of modern technology there are possibilities for real direct observational tests of the physical nature of the cosmological redshift. First crucial test of the reality of the space expansion was suggested by Sandage [40], who noted that the observed redshift of a distant object (e.g. quasar) in expanding space must be changing with time according to relation $dz/dt = (1 + z)H_0 - H(z)$. In terms of radial velocity, the predicted change $dv/dt \sim 1\,\mathrm{cm\,s^{-1}/yr}$. This may be within the reach of the future ELT telescope [34], [32]. In the case of the global gravitational redshift the change of redshift equals zero.

Even within the Solar system there is a possibility to test the global expansion of the universe. According to recent papers by Kopeikin [30], [31] the equations of light propagation used currently by Space Navigation Centers for fitting range and Doppler-tracking observations of celestial bodies contain some terms of the cosmological origin that are proportional to the Hubble constant H_0. Such project as PHARAO may be an excellent candidate for measuring the effect of the global cosmological expansion within Solar system, which has a well-predicted blue-shift effect having magnitude $\Delta\nu/\nu = 2H_0\Delta t \approx 4 \times 10^{-15}\ (H_0/70\,\mathrm{kms^{-1}\,Mpc^{-1}})\ (\Delta t/10^3\,\mathrm{s})$, where H_0 is the Hubble constant and Δt is the time of observations. In the case of the non-expanding Universe the frequency drift equals zero.

5. Conclusion

Cosmology at Small Scales is very important part of astronomy. New mathematical and physical ideas in cosmology should be discussed and tested by experiments and observations in the Local Universe from the Solar system scales up to the superclusters scales.

Surprises of recent observational cosmology of the Local Universe stimulate its further investigations. A puzzling conclusion is that the Hubble's law, i.e. the strictly linear redshift-distance relation, is observed just inside strongly inhomogeneous galaxy distribution, i.e. deeply inside fractal structure at scales $1 \div 100\,\mathrm{Mpc}$. This empirical fact presents a profound challenge to the standard cosmological model,

where the homogeneity is the basic explanation of the Hubble law, and *the connection between homogeneity and Hubble's law was the first success of the expanding world model* (Peebles et al. 1991 [36]). However the spectacular observational fact (Fig. 4) is that the Hubble's law is not a consequence of homogeneity of the galaxy distribution, as it was assumed during almost the whole history of cosmology.

New type of global physical laws can appear at cosmological scales which make cosmology especially creative science. Intriguingly, up to now there is no crucial experiment which directly measure the real increasing distance with time. The global gravitational cosmological redshift can be such new physical phenomenon which should be tested by observations and experiments.

New powerful mathematical methods of fractal structures analysis should be developed for investigation of the large scale structure of the Universe. Even new approaches for description of gravitational interaction in the frame of modern theoretical physics can be tested at all scales from Solar system up to the cosmological scales.

This is possible due to very fast development of observational techniques and theoretical models which is applied to astronomical objects. Theoretical models utilize modern theoretical physics and even its possible extensions, which can be tested by observations. In conclusion we may say that now we are entering in the golden age of cosmological physics of the Local Universe. So the research in the field of *Cosmology at Small Scales* is a perspective direction in modern physical science.

Acknowledgements

I am grateful to Pekka Teerikorpi, Georges Paturel, Luciano Pietronero, and Francesco Sylos Labini for many years of collaboration in study large scale structure of the Universe. Also I thank Daniil Tekhanovich for joint work in analysis of modern Local Universe galaxy catalogues. This work has been supported by the Saint Petersburg State University (grant No. 6.38.18.2014).

References

[1] Abell, G. O.: The distribution of rich clusters of galaxies. Astrophys. J. Suppl. Ser. **3** (1958), 211.

[2] Abell, G. O.: Evidence regarding second-order clustering of galaxies and interactions between clusters of galaxies. Astron. J. **66** (1961), 607.

[3] Baryshev, Y. V.: Field fractal cosmological model as an example of practical cosmology approach. In: Practical Cosmology, Proceedings of the International Conference held at Russian Geographical Society, 23–27 June, 2008, Vol. 2, p. 60, (arXiv:0810.0162).

[4] Baryshev, Y. V.: Paradoxes of the cosmological physics in the beginning of the 21-st century. In: Proceedings of the XXX-th International Workshop on

High Energy Physics — *Particle and Astroparticle Physics, Gravitation and Cosmology — Predictions, Observations and New Projects,* WSPC, p. 297, 2015, (arXiv:1501.01919).

[5] Baryshev, Y. V. and Teerikorpi, P.: *Discovery of cosmic fractals.* World Scientific, Singapore, 2002, 408 pp. (Polish translation: Poznawanie kosmicznego ladu Wszechswiat,WAM, Krakow, 2005; Italian translation: La scoperta dei frattali cosmici, Bollati Boringhieri, Torino, 2006).

[6] Baryshev, Y. V. and Teerikorpi, P.: The fractal analysis of the large-scale galaxy distribution. Bull. Spec. Astrophys. Obs. **59** (2006), 92.

[7] Baryshev, Y. V. and Teerikorpi, P.: *Fundamental questions of practical cosmology: exploring the realm of galaxies.* Springer, 2012, p. 328.

[8] Baryshev, Y., Sylos-Labini, F., Montuori, M., and Pietronero, L.: Facts and ideas in modern cosmology. Vistas in Astronomy **38** (1994), 419.

[9] Carpenter, E. F.: Some characteristics of associated galaxies I. A density restriction in the metagalaxy. Astrophys. J. **88** (1938), 344.

[10] de Vaucouleurs, G.: The case for a hierarchical cosmology. Science **167** (1970), 1203.

[11] de Vaucouleurs, G.: The large-scale distribution of galaxies and clusters of galaxies. Publ. Astron. Soc. Pac. **83** (1971), 113.

[12] De Vega, H., Sanches, N., and Combes, F.: Self-gravity as an explanation of the fractal structure of the interstellar medium. Nature **383** (1996), 56.

[13] De Vega, H., Sanches, N., and Combes, F.: The fractal structure of the universe: A new field theory approach. Astrophys. J. **500** (1998), 8.

[14] Ekholm, T., Baryshev, Y. V., Teerikorpi, P., Hanski, M., and Paturel, G.: On the quiescence of the Hubble flow in the vicinity of the local group: A study using galaxies with distances from the Cepheid PL-relation. Astron. Astrophys. **368** (2001), L17.

[15] Feynman, R.: *Lectures on gravitation.* California Institute of Technology, 1971.

[16] Feynman, R., Morinigo, F., and Wagner, W.: *Feynman lectures on gravitation.* Addison-Wesley Publ. Comp., 1995.

[17] Francis, M. J., Barnes, L. A., James, J. B., and Lewis, G. F.: Expanding space: the root of all evil? Publ. Astron. Soc. Australia **24** (2007), 95, (astro-ph/0707.0380)

[18] Gabrielli, A., Sylos Labini, F., Joyce, M., and Pietronero, L.: *Statistical physics for cosmic structures*. Springer, Berlin, 2005.

[19] Harrison, E. R.: The redshift-distance and velocity-distance laws. ApJ **403** (1993), 28.

[20] Harrison, E. R.: Mining energy in an expanding universe. ApJ **446** (1995), 63–66.

[21] Hubble, E.: A relation between distance and radial velocity among extra-galactic nebulae. Proc. Nat. Acad. Sci. **15** (1929), 168–173.

[22] Hubble, E.: *The observational approach to cosmology.* Clarendon, Oxford, 1937, 68.

[23] Hubble, E. and Humason, M. L.: The velocitydistance relation among extra-galactic nebulae. Astrophys. J. **74** (1931), 43.

[24] Hubble, E. and Tolman, R. C.: Two methods of investigating the nature of the nebular red-shift. Astrophys. J. **82** (1935), 302–337.

[25] Huchra, J. et al.: The 2MASS redshift survey — description and data release. Astrophys. J. Suppl. **199** (2012), 26.

[26] Karachentsev, I. D.: Some statistical characteristics of superclusters of galaxies. Astrofizika **2** (1996), 307. (English translation in Astrophysics **2**, 159.)

[27] Karachentsev, I. D.: Average statistical characteristics of systems of galaxies and the problem of the existence of hidden virial mass. Commun. Byurakan Obs. **39** (1968), 76 (in Russian).

[28] Karachentsev, I., Makarov, D. I., Sharina, M. E. et al.: Local galaxy flows within 5 Mpc. Astron. Astrophys. **398** (2003), 493.

[29] Karachentsev, I., Makarov, D., and Kaisina, E. I.: Updated nearby galaxy catalog. AJ **145** (2013), 101.

[30] Kopeikin, S.: Celestial ephemerides in an expanding universe. Phys. Rev. **D86** (2012), 064004.

[31] Kopeikin, S.: Local gravitational physics of the Hubble expansion. Eur. Phys. J. Plus **130** (2015), arXiv:1407.6667

[32] Liske, J. et al.: Cosmic dynamics in the era of extremely large telescopes. Mon. Not. R. Astron. Soc. **386** (2008), 1192.

[33] Mandelbrot, B. B.: *Fractals: form, chance and dimension.* W. H. Freeman, New York, 1977.

[34] Pasquini, L. et al.: CODEX: measuring the expansion of the Universe. The Messenger **122**, December 2005, p. 10.

[35] Peebles, P. J. E.: *Principles of physical cosmology*. Princeton Univ. Press, 1993.

[36] Peebles, P. et al.: The case for the relativistic hot big bang cosmology. Nature **352** (1991), 769.

[37] Perdang, J.: Self-gravitational fractal configuration. Vistas Astron. **33** (1990), 371.

[38] Pietronero, L.: The fractal structure of the Universe: correlations of galaxies and clusters and the average mass density. Physica A **144** (1987), 257.

[39] Sandage, A.: The ability of the 200-inch telescope to discriminate between selected world models. Astrophys. J. **133** (1961), 355.

[40] Sandage, A.: The change of redshift and apparent luminosity of galaxies due to the deceleration of the expanding universes. ApJ **136** (1962), 319.

[41] Sandage, A.: Practical cosmology: inventing the past. In: Binggeli, Buser, R. (eds.) *The deep universe*, pp. 1–232. Springer, Berlin, 1995a.

[42] Sandage A.: Astronomical problems for the next three decades. In: A. Mamaso and G. Munch (Eds.), *Key problems in astronomy and astrophysics*, Cambridge University Press, 1995b.

[43] Sandage, A., Reindl, B., and Tammann, G.: The linearity of the cosmic expansion field from 300 to 30 000 km s^{-1} and the bulk motion of the local supercluster with respect to the cosmic microwave background. Astrophys. J. **714** (2010), 1441.

[44] Shirokov, S. I., Lovyagin, N. Y., Baryshev, Y V., and Gorokhov, V. L.: Large-scale fluctuations in the number density of galaxies in independent surveys of deep fields. Astron. Rep. **60** (2016), 563.

[45] Sylos Labini, F.: Inhomogeneities in the universe classical and quantum gravity **28** (2011), 164003.

[46] Sylos Labini, F., Montuori, M., and Pietronero, L.: Scale-invariance of galaxy clustering. Phys. Rep. **293** (1998), 61.

[47] Sylos Labini, F., Tekhanovich, D., and Baryshev, Y.: Spatial density fluctuations and selection effects in galaxy redshift surveys. J. of Cosmol. and Astropart. Phys. **7** (2014), 035.

[48] Tekhanovich, D. and Baryshev, Y. M.: Global structure of the local universe according to 2MRS survey. Astrophys. Bull. **71** (2016), 155.

[49] Tully, B. et al.: Cosmic flows-2: the data. Astron. J. **146** (2013), 86.

Conference *Cosmology on Small Scales 2016*
Michal Křížek and Yurii Dumin (Eds.)
Institute of Mathematics CAS, Prague

LOCAL HUBBLE EXPANSION: CURRENT STATE OF THE PROBLEM

Yurii V. Dumin

[1]P. K. Sternberg Astronomical Institute of M. V. Lomonosov Moscow State University
Universitetskii prosp. 13, 119992, Moscow, Russia
[2]Space Research Institute of the Russian Academy of Sciences
Profsoyuznaya str. 84/32, 117997, Moscow, Russia
dumin@yahoo.com, dumin@sai.msu.ru

Abstract: We present a brief qualitative overview of the current state of the problem of Hubble expansion at the sufficiently small scales (e.g., in planetary systems or local intergalactic volume). The crucial drawbacks of the available theoretical treatments are emphasized, and the possible ways to avoid them are outlined. Attention is drawn to a number of observable astronomical phenomena that could be naturally explained by the local Hubble expansion.

Keywords: Hubble expansion, two-body problem, evolution of planetary systems

PACS: 98.80.Es, 98.80.Jk, 95.10.Ce, 95.36.+x, 96.00.00

1. Introduction: theoretical approaches to the problem of local Hubble expansion

The problem of small-scale cosmological effects has a long history: the question if planetary systems are affected by the universal Hubble expansion was posed by McVittie as early as 1933 [35], i.e., approximately at the same time when the concept of Hubble expansion became the dominant paradigm in cosmology. Although this question never was a hot topic, the corresponding papers occasionally appeared in the astronomical literature in the subsequent eight decades [1, 7, 9, 10, 12, 19, 21, 27, 33, 37, 41]. Using quite different physical models and mathematical approaches, most of these authors arrived at the negative conclusions. As a result, it is commonly believed now[1] that Hubble expansion should be strongly suppressed or absent at all at the sufficiently small scales, for example, in planetary systems or inside galaxies.

[1]One of a few exceptions is a short review by Bonnor [3], which appealed for a critical reconsideration of the available studies.

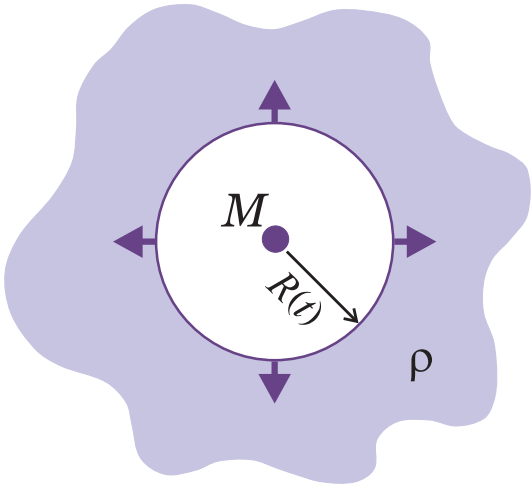

Figure 1: Schematic illustration of Einstein–Straus theorem.

However, a surprising thing is that the commonly-used arguments not only prohibit the local Hubble expansion but also strongly contradict each other. For example, the most popular criterion for the suppression of Hubble expansion (especially, among the observational astronomers) is just a gravitational binding of the system, e.g., determined by the virial theorem of classical mechanics [32]. Namely, if mass of the particles concentrated in the system becomes so large that the corresponding energy of gravitational interaction approaches by absolute value the double kinetic energy, then orbits of the particles should be bounded, i.e., no overall expansion of the system is possible. In other words, just the classical forces of gravitational attraction break the global Hubble flow in the regions of local mass enhancement.

On the other hand, yet another well-known theoretical argument against the local Hubble expansion, based on the self-consistent theoretical analysis in the framework of General Relativity (GR), is the so-called Einstein–Straus theorem [19], illustrated in Figure 1: Let us consider a uniform distribution of the background matter with density ρ and then assume that substance in a spherical volume with radius R is cut off and concentrated in its center, thereby forming the point-like mass $M = (4\pi/3)R^3\rho$. Then, according to the this theorem, there will be no Hubble expansion inside the empty cavity, but the Hubble flow is restored again beyond its boundary with the background matter distribution (and this boundary itself moves exactly with Hubble velocity).

It is important to emphasize that, as distinct from the first criterion, there is no any excessive mass in the above-mentioned sphere and, moreover, the Hubble expansion is absent just in the empty space rather than in the region of mass enhancement. In principle, this fact is quite natural: according to the standard GR formula,

Hubble constant H is related to the local energy density ρ in the spatially-flat Universe as[2]

$$H = \sqrt{\frac{8\pi G}{3}\,\rho}\,, \tag{1}$$

where G is the gravitational constant. So, from the relativistic point of view, it is not surprising that Hubble constant tends to zero when the energy density disappears[3].

Therefore, the above discussion demonstrates that the attempts to treat the problem of local Hubble expansion in terms of the classical gravitational forces can be very misleading. Indeed, the global Hubble expansion exists even in the perfectly-uniform Universe, where there are no any "classical" gravitational forces at all (since such forces can be produced only by nonhomogeneity of mass distribution). In other words, it should be kept in mind that Hubble expansion corresponds to another "degree of freedom" of the relativistic gravitational field as compared to the degrees of freedom reduced to the classical gravitational forces.

Unfortunately, a lot of textbooks tried to estimate the local Hubble expansion in terms of the "classical" gravity or just *postulated* its absence in the small-scale systems. A typical example is the famous textbook [36], where the behavior of small-scale systems (galaxies) in the globally-expanding Universe was pictorially described as a set of coins pinned to the surface of an inflating ball (see Figure 27.2 in the above-cited book), but no justification for such a picture was given.

2. Hubble expansion in the dark-energy-dominated cosmology

Because of the oversimplified geometry of the Einstein–Straus model (particularly, a presence of the void, which can hardly have a reasonable astrophysical interpretation), it is desirable to consider not so idealized situations. Unfortunately, a serious obstacle in this way is the problem of separation between the peculiar and Hubble flows of matter in a spatially inhomogeneous system. Namely, if there is no empty cavity, and boundary with the background matter distribution is not perfectly sharp, as in Figure 1, then substance in the vicinity of the central mass will experience a quite complex radial motion in the course of time, depending on the initial conditions. In general, we do not have any universal criterion to answer the question: what part of this motion should be attributed to the Hubble flow?

Fortunately, the situation is simplified very much in the case of idealized dark-energy-dominated Universe, where the entire cosmological contribution to the energy–momentum tensor of GR equations is produced by the Λ-term (cosmological constant). The Λ-term is distributed, by definition, perfectly uniform in space and, therefore, does not experience any back reaction from the additional (e.g., point-like)

[2]We use everywhere the system of units where the speed of light is equal to unity ($c \equiv 1$) and, therefore, there is no difference between the mass- and energy-density.

[3]Of course, strictly speaking, formula (1) is applicable only to the totally uniform Universe.

mass[4]. As a result, it becomes not so difficult to consider the "restricted cosmological two-body problem", i.e., motion of a test particle in the local gravitational field of the central mass embedded into the cosmological background formed by the Λ-term[5]. From our point of view, just this model enables one to get the simplest but reliable estimate for the magnitude of the local Hubble expansion, which can be used as a benchmark in more sophisticated studies.

The above-mentioned problem can be separated into two steps: Firstly, using GR equations, one needs to find a space–time metric of the point-like mass M against the Λ-background. Secondly, using the standard geodesic equations, we should calculate the trajectories of test particles in this metric.

The first task was actually solved long time ago, in 1918, by Kottler [28]. The required metric reads as[6]

$$\begin{aligned} \mathrm{d}s^2 = & -\left(1-\frac{2GM}{r}-\frac{\Lambda r^2}{3}\right)\mathrm{d}t^2 \\ & +\left(1-\frac{2GM}{r}-\frac{\Lambda r^2}{3}\right)^{-1}\mathrm{d}r^2+\, r^2(\mathrm{d}\theta^2+\,\sin^2\theta\,\mathrm{d}\varphi^2)\,, \end{aligned} \tag{2}$$

for more general discussion, see also [29].

Just this metric was widely used starting from the early 2000's — when the importance of Λ-term in cosmology was clearly recognized — to study the motion of test particles. The quite sophisticated mathematical treatments can be found, for example, in papers [2, 23]; and the respective formulas were used for the analysis of observational data on planetary dynamics in the Solar system [5, 24, 25]. Unfortunately, the original Kottler metric (2) does not possess the correct cosmological asymptotics at infinity (which is not surprising, since it was derived well before a birth of the modern cosmology). The above-cited works, of course, reveal some features of particle dynamics in the dark-energy-dominated Universe, but they are unrelated (or, probably, partially related) to the Hubble expansion by itself.

So, to study effects of the Hubble expansion *per se*, it is necessary to transform metric (2) to the standard Robertson–Walker coordinates, commonly used in the cosmological calculations. Such a procedure was performed in our paper [15]; and the resulting expressions for the "cosmological" Kottler metric can be found there. Next, this metric should be used to solve the geodesic equations for a test particle moving in the field of the central mass [17]:

[4]We do not discuss here the models with "dynamical" dark energy (where Λ-term is replaced by a new field), because they are not so necessary to explain the available observational data.

[5]According to the standard terminology of celestial mechanics, the term "restricted" implies that one of the bodies (test particle) has infinitely small mass.

[6]It is often called in the modern literature the Schwarzschild–de Sitter metric; although, from our point of view, this term is not sufficiently correct.

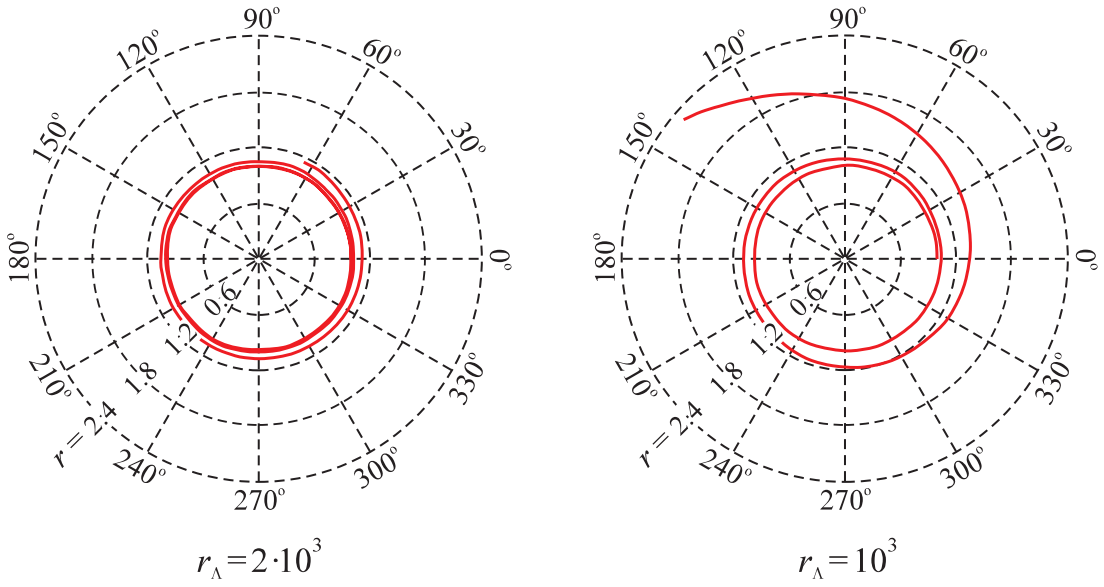

Figure 2: Orbits of a test body in the field of the central mass at $r_g = 10^{-2}$ and various values of r_Λ, assuming that $R_0 = 1$.

$$2\left[1-\frac{r_g}{r}\left(1-\frac{t}{r_\Lambda}\right)\right]\ddot{t} - 4\,\frac{r_g}{r_\Lambda}\,\ddot{r} + \frac{r_g}{r_\Lambda}\,\frac{1}{r}\,\dot{t}^{\,2} + 2\,\frac{r_g}{r^2}\left(1-\frac{t}{r_\Lambda}\right)\dot{t}\,\dot{r} + \frac{1}{r_\Lambda}\left(2+\frac{r_g}{r}\right)\dot{r}^{\,2} + 2\,\frac{r^2}{r_\Lambda}\,\dot{\varphi}^{\,2} = 0\,, \tag{3}$$

$$4\,\frac{r_g}{r_\Lambda}\,\ddot{t} + 2\left[1+2\,\frac{t}{r_\Lambda}+\frac{r_g}{r}\left(1+\frac{t}{r_\Lambda}\right)\right]\ddot{r} + \frac{r_g}{r^2}\left(1-\frac{t}{r_\Lambda}\right)\dot{t}^{\,2} + \frac{2}{r_\Lambda}\left(2+\frac{r_g}{r}\right)\dot{t}\,\dot{r} - \frac{r_g}{r^2}\left(1+\frac{t}{r_\Lambda}\right)\dot{r}^{\,2} - 2\,r\left(1+2\,\frac{t}{r_\Lambda}\right)\dot{\varphi}^{\,2} = 0\,, \tag{4}$$

$$r\left(1+2\,\frac{t}{r_\Lambda}\right)\ddot{\varphi} + 2\,\frac{r}{r_\Lambda}\,\dot{t}\dot{\varphi} + 2\left(1+2\,\frac{t}{r_\Lambda}\right)\dot{r}\dot{\varphi} = 0\,. \tag{5}$$

Here, as distinct from formula (2), t and r are the Robertson–Walker coordinates; and dot denotes a derivative with respect to the proper time of the moving particle.

An important feature of these equations is that they involve three characteristic spatial scales — Schwarzschild radius $r_g = 2GM$, de Sitter radius $r_\Lambda = \sqrt{3/\Lambda}$, and the initial radius of orbit of the test body (e.g., a planet) R_0 — which differ from each other by many orders of magnitude. For example, in the case of the Earth–Moon system (where Earth is the central mass; and Moon, the test body), we

have: $r_g \sim 10^{-2}$ m, $R_0 \sim 10^9$ m, and $r_\Lambda \sim 10^{27}$ m. This makes the problem of accurate numerical integration very hard.

However, for simplicity — just to reveal the possibility of local Hubble expansion in the gravitationally-bound system — we can consider a toy model, where these parameters differ from each other not so much, e.g., by only two or three orders of magnitude. For example, let us take the initial orbital radius as the unit of length (i.e., $R_0 \equiv 1$); and let the Schwarzschild radius be $r_g = 10^{-2}$, and de Sitter radius $r_\Lambda = 10^3$ or $2{\cdot}10^3$. The corresponding numerical orbits are presented in Figure 2. As is seen, when Λ (i.e., the dark-energy density) increases and, respectively, r_Λ decreases, the orbits become more and more spiral. In other words, *a test particle orbiting about the central mass can really experience the local Hubble expansion.* This quantitative analysis argues against the commonly-accepted intuitive point of view that the remote cosmological action would result just in a partial compensation of the gravitational attraction to the center, i.e., the orbit will be slightly disturbed but remain stationary [33]. According to our calculations, the secular (time-dependent) effects are really possible.

Unfortunately, it is not so easy to get the reliable numerical values of such an effect in the realistic planetary systems, because of the above-mentioned huge difference in the characteristic scales and the need for integration over a very long time interval. Besides, since the set of equations is strongly nonlinear, it is difficult to predict how the other kinds of celestial perturbations (e.g., by the additional planets) will interfere with the secular Hubble-type effects. Moreover, it is unclear in advance if the local Hubble expansion will follow the standard linear relation:

$$\dot{r} = H_0^{(\mathrm{loc})}\, r\,, \tag{6}$$

where $H_0^{(\mathrm{loc})}$ is the local Hubble constant (which, generally speaking, can be different from the global one). In principle, the corresponding relation in the vicinity of the central massive body might be substantially nonlinear. So, all these questions are still to be answered.

3. Observable footprints of the local Hubble expansion

A crucial factor supporting the interest to a probable manifestation of Hubble expansion at the small scales is that there is a number of observable phenomena — both in the Solar system and local intergalactic volume — that could be naturally explained by the local Hubble expansion. A detailed list of such effects in the Solar system can be found in papers [30, 31]. Particularly, they are:

- the so-called faint young Sun problem (i.e., the insufficient luminosity of the young Sun to support development of the geological and biological evolution on the Earth),

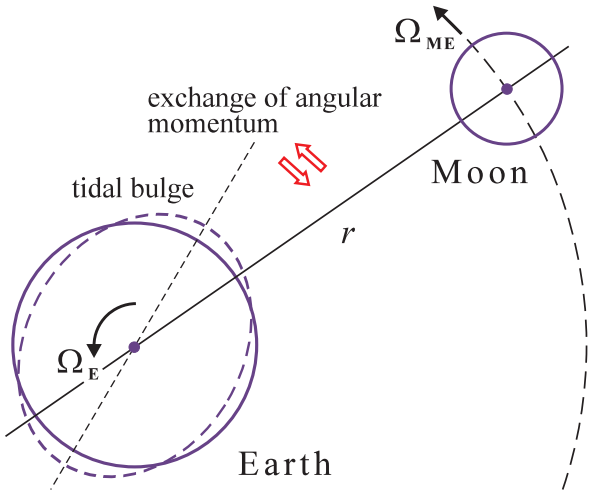

Figure 3: Sketch of the tidal interaction between the Earth and Moon.

- the problem of liquid water on Mars (which actually has the same origin as the above-mentioned one),
- the anomalous rate of recession of the Moon from the Earth (called also the lunar tidal catastrophe),
- the long-term dynamics of the so-called fast satellites of Mars, Jupiter, Uranus, and Neptune,
- the efficiency of formation of Neptune and comets in the Kuiper belt from the protoplanetary disk.

3.1. The lunar tidal catastrophe

From our point of view, the most appealing example for the existence of the local Hubble expansion is the anomalous Earth–Moon recession rate. Namely, it was known for a long time that tidal interaction results in the deceleration of *proper* rotation of the Earth $\Omega_{\rm E}$ and acceleration of *orbital* rotation of the Moon $\Omega_{\rm ME}$ [26]. This is pictorially explained in Figure 3: since $\Omega_{\rm E} > \Omega_{\rm ME}$, a tidal bulge on the Earth's surface is slightly shifted forward (in the direction of Earth's rotation) because of the finite-time relaxation effects. Such a shifted bulge pulls the Moon forward, thereby accelerating it; and simultaneously, due to the back reaction, the proper rotation of the Earth decelerates.

Method	Measurement by the lunar laser ranging	Estimate from the Earth's tidal deceleration
Effects involved	(1) geophysical tides (2) local Hubble expansion	(1) geophysical tides
Numerical value	3.8±0.1 cm/yr	1.6±0.2 cm/yr

Table 1: Relative contributions of various processes to the recession rate of the Moon from the Earth.

The increasing orbital momentum of the Moon results in the increase of its distance from the Earth with the following rate:

$$\dot{r} = k\,\dot{T}_{\rm E}\,, \tag{7}$$

where $T_{\rm E}$ is the Earth's diurnal period, and $k = 1.81{\cdot}10^5\,$cm/s [14]. So, if secular variation in the length of day is known from astrometric observations, relation (7) can be used to derive the rate of secular increase in the lunar orbit $\dot{r}$.

On the other hand, the same quantity can be measured immediately by the lunar laser ranging (LLR). This became possible since the early 1970's, when a few optical retroreflectors were installed on the lunar surface. The accuracy of LLR quickly improved in the subsequent two decades, and its errors were reduced to 2–3 cm, which enabled ones to measure immediately the secular expansion of the lunar orbit [11]. Surprisingly, the measured value of $\dot{r}$ turned out to be substantially greater than the value obtained from formula (7), as summarized in Table 1 [16].

Then, a lot of attempts were undertaken to reduce this discrepancy. Namely, the value presented in the last column of the table corresponds to

$$\dot{T}_{\rm E} = (8.77{\pm}1.04){\cdot}10^{-6}\,{\rm s/yr}\,. \tag{8}$$

It was derived from a series of astronomical observations accumulated since the middle of the 17th century, when telescopic data became available (they are compiled, for example, in monograph [42]). In principle, the period of three centuries might be insufficiently long, because the length of day $T_{\rm E}$ experience also some quasi-periodic variations on the longer time scales, which can affect the linear trend (8).

One of the ways to get around this obstacle is to employ the ancient data on eclipses, which cover the period over two millennia. Such an approach was pursued by a number of researchers (e.g., review [43]), and the obtained values of $\dot{T}_{\rm E}$ sometimes enabled them to get a reasonable agreement with LLR data. However, the various sets of ancient observations give the results different from each other by almost two times, and it is not clear *a priori* which of them are more reliable.

Yet another idea to avoid the discrepancy presented in Table 1 is to take into account a secular variation in the Earth's moment of inertia, which is commonly characterized by the second gravitational harmonic coefficient $\dot{J}_2$. Its decreasing trend at the present time is assumed to be caused by the so-called viscous rebound of the solid Earth from the decrease in load due to the last deglaciation. (Namely, the Earth was compressed by the ice caps in polar regions during the glacial period and now restores its shape.) The first determination of the above-mentioned parameter by Lageos satellite [44] led to the value $\dot{J}_2 = -3{\cdot}10^{-11}$/yr, which seemed to be consistent with LLR data. However, as was established later, such a determination may be very unreliable [4] and even can give the opposite sign of $\dot{J}_2$ [8].

In view of the above difficulties, a promising explanation of the discrepancy $2.2{\pm}0.3\,$cm/yr in Table 1 can be based just on the presence of local Hubble expansion. Assuming validity of the standard relation (6), this corresponds to the value of the local Hubble constant

$$H_0^{(\mathrm{loc})} = 56{\pm}8\ (\mathrm{km/s})/\mathrm{Mpc}\,, \tag{9}$$

which is quite close to its "global" value H_0. So, such an interpretation is not meaningless.

Unfortunately, as was mentioned in Section 2, by now we cannot reliably explain this quantity in terms of parameters of the Earth–Moon system because of the problems in the numerical integration of the equations of motion. Instead, we shall present here a more crude but universal estimate of the relation between the local and global Hubble rates, which is actually applicable to any "small-scale" system.

It is reasonable to assume that the local Hubble expansion is formed only by the uniformly-distributed dark energy (Λ-term), while the irregularly distributed (clumped) forms of matter affect the rate of cosmological expansion only at the sufficiently large distances, where they can be characterized by their average values. (At smaller distances, the clumped forms of matter manifest themselves by the "classical" gravitational forces.) So, if the Universe is spatially flat and filled only with dark energy and the dust-like matter with densities $\rho_{\Lambda 0}$ and $\rho_{\mathrm{D}0}$, respectively, then general expression (1) can be rewritten as[7]

$$H_0 = \sqrt{\frac{8\pi G}{3}}\,\sqrt{\rho_{\Lambda 0} + \rho_{\mathrm{D}0}}\,, \tag{10}$$

$$H_0^{(\mathrm{loc})} = \sqrt{\frac{8\pi G}{3}}\,\sqrt{\rho_{\Lambda 0}}\,. \tag{11}$$

Therefore, a ratio of the local to global Hubble constants will be

$$\frac{H_0^{(\mathrm{loc})}}{H_0} = \left[1 + \frac{\Omega_{\mathrm{D}0}}{\Omega_{\Lambda 0}}\right]^{-1/2}, \tag{12}$$

where $\Omega_{\Lambda 0} = \rho_{\Lambda 0}/\rho_{\mathrm{cr}}$ and $\Omega_{\mathrm{D}0} = \rho_{\mathrm{D}0}/\rho_{\mathrm{cr}}$ are the corresponding relative densities.

[7]Subscripts "0" denote here the values of the corresponding quantities at the present time.

Taking for a crude estimate $\Omega_{\Lambda 0} = 0.75$ and $\Omega_{\rm D0} = 0.25$, we arrive at

$$H_0/H_0^{(\rm loc)} \approx 1.15\,. \tag{13}$$

Consequently, the local value (9) corresponds to the global value

$$H_0 = 65{\pm}9 \;\; ({\rm km/s})/{\rm Mpc}\,, \tag{14}$$

which is in a good agreement with the modern cosmological data (especially, based on studies of type Ia supernovae).

Let us emphasize that the performed analysis crucially depends on the accepted value of secular increase in the length of day $\dot{T}_{\rm E}$. The qualitative idea of such analysis was put forward in our work [13], and in the first quantitative study of this subject [14] we used the value corrected for the ancient eclipses, $\dot{T}_{\rm E} = 1.4{\cdot}10^{-5}\,{\rm s/yr}$, which was considered by some researchers as the best option [43]. As a result, we arrived at the substantially reduced magnitude of the local Hubble constant, $H_0^{(\rm loc)} = 33{\pm}5\,({\rm km/s})/{\rm Mpc}$, which had no reasonable interpretation. On the other hand, when in the later work [16] we employed $\dot{T}_{\rm E}$ derived purely from the set of astrometric observations in the telescopic era [42] without any further corrections, the resulting value of $H_0^{(\rm loc)}$ was found to be in accordance with the large-scale cosmological data.

3.2. The faint young Sun paradox

Yet another appealing example for the existence of local Hubble expansion is the problem of insufficient flux of energy from Sun to the Earth in the past; e.g., review [22]. Namely, according to the modern models of stellar evolution, the solar luminosity increases by approximately 30 % during the period after its birth (about $5{\cdot}10^9\,{\rm yr}$). This means that the energy input to the Earth's climate system, e.g., 2–4 billion years ago was appreciably less than now and, therefore, the most part of water must be in a frozen state. This would preclude the geological and biological evolution of the Earth and contradicts a number of well-established facts on the existence of considerable volumes of liquid water in that period of time. Although a lot of attempts were undertaken to resolve this problem by the inclusion of additional influences (first of all, the atmospheric greenhouse effect), no definitive solution is available by now.

An interesting option was suggested recently by Křížek and Somer [30, 31], who proposed to take into consideration the local Hubble expansion of the Earth's orbit. As a result, the Sun–Earth distance in the past would be appreciably less than now and, consequently, the solar irradiation of the Earth's surface increased. In particular, the quantitative analysis performed in the above-cited papers have shown that at $H_0^{(\rm loc)} \approx 0.5 H_0$ expansion of the Earth's orbit compensates the increasing solar luminosity with very good accuracy; so that the Earth's surface received almost the

same flux of energy in the past $3.5{\cdot}10^9$ yr and will continue to do so for a considerable period in future.

From our point of view, the above-mentioned idea is very promising. Unfortunately, the value of local Hubble constant used in these papers is poorly consistent with the one derived from our analysis of the Earth–Moon system in Section 3.1, $H_0^{(\mathrm{loc})} \approx 0.85\, H_0$. So, it is interesting to check if the same mechanism will work at other rates of the local Hubble expansion? Such analysis was performed in our recent work [18].

Namely, let solar luminosity increase linearly with time:

$$L(t) = L_0 + (\Delta L/\Delta T)\, t\,, \tag{15}$$

where L_0 is its present-day value (at $t = 0$), and ΔL is the variation of luminosity over the time interval $\Delta T = 5{\cdot}10^9$ yr (for the sake of estimate, we shall use here the rounded values). Then, assuming validity of the standard relation (6), a temporal variation in the irradiation of the Earth's surface can be found from a simple geometric consideration. The resulting curves for a number of hypothetical solar models with $\Delta L/L_0 = 0.3,\ 0.4,\ 0.5,\ 0.6$ and various rates of the local Hubble expansion $H_0^{(\mathrm{loc})} = 0.5,\ 0.6,\ 0.7,\ 0.8,\ 0.9\, H_0$ are presented in Figure 4.

It is seen that the Křížek–Somer case ($\Delta L/L_0 = 0.3$, $H_0^{(\mathrm{loc})}/H_0 = 0.5$) really provides a very stable energy input to the Earth for a few billion years both in the past and future. At the higher rates of the local Hubble expansion (which would be more consistent with our analysis of the Earth–Moon dynamics), a quite favorable situation exists, for example, at $\Delta L/L_0 = 0.5$ and $H_0^{(\mathrm{loc})}/H_0 = 0.8$: the solar irradiation at $t < 0$ is almost as stable as in the Křížek–Somer case, and more appreciable variation at $t > 0$ is not so important because we actually do not know the Earth's evolution in the future.

Is it reasonable to consider the solar model with $\Delta L/L_0 = 0.5$? In fact, such enhanced variations ΔL were typical for the first quantitative models of the Sun [40]. However, the subsequent investigations resulted in the progressively less values of ΔL; and it is commonly accepted now that the increase in luminosity amounts to about 7 % per Gyr over the past evolution of 4.57 Gyr. Nevertheless, we may imagine processes like mixing in the solar interiors to change this value. This would imply the star with a small convective core. The problem is that the Sun is just at the limit of mass where convective cores appear [34].

Of course, one should keep in mind that the above calculations of solar irradiation cannot be immediately confronted with the relevant data from paleoclimatology, because it is necessary to take into account a lot of additional geophysical and geochemical processes, first of all, the greenhouse effect. From this point of view, the Earth–Moon system discussed in Section 3.1 represents a more "clean" case, where the probable local Hubble expansion is less obscured by other phenomena.

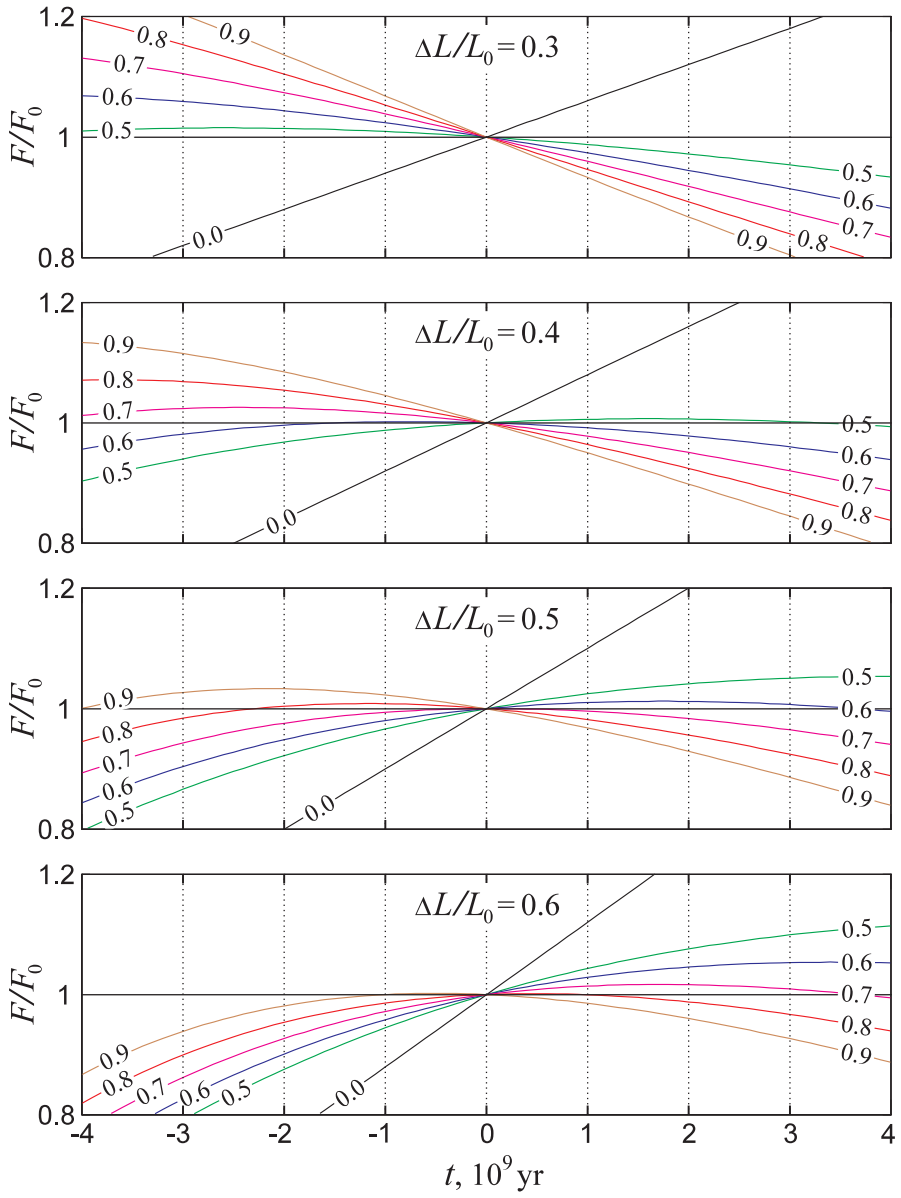

Figure 4: Temporal variations in solar irradiation of the Earth's surface F/F_0 for different models of solar evolution (characterized by $\Delta L/L_0$) and various rates of the local Hubble expansion (numbers near the curves denote the ratio $H_0^{(\mathrm{loc})}/H_0$). The straight lines marked by 0.0 correspond to the case when the local Hubble expansion is absent at all.

3.3. Other systems

A number of other effects in the Solar system that might be associated with local Hubble expansion have been already listed in the beginning of Section 3. Unfortunately, they are much less studied than the lunar tidal catastrophe and the faint young Sun paradox. So, we shall not discuss them in the present article; for more details, see papers [30, 31].

Besides, a few researchers studied dynamics of all solar-system bodies, including the major asteroids, on the basis of data by optical and radio astrometry collected in the last decades [38, 39]. Their conclusion was that, in general, a self-consistent picture of planetary motion (the high-precision ephemerides) can be obtained without taking into account any local cosmological influences. However, it should be kept in mind that such analyses involved a lot of fitting parameters, which were attributed, e.g., to the unknown masses of asteroids, solar oblateness, effects of the solar wind on radio wave propagation, etc. On the other hand, *the probable Hubble expansion was never included into their equations in explicit form.* So, the small resulting residuals might be merely a mathematical fact: it is well known from statistics that any empirical data can be fitted as accurately as desirable if the number of free parameters becomes sufficiently large.

If the local Hubble expansion is present in the Solar system, it should be naturally expected also in galaxies. Unfortunately, the entire pattern of galaxy evolution is very complicated by the formation of stars and their proper motions. So, as far as we know, the problem of cosmological effects at the scale of galaxies remains completely unexplored by now.

A much more elaborated subject is Hubble expansion in the local intergalactic volume. It was believed for a long time that the standard Hubble flow can be traced only at the distances starting from 5–10 Mpc, where it becomes possible to introduce the average cosmological matter density. Nevertheless, by the end of the 20th century, the Hubble flow was detected also at the considerably less scales, down to 1–2 Mpc. At the same time, the concept of dark-energy-dominated Universe became the main paradigm in cosmology. So, it was natural to explain both the presence of the Hubble flow at the sufficiently small scales and its regularity ("quiescence") just by the perfectly-uniform dark energy (or Λ-term) [6, 20]. Unfortunately, it remains unclear by now if the effective value of Hubble constant in the Local Group is smaller or larger than at the global scales and, therefore, if the relation (12) between $H_0^{(\mathrm{loc})}$ and H_0 is applicable in this situation?

Let us mention also that the most of available theoretical works on the dynamics of galaxies in the Local Group are based on the effective gravitational forces derived from Kottler metric (2):

$$F_{\mathrm{eff}}(r) = M_1\left(-\frac{GM_2}{r^2} + \frac{\Lambda\, r}{3}\right); \tag{16}$$

the last term often being called the "antigravity" force. Unfortunately, such treatment has a limited scope of applicability: Firstly, as was already mentioned in Section 2, the static metric (2) does not possess a correct cosmological asymptotics at infinity and, therefore, the corresponding force (16) is unable to describe the entire Hubble flow, including the large distances. Secondly, strictly speaking, the above-written effective force is adequate *only for the restricted two-body problem* (where M_1 is the mass of a test particle, and M_2 is the mass of the central gravitating body). This is evident, in particular, from the fact that masses M_1 and M_2 appear in expression (16) by different ways. So, there is no reason to assume validity of this formula when M_1 and M_2 are comparable to each other or, especially, to apply it to the many-body problem.

4. Concluding remarks

1. Despite a lot of theoretical works rejecting the possibility of local Hubble expansion, we believe that this problem is still unresolved: Firstly, the available arguments often contradict each other. Secondly, the most of them become inapplicable to the case when the Universe is dominated by the perfectly-uniform dark energy (or Λ-term). Moreover, a self-consistent theoretical treatment of the simplest models (such as the restricted two-body problem against the Λ-background) demonstrates a principal possibility of the local cosmological influences: the Hubble expansion is not suppressed completely in the vicinity of a massive body.

2. A few long-standing problems in planetology, geophysics, and celestial mechanics can be well resolved by the assumption of local Hubble expansion whose rate is comparable to that at the global scales. It is quite surprising that many theorists believe that the possibility of local cosmological influences is strictly prohibited just by the available observational data, while a lot of observers believe that there are irrefutable theoretical proofs that Hubble expansion is absent at small scales.

3. However, the important conceptual question still persists: What is the spatial scale from which the cosmological expansion no longer takes place? This is of crucial importance since otherwise, as pictorially explained by Misner et al. [36, p. 719], the "meter stick" will also expand and, therefore, it will be meaningless to speak about any expansion at all... We cannot give a definitive numerical answer to this question. However, we believe that the systems dominated by non-gravitational interactions should not experience the cosmological expansion (e.g., the meter stick, the solid Earth, etc. do not expand).

Acknowledgements

I am grateful to Yurij V. Baryshev, Sergei M. Kopeikin, Michal Křížek, André Maeder, and Marek Nowakowski for valuable discussions of the problems outlined in this paper.

References

[1] Anderson, J. L.: Multiparticle dynamics in an expanding universe. Phys. Rev. Lett. **75** (1995), 3602.

[2] Balaguera-Antolínez, A., Böhmer, C. G., and Nowakowski, M.: Scales set by the cosmological constant. Class. Quant. Grav. **23** (2006), 485.

[3] Bonnor, W. B.: Local dynamics and the expansion of the universe. Gen. Rel. Grav. **32** (2000), 1005.

[4] Bourda, G. and Capitaine, N.: Precession, nutation, and space geodetic determination of the Earth's variable gravity field. Astron. Astrophys. **428** (2004), 691.

[5] Cardona, J. F. and Tejeiro, J. M.: Can interplanetary measures bound the cosmological constant? Astrophys. J. **493** (1998), 52.

[6] Chernin, A., Teerikorpi, P., and Baryshev, Y.: Why is the Hubble flow so quiet? Adv. Space Res. **31** (2003), 459.

[7] Cooperstock, F. I., Faraoni, V., and Vollick, D. N.: The influence of the cosmological expansion on local systems. Astrophys. J. **503** (1998), 61.

[8] Cox, C. M. and Chao, B. F.: Detection of a large-scale mass redistribution in the terrestrial system since 1998. Science **297** (2002), 831.

[9] Davis, T. M., Lineweaver, C. H., and Webb, J. K.: Solutions to the tethered galaxy problem in an expanding universe and the observation of receding blueshifted objects. Amer. J. Phys. **71** (2003), 358.

[10] Dicke, R. H. and Peebles, P.J̇. E.: Evolution of the solar system and the expansion of the universe. Phys. Rev. Lett. **12** (1964), 435.

[11] Dickey, J. O. et al.: Lunar laser ranging: A continuing legacy of the Apollo program. Science **265** (1994), 482.

[12] Domínguez, A. and Gaite, J.: Influence of the cosmological expansion on small systems. Europhys. Lett. **55** (2001), 458.

[13] Dumin, Y. V.: Using the lunar laser ranging technique to measure the local value of Hubble constant. Geophys. Res. Abstr. **3** (2001), 1965.

[14] Dumin, Y. V.: A new application of the lunar laser retroreflectors: Searching for the 'local' Hubble expansion. Adv. Space Res. **31** (2003), 2461.

[15] Dumin, Y. V.: Comment on 'Progress in lunar laser ranging tests of relativistic gravity'. Phys. Rev. Lett. **98** (2007), 059 001.

[16] Dumin, Y. V.: Testing the dark-energy-dominated cosmology by the solar-system experiments. In: H. Kleinert, R. Jantzen, and R. Ruffini (Eds.), *Proc. 11th Marcel Grossmann Meeting on General Relativity*, p. 1752. World Sci., Singapore, 2008.

[17] Dumin, Y. V.: Perturbation of a planetary orbit by the Lambda-term (Dark energy) in Einstein equations. In: N. Capitaine (Ed.), *Proc. Journées 2010 Systèmes de référence spatio-temporels: New challenges for reference systems and numerical standards in astronomy*, p. 276. Observ. Paris, 2011.

[18] Dumin, Y. V.: The faint young sun paradox in the context of modern cosmology. Astronomicheskii Tsirkulyar (Astron. Circular) **1623** (2015), 1. `http://comet.sai.msu.ru/~gmr/AC/AC1623.pdf`.

[19] Einstein, A. and Straus, E. G.: The influence of the expansion of space on the gravitation fields surrounding the individual stars. Rev. Mod. Phys. **17** (1945), 120.

[20] Ekholm, T., Baryshev, Y., Teerikorpi, P., Hanski, M.O., and Paturel, G.: On the quiescence of the Hubble flow in the vicinity of the Local Group: A study using galaxies with distances from the Cepheid PL-relation. Astron. Astrophys. **368** (2001), L17.

[21] Faraoni, V. and Jacques, A.: Cosmological expansion and local physics. Phys. Rev. D **76** (2007), 063 510.

[22] Feulner, G.: The faint young sun problem. Rev. Geophys. **50** (2012), RG2006.

[23] Hackmann, E. and Lämmerzahl, C.: Geodesic equation in Schwarzschild-(anti-) de Sitter space-times: Analytical solutions and applications. Phys. Rev. D **78** (2008), 024 035.

[24] Iorio, L.: Can solar system observations tell us something about the cosmological constant? Int. J. Mod. Phys. D **15** (2006), 473.

[25] Kagramanova, V., Kunz, J., and Lämmerzahl, C.: Solar system effects in Schwarzschild–de Sitter space–time. Phys. Lett. B **634** (2006), 465.

[26] Kaula, W.: *An introduction to planetary physics: The terrestrial planets*. J. Wiley & Sons, New York, 1968.

[27] Klioner, S. A. and Soffel, M. H.: Refining the relativistic model for Gaia: Cosmological effects in the BCRS. In: C. Turon, K. S. O'Flaherty, and M. A. C. Perryman (Eds.), *Proc. Symp. The Three-Dimensional Universe with Gaia (ESA SP-576)*, p. 305. ESA Publ. Division, Noordwijk, Netherlands, 2005.

[28] Kottler, F.: Uber die physikalischen Grundlagen der Einsteinschen Gravitationstheorie. Ann. Phys. (Leipzig) **56** (1918), 401.

[29] Kramer, D., Stephani, H., MacCallum, M., and Herlt, E.: *Exact solutions of Einstein's field equations*. Cambridge University Press, Cambridge, 1980.

[30] Křížek, M.: Dark energy and the anthropic principle. New Astron. **17** (2012), 1.

[31] Křížek, M. and Somer, L.: Manifestations of dark energy in the Solar system. Grav. Cosmol. **21** (2015), 59.

[32] Landau, L. D. and Lifshitz, E. M.: *Mechanics*. Pergamon Press, Oxford, 1976, 3rd edn.

[33] Lineweaver, C. H. and Davis, T. M.: Misconceptions about the Big Bang. Sci. American **292, no. 3** (2005), 36.

[34] Maeder, A.: Private communication (2016).

[35] McVittie, G. C.: The mass-particle in an expanding universe. Mon. Not. R. Astron. Soc. **93** (1933), 325.

[36] Misner, C. W., Thorne, K. S., and Wheeler, J. A.: *Gravitation*. W. H. Freeman & Co., San Francisco, 1973.

[37] Noerdlinger, P. D. and Petrosian, V.: The effect of cosmological expansion on self-gravitating ensembles of particles. Astrophys. J. **168** (1971), 1.

[38] Pitjeva, E. V.: High-precision ephemerides of planets–EPM and determination of some astronomical constants. Solar System Res. **39** (2005), 176.

[39] Pitjeva, E. V.: Relativistic effects and solar oblateness from radar observations of planets and spacecraft. Astron. Lett. **31** (2005), 340.

[40] Schwarzschild, M.: *Structure and evolution of the stars*. Princeton Univ. Press, Princeton, N.J., 1958.

[41] Sereno, M. and Jetzer, P.: Evolution of gravitational orbits in the expanding universe. Phys. Rev. D **75** (2007), 064 031.

[42] Sidorenkov, N. S.: *Physics of the Earth's rotation instabilities*. Nauka-Fizmatlit, Moscow, 2002. In Russian.

[43] Stephenson, F. R. and Morrison, L. V.: Long-term changes in the rotation of the Earth: 700 B.C. to A.D. 1980. Phil. Trans. Royal Soc. Lond. A **313** (1984), 47.

[44] Yoder, C. F. et al.: Secular variation of Earth's gravitational harmonic J_2 coefficient from Lageos and nontidal acceleration of Earth rotation. Nature **303** (1983), 757.

Conference *Cosmology on Small Scales 2016*
Michal Křížek and Yurii Dumin (Eds.)
Institute of Mathematics CAS, Prague

SCALE INVARIANT COSMOLOGY: COSMOLOGICAL MODELS AND SMALL SCALE EFFECTS

André Maeder

Geneva Observatory
chemin des Mailletes, CH-1290 Sauverny, Switzerland
andre.maeder@unige.ch

Abstract: We make the hypothesis that the empty space, at macroscopic and large scales, is scale invariant. This leads to essential simplifications in the cosmological equations with scale invariance. There is an additional term remaining that opposes to gravity and favors accelerated expansion. This term makes a significant contribution, called Ω_λ, to the energy-density of the Universe, satisfying an equation $\Omega_\mathrm{m} + \Omega_\mathrm{k} + \Omega_\lambda = 1$. Numerical integrations of the cosmological equations for different curvature k and density parameters Ω_m are performed. The cosmological models start explosively with first a braking phase followed by a continuously accelerating expansion. The comparison with observations of supernovae SN Ia, BAO and CMB data from Planck 2015 shows that the scale invariant model with $k = 0$ and $\Omega_\mathrm{m} = 0.30$ very well fits the observations in the Ω_m vs. Ω_Λ plane and consistently accounts for the accelerating expansion or dark energy. The plot $H(z)$ vs. redshift z, the parameters q_0 and the redshift z_trans of the transition between braking and acceleration are examined. These dynamical tests are fully satisfied. The past evolution of matter and radiation density shows only minor differences with respect to the standard case. The local effects in the Newtonian approximation are also investigated. In the two-body problem, they result in a weak outwards expansion of the orbits at a rate of the order of the Hubble expansion, but not exactly. The effects behave like the ratio $(\varrho_\mathrm{c}/\varrho)^{1/2}$ of the critical density of the Universe to the density of the system considered. In clusters of galaxies, the additional expansion term may be responsible for the large excesses of the dynamical masses derived from the standard Virial theorem.

Keywords: Cosmology, theory, dark energy, cosmological parameters

PACS: 04.20.-q, 04.25.-g

1. Introduction and recalls on scale invariance

The laws of physics are generally not unchanged under a change of scale, a fact discovered by Galileo Galilei [15]. The scale references are closely related to the

material content of the medium. Even the vacuum at the quantum level is not scale invariant, since quantum effects produce some units of time and length. This point is a historical argument, already forwarded long time ago against the Weyl theory.

The empty space at macroscopic and large scales, in the sense it is used for example in the Minkowski metric, does not appear to have preferred scales of length or time. We now make the hypothesis that the empty space at large scales is scale invariant. Thus, in the same way as we may use Newton or Einstein theory at macroscopic and large scales, even if we do not have a quantum theory of gravitation, we may consider that the large scale empty space is scale invariant, even if this is not true at the quantum level.

A strong reason has been emphasized by Dirac [9]: *It appears as one of the fundamental principles of Nature that the equations expressing basic laws should be invariant under the widest possible group of transformations.* The Maxwell equations of electrodynamics in absence of charges and currents show the property of scale invariance. While scale invariance has often been studied in relation with possible variations of the gravitational constant G, no such hypothesis of variable G is considered here. We do not know whether the above hypothesis of scale invariance really applies. However, it is by carefully examining the implications of such a hypothesis that we will find whether it corresponds to Nature or not. The detailed results summarized here are presented in three recent papers [24].

Many developments on a scale invariant theory of gravitation have been performed by giants of Physics like Eddington [13], Dirac [9], and Canuto [7]. Here, we limit the recalls to the very minimum. In the 4-dimensional space of General Relativity, the element interval $ds'^{\,2}$ in coordinates $x'^{\,\mu}$ writes $ds'^{\,2} = g'_{\mu\nu} dx'^{\,\mu}\, dx'^{\,\nu}$, (the symbols with a prime refer to the space of General Relativity, which is not scale invariant). A scale (or gauge) transformation is considered to a new coordinate system x^μ with the following relation between the two systems,

$$ds' = \lambda(x^\mu)\, ds\,, \tag{1}$$

where $ds^2 = g_{\mu\nu} dx^\mu\, dx^\nu$ is the line element in the new more general framework, where scale invariance is a fundamental property in addition to the general covariance. Thus, there is a conformal transformation between the two systems,

$$g'_{\mu\nu} = \lambda^2\, g_{\mu\nu}\,. \tag{2}$$

Parameter $\lambda(x^\mu)$ is the scale factor connecting the two line elements. The Cosmological Principle demands that the scale factor only depends on time. The general scale invariant field equation is [7]

$$R'_{\mu\nu} - \frac{1}{2}\, g_{\mu\nu} R' - \kappa_{\mu;\nu} - \kappa_{\nu;\mu} - 2\kappa_\mu\kappa_\nu + 2 g_{\mu\nu}\kappa^\alpha_{;\alpha} - g_{\mu\nu}\kappa^\alpha\kappa_\alpha = -8\pi G T_{\mu\nu} - \lambda^2 \Lambda_{\rm E}\, g_{\mu\nu}\,, \tag{3}$$

where G is the gravitational constant and $\Lambda_{\rm E}$ the Einstein cosmological constant. The term κ_μ is called the coefficient of metrical connection, ";" indicates a derivative,

$$\kappa_\mu = -\frac{\partial}{\partial x^\mu}\, \ln\lambda\,. \tag{4}$$

In the scale covariant theory, it is a fundamental quantity like the $g_{\mu\nu}$. The contracted form of the Riemann-Christoffel tensor $R_{\mu\nu}$ and the total curvature R are [9, 7]

$$R_{\mu\nu} = R'_{\mu\nu} - \kappa_{\mu;\nu} - \kappa_{\nu;\mu} - g_{\mu\nu}\kappa^{\alpha}_{;\alpha} - 2\kappa_{\mu}\kappa_{\nu} + 2g_{\mu\nu}\kappa^{\alpha}\kappa_{\alpha}\,, \tag{5}$$

$$R = R' - 6\kappa^{\alpha}_{;\alpha} + 6\kappa^{\alpha}\kappa_{\alpha}\,. \tag{6}$$

There, $R'_{\mu\nu}$ and R' are the usual expressions in General Relativity. The second member of the scale invariant field equation is scale invariant, as is the first one. Thus, we have $T'_{\mu\nu} = T_{\mu\nu}$, where the right-hand term is the energy-momentum tensor in the new more general coordinate system. This has further implications, which are easily examined in the case of a perfect fluid [7]. The tensor $T_{\mu\nu}$ being invariant, one may write $(p+\varrho)u_{\mu}u_{\nu} - g_{\mu\nu}p = (p'+\varrho')u'_{\mu}u'_{\nu} - g'_{\mu\nu}p'$. The velocities u'^{μ} and u'_{μ} transform like

$$u'^{\mu} = \frac{dx^{\mu}}{ds'} = \lambda^{-1}\frac{dx^{\mu}}{ds} = \lambda^{-1}u^{\mu} \quad \text{and} \quad u'_{\mu} = g'_{\mu\nu}u'^{\nu} = \lambda^{2}g_{\mu\nu}\lambda^{-1}u^{\nu} = \lambda\, u_{\mu}\,. \tag{7}$$

Thus, the energy-momentum tensor transforms like

$$(p+\varrho)u_{\mu}u_{\nu} - g_{\mu\nu}p = (p'+\varrho')\lambda^{2}u_{\mu}u_{\nu} - \lambda^{2}g_{\mu\nu}p'\,. \tag{8}$$

This implies the following scaling of p and ϱ in the new general coordinate system

$$p = p'\,\lambda^{2} \quad \text{and} \quad \varrho = \varrho'\,\lambda^{2}\,. \tag{9}$$

Pressure and density are therefore not scale invariant, but are so-called coscalars of power -2. To avoid any ambiguity, we always keep all expressions with $\Lambda_{\rm E}$, the true Einstein cosmological constant, so that in (3), it appears multiplied by λ^2.

2. Consequences of the scale invariance of the empty space

We consider the case of the empty space, with thus an energy-momentum tensor $T_{\mu\nu} = 0$. The line-element is given by the Minkowski metric, $ds^2 = c^2dt^2 - (dx^2 + dy^2 + dz^2)$. In General Relativity, it implies that the first member of Einstein equation is equal to zero, $R'_{\mu\nu} - \frac{1}{2}\,g_{\mu\nu}\;R' = 0$. Thus, in the scale invariant field equation (3), only the following terms are remaining [27],

$$\kappa_{\mu;\nu} + \kappa_{\nu;\mu} + 2\kappa_{\mu}\kappa_{\nu} - 2g_{\mu\nu}\kappa^{\alpha}_{;\alpha} + g_{\mu\nu}\kappa^{\alpha}\kappa_{\alpha} = \lambda^{2}\Lambda_{\rm E}\,g_{\mu\nu}\,. \tag{10}$$

We are left only with a relation between some functions of the scale factor λ (through the κ-terms (4)), the $g_{\mu\nu}$ and the Einstein cosmological constant $\Lambda_{\rm E}$, interpreted as the energy density of the vacuum, and which now appears as related to the properties of scale invariance in the empty space. The problem of the cosmological constant in the empty space is not a new one. Bertotti et al. [3] are quoting the following remark they got from Professor Bondi, who stated that: *"Einstein's disenchantment with the cosmological constant was partially motivated by a desire to preserve scale invariance*

of the empty space Einstein equations". This remark is in agreement with the fact that $\Lambda_{\rm E}$ is not scale invariant as are the $T_{\mu\nu}$. The above developments show that the scale invariant theory may offer a possibility to conciliate the existence of $\Lambda_{\rm E}$ with the scale invariance of the empty space at macroscopic scales.

Only the zero component of κ_μ is non-vanishing. Thus, one has

$$\kappa_{\mu;\nu} = \kappa_{0;0} = \partial_0 \kappa_0 = \frac{d\kappa_0}{dt} \equiv \dot{\kappa}_0 \,. \tag{11}$$

The 0 and the 1, 2, 3 components of what remains from the field equation (10) become respectively

$$3\kappa_0^2 = \lambda^2 \,\Lambda_{\rm E} \quad \text{and} \quad 2\dot{\kappa}_0 - \kappa_0^2 = -\lambda^2 \Lambda_{\rm E} \,. \tag{12}$$

From (4), one has $\kappa_0 = -\dot{\lambda}/\lambda$ (with $c = 1$ at the denominator) and (12) leads to

$$3\,\frac{\dot{\lambda}^2}{\lambda^2} = \lambda^2\,\Lambda_{\rm E} \quad \text{and} \quad 2\,\frac{\ddot{\lambda}}{\lambda} - \frac{\dot{\lambda}^2}{\lambda^2} = \lambda^2\,\Lambda_{\rm E} \,. \tag{13}$$

These expressions may also be written in equivalent forms

$$\frac{\ddot{\lambda}}{\lambda} = 2\,\frac{\dot{\lambda}^2}{\lambda^2} \,, \quad \text{and} \quad \frac{\ddot{\lambda}}{\lambda} - \frac{\dot{\lambda}^2}{\lambda^2} = \frac{\lambda^2\,\Lambda_{\rm E}}{3} \,. \tag{14}$$

The first relation of (14) places a constraint on $\lambda(t)$. Considering a solution of the form $\lambda = a\,(t-b)^n + d$, we get $d = 0$ and $n = -1$. There is no constraint on b, which means that the origin b of the timescale is not determined by the above equations. (The origin of the time will be determined by the solutions of the equations of the particular cosmological model considered.) We get from (13) and (14),

$$\lambda = \sqrt{\frac{3}{\Lambda_{\rm E}}}\,\frac{1}{c\,t} \,. \tag{15}$$

The hypothesis that the empty space is scale invariant at large scales has important consequences, such as (13), (14), and (15), as well as with respect to Bondi's remark.

3. Cosmological equations and their properties

The equations of the scale invariant cosmology can be derived from the field equation (3) using the Robertson–Walker metric [7]. They can also be obtained by applying scale transformation to the current cosmological equations containing the expansion function $R(t)$. This direct method [24] is shown in the Appendix.

$$\frac{8\,\pi G\varrho}{3} = \frac{k}{R^2} + \frac{\dot{R}^2}{R^2} + 2\,\frac{\dot{\lambda}\,\dot{R}}{\lambda\,R} + \frac{\dot{\lambda}^2}{\lambda^2} - \frac{\Lambda_{\rm E}\lambda^2}{3} \,, \tag{16}$$

$$-8\,\pi G p = \frac{k}{R^2} + 2\frac{\ddot{R}}{R} + 2\frac{\ddot{\lambda}}{\lambda} + \frac{\dot{R}}{R}^2 + 4\frac{\dot{R}\,\dot{\lambda}}{R\,\lambda} - \frac{\dot{\lambda}^2}{\lambda^2} - \Lambda_{\rm E}\,\lambda^2 \,. \tag{17}$$

With expressions (13) and (14) for the empty space, which characterize λ and its properties, the two above cosmological equations simplify [24],

$$\frac{8\,\pi G\varrho}{3} = \frac{k}{R^2} + \frac{\dot{R}^2}{R^2} + 2\,\frac{\dot{R}\dot{\lambda}}{R\lambda}\,, \qquad -8\,\pi G p = \frac{k}{R^2} + 2\frac{\ddot{R}}{R} + \frac{\dot{R}^2}{R^2} + 4\frac{\dot{R}\dot{\lambda}}{R\lambda}\,. \tag{18}$$

The combination of these two equations leads to

$$-\frac{4\,\pi G}{3}\,(3p+\varrho) = \frac{\ddot{R}}{R} + \frac{\dot{R}\dot{\lambda}}{R\lambda}\,. \tag{19}$$

There, $k = 0$ or ± 1, p and ϱ are the pressure and density in the scale invariant system. These three equations differ from the classical ones only by the presence of an additional term containing $\dot{R}\,\dot{\lambda}/(R\,\lambda)$. If $\lambda(t)$ is a constant, one gets the usual equations of cosmologies for the expansion term $R(t)$. Thus at any fixed time, the effects that do not depend on the time evolution are just those predicted by General Relativity. Departures from General Relativity appear when the evolution of a physical effect over the ages is intervening.

What is the significance of this additional term? The second term on the right-hand side of (19) is negative, since according to (15) we have $\dot{\lambda}/\lambda = -\frac{1}{t}$. It represents *an acceleration that opposes gravitation*, which may particularly dominate during the advanced stages of evolution of the Universe, since according to (19) the acceleration is proportional to the relative velocity of the expansion. For the empty space, (19) directly leads to the solution $R(t) \sim t^2$ with a continuous expansion over the ages. Equations (18) to (19) incorporate the scale invariance of the field equations as well the scale invariance properties of the vacuum at large scales.

3.1. Density and geometrical parameters

The critical density corresponding to the case $k = 0$ of the flat space is from (18) and (15), with the Hubble parameter $H = \dot{R}/R$,

$$\frac{8\,\pi G\varrho^*_{\rm c}}{3} = H^2 - 2\,\frac{H}{t}\,. \tag{20}$$

We mark with a * this critical density that does not correspond to the usual definition. The parenthesis is always ≥ 0, since $2/(t\,H) = 2(dt/t)(R/dR)$ and the relative growth rate for non empty models is higher than t^2. With (18), (15), and (20), we have

$$\frac{\varrho}{\varrho^*_{\rm c}} - \frac{k}{R^2H^2} + \frac{2}{Ht}\left(1 - \frac{\varrho}{\varrho^*_{\rm c}}\right) = 1\,. \tag{21}$$

$$\text{With } \Omega^*_{\rm m} = \frac{\varrho}{\varrho{*}_{\rm c}}\,,\ \Omega_{\rm k} = -\frac{k}{R^2H^2}, \quad \text{we get} \quad \Omega^*_{\rm m} + \Omega_{\rm k} + \frac{2}{H\,t}\,(1-\Omega^*_{\rm m}) = 1. \tag{22}$$

$\Omega^*_{\rm m} = 1$ consistently implies $\Omega_{\rm k} = 0$ and reciprocally. With the usual definition of the critical density,

$$\Omega_{\rm m} = \frac{\varrho}{\varrho_{\rm c}} \quad \text{with} \quad \varrho_{\rm c} = 3\,H^2/(8\pi G)\,, \quad \text{we get} \quad \Omega_{\rm m} = \Omega^*_{\rm m}\left(1 - \frac{2}{Ht}\right)\,. \tag{23}$$

With $\Omega_{\rm m}$, relation (22) becomes simply,

$$\Omega_{\rm m} + \Omega_{\rm k} + \Omega_\lambda = 1\,, \quad \text{with} \quad \Omega_\lambda \equiv \frac{2}{H\,t}\,. \tag{24}$$

There, Ω_λ is defined by the second relation in (24). The term Ω_λ arising from scale invariance has replaced the usual term Ω_Λ. However, the difference of the physical meaning is very profound. While Ω_Λ is related to the cosmological constant or to the dark energy, Ω_λ *expresses the energy density resulting from the variations of the scale factor.* This term does not demand the existence of unknown particles. It is interesting that an equation like (24) is also valid in scale invariant cosmology.

We may also write $\Omega_{\rm m} = \Omega^*_{\rm m}(1 - \Omega_\lambda)$ and $\Omega^*_{\rm m} = \frac{\Omega_{\rm m}}{\Omega_{\rm m}+\Omega_{\rm k}}$. For $k = 0$, the ratio $2/(t\,H)$ is not a constant (except for the empty model) and thus the various Ω-parameters vary with age, except $\Omega^*_{\rm m}$ which is always equal to 1. While in Friedman's models, there is only one model corresponding to $k = 0$, in the scale invariant framework for $k = 0$ there is a variety of models with different $\Omega_{\rm m}$ and Ω_λ at time t_0. For $k = \pm 1$, $\Omega^*_{\rm m}$ is different from 1, and the terms $\Omega_{\rm m}$, Ω_λ and $\Omega_{\rm k}$ are also not constant in time. We may verify that all models have $\Omega_{\rm m} < 1$, even for $k = 1$, see [24].

We now consider the geometry parameters k, $q_0 = -\frac{\ddot{R}_0\,R_0}{\dot{R}_0^2}$ and their relations with $\Omega_{\rm m}$, $\Omega_{\rm k}$ and Ω_λ at t_0, in absence of pressure. We emphasize that t_0 is not the present age of the Universe, but the present time. The present age is $\tau = t_0 - t_{\rm in}$, where the initial time $t_{\rm in}$ depends on the considered model. From (18) and (22), we get

$$-2\,q_0 + 1 - \Omega_{\rm k} = \frac{4}{H_0 t_0} \quad \text{and} \quad q_0 = \frac{\Omega_{\rm m}}{2} - \frac{\Omega_\lambda}{2}\,. \tag{25}$$

This establishes relations between the deceleration parameter q_0 and the expressions of the matter content for a scale invariant cosmology. If $k = 0$, we have

$$q_0 = \frac{1}{2} - \Omega_\lambda = \Omega_{\rm m} - \frac{1}{2}\,. \tag{26}$$

For a present $\Omega_{\rm m} = 0.30$, we get $q_0 = -0.20$. The above relations are different from those of the ΛCDM, where one has for $k = 0$,

$$q_0 = \frac{1}{2}\Omega_{\rm m} - \Omega_\Lambda = \frac{3}{2}\Omega_{\rm m} - 1 = \frac{1}{2} - \frac{3}{2}\Omega_\Lambda\,. \tag{27}$$

For $\Omega_{\rm m} = 0.30$, we get $q_0 = -0.55$. Let us now turn to the curvature parameter k. From (18), the definition of the critical density and (24), we have at t_0,

$$\frac{k}{R_0^2} = H_0^2\,(\Omega^*_{\rm m} - 1)\left(1 - \frac{2}{t_0 H_0}\right)\,. \tag{28}$$

Values of $\Omega^*_{\rm m} > 1$ correspond to a positive k-value, values smaller than 1 to a negative k-value. With $\Omega_{\rm m}$, we obtain

$$\frac{k}{R_0^2} = H_0^2\left[\Omega_{\rm m} - \left(1 - \frac{2}{t_0 H_0}\right)\right], \quad \text{and} \quad \frac{k}{R_0^2} = H_0^2\left[2\,q_0 - 1 + \frac{4}{H_0 t_0}\right]\,. \tag{29}$$

The expansion functions corresponding to the Friedman models do not have inflexion points. In the scale invariant cosmology, there are epochs dominated by gravitational braking and other epochs by acceleration. According to (25), $q = 0$ occurs at time t when $\Omega_{\rm m} = \Omega_\lambda$. The gravitational term dominates in the early epochs and the λ-acceleration dominates in more advanced stages. The higher the $\Omega_{\rm m}$-value, the later the inflexion point occurs. The expansion functions associated to the empty models have no inflexion points, since they are accelerating continually. For a flat model with $k = 0$, we have an inflexion point for

$$1 - \Omega_\lambda = \Omega_\lambda\,, \quad \text{and thus} \quad \Omega_\lambda = \Omega_{\rm m} = \frac{1}{2}\,. \tag{30}$$

These results differ from those of the ΛCDM models. According to (27), we have $q = 0$ for a flat ΛCDM model when $\frac{1}{2}\,\Omega_{\rm m} = \Omega_\Lambda$. The acceleration term needs only to reach the half of the gravitational one in the ΛCDM model, while in the scale invariant case the inflexion point is met for the equality of the two terms.

4. Conservation laws and scale invariance

A new invariance necessarily influences the conservation laws. In addition, we have accounted for the scale invariance of the vacuum at macroscopic scales by using (13) and (14). We first rewrite (18) as follows and take its derivative,

$$8\,\pi G\varrho R^3 = 3\,kR + 3\,\dot R^2 R + 6\,\frac{\dot\lambda}{\lambda}\dot R R^2\,, \tag{31}$$

$$\begin{aligned}\frac{d}{dt}(8\,\pi G\varrho R^3) &= 3\,k\dot R + 3\,\dot R^3 + 6\,\dot R\ddot R R + 6\,\ddot R R^2\frac{\dot\lambda}{\lambda} + 6\,\dot R R^2\frac{\ddot\lambda}{\lambda} + 12\,\dot R^2 R\frac{\dot\lambda}{\lambda} - 6\,\dot R R^2\frac{\dot\lambda^2}{\lambda^2}\\ &= -3\dot R R^2\left[-\frac{k}{R^2} - \frac{\dot R^2}{R^2} - 2\frac{\ddot R}{R} - 2\frac{\ddot R}{\dot R}\frac{\dot\lambda}{\lambda} - 2\frac{\ddot\lambda}{\lambda} - 4\frac{\dot R\dot\lambda}{R\lambda} + 2\frac{\dot\lambda^2}{\lambda^2}\right]\,.\end{aligned} \tag{32}$$

equations (18), (19) and (14) lead to many simplifications,

$$\frac{d}{dt}(8\,\pi G\varrho R^3) = -3\,\dot R R^2\left[8\,\pi G p + \frac{R}{\dot R}\frac{\dot\lambda}{\lambda}\left(8\,\pi G p + \frac{8\,\pi G\varrho}{3}\right)\right]\,, \tag{33}$$

$$3\,\lambda\varrho dR + \lambda R d\varrho + R\varrho d\lambda + 3\,p\lambda dR + 3pR d\lambda = 0\,, \tag{34}$$

and

$$3\,\frac{dR}{R} + \frac{d\varrho}{\varrho} + \frac{d\lambda}{\lambda} + 3\,\frac{p}{\varrho}\,\frac{dR}{R} + 3\,\frac{p}{\varrho}\,\frac{d\lambda}{\lambda} = 0\,. \tag{35}$$

This can also be written in a form rather similar to the usual conservation law,

$$\frac{d(\varrho R^3)}{dR} + 3\,pR^2 + (\varrho + 3\,p)\frac{R^3}{\lambda}\frac{d\lambda}{dR} = 0\,. \tag{36}$$

These last two equations express the law of conservation of mass-energy in the scale invariant cosmology. For a constant λ, we evidently recognize the usual conservation law. We now write the equation of state in the general form, $P = w\,\varrho$, with $c^2 = 1$, where w is taken here as a constant. The equation of conservation (35) becomes $3\,\frac{dR}{R} + \frac{d\varrho}{\varrho} + \frac{d\lambda}{\lambda} + 3\,w\,\frac{dR}{R} + 3\,w\,\frac{d\lambda}{\lambda} = 0$, with the following simple integral,

$$\varrho\, R^{3(w+1)}\, \lambda^{(3w+1)} = \text{const.} \tag{37}$$

For $w = 0$, this is the case of ordinary matter of density $\varrho_{\rm m}$ without pressure,

$$\varrho_{\rm m}\, \lambda\, R^3 = \text{const.} \tag{38}$$

which means that the inertial and gravitational mass (respecting the Equivalence principle) within a covolume should both slowly increase over the ages. For an empty model, the change of λ is enormous from ∞ at $t = 0$ to 1 at t_0. In a flat model with $\Omega_{\rm m} = 0.30$, λ varies from 1.4938 to 1 (see Table 2). We do not expect any matter creation as in Dirac's Large Number Hypothesis [9] and thus the number of baryons should be a constant. However, since an additional fundamental invariance has been accounted for, some changes in the conservation laws are unavoidably resulting. A change of the inertial and gravitational mass is not a new fact, it is well known in Special Relativity, where the masses change as a function of their velocity. In the standard model of particle physics, the constant masses of elementary particles originate from the interaction of the Higgs field [20, 14] in the vacuum with originally massless particles. The assumption of scale invariance of the vacuum (at large scales) and of the gravitation field does not let the masses invariant and make them to slowly slip over the ages, however by a very limited amount in realistic models. We may check that the above expression (38) is fully consistent with the hypotheses made. According to (9), we have $\varrho'\lambda^2 = \varrho$, where we recall that the prime refers to the value in General Relativity. Thus expression (38) becomes, also accounting for the scale transformation $\lambda\, R = R'$, $\varrho_{\rm m}\, \lambda\, R^3 = \varrho'\, \lambda^3\, R^3 = \varrho'\, R'^3 = \text{const.}$ This is just the usual mass conservation law in General Relativity.

Let us go on with the conservation law for relativistic particles and in particular for radiation with density ϱ_γ. We have $w = 1/3$. From (37), we get

$$\varrho_\gamma\, \lambda^2\, R^4 = \text{const.} \tag{39}$$

A term λ^2 intervenes. As for the mass conservation, we may check its consistency with General Relativity. Expression (39) becomes $\varrho'_\gamma\, \lambda^4\, R^4 = \text{const.}$ and thus $\varrho'_\gamma\, R'^4 = \text{const.}$ in the Einstein framework. Another case is that of the vacuum with density $\varrho_{\rm v}$. It obeys to the equation of state $p = -\varrho$ with $c = 1$. Thus, we have $w = -1$ and from (37), $\varrho_{\rm v}\lambda^{-2} = \text{const.}$ indicating a decrease of the vacuum energy with time. With $\varrho'_{\rm v}\lambda^2 = \varrho_{\rm v}$, this gives $\varrho'_{\rm v} = \text{const.}$ in the Einstein framework, in agreement with the standard result.

5. Scale invariant cosmological models

We now construct scale invariant cosmological models and examine their dynamical properties. The solutions of the equations are searched for the case of ordinary matter with density $\varrho_{\rm m}$ and $w = 0$. We may write the first equation of (18),

$$\frac{8\,\pi G \varrho_{\rm m} R^3 \lambda}{3} = k\,R\lambda + \dot{R}^2 R\lambda + 2\,\dot{R}R^2\dot{\lambda}\,. \tag{40}$$

The first member is a constant. With $\lambda = t_0/t$ and the present time $t_0 = 1$, we have

$$\dot{R}^2 R\,t - 2\,\dot{R}\,R^2 + k\,R\,t - C\,t^2 = 0\,, \quad \text{with} \quad C = \frac{8\,\pi G \varrho_{\rm m}\,R^3\lambda}{3}\,. \tag{41}$$

At time $t_0 = 1$, we also assume $R_0 = 1$. The origin, the Big Bang if any one, occurs when $R(t) = 0$ at time $t_{\rm in}$, which is not necessarily 0. To integrate (41), we need numerical values of C, corresponding to different densities.

5.1. Cosmological models with a flat space ($k = 0$)

In view of the results of the space missions investigating the Cosmic Microwave Background (CMB) radiation with Boomerang, WMAP and the Planck Collaboration [32], this case is the most interesting one. Equation (41) becomes

$$\dot{R}^2 R\,t - 2\,\dot{R}\,R^2 - C\,t^2 = 0\,. \tag{42}$$

At t_0=1 and R_0=1, with the Hubble constant $H_0 = \dot{R}_0/R_0$, we have

$$H_0^2 - 2\,H_0 = C \quad \text{which gives} \quad H_0 = 1 \pm \sqrt{1 + C}\,, \tag{43}$$

where we take the sign +, since H_0 is always positive.

We now relate C to $\Omega_{\rm m}$ at time t_0. We have $\Omega_{\rm m} = 1 - \Omega_\lambda$ and thus from (24) $H_0 = \frac{2}{1-\Omega_{\rm m}}$. This gives H_0 (in unit of t_0) from $\Omega_{\rm m}$. We obtain C as a function of $\Omega_{\rm m}$ at t_0 with the help of (43),

$$C = \frac{4}{(1-\Omega_{\rm m})^2} - \frac{4}{(1-\Omega_{\rm m})} = \frac{4\,\Omega_{\rm m}}{(1-\Omega_{\rm m})^2}\,, \tag{44}$$

which allows us to integrate (42) for a chosen $\Omega_{\rm m}$.

The scale invariant cosmology with $k = 0$, like the ΛCDM, permits a variety of models with different $\Omega_{\rm m}$. This is an interesting property in view of the results of the CMB which support a flat Universe [32]. The parameter $\Omega_{\rm m}$ is less than 1, since $\Omega_\lambda > 0$ and (24) must be satisfied. Equation (44) shows that for $\Omega_{\rm m}$ ranging from $0 \to 1$, C covers the range from 0 to infinity.

$\Omega_{\rm m}$	C	$H_0(t_0)$	$t_{\rm in}$	q_0	τ	$\tau_{\rm Gyr}$	$H_0(\tau)$	t(q)	R(q)	Ω_λ	$H_{0\,\rm obs}$
0.001	0.0040	2.0020	0.0999	- 0.50	0.9001	37.6	1.802	0.126	0.010	0.999	127.7
0.010	0.0408	2.0202	0.2154	-0.49	0.7846	32.7	1.585	0.271	0.047	0.990	112.3
0.100	0.4938	2.2222	0.4641	- 0.40	0.5359	22.4	1.191	0.585	0.231	0.900	84.4
0.180	1.0708	2.4390	0.5645	- 0.32	0.4355	18.2	1.062	0.711	0.364	0.820	75.3
0.246	1.7308	2.6525	0.6265	- 0.25	0.3735	15.6	0.991	0.789	0.474	0.754	70.2
0.300	2.4490	2.8571	0.6694	-0.20	0.3306	13.8	0.945	0.843	0.568	0.700	67.0
0.400	4.4444	3.3333	0.7367	-0.10	0.2633	11.0	0.878	0.928	0.763	0.600	62.2
0.500	8.0000	4.0000	0.7936	0.00	0.2064	8.6	0.826	1.000	1.000	0.500	58.5
0.800	80	10	0.9282	0.30	0.0718	3.0	0.718	1.170	2.520	0.200	50.9
0.990	39600	200	0.9967	0.49	.00335	0.14	0.669	1.256	21.40	0.010	47.4

Table 1: Cosmological parameters of some models with $k = 0$ and different $\Omega_{\rm m} < 1$. The symbol $H_0(t_0)$ stands for the values of the Hubble constant at $t_0 = 1$, $t_{\rm in}$ is the time when $R(t) = 0$, $\tau = t_0 - t_{\rm in}$ is the age of the Universe in units of $t_0 = 1$, $\tau_{\rm Gyr}$ is the age in Gyr, $H_0(\tau)$ is the H-value in the unit of τ, $t(q)$ and $R(q)$ are the values of t and R at the inflexion point, "$H_{0\,\rm obs}$" is the value of H_0 in $\mathrm{km\,s^{-1}\,Mpc^{-1}}$.

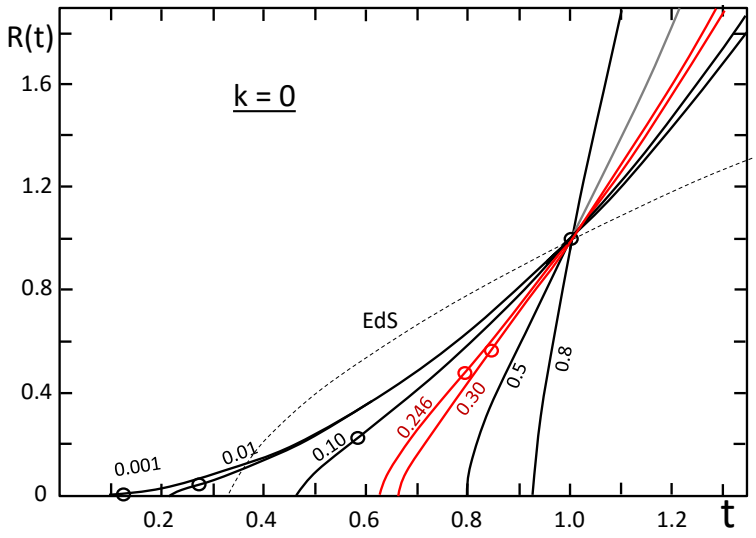

Figure 1: Some solutions of $R(t)$ for $k = 0$. The curves are labeled by the values of $\Omega_{\rm m}$ at t_0. The Einstein-de Sitter model (EdS) is indicated by a thin broken line. The small circles on the curves show the transition point between braking ($q > 0$) and acceleration ($q < 0$); for $\Omega_{\rm m} = 0.80$, this point is at $R = 2.52$. The two red curves indicate models corresponding to the observational values of $\Omega_{\rm m} = 0.246$ by Frieman et al. [18] and of $\Omega_{\rm m} = 0.30$, cf. the Planck Collaboration [32].

z	R/R_0	t/t_0	τ/t_0	age (yr)	$H(t_0)$	$H(z)$ $\mathrm{km\,s^{-1}\,Mpc^{-1}}$	λ
0.00	1	1	.3306	13.8 E+09	2.857	67.0	1.000
0.10	.9091	.9679	.2985	12.5 E+09	3.088	72.4	1.033
0.20	.8333	.9407	.2713	11.3 E+09	3.324	77.9	1.063
0.40	.7143	.8974	.2280	9.5 E+09	3.810	89.4	1.114
0.60	.6250	.8644	.1950	8.1 E+09	4.321	101.3	1.157
1.00	.5000	.8181	.1487	6.2 E+09	5.408	126.8	1.222
1.50	.4000	.7814	.1120	4.7 E+09	6.895	161.7	1.280
2.00	.3333	.7575	.0881	3.7 E+09	8.522	199.9	1.320
3.00	.2500	.7290	.0596	2.5 E+09	12.16	285.1	1.372
4.00	.2000	.7131	.0437	1.8 E+09	16.24	381	1.402
9.00	.1000	.68550	.0161	6.7 E+08	42.46	996	1.4588
9999	.0001	.66943	5.0 E-07	2.1 E+04	1.27 E+06	3.0 E+07	1.4938

Table 2: Data as a function of the redshift z for the reference model with $k = 0$ and $\Omega_\mathrm{m} = 0.30$. Column 2 gives $R(t)$ vs. time t/t_0 (column 3). Column 4 contains the age $\tau = t - t_\mathrm{in}$. The age in year is in column 5 for a present value of 13.8 Gyr. Column 6 gives the Hubble parameter $H(t_0)$ in the scale $t_0 = 1$, while the Hubble parameter $H(z)$ in $\mathrm{km\,s^{-1}\,Mpc^{-1}}$ is in column 7 for the same assumptions as in Table 1. In column 8, the scale factor λ is given with $\lambda = 1$ at present.

To integrate (42) numerically, we choose a present value for Ω_m, which determines C according to (44) and we proceed to the integration backwards and forwards in time starting from $t_0 = 1$ and $R_0 = 1$. Table 1 provides some model data for different Ω_m. In practice to get H_0 in $\mathrm{km\,s^{-1}\,Mpc^{-1}}$, we proceed as follows. The inverse of the age of 13.8 Gyr is $2.296 \cdot 10^{-18}\,\mathrm{s^{-1}}$, which in the units currently used is equal to $70.86\,\mathrm{km\,s^{-1}\,Mpc^{-1}}$. This value of H_0 corresponds to $H_0(\tau) = 1.000$ in column 8 of Table 1. On the basis of this correspondence, we multiply all values of $H_0(\tau)$ of column 8 by $70.86\,\mathrm{km\,s^{-1}\,Mpc^{-1}}$ to get the values of H_0 in the last column. The Hubble constant $H_0 = 67\,\mathrm{km\,s^{-1}\,Mpc^{-1}}$ is predicted for $\Omega_\mathrm{m} = 0.30$ in agreement with the Planck Collaboration 2015, see [32]. This agreement indicates that the expansion rate is correctly predicted by the scale invariant models for the given age of the Universe.

In Table 2, we give some basic data for the reference model with $k = 0$ and $\Omega_\mathrm{m} = 0.30$ as a function of the redshift z. Fig. 1 shows the $R(t)$ curves for models with $k = 0$ and different Ω_m.

The models show that after an initial phase of braking, there is an accelerated expansion, which goes on all the way. No curve $R(t)$ starts with an horizontal tangent, except the case of zero density. All models with matter start explosively

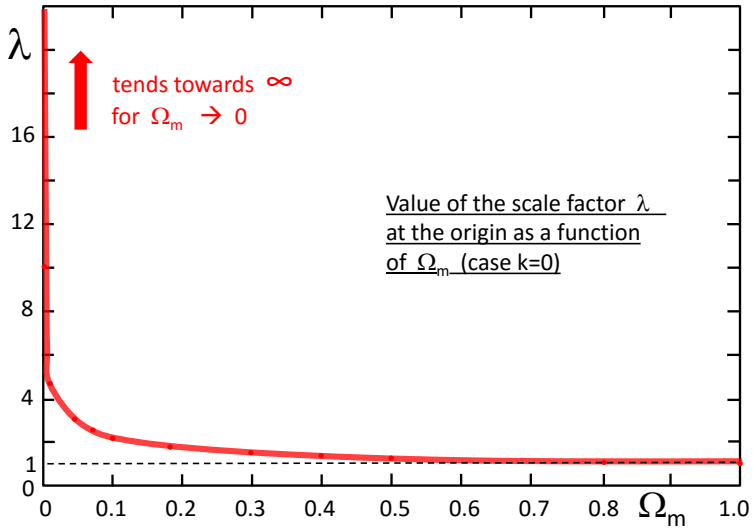

Figure 2: The scale factor λ at the origin $R(t) = 0$ for models with $k = 0$ and different $\Omega_{\rm m}$. At present time t_0, $\lambda = 1$ for all models. This curve shows that for increasing densities, the amplitudes of the variations of the scale factor λ are very much reduced.

with very high values of $H = \dot{R}/R$ and a positive value of q, indicating braking. The locations of the inflexion points, where q changes sign, are indicated for the models of different $\Omega_{\rm m}$ by a small open circle in Fig. 1. The expansion is faster for $\Omega_{\rm m} \to 1$. This suggests that for $\Omega_{\rm m} = 1$ the model inflates explosively all the way since the origin. Whether this has some implications at the origin is an open question. Models with $k = \pm 1$ have been studied in [24]. Their behaviors are not so different from that for $k = 0$, indicating curvature is not a dominant effect with respect to scale invariance.

The behavior of $\lambda(t)$ is interesting (see Fig. 2). For an empty space, the factor λ varies between ∞ at the origin to 1 at present. If matter is present, the λ-variations fall dramatically. For $\Omega_{\rm m} = 0.30$, λ varies only from 1.4938 to 1.0 between the origin and present. The presence of less than 1 H-atom per cubic meter is sufficient to dramatically reduce the variations of λ. For $\Omega_{\rm m} \to 1$, the scale factor λ tends towards 1. Thus, the domain of λ-values is consistently determined by the matter content or in other words by the departures from the scale invariant empty space.

6. Comparisons of scale invariant models and observations

Comparisons with observations are essential to invalidate or validate theories. The studies of the CMB support more and more the flatness $k = 0$ of the Universe: the last Planck results [32] give $\Omega_{\rm k} = 0.00 \pm 0.005$ at a 95 % confidence limit. Frieman et al. [18] found average values of $\Omega_{\rm m} = 0.246 \pm 0.028$ and $\Omega_\Lambda = 0.757 \pm 0.021$,

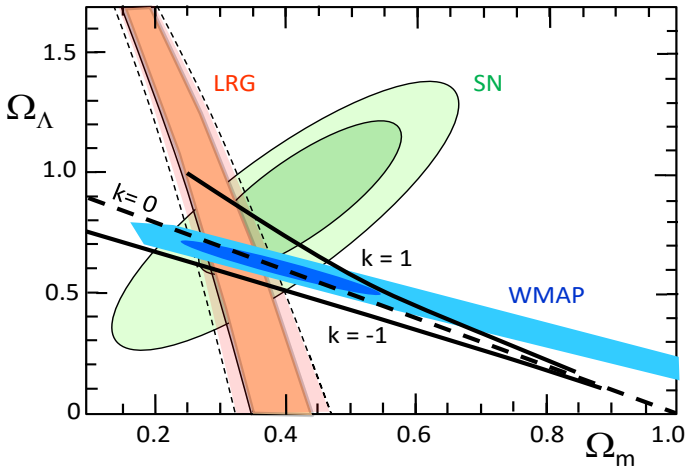

Figure 3: The constraints from the data collected by Reid et al. [34], from WMAP5, from the Union SN sample and the halo density field of luminous red galaxies of the SDSS DR7. The results of the scale invariant models are shown by black lines for the different k-values.

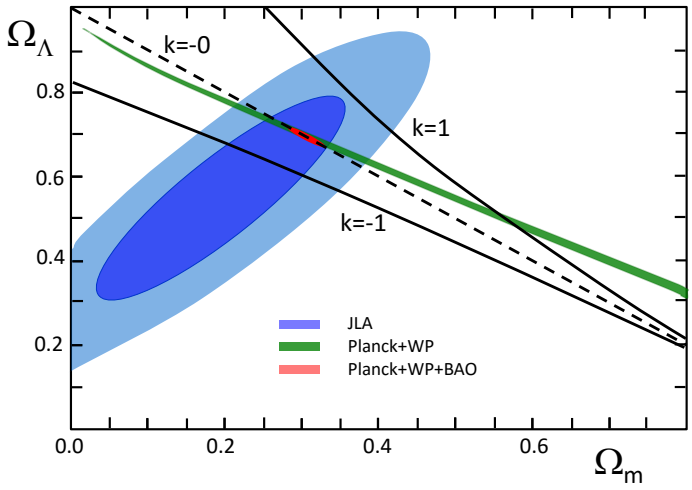

Figure 4: The Ω_Λ vs. Ω_m from data by Betoule et al. [4], cf. their Fig. 15. The SN sample from JLA is in blue, the Planck temperature and WMAP polarization measurements in green. The most stringent constraint (red) accounts for the BAO results. Scale invariant models are shown.

based on the magnitude-redshift data for supernovae, the CMB radiation measured by WMAP, the age constraints and the baryon acoustic oscillations (BAO). Reid et al. [34] examine the constraints from the clustering of luminous red galaxies in the SDSS DR7. They find $\Omega_m = 0.289 \pm 0.019$. The gas mass fraction in clusters of galax-

ies provides another interesting constraint on the density parameters. Allen et al. [1] found $\Omega_{\rm m} = 0.275 \pm 0.015$ and $\Omega_\Lambda = 0.725 \pm 0.016$. A study by Betoule et al. [4] with the project Joint Light-curve Analysis (JLA) together with CMB data from Planck and WMAP, including also the constraints from BAO, gives stringent conditions as illustrated by Fig. 4 and favors a value $\Omega_{\rm m} = 0.295 \pm 0.034$. Figs. 3 and 4 show the comparison of the observed density parameters $\Omega_{\rm m}$ and Ω_Λ with the results of our models. The flat model with $k = 0$ and $\Omega_{\rm m} = 0.30$ well fits the various constraints. The two sets of models with non-zero curvature do not agree with observations.

6.1. The value of H_0

The models provide the Hubble constant $H_0(\tau)$ as a function of the age τ of the Universe. To get H_0 in $\mathrm{km\,s^{-1}\,Mpc^{-1}}$ from the models, we need both $H_0(\tau)$ and the age, taken to be 13.8 Gyr (Sect. 5.1). Among recent determinations, a value $H_0 = 72 \pm 5$ in $\mathrm{km\,s^{-1}\,Mpc^{-1}}$ is given by Frieman et al. [18], 73 ± 4 by Freedman and Madore [17], 69.4 ± 1.6 by Reid et al. [34], 70.2 ± 1.4 by Allen et al. [1], 67.8 ± 0.9 by the Planck collaboration [32].

For values between $\Omega_{\rm m} = 0.246$ and 0.308 according to [18] and [32], we get H_0 between 70.2 and 66.5 $\mathrm{km\,s^{-1}\,Mpc^{-1}}$, a range consistent with the observed one. For an age of 13.7 Gyr, these values would have been 67.0 and 70.7 and for an age of 13.9 Gyr, 66.0 and 69.7 respectively, which would not change the conclusions. This shows that the models correctly predict the observed expansion rate.

7. Observational dynamical tests for past epochs

7.1. The expansion history

The determination of the expansion rate $H(z)$ vs. redshift z represents a direct test on the expansion $R(t)$ over the ages. For performing valid tests, the observational data must be independent on the cosmological models. The method of the "cosmic chronometer" is based on the simple relation, $H(z) = -\frac{1}{1+z}\frac{dz}{dt}$, obtained from $R_0/R = 1 + z$ and the definition of $H = \dot{R}/R$. The ratio dz/dt is estimated from of a sample of passive galaxies (with ideally no active star formation) of different z and ages by Melia and McClintock [29] and Moresco [30]. The method, however, depends on the models of spectral evolution of galaxies.

The model data are given in column 7 of Table 2. The observations are indicated in the caption of Fig. 5. We have reported the ΛCDM model and a model $R_h = c\,t$ by Melia and McClintock [29]. According to them, this last model is better supported, a claim challenged by Moresco [31]. Without entering this debate, we note the model differences at high z. Delubac et al. [8] find a 2.5 σ difference of the BAO at $z = 2.34$ with the predictions of a flat ΛCDM model. The predictions of the scale invariant model are intermediate between the ΛCDM and $R_h = c\,t$ models. They well match the observations of the expansion history $H(z)$ vs. z from cosmic chronometers.

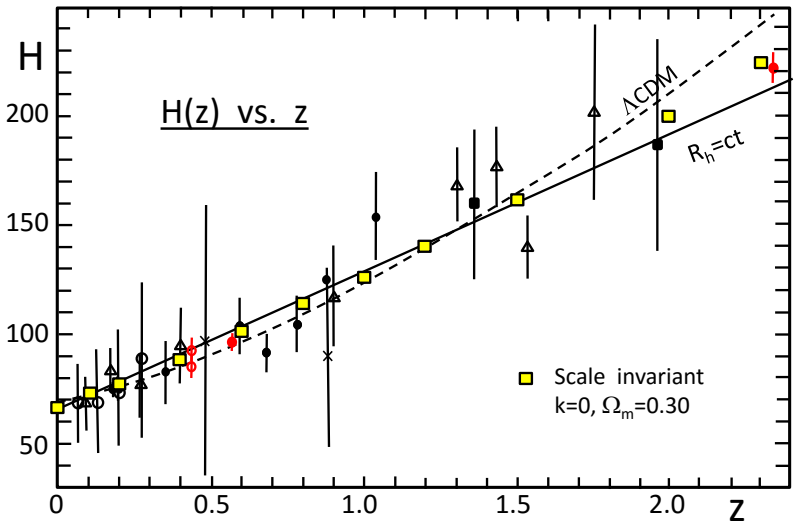

Figure 5: The $H(z)$ vs. redshift plot, with H in $\mathrm{km\,s^{-1}\,Mpc^{-1}}$. The observations are the model-independent data collected by Melia et al. [29]. The filled red point at $z = 2.34$ is from Delubac et al. [8], that at $z = 0.57$ is from Anderson et al. [2], the two open and connected red points at $z = 0.43$ are from Moresco et al. [31], interpreted with two different sets of models of spectral evolution. The curves for the ΛCDM and $R_h = c\,t$ models are by Melia et al. [29]. The yellow squares indicate the predictions of the scale invariant model for $k = 0$ and $\Omega_\mathrm{m} = 0.30$.

7.2. The values of q_0 in the ΛCDM and scale invariant models

Parameter q_0 depends on the change of the expansion rate H over recent times. The ΛCDM and the scale invariant models predict different values of q_0. For $k = 0$ and $\Omega_\mathrm{m} = 0.30$, these are respectively -0.55 and -0.20, both corresponding to an acceleration. We have $q = -\frac{\ddot{R}R}{\dot{R}^2} = -\frac{dH}{dt}\frac{R^2}{\dot{R}^2} - 1 = -\frac{dH}{dz}\frac{dz}{dt}\frac{1}{H^2} - 1$. In the limit $z \to 0$, we have $-dz/dt = H_0$, thus we get

$$\left(\frac{dH}{dz}\right)_0 = (q_0 + 1)H_0\,, \tag{45}$$

which relates q_0 and the derivative $(dH/dz)_0$ at the present time.

Fig. 6 shows the slopes $(dH/dz)_0$ for four different q_0-values. These slopes have to be considered in the zone near the origin $z = 0$. The differences between them are quite significant. For $q_0 = 1$ (strong braking), the expansion factor H was much larger in the past, thus the much steeper slope. Both the ΛCDM and scale invariant models for $\Omega_\mathrm{m} = 0.30$ are within the scatter of the observations. We may conclude that the scale invariant model shows no disagreement for this test.

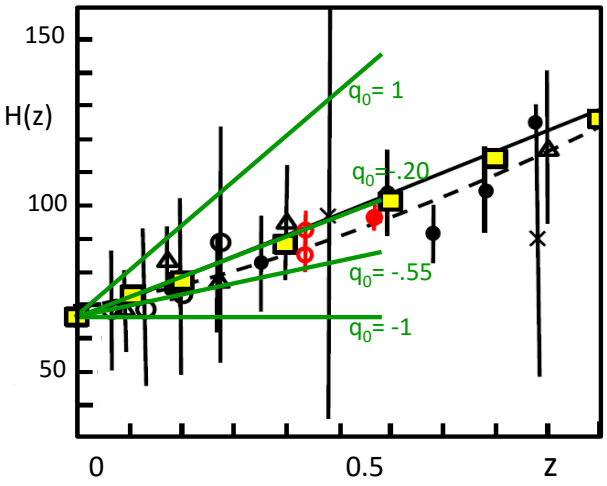

Figure 6: Lower left part of Fig. 5 with the lines indicating the slope $(dH/dz)_0$ for 4 different q_0-values. The value $q_0 = -0.55$ corresponds to the flat ΛCDM, while $q_0 = -0.20$ for the flat scale invariant model. For all models, a value $\Omega_{\rm m} = 0.30$ is assumed.

7.3. The transition from braking to acceleration

For the scale invariant model with $k = 0$, the transition ($q = 0$) from braking to acceleration occurs when $\Omega_\lambda = \Omega_{\rm m} = \frac{1}{2}$. For $\Omega_{\rm m} = 0.30$, it occurs at $R/R_0 = 0.568$ (cf. Table 1) corresponding to a transition redshift $z_{\rm trans} = 0.76$. In the flat ΛCDM model, the transition lies at $1 + z_{\rm trans} = \left(\frac{2\,\Omega_\Lambda}{\Omega_{\rm m}}\right)^{1/3}$ [36]. For the same $\Omega_{\rm m}$, this gives $z_{\rm trans} = 0.67$. Fig. 7 shows as a function of $\Omega_{\rm m}$ the values $z_{\rm trans}$ for both kinds of models. Several authors have tried to estimate the value of $z_{\rm trans}$. The estimates are often not model independent and this may introduce a bias in the comparisons. Shapiro and Turner [35] suggested $z_{\rm trans} \approx 0.3$ for $\Omega_{\rm m} = 0.30$, a value of the matter-density adopted in most studies. Melchiorri et al. [28] obtained $z_{\rm trans}$ between 0.76 ± 0.10 and 0.81 ± 0.12. The two values are connected by a thin broken line in Fig. 7. Ishida et al. [21] found 0.88 $(+.12, -.10)$. Blake et al. [5] gave ≈ 0.7 for $\Omega_{\rm m} = 0.27$. Sutherland and Rothnie [36] suggested ~ 0.7. Rani et al. [33] supported a value around 0.7. The best fit by Vitenti and Penna-Lima [37] gave ≈ 0.65. Moresco [31] found 0.4 ± 0.1 for a model of spectral evolution, while for another model they got 0.75 ± 0.15 (Fig. 7). Most of the estimates support a transition near $z_{\rm trans} = 0.75$, except two. The observations are in good agreement with the flat scale invariant models. However, the differences between the ΛCDM and the scale invariant model are small and not sufficient to discriminate between the two models.

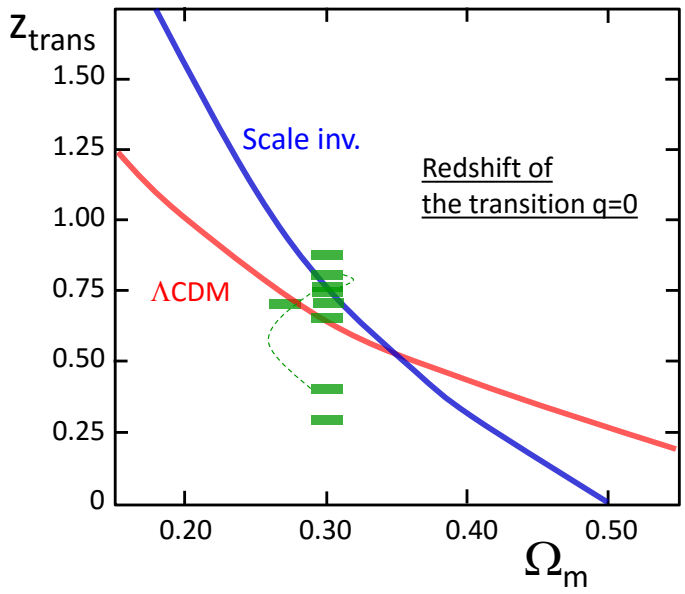

Figure 7: Redshift $z_{\rm trans}$ of the transition from the braking to acceleration vs. $\Omega_{\rm m}$ for the flat ΛCDM and scale invariant models. The "observational" values are shown by small green rectangles.

8. A brief look on the matter and thermal history

We may wonder how much different may be the past evolution of the matter and radiation densities $\rho_{\rm m}$ and ρ_γ, as well of the temperature T in the scale invariant model compared to standard models. This evolution is given by (37), which implies $T\,R\,\lambda^{\frac{1}{2}} = $ const. for the temperature. Fig. 8 shows the past evolution of these quantities versus redshift z with the scale $\log(1+z)$. For the present values, we take $\log \varrho_{\rm m} = -29.585$ ($\Omega_{\rm m} = 0.30$ and $H_0 = 67.8\,{\rm km\,s^{-1}\,Mpc^{-1}}$). The present $T_0 = 2.726$ by Fixsen [16] leads to $\log \varrho_\gamma = -33.768$. The λ-values are obtained from Table 2. On the upper side of Fig. 8, a few values of the cosmic time are given.

Amazingly, the differences in Fig. 8 are very small. As shown by Fig. 2, the variations of the λ are limited to values between 1.5 at the Big Bang and 1 at present for $k = 0$ and $\Omega_{\rm m} = 0.30$. On the whole, the evolution of matter and radiation densities is very similar, although not strictly identical, to the result of the standard case given by the classical conservation laws. Further results are discussed by [24].

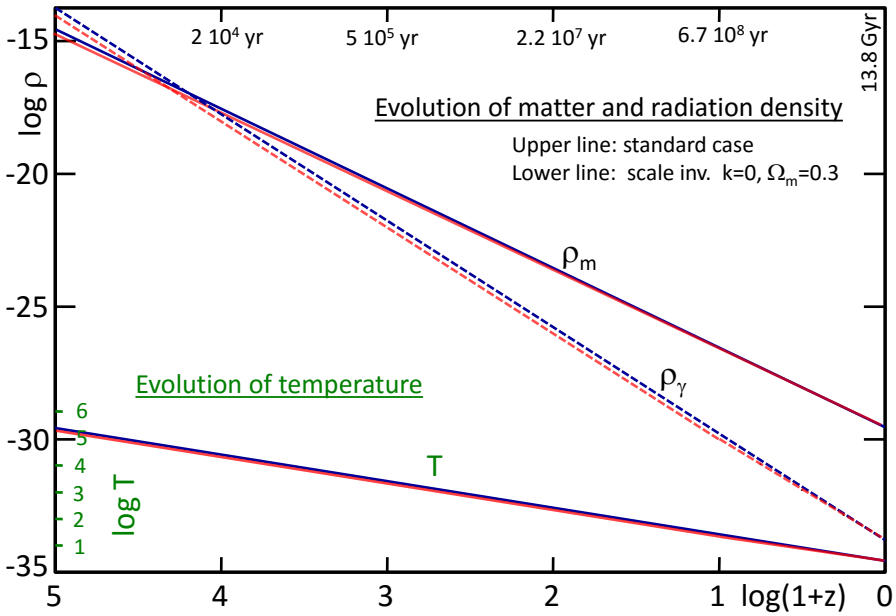

Figure 8: Evolution of $\rho_{\rm m}$, ρ_γ and T as function of redshift. The upper blue line corresponds to the classical case, the lower red line corresponds to the scale invariant solution. For T, the two lines are very close to each other. On the upper side of the frame, some ages $\tau = t(z) - t_{\rm in}$ given by the flat scale invariant model with $\Omega_{\rm m} = 0.30$ are indicated.

9. "Local" effects of the scale invariance of the field equations

Although very small, there are "local" effects resulting from scale invariance.

9.1. The equivalent to Newton's law

An analysis of the "local" effects of a scale invariance has been made long ago by Maeder [25] and Maeder and Bouvier [27]. We derived the scale invariant geodesics. The following equation was obtained (cf. their equation (38))

$$\frac{du^\varrho}{ds} + \Gamma^\varrho_{\mu\,\nu}\, u^\mu\, u^\nu - \kappa_\mu u^\mu u^\varrho + \kappa^\varrho = 0\,, \tag{46}$$

where $\Gamma^\varrho_{\mu\,\nu}$ is the ordinary Christoffel symbol. For a constant λ value, this gives the usual expression of the geodesics. The coefficient of metrical connexion κ_ν is related to the scale factor λ by (4). This equation has been applied to a weak stationary field, for a metric differing only slightly from Minkowski's,

$$g_{ii} \approx -1 \quad \text{for} \quad i = 1, 2, 3 \quad \text{and} \quad g_{00} = 1 + \frac{2\,\Phi}{c^2}\,, \tag{47}$$

where Φ is a potential created by a spherical mass M of radius r. The Christoffel symbol $\Gamma^{\varrho}_{\mu\,\nu}$ vanishes, except for

$$\Gamma^{i}_{\ 00} = \partial^i \Phi\,, \quad \text{with} \quad \partial^i = g^{i\alpha}\,\frac{\partial}{\partial x^\alpha} \tag{48}$$

and $c = 1$. For slow motions, $u^i \approx v^i = dx^i/dt$, $u^0 \approx 1$ and $ds \approx c\,dt$. We consider the equivalent to the Newtonian level of approximation. In addition, we have the coefficient of metrical connexion κ_μ. Accounting for (4) and (15), we get from the remaining components of the geodesic equation,

$$\frac{dv^i}{dt} + \partial^i\,\Phi + \frac{\dot\lambda}{\lambda}\,v^i = 0\,. \tag{49}$$

Here, we slightly differ from [25] and [27], because in the past we identified $(-\dot\lambda/\lambda)$ with the Hubble constant H. It is true that the order of magnitude is the same, since $-\dot\lambda/\lambda = 1/t$, but not the meaning. The Hubble parameter H expresses the overall expansion resulting from the initial conditions, the matter content and the scale invariance. We now keep $\kappa_0 = -\frac{\dot\lambda}{\lambda} = \frac{1}{t}$ in (49). In the Newtonian approximation of General Relativity, the potential is GM'/r'. From the scale invariance of the energy-momentum tensor (cf. (9)), we have $G\,M = \frac{r^3}{r'^3}\,G\,M'\,\lambda^2 = \frac{G\,M'}{\lambda}$. Since $r = \lambda\,r'$, the potential can be written, $\frac{G\,M'}{r'} = \frac{G\,M}{\lambda\,r'} = \frac{G\,M}{r}$. The geodesic (49) becomes,

$$\frac{d^2\vec r}{dt^2} \;=\; -\frac{G\,M}{r^2}\,\frac{\vec r}{r} + \kappa_0\,\frac{d\vec r}{dt}\,, \tag{50}$$

which is equivalent to Newton's law in the scale invariant framework [25, 27]. The additional term expresses an *outwards acceleration* opposed to gravitation. Its order of magnitude is in general very small. This equation is equivalent to (19) in a spherically symmetrical geometry for a medium with $p = 0$. We rewrite (19) as $\ddot r \;=\; -\frac{4\pi G}{3}\,\varrho\,r + \kappa_0\,\dot r$. The density ϱ associated to the mass M in a spherically symmetric system

$$\ddot r = -\frac{GM}{r^2} + \kappa_0\,\dot r\,. \tag{51}$$

Both derivations consistently predict an acceleration opposed to gravity.

9.2. Order of magnitude of the expansion term

Let us examine the order of magnitude of the additional expansion term. The ratio x of the absolute values of the two terms on the right-hand side of (50) is $x = \frac{\kappa_0\,v\,r^2}{G\,M}$. Numerically, we have $\kappa_0 = 1/(13.8\,\mathrm{Gyr}) = 70.86\,\mathrm{km\,s^{-1}\,Mpc^{-1}}$. We may write κ_0 in term of the Hubble constant H_0 for a given Ω_m, $\kappa_0 = f\,H_0$. According to Table 1, for $\Omega_\mathrm{m} = 0.30$, we have $H_0 = 67.0\,\mathrm{km\,s^{-1}\,Mpc^{-1}}$. Thus, $\kappa_0 = 1.058\,H_0$, (for H_0=71, $\kappa_0 = H_0$). We write x with the help of the critical density (23)

$$x = \left(\frac{f^2\,8\pi\varrho_\mathrm{c}v^2r^4}{3\,GM^2}\right)^{1/2} = \left(2\,f^2\,\frac{\varrho_\mathrm{c}}{\varrho}\left[\frac{v^2}{GM/r}\right]\right)^{1/2}\,, \tag{52}$$

where ϱ is the mean density of the spherical configuration of mass M and radius r. For equilibrium systems with non-relativistic velocities and a relatively small expansion term, the square bracket parenthesis is ~ 1 according to the Virial theorem. This means that

$$x \approx \left(2\, f^2\, \frac{\varrho_{\rm c}}{\varrho} \right)^{1/2} , \tag{53}$$

a conclusion obtained by [25]. For the motion of the Earth around the Sun, $x \approx 6 \cdot 10^{-12}$, while for the Earth-Moon system $x \approx 5 \cdot 10^{-13}$. The effects may be large at the level of clusters of galaxies, because there $\varrho/\varrho_{\rm c}$ tends towards 1.

9.3. Dynamical masses of clusters of galaxies

The estimate of the dynamical mass of a cluster from the standard Virial theorem (without expansion term) is known to lead to large overestimates [19]. The equivalent of the Virial theorem based on the modified Newton's equation (50) is [26],

$$\frac{1}{2}\, \overline{v^2_{\rm rad}} \left(1 - 2\, p' \frac{\kappa\, R}{\overline{\mid v_{\rm rad} \mid}} \right) \, = \, p\, \frac{G\, M}{R} \, , \tag{54}$$

where $v_{\rm rad}$ is the radial velocity of a galaxy in the cluster, $\kappa = 1/t$ for the cluster redshift z, R is the cluster radius and M the mass, $p = 1/3$ and $p' = 1/2$ for isotropic motions. The ratio of the masses M from (54) and the standard Virial theorem is

$$\frac{M}{M_{\rm stand}} = \left(1 - 2\, p' \frac{\kappa\, R}{\overline{\mid v_{\rm rad} \mid}} \right) \, . \tag{55}$$

An application of this expression to the Coma cluster leads to a ratio $M_{\rm stand}/M = 3.5$ to 10 depending on the source data. Thus, we get a M/L ratio (in scale invariant theory) of $\sim$30 (the standard value for elliptical galaxies), instead of 100 to 300 as derived from the standard Virial theorem [19]. The masses estimated from the X-ray luminosity show a smaller amount of "hidden matter", while the masses from lensing measurements are free from internal dynamical effects within the cluster [1]. The large excesses obtained with the dynamical masses may be a signature of the additional expansion term in the modified Newton's law [26].

9.4. The Earth-Moon and planetary distances

The two-body problem in the scale invariant context was studied by [25, 27], to which we refer for the details. The main conclusion was that the motion of a planet around the Sun follows trajectories similar to the Keplerian orbits, however *"with a very slight outwards superposed motion of expansion, which makes the orbits to progressively spiraling outwards"*. In the expressions given at that time, we must

replace H_0 by κ_0. The increases of the semi-major axis a and of the period P of the orbital motion are

$$\frac{\dot{a}}{a} = \frac{\dot{P}}{P} = \frac{1}{t}\,. \tag{56}$$

The increases of a and P are linear in time. For a small interval of time Δt, one has an increase $\Delta a = a\,\frac{\Delta t}{t}$. For the Earth-Sun distance, the predicted recession would be about 10.8 m per year. In this respect, it is interesting to point out that Křížek [22] supports from various arguments a recession equal to 5.3 m/yr, see also [23, 12]. Although, there is a factor of 2 between these figures, the similar trend and order of magnitude are interesting. At the time of the first bacteria on Earth, 3.5 Gyr ago, the Earth would have been about 25 % closer to the Sun than at present.

For the Earth-Moon distance, the predicted recession is 2.8 cm per year. This figure is consistent with the value of 2.2 ± 0.3 cm/yr that Dumin [10, 11] estimates from the study of the difference between the measure of the Earth-Moon distance by lunar ranging and the value estimated from the tidal deceleration of the Earth rotation. He attributes this recession to the "local" Hubble expansion produced by dark energy. Such comparisons are encouraging. They involve many complex interactions and thus need to be further studied.

10. Conclusions

Following the discovery of the accelerated expansion, the situation in cosmology is like if an interaction of an unknown nature opposes the gravitation. The hypotheses we have made about the scale invariance of the empty space at large scales together with the scale invariant cosmology seem to open a window on possible interesting cosmological models, well meeting the observational constraints. The various careful comparisons of models and observations made so far are positive and need to be pursued. In view of further tests, a point about methodology is to be strongly emphasized: to be valid, a test must be coherent and make no use of properties or inferences from the framework of other cosmological models.

A. Appendix: derivation of the basic equations

We derive here the scale invariant equations in a straightforward way. Instead of applying the Robertson-Walker metric to the scale invariant field equation, we directly apply the scale transformations to the differential equations of cosmologies obtained with the Robertson-Walker metric. These equations are

$$\frac{8\,\pi G \varrho'}{3} = \frac{k}{R'^2} + \frac{\dot{R}'^2}{R'^2} - \frac{\Lambda_{\rm E}}{3}\ , \tag{57}$$

$$-8\,\pi G p' = \frac{k}{R'^2} + 2\frac{\ddot{R}'}{R'} + \frac{\dot{R}'^2}{R'^2} - \Lambda_{\rm E}\,. \tag{58}$$

There, $\Lambda_{\rm E}$ is the Einstein cosmological constant, G is the gravitational constant, k is the curvature parameter which may take values 0 and ± 1, p' and ϱ' are the pressure and density in the system of General Relativity. Now, we make the transformations

$$R' = \lambda\, R \quad \text{and} \quad dt' = \lambda\, dt\,. \tag{59}$$

We get

$$\dot{R}' = \frac{dR'}{dt'} = \frac{\dot{\lambda}\, R + \lambda\, \dot{R}}{\lambda}\,, \tag{60}$$

where the dots indicate the time derivative in the considered system. Then, we have

$$\frac{\dot{R}'}{R'} = \frac{1}{\lambda}\left(\frac{\dot{\lambda}}{\lambda} + \frac{\dot{R}}{R}\right)\,. \tag{61}$$

The second derivative $\ddot{R}'$ becomes

$$\ddot{R}' = \frac{d(\frac{dR'}{dt'})}{dt} = \frac{1}{\lambda^2}(\ddot{\lambda} R + 2\dot{\lambda}\dot{R} + \lambda\ddot{R}) - \frac{(\dot{\lambda}\, R + \lambda\, \dot{R})}{\lambda^2}\frac{\dot{\lambda}}{\lambda}\,, \tag{62}$$

and

$$\frac{\ddot{R}'}{R'} = \frac{1}{\lambda^2}\left(\frac{\ddot{\lambda}}{\lambda} + \frac{\dot{\lambda}\,\dot{R}}{\lambda\, R} + \frac{\ddot{R}}{R} - \frac{\dot{\lambda}^2}{\lambda^2}\right)\,. \tag{63}$$

Thus, by replacing in (57) we obtain

$$\frac{8\,\pi G\varrho}{3} = \frac{k}{R^2} + \frac{\dot{R}^2}{R^2} + 2\,\frac{\dot{\lambda}\,\dot{R}}{\lambda\, R} + \frac{\dot{\lambda}^2}{\lambda^2} - \frac{\Lambda_{\rm E}\lambda^2}{3} \tag{64}$$

and from (58) after simplifications,

$$-8\,\pi G p = \frac{k}{R^2} + 2\frac{\ddot{R}}{R} + 2\frac{\ddot{\lambda}}{\lambda} + \frac{\dot{R}}{R}^2 + 4\frac{\dot{R}\,\dot{\lambda}}{R\,\lambda} - \frac{\dot{\lambda}^2}{\lambda^2} - \Lambda_{\rm E}\,\lambda^2\,. \tag{65}$$

These equations are expressed in the general system where scale invariance is a property. There, we have used the relations (9) imposed by the scale invariance of the energy-momentum tensor. Equations (64) and (65) correspond to the results by [7]. At this stage, these relations do not account for the relations (13) and (14) expressing the scale invariance of the empty space, which lead to essential simplifications.

References

[1] Allen, S. W., Evrard, A. E., Mantz, A. B.: ARAA **49** (2011), 409.

[2] Anderson, L., Aubourg, E., Bailey, S. et al.: MNRAS **441** (2014), 24.

[3] Bertotti, E. B., Balbinot, R. Bergia, S., Messina, S.: *Modern Cosmology in retrospect*, Univ. Press, Cambridge, 1990.

[4] Betoule, M, Kessler, R., Guy, J. et al.: A&A **568** (2014), A22.

[5] Blake, C., Brough, S., Colless, M. et al.: MNRAS **425** (2012), 405.

[6] Bouvier, P., Maeder, A.: Ap&SS **54** (1978), 497.

[7] Canuto, V., Adams, P. J., Hsieh, S.-H., Tsiang, E.: Phys. Rev. D **16** (1997), 1643.

[8] Delubac, T., Bautista, J. E., Busca, N. G.: A&A **574** (2015), A79.

[9] Dirac, P.: Proc. R. Soc. Lond. A **333** (1973), 403.

[10] Dumin, Yu. V.: Probl. of Practical Cosmology. In: Y. V. Baryshev, et al. (Eds.), *Proc. Internat. Conf. Russian Geogr. Soc.*, vol. 1, p. 256, 2008.

[11] Dumin, Yu. V.: The 11th Marcel Grossman Meeting on Recent Develop. in Theoretical and Exp. General Relativity. In: H. Kleinert, et al. (Eds.), p. 1752.

[12] Dumin, Yu. V.: Astron. Tsirkulyar **1623** (2015), 1, arXiv:1505.03572.

[13] Eddington, A. S.: *The mathematical theory of relativity.* Cambridge Univ. Press, 1923.

[14] Englert, F.: Ann. Phys. (Berlin) **526** (2014), 201.

[15] Feynman, R. P.: Feynman Lectures on Physics **1** (1963).

[16] Fixsen, D. J.: ApJ **707** (2009), 916.

[17] Freedman, W. L., Madore, B. F.: Ann. Rev. Astron. Astrophys. **48** (2010), 673.

[18] Frieman, J. A., Turner, M. S., Huterer, D.: ARAA **46** (2008), 385.

[19] Hartwick, F. D. A.: ApJ **219** (1978), 345.

[20] Higgs, P. W.: Ann. Phys. (Berlin) **526**, 211.

[21] Ishida, E. E. O., Reis, R. R. R., Toribio, A. V. et al.: J. Astropart. Phys. **28** (2008), 547.

[22] Křížek, M.: New Astronomy **17** (2012), 1.

[23] Křížek, M., Somer, L.: Grav. Cosmol. **21** (2015), 59.

[24] Maeder, A.: 2016abc, arXiv:1605.06314, 1605.06315, 1605.06316.

[25] Maeder, A.: A&A **65** (1978), 337.

[26] Maeder, A.: A&A **67** (1978), 81.

[27] Maeder, A., Bouvier, P.: A&A **73** (1979), 82.

[28] Melchiorri, A., Pagano, L., Pandolfi, S.: Phys. Rev. D **76** (2007), 041301.

[29] Melia, F., McClintock, T. M.: AJ **150** (2015), 119.

[30] Moresco, M., Cimatti, A., Jimenez, R. et al.: J. Cosmology Astropart. Phys. **8** (2015), 006.

[31] Moresco, M., Pozetti, L., Cimatti, A. et al.: ArXiv e-prints, 2016.

[32] Planck Collaboration 2015, arXiv 1502.01589.

[33] Rani, N., Jain, D., Mahajan, S. et al.: J. Cosmol. and Astropart. Phys. **12** (2015), 45.

[34] Reid, B. A. , Percival, W. J., Eisenstein, D. J. et al.: MNRAS **404** (2010), 60.

[35] Shapiro, C., Turner, M. S.: ApJ **649** (2006), 563.

[36] Sutherland, W., Rothnie, P.: MNRAS **446** (2015), 3863.

[37] Vitenti, S. D. P., Penna-Lima, M.: J. Cosmol. and Astropart. Phys. **9** (2015), 045.

Conference *Cosmology on Small Scales 2016*
Michal Křížek and Yurii Dumin (Eds.)
Institute of Mathematics CAS, Prague

ANTHROPIC PRINCIPLE AND THE LOCAL HUBBLE EXPANSION

Michal Křížek[1], Lawrence Somer[2]

[1]Institute of Mathematics, Czech Academy of Sciences
Žitná 25, CZ-115 67 Prague 1, Czech Republic
krizek@cesnet.cz
[2]Department of Mathematics, Catholic University of America
Washington, D.C. 20064, U.S.A.
somer@cua.edu

Abstract: We claim that a local expansion of the universe, whose rate is comparable with the Hubble constant H_0, had an essential influence on the development of intelligent life on the Earth. We present more than 10 examples showing that some antigravitational effects of the cosmological constant are observable locally in the Solar system.

It is known that the luminosity of the Sun increased approximately linearly within the last 4.5 Gyr starting at 70 % of its present value. We give several independent arguments showing that the average Earth-Sun distance increases about 5 m/yr due to antigravitational forces and such a large recession speed cannot be explained by solar wind, tidal forces, plasma outbursts from the Sun, or by the decrease of the Solar mass due to nuclear reactions. Models based on Newtonian mechanics can explain only a few cm per year. The speed $5\,\mathrm{m/yr/au} \approx 0.5\,H_0$ guarantees that the expansion of the Earth's orbit is just right for an almost constant influx of solar energy during the last 3.5 Gyr supporting the appearance of mankind and thus also the Anthropic Principle. The measured average increase in the Earth-Moon distance is 3.84 cm/yr, whereas Newtonian mechanics is able to explain only 2.1 cm/yr. We claim that this difference is also caused by a local expansion of order $0.66\,H_0$. Mars was much closer to the Sun as well, otherwise it could not have had rivers 3.5 Gyr ago, when the Sun's luminosity was only 75 % of its present value. The local Hubble expansion can again explain such a discrepancy and many other paradoxes in the Solar system as well as at cosmological distances.

Keywords: Antigravity, habitable zone, law of conservation of energy, DNA

PACS: 04.20.-q; 04.25.-g

1. Introduction

In 1973 the Australian mathematician and theoretical physicist Brandon Carter introduced the term *"Anthropic Principle"* [7]. This term was later developed and

extended in the 1986 book *The Anthropic Cosmological Principle* [2] by John Barrow and Frank Tipler. The so-called weak formulation of this principle states that all fundamental physical constants have just such values that they enabled the origin of life. Similarly, the strong formulation of this principle postulates that evolution necessarily leads to the origin of humans (= *Anthropos* in Greek).

However, no physical constant should be considered as a standard mathematical constant. For instance, the irrational numbers

$$\begin{aligned} \pi &= 3.1415926535\ldots \quad \text{(Ludolf number)},\\ \mathrm{e} &= 2.7182818284\ldots \quad \text{(Euler number)},\\ \sqrt{2} &= 1.4142135623\ldots \end{aligned}$$

have infinitely many digits. On the other hand, the third decimal digit of the Newton gravitational constant

$$G \approx 6.674 \cdot 10^{-11}\ \mathrm{m^3 kg^{-1} s^{-2}} \tag{1}$$

is probably close to four, but the other digits are not known. In the future it will be impossible to find e.g. one million digits of G, since physical constants have a completely different character from real numbers. Physical constants should be rather treated as "fuzzy numbers" or "interval arithmetic numbers" or the "density of some probabilistic distribution function".

Note that the Newtonian gravitational law represents only a certain idealization of reality, since G is well defined only purely theoretically between two mass points and no mass points exist in the real world. Therefore, the gravitational constant can never be measured and stated with absolute exactness. The product GM, where M is the mass of a star, is proportional to the pressure inside the star. Hence, the value G has an influence on the central temperature, luminosity of the star, its age, and many other parameters. If G were to be only one part per million smaller or larger than its current value, then all stars and also galaxies would evolve in a completely different way, and hence the Earth could not come into being as it is.

The same is true also for other physical constants like the speed of light, mass of the proton, charge of the electron, Planck's constant, the dimensionless constant of fine structure $\alpha \approx 137^{-1}$, etc. The expansion rate of our Universe is also an important parameter in the Anthropic principle. If this rate would be too large, galaxies and stars would not arise. It it would be too small, the Universe would collapse and life would not have enough time to appear. In this paper we will concentrate on the Hubble constant H_0 that described the expansion rate of the Universe and we show how its value contributed to the origin and evolution of life on our Earth.

When Albert Einstein established his theory of general relativity, he assumed that our Universe is stationary. He did not believe that it could expand. To avoid a gravitational collapse of the Universe, in 1917 he introduced a positive cosmological constant Λ into his system of ten nonlinear hyperbolic partial differential equations for gravitational potentials (see [13]). Its repulsive character enabled him

to consider a stationary Universe. However, when the expansion of the Universe was demonstrated by Vesto Mevlin Slipher, Gustav Strömberg, Georges E. Lemaître, and Edwin Powell Hubble (see [44], [47], [29], [19]), Einstein admitted around 1929 that the cosmological constant was the biggest blunder of his scientific career.

Nevertheless, in the seventies of the last century it was found by Beatrice Tinsley that $\Lambda > 0$ and that the expansion of the Universe is accelerating [49] (see also [17]). Later this fact was confirmed by examining supernovae of type Ia (see e.g. [37], [39], [40]) and a positive value of the cosmological constant was considered again.

2. The standard cosmological model

2.1. The Hubble parameter

Giordano Bruno in his treatise *De l'Infinito, Universo e Mondi* (1584) stated that our Universe is infinite, which is often considered as the origin of modern cosmology. However, in 1900 Karl Schwarzschild [43] predicted that the Universe has a finite volume and that it can be described by a large three-dimensional hypersphere

$$\mathbb{S}^3_r = \left\{(x, y, z, w) \in \mathbb{E}^4 \,|\, x^2 + y^2 + z^2 + w^2 = r^2\right\} \tag{2}$$

whose radius satisfies $r > 100\,000\,000$ au, where au is the astronomical unit and $\mathbb{E}^4$ is the four-dimensional Euclidean space.

According to Einstein's cosmological principle, the Universe on large scales is homogeneous and isotropic. Thus the above manifold (2) could be a good model of the Universe, since it has at all points and in all principal directions the same constant curvature $k_j = 1/r$ for $j = 1, 2, 3$, and thus also the Gauss-Kronecker curvature $k_1k_2k_3 = 1/r^3$ is constant. There are other two maximally symmetric manifolds: the three-dimensional Euclidean space $\mathbb{E}^3$ and the pseudosphere $\mathbb{H}^3_r$ (see [27] for details).

In this paper the Universe is modeled by a three-dimensional manifold that corresponds to some fixed time after the Big Bang (i.e. isochrone) in a four-dimensional spacetime. Another manifold with a different curvature is the observable universe, which can be seen only as a projection on the celestial sphere. Therefore, it is necessary to distinguish very carefully between *Universe, observable universe*, and *spacetime*, and also between model and physical reality (altogether $2 \times 3 = 6$ different entities).

The expansion of the Universe is modeled by an expanding manifold (2) with increasing radius $r = r(t)$. The expansion rate is given by the Hubble parameter $H = H(t)$ whose present measured value is

$$H_0 = H(t_0) \approx 70 \text{ km}\,\text{s}^{-1}\text{Mpc}^{-1} = \frac{70}{3.086 \cdot 10^{19}}\,\text{s}^{-1} = 2.27 \cdot 10^{-18}\,\text{s}^{-1}, \tag{3}$$

where $1\,\text{pc} = 3.086 \cdot 10^{13}\,\text{km}$ and

$$t_0 = 13.8 \text{ Gyr } = 4.355 \cdot 10^{17}\,\text{s} \tag{4}$$

is an approximate age of the Universe. In the standard cosmological model, the Hubble parameter is defined as follows:

$$H(t) = \frac{\dot{a}(t)}{a(t)}, \tag{5}$$

where a is the *expansion function* (sometimes called the *scaling parameter*) and the dot stands for the time derivative. If the Universe is modeled by (2), then the expansion function is equal to the radius, i.e., $a(t) \equiv r(t)$.

2.2. Cosmological parameters

In 1922, Alexander A. Friedmann in footnote 11 of his groundbreaking paper [14] proposed that the radius of the Universe is increasing from zero (the creation of the world) to its present value. A similar observation was made by Lemaître [29] five years later. Friedmann in [14], moreover, derived from the system of ten Einstein's equations for a perfectly symmetric space, which is for any fixed time homogeneous and isotropic (cf. (2)), the nonlinear differential equation for the expansion rate of the Universe

$$\frac{\dot{a}^2}{a^2} = \frac{8\pi G\rho}{3} + \frac{\Lambda c^2}{3} - \frac{kc^2}{a^2}, \tag{6}$$

where $a = a(t)$ is the unknown expansion function from (5), $\rho = \rho(t)$ is the mean mass density, Λ is the cosmological constant (see [32], [36]), c is the speed of light in vacuum, k/a^2 is the space curvature with $k \in \{-1, 0, 1\}$ corresponding to the pseudosphere $\mathbb{H}^3_r$, the Euclidean space $\mathbb{E}^3$, and the hypersphere $\mathbb{S}^3_r$, respectively.

Dividing the above differential equation (6) by $H^2 > 0$, we get from (5) for any time instant t the equation for three dimensionless parameters

$$1 = \Omega_{\mathrm{M}}(t) + \Omega_{\Lambda}(t) + \Omega_{\mathrm{K}}(t), \tag{7}$$

where Ω_{M} is the density of dark and baryonic matter, Ω_{Λ} is the density of dark energy, Ω_{K} is the density of spatial curvature, and

$$\Omega_{\mathrm{M}}(t) := \frac{8\pi G\rho(t)}{3H^2(t)}, \quad \Omega_{\Lambda}(t) := \frac{\Lambda c^2}{3H^2(t)}, \quad \Omega_{\mathrm{K}}(t) := -\frac{kc^2}{H^2(t)a^2(t)}. \tag{8}$$

Equation (7) thus determines the relation between the density of mass, density of energy and space curvature. According to the measurements reported in [39] and [40], we have $\Omega_{\mathrm{M}} \approx 0.3$ and $\Omega_{\Lambda} \approx 0.71$ at present which means that the Universe is nicely balanced between gravity and antigravitational forces due to dark energy, and could have a positive curvature $k = 1$ which follows from (7) and (8), see [42], i.e.,

$$\Omega_{\mathrm{K}}(t_0) = 1 - \Omega_{\mathrm{M}}(t_0) - \Omega_{\Lambda}(t_0) \approx -0.01, \tag{9}$$

where $a(t_0)$ is the present radius of the Universe. From this and (8) we find that the radius is unimaginably large,

$$a(t_0) \approx \frac{10c}{H_0} \approx 1.3 \cdot 10^{27} \text{ m} \approx 140 \text{ Gly}.$$

By (8) and (3) we find that (cf. coefficients in the Taylor expansion (40))

$$\Lambda \approx 0.71 \cdot 3H_0^2/c^2 = 1.22 \cdot 10^{-52}\,\mathrm{m}^{-2}. \tag{10}$$

For $k = 0$ we would get $\Omega_\mathrm{M} + \Omega_\Lambda = 1$. However, this equality cannot be proved by any measurements which always show some error. Finally note that for $k = -1$ the pseudosphere $\mathbb{H}^3_r$ can be isometrically imbedded into the Euclidean space $\mathbb{E}^{12}$, see [4], [27, p. 279], but it is not known whether the dimension 12 can be reduced.

3. Global and local expansion of the Universe

3.1. A possible source of the overall expansion

An extremely small deviation $\varepsilon > 0$ of the real position of some body (comet, planet, star, etc.) from Newtonian mechanics during one year may cause after one billion years a quite large and detectable value of $10^9\varepsilon$. All small deviations from Newtonian mechanics are usually not cancelled, but accumulated and then possibly observed. We show that a substantial portion of these accumulated deviations can be interpreted as dark energy.

Therefore, it seems that the conservation of energy law in reality does not hold, since we must introduce dark energy [1] in order to explain a number of surprising phenomena including the accelerated expansion of our Universe. In [25] we showed that gravitational aberration caused by the finite speed of gravitational interaction could produce the sought source for dark energy. The accelerated expansion of our Universe is then due to repulsive antigravitational forces of dark energy [15]. In this paper we survey some results on this topic from [23]–[27].

Dark energy is spread almost uniformly everywhere in the Universe. Thus it has an essential influence on the Hubble parameter $H = H(t)$ which characterizes the speed of the expansion for a given time t. In the classical monograph [32, p. 735] which appeared when dark energy was not known, it is assumed that the Hubble parameter behaves as follows

$$\tilde{H}(t) = \frac{2}{3t}, \tag{11}$$

in the matter-dominated era. We see that the function $\tilde{H} = \tilde{H}(t)$ is decreasing with time due to the Big Bang and subsequent gravitational interaction that slows down the expansion due to baryonic (and other mass particles) matter and (possible) dark matter. However, by astronomical observations (see [37], [38], [39]) we know that the expansion of the Universe has accelerated for the last 5 Gyr. It is said that the energy needed for the accelerated expansion is dark energy.

Substituting t_0 from (4) into (11), we get $\tilde{H}(t_0) = 1.53 \cdot 10^{-18}\,\mathrm{s}^{-1}$. From this and (3), we find that

$$H(t_0) - \tilde{H}(t_0) = 0.74 \cdot 10^{-18}\ \mathrm{s}^{-1}.$$

Note that this difference is very roughly of the same order as $\tilde{H}(t_0)$.

Remark 3.1. Several real-world examples below (see e.g. (17), (26), (32), (36)) indicate the local influence of $H(t_0)$ in the Solar system.

3.2. The Hubble constant rescaled to one astronomical unit

At present the *astronomical unit* is defined as follows

$$1\,\mathrm{au} = 149\,597\,870\,700\ \mathrm{m} \approx 150 \cdot 10^9\ \mathrm{m} \tag{12}$$

and it is almost equal to the semimajor axis of the Earth's elliptic orbit. Now we will recalibrate H_0 to 1 au. We claim that an equivalent value of the Hubble constant (3) is approximately

$$H_0 = 10\ \mathrm{m\,yr^{-1}au^{-1}}. \tag{13}$$

To see this we note that one sidereal year has about 31 558 150 s and 1 pc = 206 265 au. Then by (3) we find that

$$H_0 \approx 70\ \mathrm{km\,s^{-1}Mpc^{-1}} = 70\ \mathrm{m\,s^{-1}kpc^{-1}} = \frac{70 \cdot 31\,558\,150}{206\,265\,000}\ \mathrm{m\,yr^{-1}au^{-1}}.$$

Now from (12) and (13) we observe that $1\,\mathrm{m}^3$ of the space expands on average $0.2\,\mathrm{mm}^3$ per year, namely

$$\Big(1 + \frac{10}{150 \cdot 10^9}\Big)^3 \approx 1 + 3\frac{10}{150 \cdot 10^9} = 1 + 0.2 \cdot 10^{-9}. \tag{14}$$

The numbers stated above are so large that manifestations of dark energy should be detected within our own Solar system (see [26]). We will demonstrate this in Sections 4–6. In particular, the average recession speed of the Earth from the Sun is about five meters per year. This together with (13) gives the following local expansion rate

$$H_0^{(\mathrm{loc})} \approx 0.5 H_0. \tag{15}$$

Remark 3.2. Each cubic meter of the space $t = 4.5 \cdot 10^9$ years ago has increased on average at least twice its volume up to now. To see this, we take q in the interval $[0.16 \cdot 10^{-9}, 0.2 \cdot 10^{-9}]$ (cf. (14)). Then

$$(1+q)^t = \exp(t \log(1+q)) \approx\ \mathrm{e}^{qt} \in [2, 2.5].$$

Remark 3.3. Let us point out that the Solar system can be assumed to be sufficiently isolated from the influence of other stars. For instance, the gravitational force of the nearest star α-Centauri on Earth is one million times smaller than the gravitational force of Venus.

We give more than 10 examples showing that some repulsive antigravitational forces can be detected in the Solar system by means of a wide interdisciplinary approach. We present several geophysical, heliophysical, climatological, geochronometrical, paleontological, astrobiological, mathematical, computational, geometrical, and astronomical observational arguments to support this conjecture that enables us to explain a number of classical paradoxes such as the Faint Young Sun Paradox, the very large orbital momentum of our Moon, the formation of Neptune and the Kuiper

belt, an unexplained residual in the orbit of Neptune and migration of other planets, rivers on Mars, the Tidal Catastrophe Paradox of the Moon, the synchronous rotation of Iapetus, the Cosmological Constant Problem, the Accelerated Expansion of the Universe, Dark Energy Mystery, etc.

4. Slowly expanding habitable zone around the Sun and the Anthropic Principle

In this section we present three independent arguments showing that the average recession speed of the Earth from the Sun is roughly about 5 m/yr. The fourth argument is given in the end of Subsection 6.2. Dark energy is distributed almost uniformly in the Universe. There is no reason to assume that dark energy would somehow avoid the Solar system. Thus, it should also be present around the Sun. In Subsection 7.1 we show where the other authors have underestimated its existence in our neighborhood.

4.1. Stabilization of the habitable zone by dark energy

Life on Earth has existed continually for at least 3.5 Gyr and this requires relatively stable conditions during this very long time period. The constant solar flux thus would guarantee suitable conditions for life on the Earth. However, since the Sun is a star on the main sequence of the HR diagram, its luminosity increased approximately linearly within the last 4.5 Gyr (see Figure 1). The initial value of the luminosity was only 70 % of its present value. This leads to the paradox which is usually referred as the *Faint Young Sun*, see e.g. [16] and [28]. The mean temperature on the surface of Earth would have been much below the freezing point, in contrast with the absence of glaciation in the first 2.7 Gyr (see [3, p. 177]). It is believed that the greenhouse effect, higher level of radioactivity, impacts of comets, and more volcanism 3.5 Gyr ago are not able to explain this paradox.

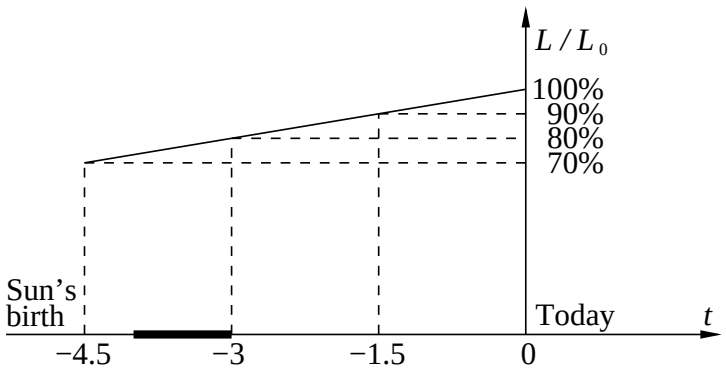

Figure 1: Relative luminosity L/L_0 of the Sun from the origin of the Solar system up to the present. The time t is given in Gyr.

Anyway, the Faint Young Sun paradox can be easily explained by dark energy, see [26]. Assume for a moment that the average recession speed of the Earth from the Sun during the last 3.5 Gyr was

$$\overline{v} = 5.2 \text{ m/yr} \tag{16}$$

which by (13) gives

$$\boxed{H_0^{(\text{loc})} \approx 0.52\, H_0} \tag{17}$$

for the expansion of the Earth-Sun system. We claim that in this case the Earth would receive an almost constant flux density of energy comparable with the solar constant[1]

$$L_0 = 1.36 \text{ kW m}^{-2} \tag{18}$$

over a very long period of the last 3.5 Gyr.

To see this we put $\tau = -3.5$ Gyr. Since the luminosity of the Sun increases approximately linearly with time and it was only about 77 % of its present value for $t = \tau$ (see Figure 1), we set

$$L(t) = \Big(1 - 0.23\frac{t}{\tau}\Big) L_0 \quad \text{for all } t \in [\tau, 0].$$

From now on, 0 will stand for the present time, i.e. $L(0) = L_0$ and we observe that $L(\tau) = 0.77\, L_0$. Since the luminosity decreases with the square of the distance, we get for

$$L_{\text{opt}}(t) = \frac{L(t)R^2}{(R + \overline{v}t)^2}, \quad t \in [\tau, 0], \tag{19}$$

where $R = 1$ au and $\overline{v}$ is given by (16), that

$$L_{\text{opt}}(t) \approx 1.36 \pm 0.005 \text{ kW m}^{-2} \quad \text{for all } t \in [\tau, 0]. \tag{20}$$

The very small interval on the right-hand side of formula (20) can be easily derived analytically by investigating the rational function $L_{\text{opt}}(t)$, see [27, p. 214].

This would, of course, guarantee very stable conditions for the development of intelligent life on Earth over a very long period of 3.5 Gyr. In particular, the amount of dark energy seems to be just right for an almost constant influx of solar energy and thus also for the appearance of mankind.

Dark energy thus presents further support for the (weak) Anthropic Principle, which states that basic physical constants are favorable for the emergence of life only if they are in very narrow intervals [26]. Moreover, the speed in (16) is optimal in the sense that any other slightly different speed would not yield an almost constant flux of the rational function in (19) on the time interval 3.5 Gyr. Thus it is probable

[1]The total solar power incident per unit perpendicularly to rays at the top of the Earth's atmosphere (corrected to 1 au given by (12)) is equal to the *solar constant*.

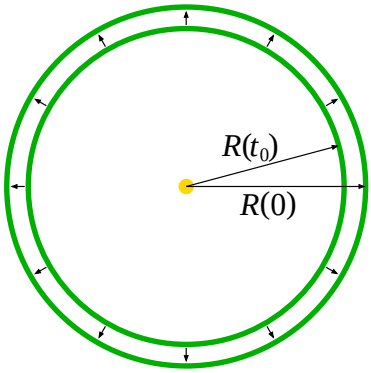

Figure 2: Schematic illustration of the expansion of the ecosphere during the last 3.5 billion years.

that the real average recession speed of the Earth from the Sun was close to the value 5.2 m/yr (see (15), (20), and Remarks 4.1–4.2 below).

The real average speed of the Earth from the Sun could be even slightly higher than (16), since the temperature of oceans 3.5 Gyr ago was about 80 °C, see [30]. It is known that a decrease of luminosity of only a few percent caused ice ages in the past. A decrease larger than 5 % would cause total glaciation of the whole planet. On the other hand, since DNA of multicellular organisms decays at temperature over 57 °C, there was not too high a temperature on the Earth during the last 500 Myr. This follows from paleontological finding over the whole surface of Earth.

A decrease or increase of the solar constant (18) up to 5 % corresponds to a ring — popularly called the *ecosphere (habitable zone)* — with radii $(0.95)^{1/2}$ au and $(1.05)^{1/2}$ au that represents a very narrow interval 145.8–153.3 million km (see Figure 2).

Remark 4.1. The recession speed (16) guarantees very stable conditions for several Gyr also in the future. For instance, during the next 3.5 Gyr from now on the luminosity of the Sun will be in the interval 1.32–1.36 kW m^{-2} if it behaves as in (19).

Remark 4.2. The linear function $L(t) = (1 - 0.23t/\tau)L_0$ (cf. Figure 1) is in some models replaced by the rational function (see e.g. [3, p. 177])

$$\hat{L}(t) = \frac{L_0}{1 + 0.3t/\tau_0}, \quad t \in [\tau, 0],$$

where $\tau_0 = -4.5$ Gyr. In this case the optimal average recession speed (guaranteeing an almost constant luminosity) is $\overline{v} = 4.36$ m/yr.

Remark 4.3. By [22], the present recession speed is only $v = 0.15$ m/yr if it is derived from classical mechanics without taking into account dark energy. However, for such a small speed v the luminosity of the Sun would very be far from being almost constant. All oceans would evaporate within less than 1 Gyr. We will return to this problem in Subsection 7.1.

4.2. Analysis of growth patterns on fossil corals from solar data

In this section we recall the method proposed by Weijia Zhang et al. [56]. The present value of the sidereal year is

$$Y = Y(0) = 365.25636 \cdot 24 \cdot 3600 \text{ s} = 31\,558\,149.54 \text{ s}. \tag{21}$$

However, the length of the sidereal year in seconds in ancient time was

$$Y(t) = n(t)(24 \cdot 3600 - f(t)t), \quad t \le 0, \tag{22}$$

where $(-t)$ is the geological age in years, $t = 0$ corresponds to the present time, $f = f(t) > 0$ characterizes the slowdown of the Earth's rotation, more precisely, $f(t)$ is the average increase of the length of the day per year during the last $(-t)$ years. Finally, $n(t)$ is the number of ancient days per year which is known from paleontological data by means of calculating the number of layers deposited during one year in fossil corals. Namely, each coral increases during one day by a few microns, more in summer and less in winter. Examining data for several consecutive years (e.g. layers that arose during twelve years are investigated in [35]), allows us to minimize the error in determining the number of days in a year. Hundreds of patterns were examined by microscope e.g. in [56, pp. 4013–4014].

One should have at least four consecutive years of data (e.g. twelve years as in [35]) to reduce the error in the calculations. In particular, for the Devonian era Zhang et al. [56], [57] found that $n(\tau) \approx 405$ days for $\tau = -370 \cdot 10^6$ years ago. A similar value of about 400 days can be found in the classic paper by Wells [54] from the seventies. Due to larger tidal forces when the Moon was closer to the Earth and the Earth was closer to the Sun, the function f is decreasing. Note that tidal forces decrease cubically with distance, see [3, p. 96]. According to [56, p. 4014], $f(\tau) = 2.6 \cdot 10^{-5}$ s per year, whereas the current value is

$$f(0) = 1.7 \cdot 10^{-5} \text{ s/yr}. \tag{23}$$

It was measured with respect to some fixed quasars at cosmological distances.

Another method uses the Babylonian timings of solar eclipses (see Figure 3),

$$\Delta t \approx f(0)Y(1 + 2 + \cdots + N),$$

where Δt is the measured value between the Ephemeris Time ET and the Universal Time UT, N is the corresponding number of years, and $Y \approx 365.25$ days is the sidereal year, i.e., $f(0) \approx 2\Delta t/(YN(N+1)) \approx 1.5 \cdot 10^{-5}$ s/yr which is close to the value given in (23). The Earth's rotational history (paleorotation) is examined e.g. in [35], [55]. Substituting the above data into (22), we get

$$Y(\tau) = 405(24 \cdot 3600 - 2.6 \cdot 10^{-5} \cdot 370 \cdot 10^6) \text{ s} = 405 \cdot 76780 \text{ s} = 31\,095\,900 \text{ s},$$

i.e., the day in the Devonian era had about 76 780 seconds (≈ 21.327 hours), cf. (21).

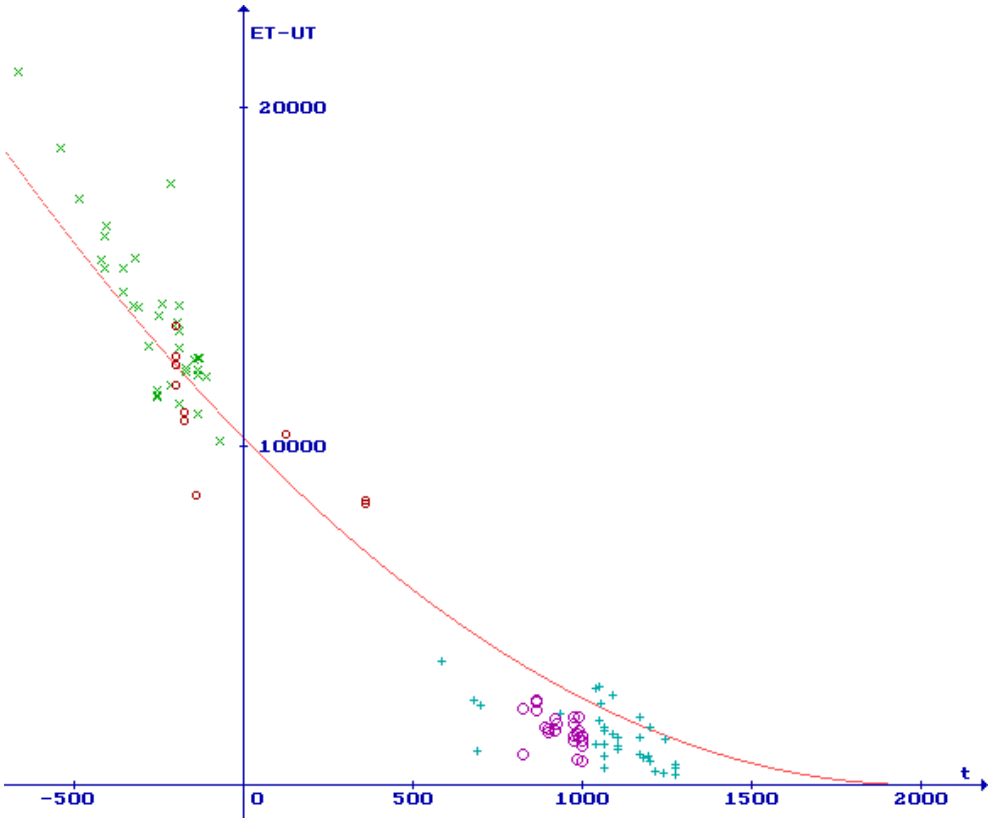

Figure 3: Secular slow-down of Earth's rotation according to [46, pp. 518–523]. The vertical axis indicates the behavior of the difference $\Delta t = \mathrm{ET} - \mathrm{UT}$ between the Ephemeris Time ET and the Universal Time UT in seconds. The horizontal axis shows the corresponding year. Babylonian timings of solar eclipses are marked by $\times$, Greek by $\circ$, Arab by o, and Chinese by $+$.

Denote by $R(t)$ the Earth's semimajor axis at time t. For a very short time period Kepler's third law

$$\frac{R^3(t)}{Y^2(t)} = \frac{GM_\odot}{4\pi^2} \tag{24}$$

describes reality quite well. Here

$$M_\odot = 1.989 \cdot 10^{30}\,\mathrm{kg} \tag{25}$$

is the Sun's mass which can be assumed to be constant as we shall derive in Subsection 5.4. Note that Kepler's laws are not reliable over long time periods, since planets migrate. Thus, applying (22)–(25) for $t = \tau$, we get

$$R(\tau) = \Big(\frac{Y^2(\tau)GM_\odot}{4\pi^2}\Big)^{1/3} = 148.1 \cdot 10^9\ \mathrm{m}.$$

This together with (12) yields the following average recession speed which has the same order of magnitude as that in (16) or Remark 4.2,

$$\overline{v} = \frac{R(\tau) - R(0)}{\tau} = \frac{(149.6 - 148.1) \cdot 10^9}{370 \cdot 10^6} = 4.01\,(\mathrm{m/yr})$$

which leads by (13) to the local Hubble expansion (cf. also [48, p. 72])

$$\boxed{H_0^{(\mathrm{loc})} = 0.4\, H_0.} \tag{26}$$

A drawback of this method is that $\overline{v}$ is sensitive to the particular choice of $n(\tau)$ and $f(\tau)$. Therefore, Zhang et al. [56, p. 4016] used hundreds of paleontological data from various epochs starting from the Cambrian era. They derived somewhat higher average recession speed

$$H_0^{(\mathrm{loc})} = 0.57 H_0,$$

which is again in good agreement with (16). From their Figure 4 of [56] we find that during the last 500 Myr the Earth-Sun distance increased about 3 million km. This implies an average recession speed of 6 m/yr leading to $H_0^{(\mathrm{loc})} = 0.6 H_0$.

Remark 4.4. By (16) the semimajor axis $R = 1$ au of Earth's orbit increases on average about $\Delta R = 5.2$ m per sidereal year. However, such a small change cannot be reliably detected, since the Newtonian barycenter of the Solar system travels hundreds of thousands km per year due to the influence of large planets [27, p. 192]. From Kepler's third law

$$\frac{(R + \Delta R)^3}{(Y + \Delta Y)^2} = \frac{R^3}{Y^2}$$

we can easily find that the increase of the orbital period of the Earth after one year would be only $\Delta Y = 1.6$ ms. In particular,

$$Y^2(R^3 + 3R^2 \Delta R + \cdots) = R^3(Y^2 + 2Y \Delta Y + \cdots).$$

Neglecting higher order terms, we get by (21) and (12) that

$$\Delta Y \approx \frac{3Y}{2R} \Delta R = 0.0016 \text{ s}. \tag{27}$$

Such a small time change also cannot be reliably detected, since one or two additional leap-seconds are usually added every year to compensate for the slowing of Earth's rotation. The increase of the orbital period by about $\Delta Y = 1.6$ ms would require one additional second after 34 years, since after two years we have to add $2\Delta Y$, after 3 years $3\Delta Y$, etc. From this we get

$$(1 + 2 + \cdots + 35)\Delta Y = (1 + 35)\frac{35}{2} \cdot 0.0016 \text{ s} \approx 1 \text{ s}.$$

This makes the evidence of a slightly increasing orbital period very difficult to obtain.

Remark 4.5. Secular variations in the ancient Earth-Sun distance were not uniform (see [57]). We believe that some nonuniformity may arise e.g. by passage of the Solar system through Galaxy arms that represent large potential holes.

4.3. Analysis of growth patterns on fossil corals from lunar data

Let $P = P(t)$ be the length of the sidereal month and $s = s(t)$ the number of sidereal months per year. At present it is $P(0) = 27.322$ days and $s(0) = 13.368$. The number $s(t)$ is known from paleontological data for many negative $t's$, since s equals one plus the number of lunar months. The number of lunar months can be manually calculated from many growth patterns on coral fossils (see [54, p. 4012]). Note that in the Cambrian era, the Moon was about 20 000 km closer to the Earth than it is now, so its angular area was more than 10 % larger than it is now and thus lunar patterns are better visible on fossil corals. In particular, $s(\tau) \approx 14.2$ for $\tau = -5 \cdot 10^8$ years according to [56, p. 4013].

Using the generalized Kepler's third law for the Earth-Moon system, we obtain the length of the year

$$Y(t) = s(t)P(t) = s(t)\Big((D + w(t)t)^3 \frac{4\pi^2}{G(M+m)}\Big)^{1/2}, \tag{28}$$

where

$$D = 384.402 \cdot 10^6 \,\mathrm{m} \tag{29}$$

is the present mean distance between the Earth and the Moon,

$$M = 5.9736 \cdot 10^{24} \,\mathrm{kg}, \quad m = 7.349 \cdot 10^{22} \,\mathrm{kg} \tag{30}$$

are their masses, and $w(t)$ is the recession speed of the Moon from the Earth. Due to larger tidal forces when the Moon was closer to the Earth, the function w is slowly decreasing from the past to the present time. By laser retroreflectors installed by the Apollo missions 11, 14, 15, and Lunokhod 2 on the Moon more than 40 years ago it has been found that the present mean distance D between the Earth and Moon increases at the present time by about

$$w(0) = 3.84 \text{ cm/yr}. \tag{31}$$

From this, (24), (28), (1), (30), and (29) we get for $t = \tau = -5 \cdot 10^8$ yr the following upper estimate

$$\begin{aligned} R(\tau) &= \Big(Y^2(\tau)\frac{GM_\odot}{4\pi^2}\Big)^{1/3} = s(\tau)^{2/3}\Big(\frac{M_\odot}{M+m}\Big)^{1/3}(384.402 \cdot 10^6 + w(\tau)\tau) \\ &< 14.2^{2/3} 328919^{1/3}(384.402 \cdot 10^6 + w(0)\tau) = 147.8 \cdot 10^9 \,(\mathrm{m}). \end{aligned}$$

This yields the following lower bound for the average recession speed of the Earth from the Sun

$$\overline{v} = \frac{R(\tau) - R(0)}{\tau} > \frac{(149.6 - 147.8) \cdot 10^9}{5 \cdot 10^8} = 3.6 \,(\mathrm{m/yr}),$$

i.e.

$$\boxed{H_0^{(\mathrm{loc})} > 0.36 H_0.} \tag{32}$$

By a thorough analysis of growth patterns on fossil corals from lunar data (which are independent of solar data) Zhang et al. [56, pp. 4013–4016] got further values of $s(t)$ for other time epochs t leading to the expansion rate $H_0^{(\mathrm{loc})} \approx 0.57 H_0$. Note that Pannella [35] derived that the synodic month was 36–39 days 1.75 Gyr ago.

5. Elimination of other possibilities for the large recession speed

5.1. Solar radiation

First we show that solar radiation is not able to explain a large speed similar to (16). The area of the cross section of our Earth is $S = \pi(6.378 \cdot 10^6)^2\,\mathrm{m}^2 = 1.277964 \cdot 10^{14}\,\mathrm{m}^2$. From this and (21), the total energy coming from the Sun during one year is

$$E = SYL_0 = 5.4 \cdot 10^{24}\ \mathrm{J}, \tag{33}$$

where L_0 is given by (18).

Now denote E_i, λ_i, ν_i, and p_i to be respectively the energy, wave length, frequency, and force impulse of the ith photon. Then we have

$$p_i = \frac{h}{\lambda_i} = \frac{h\nu_i}{c} = \frac{E_i}{c},$$

where h is Planck's constant and

$$c \doteq 3 \cdot 10^8\ \mathrm{m/s}$$

the speed of light in vacuum. Summing this equation over all photons coming to the Earth from the Sun during one year, we get by (33) that

$$p = \sum_i p_i = \frac{E}{c} = \frac{5.4 \cdot 10^{24}}{3 \cdot 10^8} = 1.8 \cdot 10^{16}\ (\mathrm{kg\,m/s}).$$

However, by (30) and (21) we find that

$$v = \frac{p}{M} = 9.5\ \mathrm{cm/yr},$$

which is a much smaller speed than that given in (16).

5.2. Tidal forces

The Earth's rotation slows down mainly due to tidal forces of the Moon (cca 68.5 %), but also of the Sun (cca 31.5 %), see [5]. Note that tidal forces (per 1 kg of the Earth) are equal to $2GM_\odot r/R^3$, where the mass $M_\odot$ of the Sun is given by (25), $R = 1\,\mathrm{au}$, and r is the Earth's radius. By the above arguments, the Earth-Sun distance increases by about only a few cm per year due to tidal forces (see [34] and [3, p. 606]).

5.3. Decrease of the Solar mass due to nuclear reactions

One atom of helium is 0.7 % lighter than 4 atoms of hydrogen. This means that at most 0.7 % of the Sun's mass changes into energy during 10 Gyr (the life period of the Sun). When the Sun was born, it already contained about 30 % helium. Hydrogen changes into helium only in central parts of the Sun and by the end of the time on the main sequence, the Sun will still contain a lot of hydrogen. Since only about 10 % of the hydrogen is converted to helium over the lifetime of the Sun, we may assume that only 0.07 % of the Sun's mass will change into energy. In this way the Sun loses $0.0007M_\odot/(10^{10}\cdot\pi 10^7) = 4.46\cdot 10^9$ kg per second due to (25) and (21). This is an essential part of the total mass losses collected in the next Subsection 5.4.

5.4. Plasma outbursts from the Sun

If the speed of a solar plasma outburst is larger than 613 (resp. 434) km/s, then plasma can escape the Solar system (resp. Sun) which reduces the Sun's mass as well. For smaller speeds plasma falls back down to the Sun.

By Noerdlinger [33] the Sun loses every second altogether $5.75\cdot 10^9$ kg of its mass due to solar wind, electromagnetic radiation, neutrino losses, and large eruptions. Taking into account that mass losses during one year (see (21)) are $1.815\cdot 10^{17}$ kg/yr, we find by (25) that

$$\frac{\dot M_\odot(t)}{M_\odot(t)} = C \quad \text{with } C = -9.13\cdot 10^{-14}\ \text{yr}^{-1},$$

where $M_\odot(0) = M_\odot$ is given by (25). Since the orbits of the planets expand at the same rate [33], we find by (12) that the average recession speed of the Earth from the Sun due to the radiative and particle loss of Sun's mass is approximately $9.13\cdot 10^{-14}\,\text{yr}^{-1}\cdot 149.6\cdot 10^{11}\,\text{cm} \doteq 1.4\,\text{cm/yr}$.

Since $M_\odot(t) = M_\odot \text{e}^{Ct}$, changes of the Sun's mass are negligible. For instance, if $t = -370\cdot 10^6$ yr (which corresponds to the Devonian era), we find that $M_\odot(t) = 1.989067\cdot 10^{30}$ kg (cf. (25)).

5.5. How much dark energy is generated by the Earth-Sun system per year?

Contributions to the recession speed of the Earth from the Sun as given in Subsections 5.1–5.4 are so small that they are not able to explain a large speed close to (16) by classical physics. So let us estimate the amount of dark energy that our Earth-Sun system continuously generates.

For simplicity first assume that the Earth has a circular orbit with radius $R = 149.6\cdot 10^9$ m around the Sun (cf. (12)). According to Kepler's third law $R^3/Y^2 = GM_\odot/4\pi^2$, where Y is the period of one year (see (21)), the total mechanical energy (kinetic + potential) can be expressed as

$$E(R) = \frac{M}{2}\Big(\frac{2\pi R}{Y}\Big)^2 - \frac{GMM_\odot}{R} = -\frac{GMM_\odot}{2R}. \tag{34}$$

Second assume that the Earth's trajectory is a spiral so that (16) holds. Then from (34), (1), (30), (25), and (12) the annual increase of total energy is

$$E(R+\Delta R)-E(R)=\frac{1}{2}GMM_{\odot}\Big(\frac{1}{R}-\frac{1}{R+\Delta R}\Big)=9.4\cdot 10^{22}\ \mathrm{J},$$

where $\Delta R = 5.2\,\mathrm{m}$ (cf. (16)). This large value corresponds by (21) to a continuous power of

$$\eta = 2975\,\mathrm{TW}$$

of dark energy that would shift the Earth 5.2 m per year further from the Sun. Such a natural perpetuum mobile produces, in fact, potential energy for free. Its amount is much larger than the total production of electricity on Earth. For another recession speed $\tilde{v}$ (different from (16)) the associated power is clearly equal to $2975\cdot\tilde{v}/\overline{v}\,\mathrm{TW}$.

6. Further testable hypotheses of the slow expansion of the Solar system

6.1. The Earth-Moon distance increases more than can be explained by tidal forces

The first observed discordance between the acceleration of the Moon's mean longitude utilizing Ephemeris Time and Atomic Time has been reported in van Flandern [50] in 1975. By laser measurements we know that the present mean distance

$$D = 384\,402\,\mathrm{km}$$

between the Earth and Moon increases by about 3.8 cm per year, see (31). Tidal forces can explain only 55 % of this value, i.e., 2.1 cm per year as we shall se below. This lunar orbital anomaly is usually referred to as the *Tidal Catastrophe Paradox* (see [51]). However, the remaining part

$$\delta = 0.45\cdot 3.8 = 1.7\ \mathrm{cm/yr} \tag{35}$$

could be due to dark energy that is determined by the local Hubble constant $H_0^{(\mathrm{loc})}$.

In [56, p. 4016] a very similar averaged value $\delta \approx 1.6\,\mathrm{cm/yr}$ during the last 500 Myr is independently obtained by measurements of growth patterns on fossil corals. This method uses geochronometrical techniques introduced in Wells [54].

The large value in (35) is derived from the following facts. Earth's rotation slows down mainly due to tidal forces of the Moon (cca 68.5 %), see Subsection 5.2. By a thorough analysis of the Ancient Babylonians' records of solar eclipses [41] we know that the length of a day increases by $1.7\cdot 10^{-5}\,\mathrm{s}$ per year during the last 2700 years (see (23)). By the conservation of the total momentum $\mathcal{M}$ of the Earth-Moon system, the value

$$\mathcal{M} = I_1\omega_1 + I_2\omega_2 + m_1R_1v_1 + m_2R_2v_2$$

has to be constant. Here I_1 and I_2 are the inertial moments of the Earth and Moon, $\omega_1 = 2\pi/Y$ and ω_2 are their angular frequencies, $m_1 = M$ and $m_2 = m$ (see (30)),

v_1 and v_2 are the speeds of the Earth and Moon, respectively, relative to their center of gravity, and the corresponding distances satisfy $D = R_1 + R_2$. Since the decrease of the Moon's angular momentum is negligible, we can derive from (23) that that $\mathrm{d}D/\mathrm{d}t = 0.674 \cdot 10^{-9}\,\mathrm{m/s}$ (for a detailed calculation see [25, pp. 1034–1037]). However, the observed value corresponding to the real recession speed of 3.8 cm/yr is much higher, namely $\mathrm{d}D/\mathrm{d}t = 1.2 \cdot 10^{-9}\,\mathrm{m/s}$. Putting these values together, we obtain by (31) that $1.7 \approx 3.8(1.2-0.674)/1.2\,\mathrm{cm/yr}$ which is the speed given in (35).

Recalibrating H_0 to the Earth-Moon distance D, we easily get by (13) and (12) that $H_0 = 2.57\,\mathrm{cm\,yr^{-1}}D^{-1}$ and thus for the expansion of the Earth-Moon system we get by (35)

$$\boxed{H_0^{(\mathrm{loc})} \approx \frac{1.7H_0}{2.57} = 0.66\,H_0} \tag{36}$$

which is in a good agreement with (15).

In 2003, Y. Dumin (see [10, p. 2463]) derived from astrometric measurements corrected to ancient eclipses the local expansion rate of

$$H_0^{(\mathrm{loc})} \approx 0.5\,H_0$$

for the Earth–Moon system. In his paper [11] from 2008 this value was increased to $H_0^{(\mathrm{loc})} \approx 0.85\,H_0$ for the data from the last three centuries (cf. (36)). His method is further developed in [12]. See also [48, p. 66].

6.2. Mars was much closer to the Sun when there were rivers

The present mean Mars-Sun distance is about $r = 225 \cdot 10^9\,\mathrm{m}$. Mars had liquid water on its surface 3–4 Gyr ago which was deduced from the number of craters in its dry riverbeds (see Figure 4). Neither wind nor lava can create such sinuous formations. At that time the Sun's luminosity was about 75 % of its current value. The bold interval on the time axis of Figure 1 indicates the period when Mars had liquid water on its surface. Since the solar power decreases with the square of the distance from the Sun, the corresponding luminosity would be by (12) only

$$L_{\mathrm{Mars}} = 0.75\,L_0\frac{150^2}{225^2} = \frac{L_0}{3},$$

which corresponds to a 67 %-decrease of the solar constant L_0 (see (18)). In this case the existence of rivers on Mars would be impossible. Note that a decrease of L_0 by only 2 % causes ice ages on the Earth, even though there is the greenhouse effect. An ancient atmosphere on Mars 3–4 Gyr ago had one-third to two-thirds of the surface atmospheric pressure as Earth has today (for details see [18]). Higher concentration of CO_2 (as suggested by [3, p. 177]) surely contributed to a higher surface temperature on Mars, but cannot fully explain liquid water there because

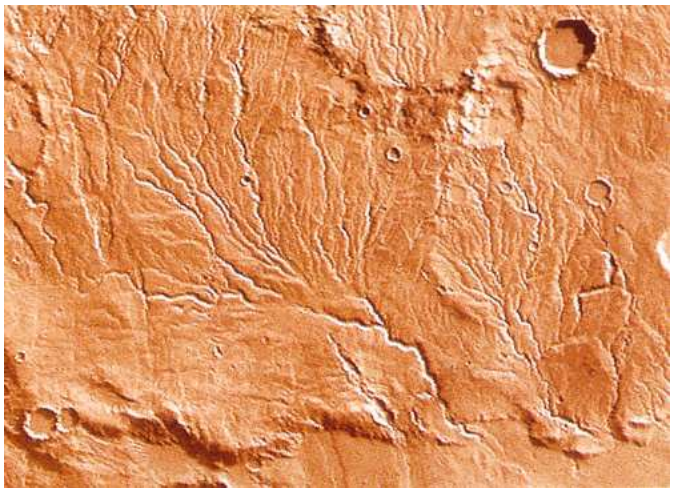

Figure 4: Dry riverbeds on Mars tending to the ancient sea at the bottom right. The center of the image (whose dimensions are $175 \times 125\,\mathrm{km}^2$) is at 42.3° south Martian latitude and 92.7° west longitude (photo NASA).

of the huge 67 %-decrease of the luminosity. Therefore, Mars must have been much closer to the Sun to account for liquid water.[2]

According to Google Mars Maps (see also Figure 4) there were many lakes and hundreds of large rivers whose dry riverbeds are now between −50° and 50° of Martian latitude. Due to measurements of the missions Viking I and II, Pathfinder, Spirit, etc., we know that the current annual average temperature (about −60°C neglecting the greenhouse effect) on Mars is very much below the freezing point of water.

By the Stefan-Boltzmann law, the equilibrium temperature T_{eq} at the distance r from the Sun satisfies $\sigma \mathrm{T}_{\mathrm{eq}}^4 = L_\odot/(4\pi r^2)$, where $L_\odot = 3.846 \cdot 10^{26}\,\mathrm{W}$ is the present value of the total Solar luminosity and $\sigma = 5.669 \cdot 10^{-8}\ \mathrm{Wm}^{-2}\mathrm{K}^{-4}$ is the Stefan-Boltzmann constant. Since Mars' surface area is four times larger than the area of its maximal cross-section, the current overall average surface temperature can be estimated by the Stefan-Boltzmann law as follows:

$$\mathrm{T}_{\mathrm{Mars}} = \frac{1}{2}\Big(\frac{(1-A)L_\odot}{\pi\sigma r^2}\Big)^{1/4} = 211\ \mathrm{K}, \tag{37}$$

where $A = 0.25$ is the present value of the Bond albedo. We see that $\mathrm{T}_{\mathrm{Mars}}$ is really very close to the yearly planetwide mean measured temperature ≈ -60°C. When the Sun's luminosity was 75 % of the present value (see Figure 1), we get from (37) only $\mathrm{T}_{\mathrm{Mars}} = 196\,\mathrm{K}$. For such a low temperature the greenhouse effect cannot explain the existence of rivers on Mars. Note that if the temperature of water is 273.16 K and

[2]Johannes Kepler inspired by Mars' elliptic trajectory formulated his famous three laws on planetary motion. We were also inspired by Mars to state that there exist antigravitational forces which very slowly push Mars away from the Sun along a spiral trajectory.

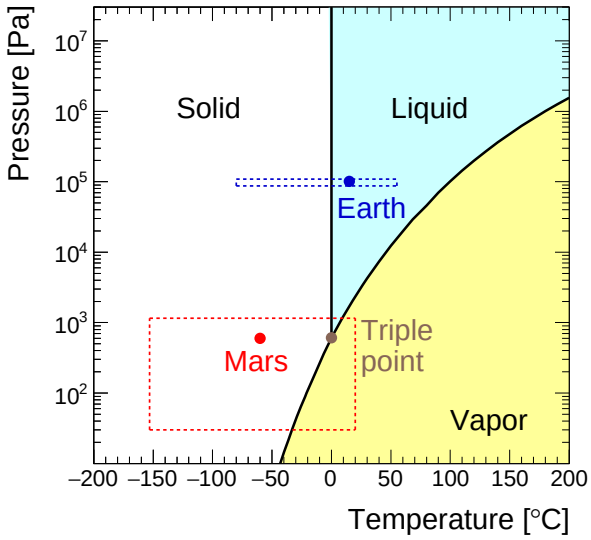

Figure 5: The triple point in the phase diagram of water. The average temperature and pressure on the Earth and Mars is indicated by a small bullet. Boxes show approximate ranges of temperature and pressure that can be achieved on the Earth and Mars. The vertical axis has the logarithmic scale.

the pressure 611.7 Pa, then water can exist simultaneously in gaseous, liquid, and solid state. This is called a *triple point* (see Figure 5). As a consequence we must conclude that Mars has been moving away from the Sun with an average speed of at least several meters per year as in (16).

When the Sun's luminosity was only $0.75L_\odot$, then similarly we would get $r = 116.782 \cdot 10^6$ km to reach the freezing point of water $\mathrm{T_{Mars}} = 273.15$ K. However, this distance is more than 100 million km smaller than the current radius $r = 225 \cdot 10^6$ km. The infrared emissivity does not change these values too much.

The above arguments show that Mars must have been closer to the Sun by several tens of million km when it had liquid water (Figure 6). By (15) and (13) recalculated to the Mars-Sun distance, we find that Mars could move further from the Sun by an amount of at least 30 ($= 4 \cdot 5 \cdot 225/150$) million km during the last 4 Gyr. Therefore, the Earth also had to be closer to the Sun. Otherwise orbits of the Earth and Mars would be unstable.

6.3. Neptune was formed much closer to the Sun than it is now

It is an open problem how Neptune could be formed as far away as $r = 30$ au from the Sun, where all movements are very slow [3]. By Kepler's third law its mean velocity is $\sqrt{GM_\odot/r} = 5.43$ km/s. To reach Neptune's mass of about 10^{26} kg during its first 100 milion years of existence, the proto-Neptune would have had to pick up an average of 30 billion kilograms of material per second in a very sparse environment.

Standish in [45] observed a small anomalous delay in Neptune position. The

Figure 6: Sediments in the Gale crater taken by the Curiosity mission represent a further proof of liquid water on Mars during a long time period. An open problem is why all layers have almost the same thickness and which physical mechanism could produce such a perfect periodicity (photo NASA).

subsequent searches for Planet X have been unsuccessful, but antigravity can again explain this paradox.

Assuming (15), Neptune could be formed more than 4.5 au closer to the Sun than it is now. Indeed, the increase d of its distance from the Sun can be bounded from below as follows:

$$d > (4.5 \cdot 10^9 \,\mathrm{yr}) \cdot (5 \,\mathrm{m}/(\mathrm{yr}\,\mathrm{au})) \cdot 30 \text{ au} = 4.5 \cdot 150 \cdot 10^9 \,\mathrm{m} = 4.5 \,\mathrm{au}.$$

Similarly to (27) we obtain that

$$\Delta P \approx \frac{3P}{2r} \Delta r,$$

where $P = 164.79\,\mathrm{yr}$ is the orbital period of Neptune around the Sun. Thus, after one period P, Neptune will be delayed by about the angle α for which

$$\tan \alpha \approx \frac{\Delta P}{r} \frac{2\pi r}{P} = \frac{2\pi \Delta P}{P} = \frac{3\pi \Delta r}{r}.$$

From this and (16) we find that

$$\alpha \approx \frac{\Delta P}{R} \frac{2\pi R}{P} = \frac{2\pi \Delta P}{P} \approx \frac{3\pi \Delta R}{R} = 0.01''.$$

Note that such small anomalous unexplained delays on the order of several milliarcseconds per century have already been observed [45].

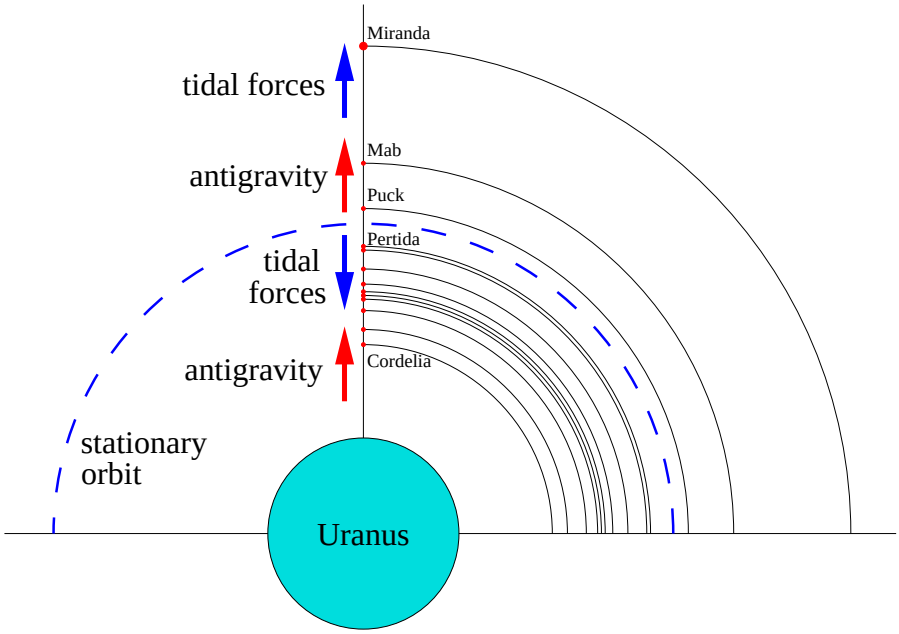

Figure 7: Eleven fast satellites of Uranus and their three neighbors (Miranda, Mab, Puck) above the stationary orbit. Below this orbit the tidal forces and antigravitational forces are subtracted, since they have opposite directions, whereas above this orbit they are summed coherently. The distances between neighboring satellites above the stationary orbit are substantially greater than below it.

To keep energy conserved, the famous Nice model assumes a breakneck exchange of large planets, but does not explain how the rich families of their moons could survive such an exchange. Also backward integration does not give initial conditions for the Nice model (see [27, p. 234] for details).

6.4. Fast satellites

In the Solar system we know of 19 satellites of Mars, Jupiter, Uranus (see Figure 7), and Neptune that are below the corresponding *stationary orbit* with radius (cf. Kepler's third law (24))

$$r_i = \left(\frac{Gm_iP_i^2}{4\pi^2}\right)^{1/3}, \tag{38}$$

where m_i is the mass of the ith planet and P_i is its sidereal rotation. We call them *fast*, since their orbital period is smaller than P_i. From a statistical point of view it is very unlikely that all these satellites would have been captured, since all of them move in the same direction on circular orbits with almost zero inclination. Therefore, they have been mostly in their orbits for approximately 4.5 Gyr even though some may be parts of larger disintegrating satellites.

By Newtonian mechanics tidal bulges continuously reduce potential energy and orbital periods of these fast satellites to keep the total orbital momentum constant.

Due to tidal forces they should approach their mother planets along spiral trajectories. Assuming their approaching speeds of 1–2 cm per year, we find that they should be 45 000–90 000 km closer to their mother planets during the 4.5 Gyr of their existence. However, this contradicts the fact that the radii of the respective stationary orbits of Uranus or Neptune are $r_7 = 82\,675$ km and $r_8 = 83\,496$ km. For the time being, their fast satellites are on very high orbits with radii cca 50 000–76 000 km. Moreover, by (38) the radii of stationary orbits were much smaller in the past (cf. [3, p. 440]), since the rotations of the planets were faster.

It is again antigravity which acts in the opposite direction than gravity and thus protects the fast satellites against crashing onto their mother planet (see Figure 7 and also [25] and [26] for details).

6.5. Mercury and Venus

The influence of antigravity over such a long duration left further footprints in the Solar system. They are recorded in the physical characteristics of planets. For instance, the rotation of Mercury is very slow (59 days) due to larger tidal forces when the planet was closer to the Sun. We know that tidal forces decrease cubically with distance. Thus, if Mercury were, e.g. 10 million km closer to the Sun 4.5 Gyr ago, then the tidal forces would be twice as large as today. This could essentially slow down the rotation of Mercury.

Since the Earth probably was 25 million km closer to the Sun 4.5 Gyr ago due to (16), leading to a distance of 125 million km from the Sun, Venus (whose present mean distance from the Sun is 108 million km) also had to be closer to the Sun. Otherwise their orbits would be unstable.

Moreover, Mercury and also Venus have no moons, since the corresponding lunar orbits would be unstable when they were closer to the Sun.

According to H. Spencer Jones [20], the measured secular accelerations of Mercury and Venus are proportional to their mean motions (see also [9]). Secular long term trends in the mean longitudes $\ell = \ell(t)$ of these planets during the last 250 years are analyzed in [21, p. 884]. The mean longitudes satisfy[3]

$$\ell(t) \approx \ell_0 + \omega t + \tfrac{1}{2}\omega H_0^{\rm loc} t^2,$$

where ℓ_0 is the initial planet longitude, $\omega = 2\pi/P$ is the mean planetary motion, P is the orbital period, and $H_0^{\rm loc} = 2\dot{\omega}/\omega$. From this and measured longitudes Igor N. Taganov [48, p. 72] derived the following local expansion rates

$$H_0^{\rm loc} \approx 0.85 H_0 \quad \text{for Mercury}$$

and

$$H_0^{\rm loc} \approx 0.82 H_0 \quad \text{for Venus.}$$

[3]The local linear Hubble expansion in radial directions produces a quadratic term in the tangential direction.

6.6. Kuiper belt

There are further arguments for the influence of antigravitational forces in the Solar system. According to [3, p. 534], there is strong evidence that the Kuiper belt of comets had been formed much closer to the Sun in a region with larger velocities. Relation (15) can explain a shift of at least 10 au during the last 4.5 Gyr due to antigravity.

6.7. Large orbital momentum of our Moon

A paradoxically very large orbital momentum of the Earth-Moon system (see [3, p. 534]) can also be explained by antigravity which causes an additional shift (35) in the recession speed of the Moon from the Earth that is not due to tidal forces.

6.8. Neptune-Triton system

The enormously large orbital angular momentum of the Neptune-Triton system is a deep mystery. Triton is probably a trapped moon (due to some N-body gravitational collision or a crash with another body), because it orbits around Neptune in the opposite direction than Neptune rotates about its axis. Such an orbit is called *retrograde.* Triton slows Neptune's rotation (as our Moon reduces Earth's rotation). However, since it circulates in the opposite direction, the tidal forces cause it to fall onto lower tracks. The spin angular momentum of Neptune takes the opposite sign than the orbital angular momentum of the Neptune-Triton system. According to the law of total angular momentum conservation, the Neptune-Triton distance should decrease.

Nevertheless, there is a natural question how such a huge body with a diameter of 2705 km could be captured at a distance greater than the radius 354 760 km of its current orbit. Triton has probably orbited Neptune for a very long time, because the eccentricity of its orbit is almost zero:

$$e = 0.000\,016.$$

This is the smallest eccentricity of all known bodies in the Solar system. When Triton was captured, its orbit was almost certainly an elongated ellipse and it took billions of years for Triton to reach a circular orbit.

There is again a quite simple explanation. Repulsive antigravitational forces continually act on Triton and, moreover, it is conceivable that at present they are even larger than the tidal forces that push Triton to Neptune, depending on initial sizes of tidal and antigravitational forces. In this way, the Neptune-Triton system could obtain its huge observed orbital angular momentum.

7. Negligible local effects of the cosmological constant

7.1. Why the other authors got much smaller values of recession speeds?

G. A. Krasinsky and V. A. Brumberg [22] derived that the present recession speed of the Earth from the Sun is equal to $v = 15\,\mathrm{cm/yr}$. Their calculation is based on the assumption that the Newtonian theory of gravitation describes all motions in the Solar system absolutely exactly. They solve an algebraic system for 62 unknown Keplerian parameters of all planets and some large asteroids and do not take into account small antigravitational forces. In other words they implicitly assume that modeling, discretization, and rounding errors are negligible. However, classical Newtonian theory assumes an infinite speed of gravitational interaction, whereas the real speed is surely finite. Hence, the modeling error is surely not zero.

Cooperstock et al. [8, p. 62] derive a tiny outward acceleration of the Earth of $3.17 \cdot 10^{-47}\,\mathrm{m/s^2}$, but the large value of the Hubble constant itself $H_0 = H(0) = 10\,\mathrm{m\,yr^{-1}au^{-1}}$ (see (13)) is not taken into account. The time derivative $\dot{H}(0)$ is, of course, extremely small. By (5) we get

$$\dot{H} = \frac{\ddot{a}}{a} - H^2 = -qH^2 - H^2, \tag{39}$$

where $q := -\ddot{a}a/\dot{a}^2$ is the dimensionless *deceleration parameter* which characterizes deceleration or acceleration of the expansion of the universe. Expressing the expansion function $a = a(t)$ as a Taylor series in time $t_0 = 0$, which corresponds to the present time, we have by (5) and (8)

$$\begin{aligned} a(t) &= a(0) + \dot{a}(0)t + \frac{1}{2}\ddot{a}(0)t^2 + \cdots = a(0)\left(1 + H_0 t - \frac{1}{2}q_0 H_0^2 t^2 + \dots\right) \\ &= a(0)\left(1 + H_0 t - \frac{1}{2}\Lambda q_0 \frac{c^2}{3\Omega_\Lambda(0)} t^2 + \dots\right), \end{aligned} \tag{40}$$

where $H_0 = H(0)$ and $q_0 = q(0) = -0.6$ is the usually accepted value of the deceleration parameter (see [40, p. 110]) which is negative, since the expansion of the universe accelerates.

M. Carrera and D. Giulini [6, p. 175] correctly derive that at the distance of Pluto (i.e. about 40 au) the acceleration of the expansion of the universe is only $2{\cdot}10^{-23}\,\mathrm{m/s^2}$ which is indeed an entirely negligible quantity. A similar tiny value was derived by B. Mashhoon et al. [31, p. 5041]. However, all these authors concentrated only on the single quadratic term in expansion (40) and did not consider the large value of the Hubble constant (13) which stands at the linear term in (40). In other words, an accelerated expansion does not manifest itself on scales of the Solar system, but the expansion itself is observable. In particular, we have

$$|H_0 t| \gg \frac{1}{2}|q_0| H_0^2 t^2 = \frac{1}{2}|q_0| \frac{\Lambda c^2}{3\Omega_\Lambda(0)} t^2$$

for t close to 0. Consequently, the accelerated expansion given by the quadratic term only appears at cosmological distances. In spite of that, the single quadratic term is so small that the linear term $|H_0 t|$ from (40) essentially dominates not only in the neighborhood of 0, but for all t in the whole interval $(-1/H_0, 0)$, since we have

$$0.3 \cdot |H_0 t| > \frac{1}{2}|q_0| H_0^2 t^2,$$

where $\frac{1}{2}|q_0| = 0.3$.

Without dark energy the expansion of our universe would slow down due to gravity (see (11)). Therefore, not only the quadratic term in (40), but also the linear term depends on dark energy.

7.2. Is the cosmological constant a fundamental physical constant?

In the standard cosmological model, the last term in (6) containing the cosmological constant Λ plays the principal role for $t \to \infty$, since the density $\rho(t)$ is proportional to $a^{-3}(t)$. However, if gravitational aberration [25] has a continual influence on the expansion rate of our Universe (at least partly), as shown in previous sections, then Λ has to depend on time, i.e., $\Lambda = \Lambda(t)$. It should also depend locally on many other quantities (mass distribution, velocities, distances, etc.). In another words, Λ is probably not a fundamental physical constant like the gravitational constant G, but it represents only some averaged value due to gravitational aberration effects of all free bodies in the Universe. Its present value $\Lambda(t_0)$ is of order $10^{-52}\,\mathrm{m}^{-2}$ (see (10)), but in the future it can became smaller. Note that the Hubble constant $H = H(t)$ depends on time, too.

The cosmological constant Λ thus could depend on particular masses and their positions and velocities in every system of free bodies that gravitationally interact. An "anthropic" upper bound on Λ is given in [52] and [53].

8. Conclusions

We have shown that antigravity acts not only on large scales but also on small scales. It essentially contributes to the migration of planets and their moons, it also causes many star clusters to dissipate, it helps to reduce the frequency of collisions of galaxies and stars. It has also created suitable habitable conditions on the Earth for several billion years.

Let us emphasize that the evolution of life is not a deterministic process, but very chaotic. It does not have any prescribed direction of its future development. For instance, if the asteroid, which caused the extinction of dinosaurs 65 million years ago, would closely miss the Earth, then man would have not appeared, even though all physical constants would be the same. This means that fundamental constants were not designed just for man to appear. But their values enabled the rise and evolution of life under natural selection which led to intelligent life. The Anthropic Principle should be considered in this way. Evolution of living organisms is chaotic. It has no prescribed goal.

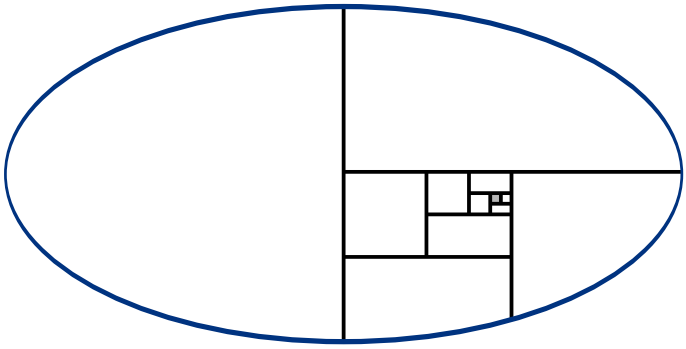

Figure 8: An illustration that the universe has to expand somewhere locally.

The local Hubble expansion certainly had a great impact on the origin of life. To demonstrate the influence of antigravity in the Solar system we must either measure very precisely (e.g. the Earth-Moon distance), or we have to consider very long time intervals, where small deviations from Newtonian mechanics are not canceled, but accumulated and then possibly observed (see [9], [10], [20], [21], [27], [48], [56]). **An extremely small deviation $\varepsilon > 0$ during one year may cause after one billion years a quite large and detectable value of $10^9\varepsilon$ which is then interpreted as dark energy**. Thus we should never identify any mathematical model with reality, since the above argument can be applied to any non-Newtonian model as well.

Newtonian mechanics is formulated so that the laws of conservation of energy and momentum hold. However, the Universe is designed so that these laws do not hold, since its expansion is accelerating. We gave more than 10 other examples showing that something is wrong with classical fundamental conservation laws in the Universe, since dark energy is slightly but continually generated by any system of two or more free bodies.

Note that there exist close binary pulsars whose orbits do not expand with time, but decay. In this case, strong magnetic and gravitational fields are present and the system loses energy due to electromagnetic and gravitational waves. These effects are much stronger than weak effects coming from antigravitational forces. Also various resonances may be significantly larger than antigravity and tidal forces.

The unknown source of dark energy that is needed for the accelerated expansion of the Universe may come partly from a finite speed of gravitational influence [24] that causes gravitational aberration which is much smaller than the aberration of light, but positive due to causality [25].

Another source of dark energy could be time-varying fundamental constants. Note that the observed accelerating expansion of the Universe is sometimes explained by the so-called energy of the vacuum. However, to get the observed values of acceleration, the density of vacuum energy should be $2 \cdot 10^{110}$ erg/cm^3, whereas its measurement gives only a smaller value of $2 \cdot 10^{-10}$ erg/cm^3, which is smaller by 120 orders of magnitude (where $1\,\mathrm{erg} = 10^{-7}\,\mathrm{J}$). From this it is evident that the vacuum energy is not the main reason of the accelerated expansion of the Universe.

It seems that a single gravitational force is not able to keep the Universe together. Most cosmologists believe that the universe expands globally, but not locally. However, this immediately leads to a mathematical contradiction. If the universe expands globally, then it has to expand in its left or right half (see Fig. 8). If it expands in the right half, for example, then it must expand in the upper or lower quarter. Let us therefore assume that it expands in the lower quarter, for instance. Then we again halve it. In this way, we can proceed as shown in Fig. 8 and obtain that the universe must expand somewhere locally.

Acknowledgements

The authors thank to Filip Křížek, Vladimír Novotný, and Jan Vondrák for valuable suggestions and comments. The article was supported by RVO 67985840.

References

[1] Amendola, L. and Tsujikawa, S.: *Dark energy – theory and observations*. Cambridge University Press, 2010.

[2] Barrow, J. D. and Tipler, F. J.: *The anthropic cosmological principle*. Oxford University Press, 1986.

[3] Bertotti, B., Farinella, P., and Vokrouhlický, D.: *Physics of the Solar system*. Kluwer, Dordrecht, 2003.

[4] Brander, D.: *Isometric embeddings between space forms*. Master Thesis, University of Pennsylvania, 2003, 1–48.

[5] Burša, M. and Peč, K.: *Gravity field and dynamics of the Earth*. Springer, Berlin, 1993.

[6] Carrera, M. and Giulini, D.: Influence of global cosmological expansion on local dynamics and kinematics. Rev. Mod. Phys. **82** (2010), 169–208.

[7] Carter, B.: Large number coincidences and the Anthropic Principle in cosmology. In: M. S. Longair (Ed.), *IAU Symposium 63: Confrontation of Cosmological Theories with Observational Data*, pp. 291–298. Riedel, Dordrecht, 1974.

[8] Cooperstock, F. I., Faraoni, V., and Vollick, D. N.: The influence of the cosmological expansion on local systems. Astrophys. J. **503** (1998), 61–66.

[9] De Sitter, W.: On the secular accelerations and the fluctuations of the longitudes of the Moon, the Sun, Mercury and Venus. Bull. Astron. Inst. Netherlands **4** (1927), 21.

[10] Dumin, Y. V.: A new application of the Lunar laser retroreflectors: Searching for the "local" Hubble expansion. Adv. Space Res. **31** (2003), 2461–2466.

[11] Dumin, Y. V.: Testing the dark-energy-dominated cosmology by the Solar-System experiments. In: H. Kleinert, R. T. Jantzen, and R. Ruffini (Eds.), *Proc. of the 11th Marcel Grossmann Meeting on General Relativity*, pp. 1752–1754. World Sci., Singapore, 2008, , arXiv: 0808.1302.

[12] Dumin, Y. V.: The faint young Sun paradox in the context of modern cosmology. Astron. Tsirkulyar **1623** (2015), 1–5, arXiv: 1505.03572v1.

[13] Einstein, A.: Kosmologische Betrachtungen zur allgemeinem Relativitätstheorie. Preuss. Akad. Wiss. Berlin, Sitzber, 1917, 142–152.

[14] Friedmann, A.: Über die Krümmung des Raumes. Z. Phys. **10** (1922), 377–386.

[15] Glanz, J.: Astronomers see a cosmic antigravity force at work. Science **279 (5355)** (1998), 1298–1299.

[16] Goldblatt, C. and Zahnle, K. J.: Faint young Sun paradox remains, arXiv: 1105.5425v2 [astro-ph.EP] 30 May 2011.

[17] Gunn, J. E. and Tinsley, B.: An accelerating Universe? Nature **257** (1975), October, 454–457.

[18] Hartmann, W. K.: *Mars*. Workman Publ., New York, 2003.

[19] Hubble, E.: A relation between distance and radial velocity among extra-galactic nebulae. Proc. Nat. Acad. Sci. USA **15** (1929), 168–173.

[20] Jones, H. S.: The rotation of the Earth, and secular acceleration of the Sun, Moon and planets. Mon. Not. R. Astron. Soc. **99** (1939), 541–558.

[21] Kolesnik, Y. B. and Masreliez, C. J.: Secular trends in the mean longitudes of planets derived from optical observations. Astron. J. **128** (2004), 878–888.

[22] Krasinsky, G. A. and Brumberg, V. A.: Secular increase of astronomical unit from analysis of the major planet motions, and its interpretation. Celest. Mech. Dyn. Astr. **90** (2004), 267–288.

[23] Křížek, M.: Numerical experience with the three-body problem. J. Comput. Appl. Math. **63** (1995), 403–409.

[24] Křížek, M.: Numerical experience with the finite speed of gravitational interaction. Math. Comput. Simulation **50** (1999), 237–245.

[25] Křížek, M.: Does a gravitational aberration contribute to the accelerated expansion of the Universe? Comm. Comput. Phys. **5** (2009), 1030–1044.

[26] Křížek, M.: Dark energy and the Anthropic principle. New Astronomy **17** (2012), 1–7.

[27] Křížek, M., Křížek, F., and Somer, L.: *Antigravity — its origin and manifestations*. Lambert Acad. Publ., Saarbrücken, 2015, 1–348.

[28] Lang, K. L.: *Cambridge encyclopedia of the Sun*. Cambridge University Press, Cambridge, 2001.

[29] Lemaître, G. E.: Un Univers homogène de masse constante et de rayon croissant rendant compte de la vitesse radiale des nébuleuses extragalactiques. Ann. Soc. Sci. de Bruxelles, April (1927), 49–59.

[30] Linewaver, C. H. and Schartzmann, D.: Cosmic thermobiology. In: J. Seckbach (Ed.), *Origins*, pp. 233–248. Kluwer, Dordrecht, 2003.

[31] Mashhoon, B., Mobed, N., and Singh, D.: Tidal dynamics in cosmological spacetimes. Classical Quant. Grav. **24** (2007), 5031–5046.

[32] Misner, C. W., Thorne, K. S., and Wheeler, J. A.: *Gravitation*, (20th edition). W. H. Freeman and Company, New York, 1997.

[33] Noerdlinger, P. D.: *Solar mass loss, the astronomical unit, and the scale of the Solar system*, 2008, arXiv:0801.3807.

[34] Novotný, O.: Motions, gravity field and figure of the Earth. Lecture Notes, Univ. Federal da Bahia, Salvador, 1998.

[35] Pannella, G.: Paleontological evidence on the Earth's rotation history since early precambrian. Astrophys. Space Sci. **16** (1972), 212–237.

[36] Peebles, P. J. E.: *Principles of physical cosmology*. Princeton University Press, New Jersey, 1993.

[37] Perlmutter, S. and Aldering, G. et al.: Measurements of Ω and Λ from 42 high-redshift supernovae. Astrophys. J. **517** (1999), 565–586.

[38] Perlmutter, S. and Gabi, S., et al.: Measurements of the cosmological parameters Ω and Λ from the first seven supernovae at $z \geq 0.35$. Astrophys. J. **483** (1997), 565–581.

[39] Riess, A. G. and Filippenko, A. V. et al.: Observational evidence from supernovae for an accelerating universe and a cosmological constant. Astron. J. **116** (1998), 1009–1038.

[40] A. G. Riess and L.-G. Strolger, et al., New Hubble space telescope discoveries of Type Ia supernovae at $z >= 1$: Narrowing constraints on the early behavior of dark energy. Astrophys. J. **659** (2007), 98–121.

[41] Said, S. S. and Stephenson, F. R.: Solar and lunar eclipse measurements by medieval Muslim astronomers. J. Hist. Astron. **27** (1996), 259–273.

[42] Schwarzschild, B.: Discoverers of the Hubble expansion's acceleration share Nobel physics prize. Physics Today **64** (2011), Dec., 14–17.

[43] Schwarzschild, K.: Über das zulässige Krümmungsmaaß des Raumes. Vierteljahrsschift der Astronomischen Gesellschaft **35** (1900), 337–347.

[44] Slipher, V. M.: Spectrographic observations of nebulae. Amer. Aston. Soc., Popular Astronomy **23** (1915), 21–24.

[45] Standish, E. M.: Planet X: no dynamical evidence in the optical observations. Astronom. J. **105** (1993), 2000–2006.

[46] Stephenson, F. R.: *Historical eclipses and Earth's rotation*. Cambridge University Press, 1997.

[47] Strömberg, G.: Analysis of radial velocities of globular clusters and non-galactic nebulae. Astrophys. J. **LXI** (1925), 353–362.

[48] Taganov, I. N.: *Irreversible time physics*. Russian Acad. Sci., Saint Petersburg, 2016.

[49] Tinsley, B.: Accelerating Universe revisited. Nature **273** (1978), May, 208–211.

[50] van Flandern, T. C.: A determination of the rate of change of G. Mon. Not. R. Aston. Soc. **170** (1975), 333–342.

[51] Verbund, F.: *The Earth and Moon: from Halley to lunar ranging and shells*. Preprint, Utrecht University, 2002, 1–10.

[52] Weinberg, S.: Anthropic bound on the cosmological constant. Phys. Rev. Lett. **59** (1987), 2607–2610.

[53] Weinberg, S.: The cosmological constant problem. Rev. Modern Phys. **61** (1989), 1–23.

[54] Wells, J. W.: Coral growth and geochronometry. Nature **197** (1963), 948–950.

[55] Williams, G. E.: Geological constraints on the Precambrian history of Earth's rotation and the Moon's orbit. Rev. Geophys. **38** (2000), 37–60.

[56] Zhang, W. J., Li, Z. B., and Lei, Y.: Experimental measurements of growth patterns on fossil corals: secular variation in ancient Earth-Sun distance. Chinese Sci. Bull. **55** (2010), 4010–4017.

[57] Zhang, W. J., Sun, Y. L., Kelley, N., Lei, Y., and Li, Z.: The D" layer's key position in the long-term electromagnetic core-mantle coupling and observational evidence. Eur. Phys. J. Plus **126** (2011), 1–12.

Conference *Cosmology on Small Scales 2016*
Michal Křížek and Yurii Dumin (Eds.)
Institute of Mathematics CAS, Prague

A LOCAL PORTRAIT OF THE COSMOLOGICAL CONSTANT

Marek Nowakowski

Departamento de Fisica, Universidad de los Andes
Cra 1E, 18A-10, Bogotá, Colombia
mnowakos@uniandes.edu.co

Abstract: The cosmological constant is one of the most controversial constants of nature. Many scientists would prefer to see its value to be zero and its effect replaced by some other mechanism. The reason for this disliking is partly historical and partly based on some unpleasant features of the cosmological constant Λ. In spite of its problems we take here a pragmatic point of view that Λ is still the simplest theory to account for the acceleration of the expansion. Taking it more seriously implies that we should probe also into possible local effects of this constant i.e., at astrophysical scales. A priori, this is possible since Λ is part of the Einstein tensor and the question arises as to how large its effects are. We will argue that the effects can either be numerically sizable due to a combination of two scales (one connected to Λ, the other to the Newtonian constant) or they are theoretically interesting.

Keywords: Cosmological constant, cosmology, gravitational equilibrium

PACS: 95.36.+x, 98.80.Es, 04.30.Nk, 04.70.Dy, 04.50.Bc

1. Introduction

Nature has provided us with many constants, some more fundamental like Planck's constant $\hbar$ and the speed of light c (which we will put to one here), some connected with the strength of an interaction like the fine structure constant α or Newton's gravitational constant G_N. We accept the numerical values of these quantities found by experiment and we agree that up to date we do not have a convincing theory to explain why these constants have the particular values found in our universe (we also agree that universes with other set of constants are, in principle, consistent and possible). There is, however, one constant which has had a more turbulent history than all others and is still a matter of debate. This is the cosmological constant Λ which has started as a theoretical possibility (indeed, a most general Einstein tensor has to contain this constant), among others to allow Einstein's static universe [20], has been disfavored for decades and partly made an unexpected return when the accelerated expansion of the universe was discovered [47]. The adjective "partly" has

a deeper meaning here since not everybody is ready to accept this re-entry of Λ into the gravitational theory. The reasons are manifold, but one of the most frequently quoted one is the fact that Λ can be re-cast into a constant density $\rho_{\rm vac}$ which interpreted as vacuum energy density will receive other contributions, e.g., from the zero-point energy in quantum field theory. The latter is a divergent quantity and the argument that $\rho_{\rm vac}$ should be governed by the Planck mass relies on a cut-off at the Planck scale. Hence, there is a huge mismatch of scales between what is expected and what we would like to have to explain the accelerated expansion. This argument is often used to discard the cosmological constant, but it does not provide us with an explanation. Indeed, the epistemological status of Λ will be the same if we discard it (which normally amounts to putting its value to zero) or accept a non-zero but small value of $\rho_{\rm vac}$ of the order of the critical density. The argument of the mismatch applies to both cases. Of course, there might be a natural mechanism why its value has to be zero, but in spite of many years of looking for a such a mechanism none has been found (or at least, none is generally accepted). Moreover, explicit examples exist where the use of a hadronic energy-momentum tensor in the early universe implies that the bound on the cosmological constant comes from the low energy hadronic particles [13] which is rather an unexpected result and could lead to a shift in the cosmological constant controversy. We therefore take here the point of view that the cosmological constant whose values we infer from cosmology could be a physical reality. This in turn calls for a more detailed investigation of the effects of Λ apart from the obvious cosmological implication. In other words we are looking for fingerprints of Λ in an astrophysical setting. Making a connection between cosmology and astrophysics is not new. For instance, the question if the expansion of space has an impact on astrophysical matter has been put forward already by Einstein and Strauss [21] and pursued till now [10, 16, 33, 34]. We will follow another path here and make use of the fact that Λ is part of the Einstein tensor and as such its presence will be felt in any general relativistic phenomenon (see however [17]). The question is, however, how big and how relevant the effects are. In the first part of the paper we will briefly introduce the cosmological constant via the Einstein equation and cosmology. Here the relevant scales of Λ will also be touched upon. In the next section we will probe if Λ has an impact in the astrophysical concepts of equilibrium like the virial or hydrostatic equilibrium. This will be followed by a discussion on the geodesic equation of motion. We will address the question regarding how Λ changes the motion of a test particle at large astrophysical distances. The strong gravity aspect will be covered in Section 5 where we use a Generalized Uncertainty Principle to derive limits on the black hole temperature. Finally, in Section 6 we will linearize the Einstein equation with Λ to examine the effect of this constant on gravitational waves. In the last Section we will draw our conclusions.

There exists a number of very good reviews [14, 15, 18, 30, 41, 42, 45, 46, 50, 51] on the cosmological constant, describing the problem from different angles. We adopt here yet another point of view and, as mentioned above, look for signals of this constant outside its normal habitat which is cosmology.

2. Cosmological preliminaries: Λ in cosmology

Cosmology has a long scientific tradition where observations have either matched or contradicted theoretical predictions. Alone the fact that galaxies on the average move away from each other is measurable and was probably the first step of a scientific tradition of cosmology based on general relativity (today we also have another tool which is the cosmic microwave background radiation). Indeed, the accelerated expansion of space is one possible prediction of general relativity and it was the discovery of the acceleration of the expansion which in the new century changed our picture of the universe.

2.1. Einstein equations

Einstein equations have the general form

$$G_{\mu\nu}(g_{\alpha\beta}, g_{\alpha\beta,\sigma}, g_{\alpha\beta,\sigma\rho}) = \kappa T_{\mu\nu}, \quad \kappa = 8\pi G_N\,, \tag{1}$$

where the indices after the commas indicate derivatives and G_N is the Newtonian constant. The geometrical left-hand side, known as the Einstein tensor, has to be constructed under some minimal assumptions. The right-hand side is the energy-momentum tensor usually taken from relativistic hydrodynamics or derived from the matter Lagrangian (like, e.g., the Lagrangian for electrodynamics resulting in the energy-momentum tensor of the Maxwell theory). There is a theorem proved by Lovelock in a series of papers [27, 28, 29] which assures the most general form of $G_{\mu\nu}$. The assumptions of the theorem are based on physical requirements: (i) as any other field theory we allow the equations to contain the field itself and the first as well as the second derivatives of the field, (ii) since $T_{\mu\nu}$ is symmetric, $G_{\mu\nu}$ should enjoy the same property and (iii) since $T_{\mu\nu}$ is conserved, i.e., the total divergence is zero we demand the same for the Einstein tensor. In four space-time dimensions on a pseudo-Riemannian manifold the full theorem reads:

Theorem (Lovelock's Theorem). *In a four-dimensional space the only tensor whose components $G_{\mu\nu}$ satisfy the conditions (a) $G_{\mu\nu} = G_{\nu\mu}$, (b) $\nabla^\mu g_{\mu\nu} = 0$ (metricity), (c) it contains the metric, its first and second derivatives, is*

$$G_{\mu\nu} = R_{\mu\nu} - \frac{1}{2}Rg_{\mu\nu} + \Lambda g_{\mu\nu}\,. \tag{2}$$

This theorem assures that a general Einstein tensor has a cosmological constant Λ. Its value is a priori not known (indeed, the sign of Λ is also crucial in cosmological considerations) and, in principle, nature could have chosen $\Lambda = 0$ which however would call for an explanation. Although the final result of the theorem looks simple, the proof is long and complicated partly due to the fact that it starts with few assumptions, for instance, one drops any requirement on linearity. In the light of Loevlock's theorem, should we be surprised if observationally we find a non-zero value for this constant? Theoretically many mechanisms have been tried to put the cosmological constant to zero in a natural way (say, by invoking a symmetry).

None of them has been successful and yet very often scientists view a non-zero Λ as something unnatural. They do so, because Λ, as we will see later, can receive contributions outside the realm of General Relativity and these contributions seem to give a wrong scale for this constant (see below). In any case, apart from different contributions, Lovelock's theorem assures the existence of a bare cosmological constant Λ_0. The final Λ would be a sum of this bare value plus other contributions. We will come back to this point at the end of this section.

One point is worthwhile mentioning. The cosmological constant is part of the Einstein tensor and not the energy-momentum tensor. This means that it will appear everywhere where General Relativity is used, in the cosmological solutions as well as in the local metrics. The name "cosmological constant" might have been a misnomer were it not for the actual value of Λ (provided the accelerated expansion of the universe, which we will discuss below, is attributed to this constant) whose value is such that its most prominent effects are in the cosmological realm. But we will see later that mixing of scales can happen with the effect that Λ can be "felt" at astrophysical distances.

Two solutions of the Einstein equations will be of importance for us. The first one, the cosmological one (Friedmann equations) and the other is the local Schwarzschild metric (here $\Lambda = 0$) or Schwarzschild-de Sitter metric when the cosmological constant is positive (in the opposite case when it is negative it is called Schwarzschild-anti de Sitter). Based on isotropy and homogeneity the Friedmann-Robertson-Walker metric is

$$ds^2 = -dt^2 + a^2(t)R_0^2\left[\frac{dr^2}{1-kr^2} + r^2 d\Omega\right], \tag{3}$$

where $a = R/R_0$, R_0 is the value today, and k denotes the spatial curvature which is zero in our universe. The Einstein equations are now reduced to differential equations (Friedmann equations) for a and the conservation of the energy-momentum tensor gives an equation for the energy density ρ. More explicitly involving the Hubble parameter H, we have,

$$H^2 \equiv \left(\frac{\dot{a}}{a}\right)^2 = \frac{8\pi G_N}{3}\rho + \frac{\Lambda}{3} - \frac{k}{a^2 R_0^2}, \quad k = \pm 1,\, 0\,, \tag{4}$$

and a second differential equation of the form

$$\frac{\ddot{a}}{a} = -\frac{4\pi G_N}{3}(\rho + 3p(\rho)) + \frac{\Lambda}{3}\,. \tag{5}$$

The conservation law reads

$$\dot{\rho} = -(\rho + p(\rho))\frac{\dot{a}}{a}\,. \tag{6}$$

These equations are not fully independent of each other. The first one is often written in a convenient form (from which the sign of k can also be deduced)

$$\Omega_{m0} + \Omega_{\Lambda 0} + \Omega_{k0} = 1 \to k = \mathrm{sgn}(\Omega_{m0} + \Omega_{\Lambda 0} - 1)\,, \tag{7}$$

where the 0 denotes the time today, but (7) is valid at any time. The definitions entering this equation are as follows

$$\begin{aligned} \Omega_{m0} &= \frac{\rho_0}{\rho_{\rm crit}}, \quad \rho_{\rm crit} = \frac{3H_0^2}{8\pi G_N}, \\ \Omega_k &= -\frac{k}{R_0^2 H_0^2}, \\ \Omega_{\Lambda 0} &= \frac{\rho_{\rm vac}}{\rho_{\rm crit}}, \quad \Lambda = 8\pi G_N \rho_{\rm vac}\,. \end{aligned} \tag{8}$$

In $\rho_{\rm vac}$ we encounter the first scale set by the cosmological constant in the form of a constant density. It is this scale which cosmologists interpret as vacuum density (being defined everywhere in space) and which can receive contributions from elsewhere.

An intuitive and fast understanding of the cosmological effect of Λ is provided by the Newtonian limit. For a spherically symmetric object with mass M we can use the Schwarzschild-de Sitter metric whose line element is

$$ds^2 = -{\rm e}^{\nu(r)}dt^2 + {\rm e}^{-\nu(r)}dr^2 + r^2 d\theta^2 + r^2 \sin^2\theta d\phi^2\,, \tag{9}$$

with

$$g_{00} = {\rm e}^{\nu(r)} = 1 - \frac{2r_s}{r} - \frac{r^2}{3(r_\Lambda)^2}, \quad r_s \equiv G_N M, \quad r_\Lambda \equiv \frac{1}{\sqrt{\Lambda}}\,. \tag{10}$$

Two length scales appear: the Schwarzschild radius $2r_s$ and r_Λ. With the connection of the 00 component of the metric to the gravitational potential, i.e.,

$$g_{00} \simeq -(1 + 2\Phi)\,, \tag{11}$$

we obtain the Newtonian limit in the form

$$\Phi(r) = -\frac{r_s}{r} - \frac{1}{6}\frac{r^2}{(r_\Lambda)^2}\,. \tag{12}$$

The first term is the standard Newtonian potential. Its form will change when we consider a non-spherically symmetric mass distribution. But the second term will remain as it is. Indeed, it is an external force which for a positive cosmological constant plays the role of a repulsive external force with the interpretation that two points in space separate. The Galilean spacetime gets replaced by Newton-Hooke spacetime [6] in which two space points go apart due to the cosmological constant (this is the part of the cosmological expansion which survives the Newtonian limit).

2.2. Accelerated expansion

Observation of standard candles like type II Supernovae led us to conclude that the expansion of the Universe as compared to the standard Friedmann model is accelerated [44, 43]. The Supernovae are dimer than expected in a standard Friedmann

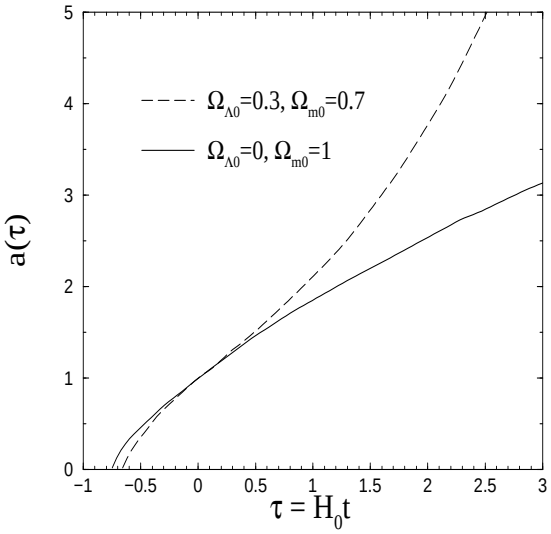

Figure 1: Two fates of matter-filled Universes. The present epoch is at $\tau = 0$.

model, hence they have to be further away than expected. The universe must have expanded faster than expected. Of course there could be other explanations also, like dust and dimming due to photon-axion conversion in the presence of magnetic fields. But by now this fact is fairly established and corroborated by other observations [48]. Indeed, the discovery won a Nobel Prize in 2013. It is easy to understand what this accelerated expansion means. The Friedmann equations (4)–(7) tell us that an acceleration simply means $\ddot{a} > 0$ and this as such cannot happen if $\Lambda = 0$. Indeed, a non-zero positive cosmological constant leads to an accelerated expansion as depicted in Figure 1 and already inferred from the Newtonian limit. For the case of dust ($p = 0$) and spatial flatness which describes our epoch, the relevant Friedmann equation $\ddot{a}/a = -4\pi G_N/3[\rho - 2\rho_{\rm vac}]$ tells us that in order to have a cosmic acceleration we have to insist on $\rho < 2\rho_{\rm vac}$. Since $\Omega_m + \Omega_\Lambda = 1$ we obtain the limits: $\Omega_m \leq 2/3$ and $\Omega_\Lambda \geq 1/3$. If by ρ we mean the total energy density, i.e., $\rho = \rho_m + \rho_{\rm vac}$ then we can retain the Friedmann equation in the form $\ddot{a}/a = -4\pi G_N/3[\rho + 3p]$ with $p = -\rho_{\rm vac}$ playing the role of an equation of state. Of course, many other explanations are possible. What they all have in common is that they go beyond standard General Relativity as defined by the Einstein tensor. They either postulate new Einstein equations based on a more complicated Lagrangian (modified gravity) or invoke a scalar field (quintessence model) [24] or modify the standard equation of state which reads $p = (\gamma - 1)\rho$ (Chaplygin gas model [26]) or use an even more complicated set-up. In some of these extensions the Einstein tensor will still appear and the question we have to face then is what do we do with value of the cosmological constant in such models? Normally it is put to zero by hand.

If we hold Λ responsible for the accelerated stage then a recent measurement tells us that $\Omega_{\Lambda 0} = 0.6$.

The cosmological constant bears more theoretical surprises. In non-spatially flat universes there exists a $\Lambda_{\rm crit}$ expressed in terms of H_0 and Ω_{m0} such that for $\Lambda = \Lambda_{\rm crit}$ the universe is semi-static and "coasting" whereas for $\Lambda > \Lambda_{\rm crit}$ there is no Big Bang, i.e., the universe contracts coming form minus infinity (in time), hits a minimum scale and starts expanding [22].

2.3. Scales of Λ

All our numerical predictions are based on two scales: the parameters entering the theory and the initial values we choose. A combination of constants and parameters yields different physical scales. For instance, as we all know $\hbar$, c and G_N combine to give Planck length $l_{\rm pl}$, time $t_{\rm pl}$, and mass $m_{\rm pl}$. Similarly, Λ alone or in conjunction with other constants sets certain scales which will appear in any calculation. We already came across the density parameter $\rho_{\rm vac}$.

In the following context two definitions turn out to be useful

$$\rho_{\rm crit} = \frac{3H_0^2}{8\pi G_N} = \frac{3}{8\pi} H_0^2 m_{\rm pl}^2 \,, \tag{13}$$

which is the critical density of the universe where H_0 is the present value of the Hubble parameter, and

$$\rho_{\rm vac} = \frac{\Lambda}{8\pi G_N} \,, \tag{14}$$

which is a combination of Λ and G_N. Using the two equations we are able to write a useful relation

$$\Lambda = 3 \left(\frac{\rho_{\rm vac}}{\rho_{\rm crit}} \right) H_0^2 \,. \tag{15}$$

In the following we will briefly introduce the different scales of Λ [39]:

- **Length**

It is convenient to define

$$r_\Lambda = \frac{1}{\sqrt{\Lambda}} = \frac{1}{\sqrt{3}} \left(\frac{\rho_{\rm vac}}{\rho_{\rm crit}} \right)^{-1/2} H_0^{-1}. \tag{16}$$

This equation tells us that r_Λ is practically the Hubble length. This is a coincidence, since neither was it so in the past nor will it be the same in the future. The same applies to the coincidence $\rho_{\rm vac} \sim \rho_{\rm crit}$. Let us now compare the two constants entering Einstein gravity. To this end recall that the Planck length is given by ($\hbar = c = 1$)

$$l_{\rm pl} = G_N^{1/2} \sim 1.5 \times 10^{-33} \, {\rm cm} \,. \tag{17}$$

Hence, this gives

$$\frac{r_\Lambda}{l_{\rm pl}} \sim 10^{61} \,. \tag{18}$$

- **(Small) Mass**

We define

$$m_\Lambda \equiv \sqrt{\Lambda} \sim 3 \times 10^{-42}\text{GeV}\,, \tag{19}$$

which is strangely close to the inverse of the Dirac large number (Dirac's large numbers appear, for instance, in the expression $\frac{1}{G_N m_p m_e} \sim 10^{41}$). An even better approximation to the Dirac large number is the ratio

$$\frac{m_p}{m_\Lambda} \sim 10^{41}\,, \tag{20}$$

where m_p is the mass of proton. On the other hand, we also have:

$$\frac{m_{\rm pl}}{m_\Lambda} \sim 10^{60}\,, \tag{21}$$

using the Planck mass $m_{\rm pl}$.

- **(Large) Mass**

A quantity of dimensions of mass (apart from $m_{\rm pl}$ and m_Λ) can be also defined as a combination of Λ and G_N

$$M_\Lambda \equiv \frac{1}{G_N\sqrt{\Lambda}} = 3.6 \times 10^{22} h_o^{-1} \left(\frac{\rho_{\rm vac}}{\rho_{\rm crit}}\right)^{-4} M_\odot\,, \tag{22}$$

where as usual $M_\odot$ is the solar mass. This gives the comparison

$$\frac{M_\Lambda}{m_{\rm pl}} \sim 10^{60}\,. \tag{23}$$

From these simple considerations it is clear that G_N and Λ lie far apart from each other (indeed, some sixty orders of magnitude). It is a priori not clear why the Dirac large number appears and why we encounter the strange coincidences at the present epoch. In the subsequent section we will see how useful the definition of the different scales is. We can appreciate it by taking an example of the Newtonian limit for a general mass distribution given by [35]

$$\nabla^2\Phi = 4\pi G_N \rho - \Lambda\,. \tag{24}$$

This limit holds if the potential is weak, i.e.,

$$|\Phi(r)| \ll 1 \to r_s \ll d(r) \equiv r - \frac{1}{6}\frac{r^3}{(r_\Lambda)^2}. \tag{25}$$

The function $d(r)$ has a local maximum at $r_+ = \sqrt{2} r_\Lambda$. Hence, we conclude

$$\frac{2\sqrt{2}}{3} M_\Lambda \gg M\,. \tag{26}$$

On the other hand, solving

$$r_s = d(r)\,, \tag{27}$$

we conclude that

$$\sqrt{6} r_\Lambda \gg r \gg r_s\,. \tag{28}$$

Since r has now a maximum value, we have a problem to put the Dirichlet boundary condition at infinity as we are used to do when $\Lambda = 0$. Although we will devote a section to astrophysical equilibria, we can have a glimpse already here of how the scales enter a spherically symmetric object under hydrostatic equilibrium. To this end we use the Buchdahl inequalities which are based on the existence of a global solution (general relativistic spherically symmetric object in hydrostatic equilibrium). For the case of a non-zero cosmological constant one has [7]

$$3r_s \leq \frac{2}{3}R + R\sqrt{\frac{4}{9} - \frac{1}{3}\frac{R^2}{(r_\Lambda)^2}}\,. \tag{29}$$

Evidently, we have to satisfy

$$R \leq \sqrt{\frac{4}{3}} r_\Lambda \sim R_{\max}\,. \tag{30}$$

Hence, we also get

$$M_{\max} \sim \frac{2}{3}\sqrt{\frac{4}{9}} M_\Lambda \geq M\,. \tag{31}$$

We have mentioned above that one of the undesired features of the cosmological constant is the fact that if we interpret $\rho_{\rm vac}$ as the energy density of vacuum, there might be different contributions to this quantity. One of them is the zero-point vacuum energy from quantum field theory which per se is divergent and needs regularization. From $\int d^4k(\omega_k \hat{N}_k + \frac{1}{2}\omega_k)$, ($\hat{N}_k$ is the number operator) we retain only the vacuum energy of quantized fields, i.e, $\int d^3k \frac{1}{2}\omega_k$ [14]. Since $\omega_k = k$ at large energies the integrand is divergent. The standard wisdom is to introduce a cut-off $k_{\max}$, so that

$$\langle \rho \rangle = 2\pi \int_0^{k_{\max}} dk k^3 = \frac{2\pi}{4} k_{\max}^4 = \frac{\pi}{2} k_{\max}^4\,. \tag{32}$$

It might be dangerous to base arguments on a cut-off scale in a fundamental theory. Indeed, a recent result [13] seems to confirm this. Be it as it may it is often argued that the only natural scale for $k_{\max}$ is $m_{\rm pl}$. In such a scenario the contribution to $\rho_{\rm vac}$ would be much too large!

As already mentioned, the above argument is strongly cut-off dependent and based only on arguments of scales. Therefore, we might be entering here a realm of physics which we do not really understand. Indeed, according to the Lovelock's theorem, a 'bare' scale Λ_0 (i.e. the value of Λ without any outside contribution) exists. The true value of $\rho_{\rm vac}$ (and hence also of Λ) would then be

$$\rho_{\rm vac} = \rho_{\rm vac}^0 + \beta k_{\max}^4\,, \tag{33}$$

where $\beta \sim \mathcal{O}(1)$ (e.g. $\frac{\pi}{2}$) and $\rho^0_{\rm vac} = \frac{\Lambda_0}{8\pi G_N}$. Now we still have two universal gravitational constants: G_N and Λ_0. Why then should we choose $k_{\rm max}$ containing only $G_N = m_{\rm pl}^{-2}$? We could also try a combination of scales such as $k_{\rm max} \sim \sqrt{\Lambda_0}$ or $\sqrt{m_{\Lambda_0} m_{\rm pl}}$, where $m_{\Lambda_0} = \sqrt{\Lambda_0}$. In the latter case we would end up with

$$\frac{\Lambda_0}{8\pi G_N} + \beta\Lambda_0^2 = \rho_{\rm vac} = 0.6\rho_{\rm crit}\,, \tag{34}$$

whereas the first choice gives

$$\frac{\Lambda_0}{8\pi G_N} + \beta m^2_{\Lambda_0} m^2_{\rm pl} = \frac{\Lambda_0}{8\pi} m^2_{\rm pl} + \beta\Lambda_0 m^2_{\rm pl} = \rho_{\rm vac} = \frac{3}{8\pi} H_0^2 m^2_{\rm pl}\,. \tag{35}$$

Solving the linear equation, we obtain

$$\Lambda_0 = m^2_{\Lambda_0} = \frac{3H_0^2}{1+8\pi\beta}\,, \tag{36}$$

which is roughly of the same order as $\Lambda = 3\left(\frac{\rho_{\rm vac}}{\rho_{\rm crit}}\right) H_0^2$ and therefore the above solution avoids the tuning problem (i.e. the difference between the actual value of Λ and the induced contribution of the end-point energies). The quadratic equation has the solution:

$$\Lambda_0 = -\frac{1}{2}\frac{1}{8\pi\beta}\sqrt{\rho_{\rm pl}} \pm \frac{1}{2}\frac{1}{8\pi\beta}\sqrt{\rho_{\rm pl}}\sqrt{\Lambda + \frac{\rho_{\rm vac}}{\rho_{\rm pl}}(8\pi\beta)^2}\,, \tag{37}$$

with $\rho_{\rm pl}$ being the Planck density. Since $\rho_{\rm pl} \gg \rho_{\rm vac}$ we can approximate

$$\Lambda_0 \simeq -\frac{1}{16\pi\beta}\sqrt{\rho_{\rm pl}} \pm \frac{1}{16\pi\beta}\sqrt{\rho_{\rm pl}}\left(1 + \frac{1}{2}(8\pi\beta)^2\frac{\rho_{\rm vac}}{\rho_{\rm pl}}\right)\,. \tag{38}$$

If we allow for the case $\Lambda_0 < 0$ (anti-de Sitter case) we can choose the negative sign in the solution

$$\Lambda_0 \simeq -\frac{1}{4}8\pi\beta\frac{\rho_{\rm vac}}{\sqrt{\rho_{\rm pl}}} = -2\pi\beta\frac{3H_0^2}{8\pi} = -\frac{3}{4}H_0^2\,. \tag{39}$$

Now $|\Lambda_0| \sim \mathcal{O}(\Lambda)$, but it is negative, i.e., we go from anti-de Sitter case (in the case of the pure Λ_0) to the de Sitter case when adding to Λ_0 the end-point energies of vacuum energies from quantum field theory. Those two examples relying on Lovelock's theorem, demonstrate in reality that we have a poor understanding of the induced contributions to Λ.

3. Equilibria Concepts: Λ in the local universe

If the cosmological constant sets only cosmological scales, can it happen that it is of some relevance at astrophysical scales [9, 11, 36, 37]. In case of the equilibria

concepts this happens for non-spherical objects with at least two length scales as we will see below.

Let us first consider the non-relativistic gravitational equilibrium via the virial equations. The standard non-relativistic virial theorem reads

$$\frac{d^2 I_{jk}}{dt^2} = 4K_{jk} + 2W_{jk}\,, \tag{40}$$

where I_{jk} is the inertial tensor defined by

$$I_{jk} = \int \rho x_j x_k d^3x\,, \tag{41}$$

K_{jk} is the kinetic tensor

$$K_{jk} = \frac{1}{2}\int \rho \bar{v}_j \bar{v}_k d^3x\,, \tag{42}$$

assuming for simplicity no dispersion, and W_{jk} is the gravitational potential tensor given by

$$W_{jk} = -\frac{1}{2}\int\int \rho(\mathbf{r})\rho(\mathbf{r}')\frac{(x'_j - x_j)(x'_k - x_k)}{|\mathbf{r}' - \mathbf{r}|^3|} d^3x' d^3x\,. \tag{43}$$

If an external force is exerted on the object, we have to add to the right-hand side of the equation the term [12]

$$V_{jk} = -\frac{1}{2}\int \rho\left(x_k \frac{\partial \Phi_{\rm ext}}{\partial x_j} + x_j \frac{\partial \Phi_{\rm ext}}{\partial x_k}\right) d^3x\,, \tag{44}$$

where $\Phi_{\rm ext}$ is the external potential and in the case of a cosmological constant it corresponds to

$$\Phi_{\rm ext} = -\frac{1}{6}\Lambda r^2\,. \tag{45}$$

Therefore, the new virial theorem which accounts for the cosmological constant takes the form [36]

$$\frac{d^2 I_{jk}}{dt^2} = 4K_{jk} + 2W_{jk} + \frac{2}{3}I_{jk}\Lambda\,. \tag{46}$$

This equation (and the rest of the equations derived below) does not include pressure or magnetic fields. Formally, it looks like a differential equation for the inertial tensor. It is very often more convenient to consider a less demanding task by simply noting that the trace W of W_{jk} is negative whereas the trace K of K_{jk} is positive definite. Then the gravitational equilibrium, i.e., $d^2 I_{jk}/dt^2 = 0$ leads to the inequality

$$-\frac{1}{3}\Lambda I + |W| \geq 0\,, \tag{47}$$

where I denotes the trace of the inertial tensor I_{jk}. To appreciate the meaning of this inequality we specialize to the case of constant density. It is then easy to show that

$$8\pi G_N \rho \geq A\Lambda, \;\; \rho \geq A\rho_{\rm vac}\,, \tag{48}$$

where the quantity A depends only on the geometry of the object under consideration, i.e.,

$$A = \frac{16\pi}{3} \frac{\int r^2 d^3x}{\int \frac{|\Phi_{\rm N}|}{\rho} d^3x} \,, \tag{49}$$

where $\Phi_{\rm N}$ is the Newtonian part of the non-relativistic gravitational potential. For spherically symmetric objects one easily calculates $A = 2$ and therefore the virial inequality is simply

$$4\pi G_N \rho \geq \Lambda, \;\; \rho \geq 2 \; \rho_{\rm vac} \,. \tag{50}$$

Let us consider a non-spherical object. Instead of the inequality we can also calculate from the virial theorem the mean velocity of the ingredient of the object

$$\langle v^2 \rangle = \frac{|W|}{M} - \frac{8\pi}{3} \frac{\rho_{\rm vac}}{M} I \,. \tag{51}$$

To estimate the effect of Λ we assume a constant density and the shape of the astrophysical object to be an ellipsoid. The mean velocity can be now written as

$$\begin{aligned} \langle v^2 \rangle_{\rm ellipsoid} &= \frac{32\pi}{45M} \rho \rho_{\rm vac} a_1 a_2 a_3 \left(a_1^2 + a_2^2 + a_3^2 \right) \\ &\times \left(\frac{3}{4} \frac{\rho}{\rho_{\rm vac}} \Gamma_{\rm ellipsoid} - 1 \right) \,. \end{aligned} \tag{52}$$

The prolate case ($a_1 = a_2 < a_3$, $\bar{e} = \sqrt{1 - a_1^2/a_3^2}$) gives

$$\Gamma_{\rm prolate} = \frac{\left(\frac{a_1}{a_3} \right)^3}{1 + 2 \left(\frac{a_1}{a_3} \right)^2} \frac{\ln \left(\frac{1+\bar{e}}{1-\bar{e}} \right)}{\bar{e}} \,. \tag{53}$$

Notice that for a flattened prolate ellipsoid we can approximate

$$\Gamma_{\rm prolate} \simeq \left(\frac{a_1}{a_3} \right)^3 \ln \left(\frac{1+\bar{e}}{1-\bar{e}} \right) \,. \tag{54}$$

Since the nowadays preferred value of $\rho_{\rm vac}$ is $0.6 \rho_{\rm crit}$, we can say that if the constant $\rho/\rho_{\rm crit}$ is, say, 10^3, it suffices for the ellipsoid to have the ratio $a_1/a_3 \sim 10^{-1}$ in order that the mean velocity of its components approaches zero. This is valid always under the assumption that the object is in gravitational equilibrium. This effect is due to the cosmological constant. In general, we can say that in flattened astrophysical systems in gravitational equilibrium, the mean velocity gets affected by the cosmological constant. The denser the system, the bigger should be the deviation from spherical symmetry to have a sizable effect.

Next we probe the same scales in a hydrostatic equilibrium for spherically symmetric objects [7]. Note that in the virial equations used above no pressure appeared

(indeed, with pressure the virial equations change), but the non-relativistic hydrostatic equilibrium is defined by

$$\nabla P = -\rho \nabla \Phi, \quad \nabla^2 \Phi = 4\pi G_N \rho - \Lambda \,. \tag{55}$$

This condition applied for the spherically symmetric case reads

$$P'(r) = -r\rho(r) \left(G_N \frac{m(r)}{r^3} - \frac{\Lambda}{3} \right) , \tag{56}$$

which is sometimes called the "fundamental equation of Newtonian astrophysics". The mass function is as usual defined by

$$m(r) = \int_0^r 4\pi \rho(s) s^2 ds \,. \tag{57}$$

Furthermore, let the mean density be defined by

$$\bar{\rho}(r) = \frac{3}{4\pi} \frac{m(r)}{r^3} \,. \tag{58}$$

Then

$$P'(r) = -r \frac{\rho(r)}{3} \Big(4\pi G_N \bar{\rho}(r) - \Lambda \Big) \,. \tag{59}$$

For any physically reasonable astrophysical object, the pressure and density must be monotonically decreasing functions of the object's radius. Hence, negativity of the derivative of the pressure implies

$$\Lambda < 4\pi G_N \bar{\rho}_b \,, \tag{60}$$

where the index b denotes that we are evaluating the density at the boundary. In its form the above inequality is similar to what we obtained in the virial case. One can arrive at the same result via the general relativistic Tolman–Oppenheimer–Volkoff equation

$$P'(r) = -r \frac{\rho(r)}{3} \Big(1 + \frac{P(r)}{\rho(r)} \Big) \left(\frac{12\pi P(r) + 4\pi G_N \bar{\rho}(r) - \Lambda}{1 - \frac{8\pi}{3} G_N \bar{\rho}(r) r^2 - \frac{\Lambda}{3} r^2} \right) . \tag{61}$$

This equation is well defined if the denominator is positive definite and we impose the boundary condition $P_{\text{boundary}} = 0$.

At the end of this section let me quote from a book "The measure of the Universe: A History of Modern Cosmology" by John David North:

> *The essential difficulty with a relativistic theory in which λ [the Cosmological Constant] is positive is that of accounting for the formation and condensation in terms of gravitational instability; for, to use the 'force' metaphor, the present expansion indicates that the force of cosmic repulsion exceeds those of gravitational attraction. This is not likely to disturb the stability of systems (such as the galaxy) of high average density, but it is likely to prevent new condensation in regions of low density.*

Of course, this picture will not be true if the cosmological constant is not too large (as it happens in our universe).

4. Λ in the local universe: equation of motion

In a theory with two scales a physically relevant combination of them can occur even if the two scales lie numerically apart [8]. Below we show that this happens also in Einstein gravity in a local Schwarzschild–de Sitter metric where r_Λ combines with a smaller length scale r_s to give a meaningful quantity.

Consider the motion of test particles in a spherically symmetric and static spacetime with a cosmological constant. The Schwarzschild–de Sitter metric takes the form

$$\begin{aligned} ds^2 &= -\mathrm{e}^{\nu(r)}dt^2 + \mathrm{e}^{-\nu(r)}dr^2 + r^2 d\theta^2 + r^2\sin^2\theta d\phi^2, \\ \mathrm{e}^{\nu(r)} &= 1 - \frac{2r_s}{r} - \frac{r^2}{3(r_\Lambda)^2}\,. \end{aligned} \tag{62}$$

The equation of motion for a massive particle with proper time τ in the Schwarzschild–de Sitter metric can be written elegantly as

$$\frac{1}{2}\left(\frac{dr}{d\tau}\right)^2 + U_{\text{eff}} = \frac{1}{2}\left(\mathcal{E}^2 + \frac{L^2\Lambda}{3} - 1\right) \equiv C = \text{constant}\,, \tag{63}$$

where $\mathcal{E}$ and L are conserved quantities (the analogs of energy and angular momentum in classical mechanics) defined by

$$\mathcal{E} = \mathrm{e}^{\nu(r)}\frac{dt}{d\tau}, \;\; L = r^2\frac{d\Phi}{d\tau}\,, \tag{64}$$

where Φ is the azimuthal angle and U_{eff} is defined by [8]

$$U_{\text{eff}}(r) = -\frac{r_s}{r} - \frac{1}{6}\frac{r^2}{(r_\Lambda)^2} + \frac{L^2}{2r^2} - \frac{r_s L^2}{2r^3}\,, \tag{65}$$

which is the analog of an effective potential in classical mechanics. This form of the equation of motion is, of course, equivalent to the geodesic equation of motion from which it has been derived.

We now consider radial motion with $L = 0$. From the definition of C we obtain the inequality

$$C \geq -\frac{1}{2}\,, \tag{66}$$

which will play a crucial role later in the derivation. For the limiting value $C = -\frac{1}{2}$, we have $\mathcal{E} = 0$ which signals an artifact of the Schwarzschild coordinates. Indeed, $\mathcal{E} = 0$ means that $g_{00} = 0$ and this equation determines the horizons. More specifically, in the Schwarzschild–de Sitter metric the equation for the horizons is the cubic

$$\begin{aligned} 0 &= y^3 - 3y + 6x\,, \\ y &= \frac{r_\star}{r_\Lambda}\,, \\ x &\simeq \frac{r_s}{r_\Lambda} = 1.94\times 10^{-23}\left(\frac{M}{M_\odot}\right)\left(\frac{\rho_{\text{vac}}}{\rho_{\text{crit}}}\right)^{1/2} \ll 1\,. \end{aligned} \tag{67}$$

The two positive roots corresponding to the Schwarzschild radius (here with corrections) and the cosmological one are

$$r_\star^{(1)} = \sqrt{3} r_\Lambda - r_s, \quad r_\star^{(2)} = 2 r_s \left(1 - \frac{1}{6} \left(\frac{r_s}{r_\Lambda} \right)^2 \right) . \tag{68}$$

In other words, the condition $C = -1/2$ is satisfied at the Schwarzschild radius and at the edge of the universe. With this limiting value, we have $|U_{\text{eff}}(r_\star)| = \frac{1}{2}$. The motion with $|U_{\text{eff}}(r)| \geq \frac{1}{2}$ becomes unphysical, since it corresponds to allowing the trajectory of test particles inside the Schwarzschild radius and beyond the observed universe. The latter is a result of the coincidence in the sense that r_Λ sets the scale of the horizon of the universe. Hence, the particles are allowed to be at some r such that

$$R_{\min} \simeq r_s < r < \sqrt{3} r_\Lambda \simeq R_{\max} \tag{69}$$

with

$$|C| < |U_{\text{eff}}(r)| < \frac{1}{2} \tag{70}$$

for negative C and U_{eff}. It is clear that at certain distance, the terms $-r_s/r$ and $r^2/(r_\Lambda)^2$ will become comparable (see Figure 2) leading to a local maximum located at

$$r_{\max} \simeq \left(3 r_s r_\Lambda^2 \right)^{1/3} \simeq 10^{-4} \left(\frac{M}{M_\odot} \right)^{1/3} \left(\frac{\rho_{\text{crit}}}{\rho_{\text{vac}}} \right)^{1/3} \text{Mpc} \, . \tag{71}$$

The value of the effective potential at this point is given by

$$U_{\text{eff}}(r_{\max}) \simeq -7.51 \times 10^{-16} \left(\frac{M}{M_\odot} \right)^{2/3} \left(\frac{\rho_{\text{vac}}}{\rho_{\text{crit}}} \right)^{1/3} . \tag{72}$$

Beyond $r_{\max}$, U_{eff} is a continuously decreasing function. This implies that $r_{\max}$ is the maximum value within which we can find bound solutions for the orbit of a test body.

Consider now the following chain of matter conglomeration of astrophysical objects: the smallest are star clusters (globular and open) with stars as members (i.e., we can set $M = M_\odot$) and a total mass of roughly $10^6 M_\odot$. We proceed to galaxies and galactic clusters. Within this chain, we find for $r_{\max}$ the following values as a function of mass:

$M/M_\odot$	$r_{\max}/\alpha$ (pc)
1	75
10^6	7.5×10^3
10^{11}	3.5×10^5
10^{13}	1.6×10^6

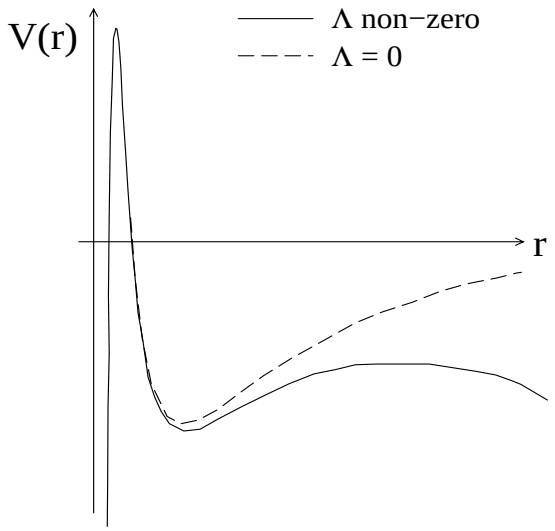

Figure 2: The effective potential drawn schematically, i.e, not to scale.

with $\alpha \simeq (\rho_{\rm vac}/\rho_{\rm crit})^{-1/3}$. The value of $r_{\rm max}/\alpha$ in the first line is of the order of magnitude of the tidal radius of globular clusters. The value in the second line is only one order of magnitude below the extension of an average galaxy including the Dark Matter halo. The reason could be that unlike the other three ones, where the argument M of $r_{\rm max}$ has been taken to be the mass of the average members of the astrophysical object, we have used in this case the mass of a globular cluster. It might appear unjustified to take the mass of the globular cluster to obtain the extension of the galaxy. However, in view of the fact that globular clusters are very old objects and are thought to be of importance in the formation of the galaxy, this choice seems to be justified. In principle, we could interpret $M = 10^6 M_\odot$ also as the black hole mass at the center of a galaxy.

The next two values of $r_{\rm max}$ are about the size of a galaxy cluster. The value $10^{13} M_\odot$ corresponds to a giant elliptic galaxy encountered often at the center of the clusters.

In conclusion, r_Λ in combination with r_s gives us surprisingly good estimates of astrophysical scales. The combination $r_{\rm max} = (3 r_s (r_\Lambda)^2)^{1/3}$ from which these scales where calculated is not an arbitrary combination with length dimension, but it is the distance beyond which we cannot find bound orbits. Therefore, we would indeed expect that $r_{\rm max}$ sets a relevant astrophysical scale. Of course, we are talking here about scales neglecting angular momentum and dynamical aspects of many body interactions, but no doubt $r_{\rm max}$ is roughly the scale to be set for bound systems.

A generalization of our theory is presented in [33].

It is justified to ask what happens in the case of non-zero $r_l \equiv L \neq 0$? The polynomial equations will become of higher order and it is not always easy to arrive at an analytical result. We will make an approximate estimate by determining first

a limiting value of r_l and using it in the Newtonian theory. To this end we look first for a saddle point, i.e.,

$$\frac{dU_{\rm eff}}{dr} = \frac{d^2U_{\rm eff}}{dt^2} = 0\,. \tag{73}$$

The two conditions lead to the position of the saddle point and a condition on one parameter, say for $x_l \equiv \frac{r_l^2}{(r_\Lambda)^2}$ in the form

$$x_l^4 - \left(\frac{3r_s}{4r_\Lambda}\right)^4 x_l - 12\left(\frac{3r_s}{4r_\Lambda}\right)^6 = 0\,. \tag{74}$$

To solve this fourth order equation we have to solve the associated third order equation, handle hyperbolic functions and their inverses, going through complex numbers and their roots. In the end we obtain the approximate simple expression

$$r_l^{\rm max} = 0.9(r_s^2 r_\Lambda)^{1/3}\,, \tag{75}$$

provided $r_s/r_\Lambda \ll 1$. For $r_l \geq r_l^{\rm crit}$ the local minimum and the second local maximum fall together and there are no more bound orbits. Taking now from non-relativistic mechanics the expression for the order of magnitude of a bound orbit, we conclude that

$$R_{\rm orbit} \sim \frac{r_l^2}{r_s} \to R_{\rm orbit}^{\rm max} \sim 0.55 r_{\rm max}\,, \tag{76}$$

which is a very satisfying result as it does not change the order of magnitude of the estimate with zero angular momentum and confirms our previous result.

A small note is in order here. To ensure the existence of the first local maximum and minimum of $U_{\rm eff}$ one has to require [23]

$$r_l^{\rm min} = 2\sqrt{3}r_s\,. \tag{77}$$

4.1. Velocity bounds

In connection with the geodesic equation of motion it is also possible to set a lower and upper bound on the radial velocity (assuming $r_l = 0$) v_0 at a distance r_0 [8, 5].

Starting with the obvious inequality

$$2{\rm e}^{2\nu(r)}|U_{\rm eff}(r_{\rm max})|(2|U_{\rm eff}(r)| - 1) < 0\,, \tag{78}$$

we arrive at

$$\Xi(r) < 2{\rm e}^{2\nu(r)}|U_{\rm eff}(r)| < {\rm e}^{2\nu(r)}\,, \tag{79}$$

with

$$\Xi(r) \equiv 2{\rm e}^{2\nu(r)}\left[\frac{|U_{\rm eff}(r)| - |U_{\rm eff}(r_{\rm max})|}{1 - 2|U_{\rm eff}(r_{\rm max})|}\right]\,. \tag{80}$$

The next step is to write the constant C as a function of the radial velocity (central in-fall) v_0 and r_0. This gives us

$$C = C(v_0, r_0) = \frac{v_0^2 + 2{\rm e}^{2\nu(r_0)}U_{\rm eff}(r_0)}{2\left({\rm e}^{2\nu(r_0)} - v_0^2\right)}\,. \tag{81}$$

Recall that satisfying

$$r_\star^{(2)} < r < r_\star^{(1)}\,, \tag{82}$$

is equivalent to

$$|U_{\rm eff}(r)| \leq 1/2\,. \tag{83}$$

Suppose now that we insist on a value v_0 such that

$$v_0 > {\rm e}^{\nu(r_0)}\,, \tag{84}$$

then we will violate the fundamental inequality i.e. $C \geq -1/2$. For, choosing $C > 0$ we automatically get

$$v_0^2 < 2{\rm e}^{2\nu(r_0)}|U_{\rm eff}(r_0)| < {\rm e}^{2\nu(r_0)}\,, \tag{85}$$

violating the assumption. If $C < 0$, then $|C| \leq 1/2$ leads to $|U_{\rm eff}(r_0)| \geq 1/2$ violating again one of the restrictions. Hence, for any r_0 which we parametrize as $r_0 = \zeta r_{\rm max}$ we are led to

$$\begin{aligned} v_{\rm max}(\zeta) &= {\rm e}^{\nu(r_0)} = 1 - \left(\frac{8}{3}\right)^{1/3} x^{2/3} f(\zeta) \\ &= 1 - 1 \times 10^{-15} \left(\frac{M}{M_\odot}\right)^{2/3} \left(\frac{\rho_{\rm vac}}{\rho_{\rm crit}}\right)^{1/3} f(\zeta)\,, \end{aligned} \tag{86}$$

with $f(\zeta) \equiv (2+\zeta^3)/2\zeta$. This represents the maximal value of the initial velocity at any r_0. The expression consists of a 1 (velocity of light) minus some corrections which are proportional $\rho_{\rm vac}$ manifesting another effect of the cosmological constant.

Let us turn our attention to the lower bound. Particles starting beyond the astrophysical scale $r_{\rm max}$ with velocity v_0 and at the position r_0 such that

$$C(v_0, r_0) < U_{\rm eff}(r_{\rm max}) < 0\,, \tag{87}$$

do not reach our Galaxy due to the potential barrier beyond $r_{\rm max}$. To determine what this exactly means, let us resolve the above inequality in terms of the velocity in dependence of the position. We obtain an inequality of the form

$$v_0^2 < \Xi(r_0) < 2{\rm e}^{2\nu(r_0)}|U_{\rm eff}(r_0)| < {\rm e}^{2\nu(r_0)}\,, \tag{88}$$

which means that particles whose velocity is smaller than

$$\begin{aligned} v_{\rm min}(\zeta > 1) &= \sqrt{\Xi(r_0)} = x^{1/3} \left(\frac{1}{3}\right)^{1/6} \\ &\times \left[1 - \left(\frac{8}{3}\right)^{1/3} x^{2/3} f(\zeta)\right] \sqrt{\frac{2f(\zeta)-3}{1-(3x)^{2/3}}}\,, \end{aligned} \tag{89}$$

do not reach the central object with mass M due to the potential barrier caused by Λ.

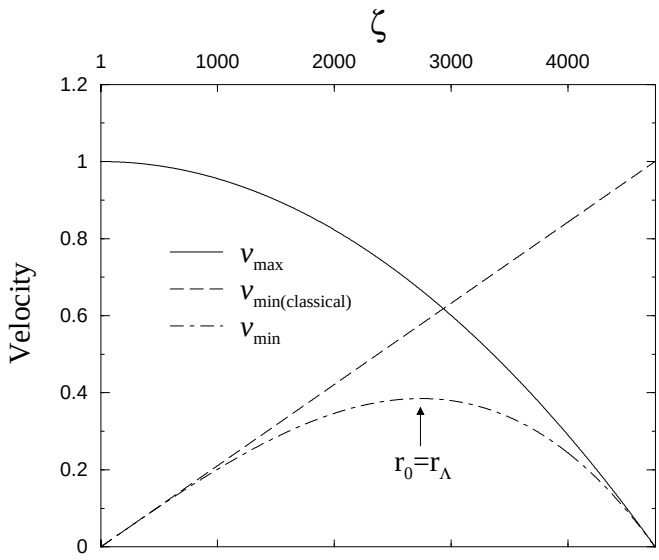

Figure 3: $v_{\max}$ and $v_{\min}$ against ζ. The window between $v_{\max}$ and $v_{\min}$ is the allowed region for initial velocities to reach the central object with mass M. The mass ratio is 10^{12}.

The results are summarized in Figures 3 and 4. Due to the restriction $C \geq -1/2$ the region $v_0^2 > \mathrm{e}^{2\nu(r_0)}$ is not accessible. Only, if the velocity lies in the range $\sqrt{\Xi(r_0)} < v_0 < \mathrm{e}^{\nu(r_0)}$, it can reach the origin. If $\sqrt{\Xi(r_0)} > v_0$ the test particle does not reach the central object. In our estimate, we neglect the fact that e.g. many galaxies are of spiral type and not spherically symmetric. This however, does not play a role, since r_0 is of the order of magnitude of Mpc. We do not consider here the details of what happens close to the galaxy.

5. The strong gravity scenario: Λ in black hole physics

So far we have explored different local aspects of the cosmological constant in the weak regime of gravity. We now turn to black holes and probe the effects of Λ via a Generalized Uncertainty Principle (GUP) [39, 4]. The keywords will be:

- black hole remnant with a minimum mass connected to a maximum temperature
- deformation of the standard (Hawking) dispersion relation $T(M)$ near the horizon $2r_s$
- maximum possible mass related to a minimum temperature which is an effect of Λ.

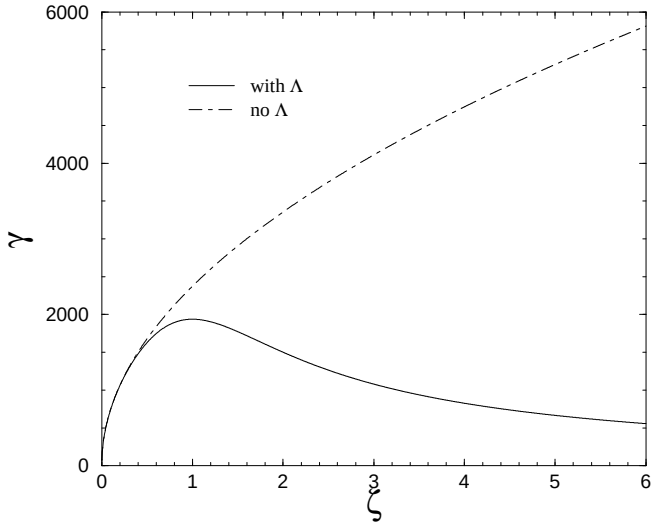

Figure 4: $\gamma = (1 - v^2_{\rm max}(\zeta))^{-1/2}$ versus ζ. The mass ration is 10^{12}.

Let us start with the GUP for the case of zero cosmological constant. This review will be brief and we refer the reader to the literature for more details [2, 3]. With $E = p$ we could tentatively write

$$a_G = \frac{G_N E}{r^2}\,. \tag{90}$$

As an order of magnitude estimate one sets

$$\Delta x_G \simeq \frac{G_N E}{r^2} L^2 \simeq G_N E = G_N p\,, \tag{91}$$

where we used $r \sim L$. Further, using $\Delta p \sim p$ we arrive at a new uncertainty relation (GUP) in the form

$$\Delta x \geq \frac{1}{2\Delta p} + \frac{G_N \Delta p}{2}\,. \tag{92}$$

Identifying $\Delta x \sim 2r_s = 2G_N M$ and $\Delta p \sim E \sim T$, we obtain via the GUP relation

$$2G_N M = 2\frac{M}{m_{\rm pl}} = \frac{1}{2T} + \frac{T}{m_{\rm pl}}\,. \tag{93}$$

Solving this equation for $T = T(M)$ and introducing a calibration factor $(2\pi)^{-1}$ gives

$$T(M) = \frac{1}{2\pi}\left(M - \sqrt{M^2 - m^2_{\rm pl}/2}\right)\,. \tag{94}$$

This short and intuitive road to Hawking's theory of black hole evaporation has several distinct features worth mentioning:

- The $T(M)$ dispersion relation reduces to Hawking's formula for large M, i.e., $T(M) = \frac{m_{\rm pl}^2}{8\pi M}$.
- However, it differs from the standard result for small masses. Indeed, we find a black hole remnant as
$$M > \mathcal{M}_{\rm min} = \frac{m_{\rm pl}}{2}\,. \tag{95}$$
This corresponds to $T_{\rm max} = m_{\rm pl}/4\pi$. We might expect such a result if the scales of the Newtonian constant set limiting values on physical parameters. We could also re-write the dispersion relation to obtain
$$T = \frac{1}{\pi}\frac{r_s}{l_{\rm pl}^2}\left(1 - \sqrt{1 - \frac{1}{4}\left(\frac{l_{\rm pl}}{r_s}\right)^2}\right)\,. \tag{96}$$
Hence, we again find a limit, this time on the the length scale, i.e., $L_{\rm min} = l_{\rm pl}/2$.

As a check of the black hole remnant we could also use a different approach [31, 32]. Starting with
$$0 < g_{00} = 1 - \frac{2G_N M}{R} = 1 - (8\pi/3)G_N\rho R^2\,, \tag{97}$$
we easily arrive at
$$\rho < \frac{3}{8\pi}\frac{1}{G_N R^2}\,. \tag{98}$$
Using the Stefan-Boltzmann law, $\rho = \sigma T^4$, leads to a limiting value on the temperature, namely,
$$T^4 < \frac{3}{8\pi}\frac{1}{\sigma G_N R^2}\,. \tag{99}$$
It is argued in [31, 32] that we necessarily have to have $R > 1/T$ which finally gives
$$T < T'_{\rm max} = \sqrt{\frac{45}{8\pi^2}}m_{\rm pl}\,. \tag{100}$$
Inserting into Hawking's formula yields another minimum mass (but the order of magnitude is the same as before)
$$M'_{\rm min} = \left(\frac{2}{5}\frac{1}{8\pi}\right)m_{\rm pl}\,. \tag{101}$$
Yet, another derivation of the same result has been done by Sakharov who also found a black hole remnant of the order of Planck mass.

Repeating the above steps with $\Lambda \neq 0$, we first assure that
$$0 < g_{00} = 1 - \frac{2r_s}{R} - \frac{R^2}{3r_\Lambda^2}\,. \tag{102}$$

This can be paraphrased as

$$0 < \rho < \frac{3}{8\pi}\frac{m_{\rm pl}^2}{R^2} - \frac{1}{3}\frac{3}{8\pi}m_{\rm pl}^2 m_\Lambda^2 \,. \tag{103}$$

Finally, using again $R > 1/T$, we obtain

$$\frac{1}{\sqrt{3}}m_\Lambda = T'_{\rm min} < T < T'_{\rm max} \,. \tag{104}$$

It is amazing how the two scales in gravitation, G_N and Λ, conspire to set a maximum and minimum value of a physical parameter. With $\Lambda = 0$ we had at least two independent ways to arrive at one and the same result (at least, viewing it as an order of magnitude estimate). Therefore, it is worthwhile to check if the same is possible for $\Lambda \neq 0$ confirming in this way the minimum temperature result and looking for maximum mass connected to the minimum temperature. To this end we will attempt a GUP which involves the cosmological constant. In doing so we will repeat many steps used in the derivation above.

The gravitational potential Φ for a spherically symmetric mass distribution with Λ

$$\Phi = -\frac{r_s}{r} - \frac{1}{6}\frac{r^2}{r_\Lambda^2} \,. \tag{105}$$

Then following the arguments from above the gravitational force per mass attributed to Λ is $\frac{|\vec{F}_\Lambda|}{m} = \frac{1}{3}\Lambda L$ where L is again a typical length scale in the problem under consideration. The corresponding displacement is $\Delta x_\Lambda \sim \frac{1}{3}m_\Lambda^2 L^3$. We now use the additional assumption $L \sim \frac{1}{\Delta p}$. This assumption is equivalent to saying that the precision of the momentum is inversely proportional to the typical length scale and can be found e.g. in textbooks in connection with wave packets. It is analogous to similar assumptions like $\Delta t \sim E^{-1}$ in the context of estimating the pion mass in Yukawa's theory or $\Delta x \sim p^{-1}$ in case we want to estimate the precision of the position. The proposed relation for GUP with the inclusion of the cosmological constant emerges then as [4]

$$\Delta x \sim \frac{1}{2\Delta p} + \frac{\Delta p}{2m_{\rm pl}^2} - \frac{\gamma}{3}\frac{m_\Lambda^2}{\Delta p^3} \,, \tag{106}$$

where we have taken into account the relative sign difference between the cosmological constant contribution and the standard Newtonian part. We also include a factor $\gamma \sim \mathcal{O}(1)$ which accounts for the fact that we are dealing with orders of magnitude estimates. As before in the context of Hawking radiation the uncertainty in position is associated with the event horizon. Then the Generalized Uncertainty Principle applied to black hole evaporation gives the equation

$$\frac{2M}{m_{\rm pl}^2} = \frac{1}{2T_*} + \frac{T_*}{2m_{\rm pl}^2} - \frac{\gamma}{3}\frac{m_\Lambda^2}{T_*^3} \,. \tag{107}$$

It is worth noting that for high temperatures, the previous results for $\Lambda = 0$ are recovered. Therefore, $T_{\rm max}$ in conjunction with $M_{\rm min}$ also follows from the above equation. For small temperatures, GUP can be approximated to

$$\frac{2M}{m_{\rm pl}^2} \approx \frac{1}{2T_*} - \frac{\gamma}{3}\frac{m_\Lambda^2}{T_*^3}\,, \tag{108}$$

which amounts to solving a third order polynomial equation of the form

$$T_*^3 - \left(\frac{m_{\rm pl}^2}{4M}\right) T_*^2 + \frac{\gamma}{6}\frac{m_\Lambda^2 m_{\rm pl}^2}{M} \;= 0\,. \tag{109}$$

In order to extract some physically relevant information we have to solve this third order polynomial. We skip all the technical steps and concentrate on the main aspects.

The crucial parameters in solving the third order equations turn out to be

$$\begin{aligned} p &= -\frac{m_{\rm pl}^4}{48M^2} \;< 0, \\ q &= \frac{m_{\rm pl}^4}{M}\left(-\frac{1}{864}\frac{m_{\rm pl}^2}{M^2} + \frac{\gamma}{6}\frac{m_\Lambda^2}{m_{\rm pl}^2}\right), \\ D &= \frac{1}{4}\frac{m_{\rm pl}^6 m_\Lambda^2}{M^2}\left(\frac{\gamma^2}{36}\left(\frac{m_\Lambda^2}{m_{\rm pl}^2}\right) - \frac{\gamma}{3(864)}\left(\frac{m_{\rm pl}^2}{M^2}\right)\right), \end{aligned} \tag{110}$$

where D is the discriminant of the system. It can be demonstrated that for $D > 0$ there are no physical solutions and only $D < 0$ is of interest to us. A limit on the value of M is set by putting $D = 0$. We find

$$M_{\rm max}^* = \frac{1}{6\sqrt{2\gamma}}\frac{m_{\rm pl}^2}{m_\Lambda}\,. \tag{111}$$

The explicit solutions are classified according to the sign of q. We introduce $M = \frac{M_{\rm max}^*}{\zeta}$ where $\zeta = 1$ corresponds to $M_{\rm max}^*$. For the branch $q > 0$ ($1 < \zeta < \sqrt{2}$), i.e., large masses we find

$$T(\zeta) = -\frac{\sqrt{2\gamma}m_\Lambda}{2\pi\zeta}\left(\cos\left(\frac{1}{3}\left(\cos^{-1}\left(-1 + \frac{2}{\zeta^2}\right) + 2\pi\right)\right) - \frac{1}{2}\right) \tag{112}$$

which is a monotonically decreasing function of ζ. This implies

$$T(1) = T_{\rm min} = \frac{\sqrt{2\gamma}}{2\pi}m_\Lambda \sim T'_{\rm min}\,. \tag{113}$$

For completeness, we quote also the explicit solution for the branch $q < 0$ ($\zeta > \sqrt{2}$) which is valid for smaller masses

$$T(\zeta) = \frac{\sqrt{2\gamma}m_\Lambda}{2\pi}\zeta\left(\cos\left(\frac{1}{3}\cos^{-1}\left(1 - \frac{2}{\zeta^2}\right)\right) + \frac{1}{2}\right)\,. \tag{114}$$

In conclusion, we have ascertained the existence of the following limiting values in the evaporation of a black hole

$$\begin{aligned} T_{\min} &\sim m_\Lambda \leftrightarrow M_{\max} \sim \frac{m_{\rm pl}^2}{m_\Lambda} \sim M_\Lambda \\ T_{\max} &\sim m_{\rm pl} \leftrightarrow M_{\min} \sim m_{\rm pl}\,. \end{aligned} \tag{115}$$

We draw the attention of the reader to the dual nature of the Newtonian and cosmological constant. If one sets a maximum (minimum) value, the other does the opposite, i.e., it defines the minimum quantity.

6. Λ and the gravitational waves

In testing Einstein's theory of gravity, its modifications and ramifications, two important sub-areas (among others) of research can be explored and explained in more detail. The first one has to do with cosmology and goes back to the discovery of dark energy which drives the acceleration of the universe. The second one is the possibility to detect gravitational waves directly. We all heard the news about the discovery of gravitational waves in 2016 [1] predicted by Einstein in 1916 [19]. Although we already had an indirect evidence through the Hulse–Taylor binaries in 1974 [25] (awarded Nobel Prize in 1993) we can still say that it took hundred years to confirm a prediction directly. We are interested in knowing if the cosmological constant has any effect on the propagation of the gravitational waves or, equivalently, if the length scale r_Λ will appear in the solutions of the linearized Einstein equations. The question does not address the cosmological aspect of Λ (the fact that the cosmological constant is part of the Friedmann equations) where the wave is interpreted as a ripple on the cosmological background. Since Λ is part of the Einstein tensor, it will also play a role in the linearized Einstein equations.

With the usual split of the metric

$$g_{\mu\nu} = \eta_{\mu\nu} + h_{\mu\nu}\,, \tag{116}$$

where $\eta_{\mu\nu}$ is the Minkowski metric the Einstein's equations in first order read

$$R^{(1)}_{\mu\nu} = -8\pi G S_{\mu\nu} - \Lambda\eta_{\mu\nu}\,. \tag{117}$$

In this equation we have used the trace-reversed part of the energy-momentum tensor

$$S_{\mu\nu} \equiv T_{\mu\nu} - \frac{1}{2}\eta_{\mu\nu}T\,. \tag{118}$$

The linearized expression of the Ricci tensor reads

$$R^{(1)}_{\mu\nu} \equiv \frac{1}{2}(\Box h_{\mu\nu} - \partial^\lambda\partial_\mu h_{\lambda\nu} - \partial^\lambda\partial_\nu h_{\lambda\mu} + \partial_\mu\partial_\nu h)\,, \tag{119}$$

such that the linearized equations take the form

$$\Box h_{\mu\nu} - \partial^\lambda \partial_\mu h_{\lambda\nu} - \partial^\lambda \partial_\nu h_{\lambda\mu} + \partial_\mu \partial_\nu h = -16\pi G S_{\mu\nu} - 2\Lambda \eta_{\mu\nu} \,. \tag{120}$$

Without the cosmological constant this equation is known as the Fierz–Pauli equation for a massless spin-2 object. The constant Λ does not play the role of a mass term in this equation as several other terms which could make it a mass term m_Λ^2 are missing.

This equation is clearly covariant under the local gauge transformation

$$h_{\mu\nu} \to h_{\mu\nu} + \partial_\mu \epsilon_\nu + \partial_\nu \epsilon_\mu \,, \tag{121}$$

as imposed by the general diffeomorphic covariance of the Einstein's equations with Λ. Any attempt to make the cosmological constant more dynamical by replacing $\Lambda \eta_{\mu\nu} \to \Lambda g_{\mu\nu}$ would spoil this gauge convariance. The gauge freedom allows us to fix the gauge which we choose to be the de Donder condition:

$$\partial^\mu h_{\mu\nu} = \frac{1}{2} \partial_\nu h. \tag{122}$$

The equation to be solved now becomes a wave equation with two kinds of inhomogeneities: one the standard source $S_{\mu\nu}(x)$ and the other a constant term proportional to the cosmological constant, i.e., [40]

$$\Box h_{\mu\nu} = -16 G S_{\mu\nu} - 2\Lambda \eta_{\mu\nu} \,. \tag{123}$$

A small check via the Veltmann Lagrangian

$$\mathcal{L}_h = -2\Lambda \left(1 + \frac{1}{2} h\right) - \frac{1}{4} \partial_\nu h_{\alpha\beta} \partial^\nu h^{\alpha\beta} + \frac{1}{4} \partial_\mu h \partial^\mu h - \frac{1}{2} \partial_\beta h \partial_\mu h^{\beta\mu} + \frac{1}{2} \partial_\alpha h_{\nu\beta} \partial^\nu h^{\alpha\beta} \tag{124}$$

is in order. Veltmann while deriving Feynman rules for graviton scattering derived the above Lagrangian which is invariant under gauge transformations. We use it to show that the Euler–Lagrange equations give the same linearized equation as above.

Since the equation is linear, we can split its solution in two parts

$$h_{\mu\nu} = \gamma_{\mu\nu} + \xi_{\mu\nu} \,, \tag{125}$$

where

$$\gamma_{\mu\nu} = e_{\mu\nu}(\mathbf{r}, \omega) \mathrm{e}^{i k_\alpha x^\alpha} + \text{c.c.} \,, \tag{126}$$

is the standard retarded solution written here for a monochromatic source at a distance far away from the source. The tensor $\xi_{\mu\nu}$ solves

$$\Box \xi_{\mu\nu} = -2\Lambda \eta_{\mu\nu} \tag{127}$$

and should satisfy the de Donder gauge. In addition, we demand that up to a diffeomorphism its asymptotic form is of the de Sitter metric. Such a solution satisfying these conditions is given by [40]

$$\begin{aligned} \xi_{00} &= -\Lambda t^2, \\ \xi_{0i} &= \frac{2}{3}\Lambda t x_i, \\ \xi_{ij} &= \Lambda t^2 \delta_{ij} + \frac{1}{3}\Lambda \epsilon_{ij}\,, \end{aligned} \tag{128}$$

where, $\epsilon_{ij} = x_i x_j$ for $i \neq j$ and 0 for $i = j$. This solution is to be used in the energy momentum pseudo–tensor $\hat{t}_{\mu\nu}$ for the gravitational waves. This pseudo-tensor $t_{\mu\nu}$ leading to the gravitational Poynting vector is well known to be [49]

$$(G_{\mu\nu} - G^{(1)}_{\mu\nu})/8\pi G\,, \tag{129}$$

where, again, the index 1 indicates that we expand the tensor in the order of $\mathcal{O}(\mathbf{h})$ and $G_{\mu\nu}$ needs to be expanded up to second order in $\mathcal{O}(\mathbf{h})$. After this expansion the tensor takes the form

$$\hat{t}_{\mu\nu} = t_{\mu\nu} - \frac{1}{8\pi G}\Lambda h_{\mu\nu}\,, \tag{130}$$

where $t_{\mu\nu}$ is the standard part defined by

$$t_{\mu\nu} = \frac{1}{8\pi G}\left(-\frac{1}{2}h_{\mu\nu}R^{(1)} + \frac{1}{2}\eta_{\mu\nu}h^{\sigma\rho}R^{(1)}_{\sigma\rho} + R^{(2)}_{\mu\nu} - \frac{1}{2}\eta_{\mu\nu}\eta^{\sigma\rho}R^{(2)}_{\sigma\rho}\right) + \mathcal{O}(\mathbf{h}^3)\,. \tag{131}$$

It remains to calculate the averaged gravitational Poynting vector. We quote the final result

$$\langle \hat{t}^{03}\rangle_{\rm wave} = \langle t^{03}\rangle_{\rm wave} = \frac{\omega^2 \hat{h}^2}{8\pi G}, \quad \langle \hat{t}^{03}\rangle_{\Lambda} = -\frac{1}{8\pi G}\frac{5}{18}\frac{1}{r_\Lambda^4}L^2\,, \tag{132}$$

where $\hat{h}$ is either $|e_{11}|$ or $|e_{12}|$ and L is the scale over which we average. Notice that due to Λ, the power

$$\frac{dP}{d\Omega} = r^2\frac{x_i}{r}\langle \hat{t}^{0i}\rangle \tag{133}$$

receives a negative contribution. The power is only well defined, i.e., positive definite below a certain critical distance $\mathcal{L}_{\rm crit}$ below which the oscillatory character of the solution dominates. To calculate this critical distance it suffices to compare the magnitudes of the two contributions to $\langle \hat{t}^{03}\rangle$. The result is [40]

$$\mathcal{L}_{\rm crit} = \frac{6\sqrt{2}\pi f \hat{h}}{\sqrt{5}} r_\Lambda^2\,, \tag{134}$$

where f is the frequency. Notice that what we are really comparing is the averaged solution proportional to Λ with the averaged wave component of the solution. We

then say that the wave character of the solution is lost when both are comparable. For a neutron star- neutron star (black hole-black hole) binary with a frequency of 100 Hz and $\hat{h} = 10^{-23}$ (10^{-22}) at a distance of 10^8 pc (2^8 pc) we get 0.13×10^8 pc (1.3×10^8 pc) which is smaller than the distance from the objects and hence the wave character would be lost at our position.

One might argue that a better approach to the problem is to expand the solution around the de Sitter background and not the Minkowski one as we have done above. In such a case Λ is part of the background and not part of the solution as in our case. If we do that, we consider the de Sitter spacetime as the tangential one. Then we should ask ourselves the question if being consistent we should not do the same for all other problems, especially in the framework of quantum field theory (replacing the Poincaré group by the de Sitter group). One of the consequences would be a change in the Casimir operators, i.e., the way we classify the elementary particles according to mass and spin. Be it as it may, I would like to close with a quote of Isaac Asimov

> *The most exciting phrase to hear in science, the one that heralds new discoveries, is not Eureka! (I found it!), but rather, hmm, thats funny.*

7. Conclusions

The cosmological constant is still a controversial quantity, but it has gained some popularity since the discovery of the accelerated expansion of the universe. Its main effect remains within the realm of cosmology, but since it is part of the Einstein tensor it affects also local physics. The most prominent local effects are:

- The existence of a last bound orbit due to a meaningful combination of large scales and small scales e.g. $r_{\max} \sim (r_s r_\Lambda^2)^{(1/3)}$ which enters the geodesic equation of motion and is of astrophysical orders of magnitude.

- The cosmological constant will change the equilibria concepts, especially for astrophysical objects far away from spherical symmetry. This is manifest in the inequality for constant density $\rho > A\rho_{\text{vac}}$ where A is purely of geometrical nature.

- If we linearize Einstein gravity around the Minkowski spacetime, Λ will change our understanding of the propagation of gravitational waves at large distances We derived a condition for the distance, i.e., $r < \mathcal{L}_{\text{crit}}(\Lambda)$ in order for the 'wavy' character to dominate and the power to be positive-definite.

Even in black hole physics Λ leaves its fingerprints, not as a sizeable effect, but rather by setting certain limiting values. Since this happens also elsewhere in connection with the cosmological constant we give a brief summary below

- The Newtonian limit demands

$$R_{\min} \sim 2r_s \ll r \ll R_{\max} \sim r_\Lambda \,. \tag{135}$$

- Demaning the existence of a bound orbit leads to

$$L_{\min} \sim r_s \ll L \ll L_{\max} \sim (r_s^2 r_\Lambda)^{(1/3)} \,, \tag{136}$$

  where we can see the combination of different scales at work.

- Finally, via a Generalized Uncertainty Principle one can establish limits on the temperature and mass, namely

$$\begin{aligned} T_{\max} &\sim m_{\rm pl} \leftrightarrow T_{\min} \sim m_\Lambda \\ M_{\min} &\sim m_{\rm pl} \leftrightarrow M_{\max} \sim m_{\rm pl}^2/m_\Lambda \,. \end{aligned} \tag{137}$$

  One cannot help but see the dual role of the Newtonian and cosmological constant in these limiting values.

Let me end this small review by quoting D. Adams in 'The Hitch-hiker's guide to the Galaxy':

> *"There is a theory which states that if ever anyone discovers exactly what the Universe is for and why it is there, it will instantly disappear and be replaced by something even more bizarre and inexplicable.*
> *There is another theory which states that this has already happened."*

This fits the theory and history of the cosmological constant: Einstein has introduced it to construct his static universe which after all decided to be more dynamical and expand. After this the cosmological constant fell from grace so much so that people were looking for explanations why it should be zero. Another twist in the story (the discovery of the accelerated expansion) forced us to re-consider the status of this constant and we are now trying to explain why it is non-zero (or replace it by other more complicated theories).

Acknowledgment

The author acknowledges the support from the Faculty of Science of the Universidad de Los Andes, Bogotá and would like to thank the administrative department of science, technology and innovation of Colombia (COLCIENCIAS) for financial support.

References

[1] Abbott, B. P., et al.: Phys. Rev. Lett. **116** (2016), 061102.

[2] Adler, R. J., Santiago, D. I.: Mod. Phys. Lett. **A14** (1999), 137.

[3] Adler, R. J., Chen, P., Santiago, D. I.: Gen. Rel Grav. **33** (2001), 2108.

[4] Arraut, I., Batic, D., Nowakowski, M.: Class. Qunat. Grav. **26** (2009), 125006.

[5] Arraut, I., Batic, D., Nowakowski, M.: Central. Eu. J. Phys. **9** (2011), 926.

[6] Balaguera-Antolinez, A., Nowakowski, M.: Astron.- Astrophys. **441** (2005), 23.

[7] Balaguera-Antolinez, A., Boehmer, C. G., Nowakowski, M.: Int. J. Mod. Phys. **D14** (2005), 1507.

[8] Balaguera-Antolinez, A., Boehmer, C. G., Nowakowski, M.: Class. Quant. Grav. **23** (2006), 485.

[9] Balaguera-Antolinez, A., Mota, D. F., Nowakowski, M.: Class. Quant. Grav. **23** (2006), 4497.

[10] Balaguera-Antolinez, A., Nowakowski, M.: Class. Quant. Grav. **24** (2007), 2677.

[11] Balaguera-Antolinez, A., Mota, D. F., Nowakowski, M.: MNRAS **382** (2007), 621.

[12] Binney, J., Tremaine, S.: *Galactic Dynamics*. Princeton Univresity Press, Prenceton 1987.

[13] Canfora, F., Giacomini, A., Pavluchenko, S.: Phys. Rev. **90** (2014), 04354.

[14] Carroll, S.: Living Reviews in Relativity, (2001), 4:1.

[15] Carroll, S., Press, W., Turner, E.: Rev. Astro. Astrophys. **30** (1992), 499.

[16] Copperstock, F. I., Faraoni, V., Vollick, D. N: Astrophys. J. **503** (1998), 61.

[17] Dumin, Y. : Phys. Rev. Lett. **98** (2007), 059001.

[18] Dyson, L., Kleban, M., Susskind, L.: JEHP (2002), 0210:011.

[19] Einstein, A.: Situngzber. Pruess. Akad. Wiss, part 1 **688**, 1916.

[20] Einstein, A.: Sitzungsber. Preuss. Akad. Wiss., Phys.-math. Klasse Vi **442** (1917).

[21] Einstein, A., Strauss, E. G: Rev. Mod. Phys. **17** (1945), 120.

[22] Felten, J. E., Isaacsman, R.: Rev. Mod. Phys. **58** (1986), 689.

[23] Fliessbach, T.: *Allgemeine Relativitätstheorie*. Spectrum Akademischer Verlag, Heidelberg 2003.

[24] Frieman, J. A., Turner, M. S., Huterer, D.: Ann. Rev. Astro. Astrophys. **46** (2008), 385.

[25] Hulse, R. A., Taylor, J. H.: Astrophys. J. **191** (1974) L59.

[26] Kamenshchik, A. Y., Moschellai, U., Pasquier, V.: Phys. Lett. **B511** (2001), 265.

[27] Lovelock, D.: Aequat. Math. **4** (1970), 127.

[28] Lovelock, D.: J. Math. Phys. **12** (1971), 498.

[29] Lovelock, D.: J. Math. Phys. **13** (1972), 874.

[30] Martin, J.: Comptes Rendus d'Academie des Sciences **13** (2012), 566.

[31] Massa, C.: Am. J. Phys. **54** (1986), 733.

[32] Massa, C.: Am. J. Phys. **57** (1989), 01.

[33] Nandra, P., Lasenby, A. N., Hobs, M. P.: MNRAS **422** (2012), 2931.

[34] Noerdlinger, P. D., Petrosina, V.: Astrophys. J. **168** (1971), 1.

[35] Nowakowski, M.: Int. J. Mod. Phys. **D10** (2001), 649.

[36] Nowakowski, M., Sanabria, J. C., Garcia, A.: Phys. Rev. **D66** (2002), 023003.

[37] Nowakowski, M., Balaguera-Antolinez, A.: AIP Conf.Proc. 861 (2006), 1001–1008.

[38] Nowakowski, M., Arraut, I.: Braz. J. Phys. **38** (2008), 425.

[39] Nowakowski, M., Arraut, I.: Mod. Phys. Lett. **A24** (2009), 2133.

[40] Nowakowski, M.: Acta. Phys. Polon. **41** (2010), 911.

[41] Padmanabhan, T.: Phys. Rep. **380** (2003), 235.

[42] Peebles, P. J. E., Ratra, B.: Rev. Mod. Phys. **75** (2003), 559.

[43] Perlmutter, S. et al.: Astrophys. J. **517** (1999), 565.

[44] Riess, A. et al.: Astron. J. **116** (1998), 1009.

[45] Rugh, S., Zinkernagel, H.: Studies on History and the Philosophy of Modern Physics **33** (2001), 663.

[46] Sahni, V., Starobinsky, A.: Inter. J. Mod. Phys. **D9** (2000), 373.

[47] Straumann, N.: arXiv: gr-qc/0208027.

[48] Weinberg, D. H. et al.: Phys. Rep. **530** (2013), 87.

[49] Weinberg, S.: *Gravitation and Cosmology*. John Wiley and Sons, 1972.

[50] Weinberg, S.: Rev. Mod. Phys. **61** (1989), 1.

[51] Weinberg, S.: arXiv: astro-ph/0005265.

Conference *Cosmology on Small Scales 2016*
Michal Křížek and Yurii Dumin (Eds.)
Institute of Mathematics CAS, Prague

THEORETICAL ESTIMATION OF THE HUBBLE CONSTANT

Igor N. Taganov

Russian Geographical Society;
International Interdisciplinary Research Project "Time Pace"
(`www.timepace.net` and `www.spiraltime.org`)
Grivtsova Str. 10, Saint Petersburg, 190000 Russian Federation
taganov.igor@mail.ru

Abstract: Applying metrological interpretation of the Hubble constant is possible using "metaphysical" principles – the Principle of least action and the Principle of measurement relativity to obtain a theoretical estimate of its value:

$$H = 9G\hbar/16c^2r_e^3 = 1.97 \cdot 10^{-18}\,\mathrm{s}^{-1}(\approx 61.6\,\mathrm{km/s/Mpc}), \quad r_e = e^2/m_ec^2$$

Metrological interpretation also makes it possible obtaining estimates of the value of the Hubble constant from astronomical observations of motion deviations of the Earth, the Moon, Mercury and Venus: $H_a = (2.08 \pm 0.24) \cdot 10^{-18}\,\mathrm{s}^{-1}(65 \pm 7.5\,\mathrm{km/s/Mpc})$, as well as from statistics of isotopic estimates of the age of rocks from the Earth and the Moon: $H_I = (2.15 \pm 0.2) \cdot 10^{-18}\,\mathrm{c}^{-1}(67.2 \pm 6\,\mathrm{km/s/Mpc})$. The proposed methodology allows developing of the Metaphysical cosmology (MC), in which the key parameters of the Universe are determined by the metaphysical principles — the Principle of least action and the Principle of measurement relativity, and their values are defined by laconic functions of the fundamental physical constants.

Keywords: Metaphysical cosmology, Hubble constant, redshift, Solar system

PACS: 04.20.Gz, 98.80.-k, 96.15.De, 05.30.Ch

In the modern methodology of Natural sciences the Metrological doctrine is defined by the Principle of the measurement relativity, which asserts that the essence of laws of nature do not depend on the standards used in the measurements of physical characteristics that are included in these laws. One of the consequences of the Principle of the measurement relativity is the constancy of the ratio of two absolute values of a physical quantity when the standards used in the measurements change.

The Principle of measurement relativity unambiguously determines the functional structure of the dimensions of physical quantities $[F]$ in the form of power monomials: $[F] = L^aM^bT^c$ of basic, primary dimensions, such as the fundamental triad

– "space L – mass M – time T" (e.g. the dimension of energy in the CGS system is $\mathrm{g\,cm^2\,s^{-2}}$).

Mathematical operations with dimensional quantities are only possible in the case when the permanent relations for the basic, primary dimensions are known. For example, it is necessarily to know two independent relations for three basic dimensions. In the modern dimensional analysis such relations are: Newton's law of gravity with standardized value of the Earth gravitational acceleration $9.80665\,\mathrm{m/s^2}$, which are necessary for using the international standard of mass — the platinum-iridium weight, stored at the International Board of Weights and Measures in Sevres (France). Second "canonized" relation for the base units is the postulate of the universal constancy of the speed of light: $c = \mathrm{const} = 299\,792\,458\,\mathrm{m/s}$, which has been adopted for the creation of modern international standards of length ("meter") and time ("atomic second").

The existence of "canonized" fundamental constants as a part of the modern systems of units provides the possibility of reducing the number of independent basic units of measurement and dimensions. For example, the principle of the constancy of the speed of light makes it possible to introduce the relation between units of length and time: $1\ \mathrm{s} = 2.998 \cdot 10^{10}$ cm, and the gravitational constant defines the relation: $1\ \mathrm{g} = 1.347 \cdot 10^{28}$ cm.

Since the dimensions of the physical quantities used in the Natural sciences are determined by power monomials of the form $[F] = L^a M^b T^c$, the application of two independent relations between the basic primary units of the fundamental triad allows one to select any of the basic units as a single, "unitary" basic dimension for all physical quantities: $[F] \propto L^n$ or M^n or T^n with $n = 0, \pm 1, \pm 2 \ldots$ In particular, the permanent relations between the basic units allow the dimensions of all physical quantities to be reduced to a "geometrical" form: $[F] = L^a M^b T^c \propto L^{n=a+b+c}$. For example, using the relations between the basic units, one can determine the geometric dimension of the elementary electric charge from the constant of fine structure $\alpha = e^2/hc = 7.297 \cdot 10^{-3}$:

$$e = 1.86 \cdot 10^{-6}\,\mathrm{cm}, \quad e/m_e = 1.516 \cdot 10^{-7}. \tag{1}$$

An important consequence of the Principle of measurement relativity is the independence of scale-factors a_i on the physical nature of the standards used for the basic units. For example, it is assumed that any length can be measured as by finite macroscopic intervals of length r_i and with the help of microscopic, quantum characteristics, for example, using the wavelengths of photon λ_i. With independence of the basic units on the physical nature of standards used for scales R_0, λ_0 the following relation for the scale-factor holds:

$$a = r/R_0 = \lambda/\lambda_0 = 1 + z, \quad z = \lambda/\lambda_0 - 1, \tag{2}$$

where z is called the *redshift*.

Relations (2) allow the use of the selected basic system of units for measuring physical characteristics of objects, regardless of their size. For example, in the SI system, we define the radius of the Earth and the radius of the proton in "meters". Belief in the independence of the reference values of the basic units on physical nature of the used material standards embodied in modern metrology justifying the use of microscopic quantum devices, as standards of international macroscopic basic units — "meter" and "second".

The use of kinematic relation between the wavelength of a photon λ_0 and the period δt_0 associated with the photon oscillations: $\lambda_0 = c \cdot \delta t_0$ enables us to represent the scale-factor in the form of: $a = r/R_0 = \lambda/c\delta t_0$. When we measure macroscopic distances $r >> \lambda$ using light pulses, as it occurs in the modern standard of "meter", this ratio can be approximated: $\lambda \approx dr; \delta t_0 \approx dt$ and then the relation (2) becomes:

$$a = c/R_0 \cdot r = dr/dt = 1 + z. \tag{3}$$

In 1933–1944, developing the "Kinematic cosmology", Edward Milne and Arthur Walker proved [2] that the central relation in (3): $dr/dt \propto r$ is one of the possible form of the condition of isotropy of spherically symmetric volume of space, which explores an observer. Earlier, in 1910, Vladimir Ignatovsky demonstrated the possibility of an axiomatic formulation of the Special theory of relativity (STR), based on the following assumptions [1]:

1. Principle of relativity, asserting the equivalence and equality of inertial reference systems.

2. The assumption of the linear form of coordinate transformations between inertial reference frames.

3. The assumption of space isotropy.

In axiomatic STR, the Poincaré-Einstein postulate of independence of speed of light from the motion of its source is not used as the initial assumption, and the relativistic velocity addition rule becomes one of results of the Ignatowsky's axiomatic STR. The assertion that a photon moving at the speed of light in one reference frame, will move with the same speed in any other frame of reference has lost the status of a postulate, becoming the proven theorem in the axiomatic STR.

In (2), (3) the equality of the second and fourth terms: $c/R_0 \cdot = 1 + z$ is the "Hubble law": $cz = Hr$ in the coordinate system corresponding to the condition: $r = 0 : z = 0$ with the "Hubble constant" $H = c/R_0$. In the approximate formulation of the Principle of measurement relativity (3) $V = dr/dt$ defines the "apparent" velocity of the Universe expansion. Consequently, the redshift phenomenon not at all indicates expansion of the Universe, but is a result of the universal application of the Principle of measurement relativity for measuring both the microscopic characteristics of photons (λ) and giant cosmic distances (r).

The basis of modern theoretical cosmology is the definition of a 4-dimensional radial interval in a spherically symmetric "flat" spacetime by the Robertson-Walker metric with Newtonian time (t):

$$ds^2 = c^2dt^2 - a^2(t) \cdot dr^2. \tag{4}$$

Cosmological models studied in cosmology differ only in the form of the dependence of the scale–factor on time $a(t)$, which in the doctrine of the expanding Universe is often interpreted as a change of the observable Universe radius: $a(t) = R(t)/R_0$.

As was already noticed in 1930s by Richard Tolman the non-static metric with interval (4) does not provide the constancy of the speed of light — for a photon trajectory ($ds = 0$) from (4) it follows a variable speed of light: $dr/dt = c/a(t) \neq \text{const}$.

The variability of the speed of light in (4) is a serious drawback of many cosmological models, since, firstly, it contradicts to the relativistic physics of photons and disagrees with the Metrological doctrine of modern Natural sciences, which presupposes the universal constancy of the speed of light. Secondly, it makes the cosmological research of the past of the Universe misleading, since most of the important physical equations cannot be used with variable speed of light.

It is reasonable to use a generalization of the interval (4) changing the reversible Newtonian time (t), by more general irreversible "physical" time (τ):

$$ds^2 = c^2d\tau^2 - a^2(\tau) \cdot dr^2. \tag{5}$$

The equations for the derivatives of scale-factor $a = r/R_0 : da/dt = \dot{a}$ and $da/d\tau = \acute{a}$ may be obtained from (5) using the condition of the universal constancy of the speed of light on the all trajectories of photons $(ds = 0) : dr/dt = adr/d\tau = c = \text{const}$. Hence:

$$d\tau/dt = a, \quad \dot{a} = \acute{a} \cdot a \tag{6}$$

The Principle of least action: $dS/d\tau = 0 \rightarrow S = \text{const}$ can be represented, in particular, as the constancy of the product of momentum p, per unit mass of the moving body by its radial path: $S = p_r \cdot r = r' \cdot r = \text{const}$. From this definition of constant action for the moving body with the scale-factor: $a = r/R_0; R_0 = \text{const}$ it follows the equation: $a' \cdot a = A = \text{const}$. The solution of this equation for the initial condition: $\tau = 0 : a = 1$ is the function: $a = (1 + 2A\tau)^{1/2}$. Substituting this function into (6), we obtain the equation: $d\tau/dt = (1 + 2A\tau)^{1/2}$, the solution of which for the initial condition: $t = 0 : \tau = 0$ leads to relations:

$$\begin{aligned} &\tau = t + At^2/2, && a = (1 + 2A\tau)^{1/2}, \\ &t = A^{-1}[(1 + 2A\tau)^{1/2} - 1], && a = (1 + At). \end{aligned} \tag{7}$$

Visual representations of physical processes with the use of potentials play an important role in physics, allowing the wide use of general equation: $\bar{q} = \nabla\phi$, in which the vector characteristic of a process – "flux" or "flow" $\bar{q}$ is determined by the

gradient of potential ϕ. This representation is used, for example, in electrodynamics, hydrodynamics, and thermodynamics to describe physical "flows". With the help of (7) the "flow" of physical time can be presented in the same visual form:

$$q_\tau = d\tau/dt = \nabla_t \tau = (1 + 2A\tau)^{1/2} = 1 + At. \tag{8}$$

The flow of physical time is directed from the past with smaller characteristic intervals into the future with larger characteristic intervals.

To determine the constant A in (7), (8) we can use the formulation of the Principle of measurement relativity (3), which corresponds to Milne–Walker postulate about isotropy of spherically symmetric volume of space: $dr/dt = \nu \propto r$ and to the empirical Hubble law: $H = \dot{a}/a = \text{const}$. For (7) this relation is: $H = \dot{a}/a = A/(1 + At)$ and for cosmologically short-term observations $(1 + At \approx 1)$ it determines the approximate estimate: $A \approx H$.

Equations (7) demonstrate a progressive increase of physical time intervals comparing to the scale of constant intervals of Newtonian time, which is a kind of "expansion" or "acceleration" $(d\tau/dt = a > 0)$ of the physical time. Modern cosmology often uses the term "expansion of space". However, instead of rather tongue-tied words "expansion of time" seems appropriate to use the more precise term "deceleration of the pace of time". Poincaré, Einstein, and Minkowski have already started to apply the term "time pace" already during development of the STR. The pace (or "rate", "course", or "flow") of physical time $\Delta\tau^{-1}(s^{-1})$ having dimension of frequency is defined as the parameter inverse with respect to some characteristic time interval $\Delta\tau$. Increase of the characteristic time intervals as is the case in (7) and (8) corresponds to decrease of magnitude of the time pace, that is, corresponds to the "deceleration of physical time pace".

Direction of the "Arrow of time" and "flow of time" is defined by the pace of time. There is no direction of the reversible Newtonian time: $t + (-t) = 0$. Orientations of the "Arrow of physical time": $\tau(t) + \tau(-t) > 0$ and the "time flow" (8) define an objective difference between the future and the past. In accordance with (7) for $A \approx H$ the use of the "present" standard of time interval leads to a linear decrease of the physical and Newtonian intervals ratio in the past (negative t and τ): $\tau/t = 1 - H/2 \cdot t$. On the contrary, this ratio linearly increases for time intervals in the future (positive t and τ):$\tau/t = 1 + H/2 \cdot t$.

The phenomenon of pace deceleration of irreversible physical time is consistent with the general concept of relativistic time dilation. In STR, time dilation is defined by Lorentz transformations for two inertial reference systems. More generally, the time dilation is defined by the coordinate transformations that take into consideration the relative acceleration of reference systems. In the concept of equivalence of inertial and gravitational masses (in General theory of relativity — GTR) time dilation is determined by the difference in gravitational potentials of compared frames of reference. The phenomenon of the cosmological deceleration of time pace is result of comparing the reference systems of different scales — the microscopic frame of

reference with quantum kinematics and the macroscopic one used, for example, in cosmology.

Hubble law in the form: $r = c/H \cdot (\lambda - \lambda_0)/\lambda_0$ can be regarded as a transformation of the spatial coordinate of the line of sight in the microscopic quantum system of reference for sole photon into macroscopic system of reference. In the complete transformation of the coordinate system, the appropriate transformation of time should be defined in addition to the transformation of the spatial coordinate. The relation (7) for $A \approx H : \tau = t + H/2 \cdot t^2$ complements the Hubble law, determining the appropriate transformation of time, when comparing the microscopic quantum systems of reference with macroscopic ones.

The physical nature of observed manifestations of the cosmological deceleration of the pace of time is rooted in the fact that all uniform motions in decelerating physical time analyzed with the use of invariable uniform Newtonian time scale look as accelerating under influence of virtual forces (Taganov, Saari [4, 5]).

Most impressively cosmological phenomenon of time pace deceleration is manifested in the apparent secular growth of the Earth's rotation. Recently, the international services of exact time started quite accurately measuring of the secular acceleration of the Earth's rotation, which appeared should lead to a decrease in the average Length of day (LOD) after exclusion of all tidal influences by about: $1.7 - 2.3 = -0.6\,\mathrm{ms/century}$. For the standard length of the day 86 400 s and 36 525 days of Julian century, the average rate of this LOD decrease can be estimated as: $d\Delta/dt$; $[(1.7 - 2.3) \cdot 10^{-3} \cdot 36525]/(86400 \cdot 36525) = -6.94 \cdot 10^{-9}$.

This apparent Earth acceleration is the manifestation of the cosmological deceleration of time for which from (7) with $A \approx H$ follows: $\Delta t = t - \tau = -H/2 \cdot t^2$. This relation and the Hubble constant value (e.g. the estimation $H_0 = (2.17 \pm 0.02) \cdot 10^{-18}\mathrm{s}^{-1}$ by the international research project "Planck" in 2013) allow for the theoretical estimation of the potential LOD decrease rate: $d\Delta t/dt = -Ht = 2.17 \cdot 10^{-18} \cdot 86400 \cdot 36525 = -6.85 \cdot 10^{-9}$. Comparing these two estimations one sees that theoretical estimate differs from observational one less than in 2 %, which is significantly less than the mean uncertainty of the observational data.

Astronomical observations of the Moon, the Earth, Venus and Mercury revealed unexplained accelerations of planet movements that are proportional to their average orbital motions, see references in [4, pp. 115, 118, 119] or [5, pp. 126, 130, 131]. In accordance with Kepler and Newton laws the longitude of a planet is described by equation: $L_t = L_0 + nT_c$ where n is the mean motion of the planet in arc seconds per century (as/cy) and T_c is the time measured in Julian centuries. However, the use of (7) with $A \approx H$ for decelerating physical time leads to another equation: $L_\tau = L_0 + nT_c + n \cdot H_c/2 \cdot T_c^2$ (here $H_c = 6.217 \cdot 10^{-9}$ 1/year, corresponding to (25)). The last term in the right-hand side of this equation describes "accelerations" of planets which astronomers observe.

The value of a planet longitude deviation from Kepler and Newton laws is estimated in astronomy by the longitude correction δL , which is equal to the difference between the theoretical longitude: $L_t = L_0 + nT_c$ and observed longitude. Using this

equation and (7) with $A \approx H$, which determines the deceleration of physical time pace, we can get an estimate of the "cosmological correction" for the longitude of a planet:

$$\delta L = L_t - L_\tau = -n \cdot H_c/2 \cdot T_c^2. \tag{9}$$

The comparison of the theoretical values of cosmological corrections (9) for the planet motions with their observational estimations shows that the discrepancy between them does not exceed the statistical observation uncertainties.

The Moon ($n = 1.74 \cdot 10^9$ as/cy). Cosmological correction (9): 5.41 as/cy^2. Average correction in accordance with observations: $\langle \delta L \rangle = 6.2 \pm 0.7$ as/cy^2, see references in [4, p. 115] or [5, p. 126].

The Mercury ($n = 5.4 \cdot 10^8$ as/cy). Cosmological correction (9): 1.68 as/cy^2. Average correction in accordance with observations: $\langle \delta L \rangle = 1.62 \pm 0.26$ as/cy^2, see references in [4, pp. 118–119] or [5, pp. 130–131].

The Venus ($n = 2.1 \cdot 10^8$ as/cy). Cosmological correction (9): 0.66 as/cy^2. Average correction in accordance with observations: $\langle \delta L \rangle = 0.61 \pm 0.1$ as/cy^2, see references in [4, pp. 118–119] or [5, pp. 130–131].

The Earth ($n = 1.296 \cdot 10^8$ as/cy). Cosmological correction (9): 0.4 as/cy^2. Average correction in accordance with observations: $\langle \delta L \rangle = 0.47 \pm 0.23$ as/cy^2, see references in [4, p. 115] or [5, p. 126].

The phenomenon of cosmological deceleration of time pace gives a unique opportunity to estimate the value of the Hubble constant not from the redshifts of distant galaxies, but from the observations of orbital motion of the Earth, the Moon, Venus, and Mercury. From (9) for $T_c = 1$ cy we can get the formula for the observational estimation of the Hubble constant: $H_{c(\mathrm{obs})} = 2\langle \delta L \rangle / n$. This formula with average observational values of $\langle \delta L \rangle$ for planets gives the following average observational estimation of the Hubble constant: $H_{\mathrm{obs}} = (6.55 \pm 0.75) \cdot 10^{-9}\,\mathrm{cy}^{-1} = (2.08 \pm 0.24) \cdot 10^{-18}\,\mathrm{s}^{-1}(65 \pm 7.5\,\mathrm{km/s/Mpc})$. This estimation is close to the theoretical value of the Hubble constant (25): $H = 1.97 \cdot 10^{-18}\,\mathrm{s}^{-1}(61.6\,\mathrm{km/s/Mpc})$ and corresponds well to the recent estimation of Hubble constant by international astrophysical project "Planck": $(2.17 \pm 0.02) \cdot 10^{-18}\,\mathrm{s}^{-1}(67.8 \pm 0.77\,\mathrm{km/s/Mpc})$.

Manifestations of the phenomenon of the cosmological deceleration of time pace can be observed not only in the grand scale of the Universe or the Solar system, but also in microcosm. In particular, the deceleration of physical time pace with respect to the uniform invariable Newtonian time scale reveals itself in the analysis of the radioactive decay data (Taganov 2003–2013 [3, 4]).

In accordance with (7) for $A \approx H$ the radioactive isotope decay in physical time is described by the modified Rutherford law:

$$N_\tau^I = N_0^I \exp(-\lambda_\tau^I \tau) = N_0^I \exp[-\lambda_\tau^I (t + Ht^2/2)].$$

In order that for a shorter interval of physical time disintegrated the same amount of isotope atoms as for larger interval of Newtonian time the physical decay constant λ_τ^I should be larger than the Newtonian decay constant λ_t^I, and therefore in the retrospective analysis of isotope decay always: $\lambda_\tau^I > \lambda_t^I$.

From this analysis follows that simultaneous estimation of the sample age in Newtonian time scale with two isotopes with different decay rate constants gives two different values with the difference:

$$t_e^{(1)} - t_e^{(2)} = t_e^{(1)} \cdot [1 - (\lambda_t^{(1)}\lambda_\tau^{(2)})/(\lambda_\tau^{(1)}\lambda_t^{(2)})], \quad \lambda_t^{(1)} > \lambda_t^{(2)}. \tag{10}$$

The estimations of sample's Newtonian age made with isotope with larger lifetime will give the smaller age estimation.

Analysis of publications with evaluations of geological sample ages performed using simultaneously (U/Pb), (Rb/Sr), and (Sm/Nd) isotopic methods reliably confirms the predicted discrepancy of isotope age estimations [3]– [6].

Using the statistics of differences in isotopic estimations of the age of geological samples we can calculate the estimate of the Hubble constant: $H_I = (2.15 \pm 0.2) \cdot 10^{-18}\,\mathrm{s}^{-1}(67.2 \pm 6\,\mathrm{km/s/Mpc})$. This estimation is close to the theoretical value of the Hubble constant (25): $H = 61.6\,\mathrm{km/s/Mpc}; (1.97 \cdot 10^{-18}\,\mathrm{s}^{-1})$ and correspond to the commonly used in astrophysics interval: $H_0 = 60 - 75\,\mathrm{km/s/Mpc}$.

The model of physical time with decelerating pace provides basic formulae of cosmography, which can be compared with observations. From (7) with $A \approx H$ it is possible to derive the analogue of the Hubble law for decelerating physical time and the definition of the metric distance:

$$z = (1+2H\tau)^{1/2} - 1 \Rightarrow z = (1+2H/c \cdot r_\tau)^{1/2} - 1 \Rightarrow r_\tau(z) = c/2H \cdot [(1+z)^2 - 1]. \tag{11}$$

1. In contrast to the non–relativistic cosmological models, in relativistic models photometric distance coincides with the metric distance, and the equation for the radiation flux is: $F = L_0/4\pi r_\tau^2(z)$. The formula for the distance module (distances r_τ in Mpc) is:

$$\mu_\tau = 51g[r_\tau(z)] + 25. \tag{12}$$

2. As in the "standard" cosmological model of GRT the dependence of the angular size of the extended space object on the redshift is given by relation:

$$\theta \propto (1+z)/r_\tau(z). \tag{13}$$

3. For estimation of the average surface brightness of a space object $\langle sb \rangle = F/\theta^2$ in contrast with "standard" cosmological model GRT, where $\langle sb \rangle_t = F/\theta^2 \propto (1+z)^{-4}$ the formulae (12,13) lead to the relations:

$$\langle sb \rangle_\tau \propto (1+z)^{-2}, \quad \langle sbm \rangle_\tau = \langle sbm \rangle_{0\tau} + 2.5 \cdot \lg[(1+z)^2], \tag{14}$$

where $\lg x = \log_{10} x$.

Analysis of cosmographical calculations using formulae (12)–(14) convincingly demonstrates the superiority of the cosmological model of the Universe with decelerating physical time, which has the lowest standard deviations (RMS) of theoretical formulae from observational data in all classical cosmological tests. If we estimate the mean ratios of RMS of cosmographical formulae to the average uncertainties of corresponding observations, it appears that the "standard" ΛCDM-model of GRT has these ratios in the range $0.8 \div 2.7$ and in average about 1.8. The same ratios for the cosmography of the Universe with decelerating physical time are in the range $0.4 \div 1.35$ and in average about 1.0 (see details in [4]).

Apart from the cosmographical formulae that determine the basic geometrical characteristics of observable part of the Universe, a complete cosmology must use certain thermodynamic equation of state for the Universe. From the Principle of least action: $\partial S/\partial\tau = 0 \Rightarrow S = E\tau = \text{const}$ for constant volume $V = \text{const}$ and energy density: $\rho_E = E/V$ follows the relation: $\rho_E = \text{const}/\tau$. The form of Principle of least action: $S = p_r \cdot r \propto r' \cdot r = \text{const}$ can be considered as a differential equation that has a solution: $r^2 = \text{const} \cdot \tau$. With this solution, the relation $\rho_E = \text{const}/\tau$ may be represented in the form:

$$\rho_E \tau = \text{const}, \qquad \rho_E = \text{const}/r^2. \tag{15}$$

This equation, which is one of the possible forms of the Principle of least action, is used in the Metaphysical cosmology (MC) with decelerating physical time as the equation of state for the Universe.

The finite volume of Universe is considered as relativistic object with the total energy equal to zero: $E = 0$, and gravitational energy: $E_G = -3Gm^2/2r$. The total energy is: $E = mc^2 + E_U - (3Gm^2/2r) = 0$ where E_U is an internal energy, including the kinetic energy of the non–relativistic subsystems, which can be estimated as $E_U = -U_G/2 = 3Gm^2/4r$ in accordance with the non-relativistic virial theorem. With these assumptions, the total energy of the finite volume of Universe is

$$mc^2 - (3Gm^2/4r_\tau) = 0. \tag{16}$$

Substituting into (16) the transformed relation (7) with $A \approx H : R = R_0(1 + 2H\tau)^{1/2}$ one can get an estimate for the process of growth of the Universe mass:

$$m = 4c^2 R_0/3G \cdot (1 + 2H\tau)^{1/2}. \tag{17}$$

In contrast to the cosmology of the GRT with the Big Bang, in which the whole matter of the Universe was born in the process of inflation almost instantly (during $10^{-36} - 10^{-34}$ seconds), MC of the Universe with decelerating physical time predicts a gradual increase of the mass of the Universe (17), that is, the existence of the processes of synthesis of new matter. The average rate of synthesis of new matter can be estimated by cosmological scales (20)–(22): $Q_H = M_H/T_H V_H = 8H^3/27\pi \approx 10^{-47}\,\mathrm{g\,s^{-1}cm^{-3}}$. This rate of mass growth means, for instance, that in the whole

volume of the Earth during all its history could appear no more than $2 \cdot 10^{-3}$ gram of hydrogen, not enough to fill a child's balloon. Yet in the whole Universe this mass growth means the birth of new cosmic objects with the total mass of more than 10^5 solar masses, i.e. of the same order as masses of new globular star cluster or a dwarf galaxy, emerging every second.

The estimated characteristics of the Universe mass growth discussed above by no means suggest uniform matter synthesis across the Universe. It seems rather that high-energy processes of matter synthesis occur in relatively few centers, like quasars or active nuclei of massive galaxies.

From the energy balance (16) we can obtain the relations for the mass and the mass density $\rho_m = m/V = 3m/4\pi r_\tau^3$, defined as extensive parameters of the finite volumes and masses of the relativistic matter:

$$m = 4c^2 r_\tau / 3G, \quad \rho_m = (c^2/\pi G) \cdot r_\tau^{-2} \quad \langle m \rangle \propto \langle r_\tau \rangle \quad \langle \rho_m \rangle \propto \langle r_\tau \rangle^{-2}. \tag{18}$$

In Metaphysical cosmology of the Universe with decelerating physical time we use a new doctrine.

The integrity of the Universe as an interconnected system consisting of two major subsystems — the micro world and the mega world is provided by system–forming relations between key characteristics of the micro world and the mega world.

The important feature of the methodology of Natural sciences is the definition and use of the characteristic scales of the objects and physical processes. The "cosmological scales" can also be introduced for the observable part of the Universe. Estimates of the cosmological scales of time (the "age of the Universe") and distance (the "radius of the Universe") can be obtained using the relation (7) with $A \approx H$. The estimate of the Newtonian age of the Universe can be determined from the condition $\tau = 0$ for which the equation (7) has the form: $\tau = 0 = -t + H/2 \cdot t^2$. Hence: $-1 + H/2 \cdot t = 0$ and respectively:

$$t_p = 2/H = 32.15\,\text{Gyr}. \tag{19}$$

The velocity of the apparent Universe expansion $V = cz$ reaches the limit of the speed of light at $z = 1$. For this value of redshift the relation (7) has the form: $r = c\tau = c/2H \cdot [(1+z)^2 - 1]$ from which for $z = 1$ follows: $\tau = 1/2H \cdot [(1+1)^2 - 1]$ and then:

$$\tau = T_H = 3/2H = 7.618 \cdot 10^{17}\,\text{s}\,(\approx 24.15\,\text{Gyr}). \tag{20}$$

In (19), (20), and henceforth in the calculations of the numerical values of cosmological scales we use the theoretical value of Hubble constant (25) derived a half page below.

The relation $R_H = cT_H$ together with (20) gives the estimation of the cosmological distance scale ("radius of the Universe"):

$$R_H = cT_H = 3c/2H = 2.283 \cdot 10^{28}\,\text{cm}. \tag{21}$$

From the first relation in (18) it can be obtained the estimate for mass of the Universe with $r = R_H$:

$$M_H = 4c^2 R_H/3G = 2c^3/GH = 4.099 \cdot 10^{56}\ \text{g}. \tag{22}$$

For cosmological scales (20)–(22) with the help of (18) we can estimate the average density of action:

$$\rho_s = \rho_E T_H = \rho_m c^2 T_H = 2c^2 H/3\pi G = 5.627 \cdot 10^9\,\text{erg}\,\text{s}\,\text{cm}^{-3}. \tag{23}$$

From the Principle of least action: $S = E\tau = \text{const}$ for constant volume $V_H = \text{const}$ from (23) follows the relation: $\rho_{SH} = 2c^2 H/3\pi G = \text{const}$ defining constancy of action density in mega world. Planck equation $\varepsilon\delta t = h/2 = \text{const}$ can also be represented as an assertion of constancy of action density in the micro world, if we assume the existence of a finite volume $\nu_{PL} = \text{const}$ for the quantum of action: $\varepsilon\delta t/\nu_{Pl} = \text{const}$. We may also assume that the quantum of action is defined in the same volume as the elementary charge that is in the spherical volume: $\nu_{Pl} = 4\pi r_e^3/3$ with the classical electron radius: $r_e = e^2/m_e c^2$. Corresponding action density in the micro world will be: $\rho_{SPl} = \hbar/2\nu_{Pl} = 3\hbar/8\pi r_e^3 = \text{const}$. Universality of the Principle of least action allows us to formulate the conditions of dynamic unity of the micro world and the mega world in the form of a condition of universal constancy of action density:

$$\rho_{SH} = \rho_{SPl} \longrightarrow K_\tau = 2c^2 H/3G = 3\hbar/8r_e^3 = 1.768 \cdot 10^{10}\,\text{erg}\,\text{s}\,\text{cm}^{-3}. \tag{24}$$

This relation allows representing the Hubble constant and many other key parameters of the Universe as simple functions of fundamental constants:

$$H = 9G\hbar/16c^2 r_e^3 = 1.97 \cdot 10^{-18}\,\text{s}^{-1} (\approx 61.6\,\text{km/s/Mpc}), \quad r_e = e^2/m_e c^2. \tag{25}$$

Application of the Principle of least action and relations (24) in the MC of the Universe with decelerating physical time allows determination of the interdependence of key parameters of the Universe and the basic processes of the microcosm represented by fundamental constants (for details, see [3, 4]).

1. The relations (21), (22), and (25) lead to the estimation of the average mass density of the Universe:

$$\rho_m = M_H/V_H = 4H^2/9\pi G = 9\hbar^2 G/64\pi c^4 r_e^6 = 8.227 \cdot 10^{-30}\,\text{g}\,\text{cm}^{-3}. \tag{26}$$

   Estimates of average mass density by astrophysical observations correspond to the range: $\rho_m = (5 \div 10) \cdot 10^{-30}\,\text{g}\,\text{cm}^{-3}$.

2. Equation (15) $\rho_E \tau = \text{const}$ with invariant equation of state of relativistic matter (16) must be true for any time and, in particular, for the cosmological scale

of physical time (20): $\tau = T_H = 3/2H$. Using this relation and the theoretical formula (25) one can define a constant in (15) and present it in the form:

$$\rho_E \tau = k_\tau, \quad k_\tau = 2c^2 H/3\pi G = 3\hbar/8\pi r_e^3 = 5.629 \cdot 10^9 \,\mathrm{erg\,s\,cm^{-3}}. \tag{27}$$

If we define the characteristic time in the equation (27), using the relation: $\tau = r/c$ and taking into account that $\rho_E = \rho_m c^2$, the equation for mass density takes the form:

$$\rho_m = (2cH/3\pi G) \cdot r^{-1} = (k_\tau/c) \cdot r^{-1} = 1.878 \cdot 10^{-1} \cdot r^{-1} \,\mathrm{g\,cm^{-3}}. \tag{28}$$

For the fractals there can be defined with the help of the relation $m \propto r^D$ the Hausdorff dimension D, which is connected with the mass density by the relation: $\rho_m \propto r^{-(3-D)}$. Comparing this formula with (28) we arrive to the conclusion that the relation (28) should generate the fractal distribution of matter in the Universe with the fractal dimension $D = 2$. Therefore, statistical methods for analyzing the 3D–distribution of galaxies in space, which use the Hubble's law to determine the one of galaxy's coordinates, shall, in accordance with the equation (28) to detect the fractal dimension of the large–scale structure of the Universe of about $D = 2$. This prediction is well confirmed by observations up to distances about 1 000 Mpc.

3. Application of quantum scaling in the MC of the Universe with decelerating physical time allows evaluating of the energy density and the temperature of the cosmic microwave background:

$$\rho_{CMB} = \rho_m \cdot e^4/\hbar^2 \cdot (1 + m_e/m_p) = 3.931 \cdot 10^{-13} \,\mathrm{erg\,cm^{-3}},$$
$$T_{CMB} = (\rho_{CMB}/\sigma)^{1/4} = 2.685 \,\mathrm{K}. \tag{29}$$

The most impressive manifestation of cosmological deceleration of time in distant cosmos is the illusion of accelerating expansion of the Universe. Recently, the scientific community lively discussed the possible evidence of "accelerating expansion" of the Universe, discovered independently by two teams of researchers (Perlmutter et al., Riess et al.). In order to detect the phenomenon of "accelerating expansion" scientists used estimates of the so–called cosmological parameters Ω_M, Ω_Λ in the "standard" model of GRT cosmology, obtained by processing the results of the study of supernovae SNe Ia explosions. These research projects evaluated the following estimates of the cosmological parameters: $\Omega_{Me} = 0.28^{+0.09}_{-0.08}$ and $\Omega_{Me} = 0.29^{+0.05}_{-0.03}$. Relation $\Omega_M + \Omega_\Lambda \approx 1$ allows for a standard "flat" cosmological model to estimate the value of Ω_Λ and then using the formula: $q_t = \frac{1}{2}\,\Omega_M - \Omega_\Lambda$ to calculate the "deceleration parameter" for Newtonian time: $q_{te} = -0.56 \pm 0.11$. This negative deceleration parameter allowed concluding that in our epoch the Universe expands with acceleration.

In the concept of decelerating physical time, the apparent evidence of "accelerating expansion" of the Universe has an ordinary explanation (Taganov 2005 [3, 4]). In accordance with the equations (6) the relation between the cosmological deceleration parameter for physical time: $q_\tau = -aa''/a'^2$ and the deceleration parameter $q_t = -a\ddot{a}/\dot{a}^2$ for Newtonian time is: $q_t = q_\tau - 1$. From this relation follows that the moderate ($q_\tau < +1$) deceleration of the Universe expansion in physical time seems an accelerating expansion ($q_t < 0$) in the Newtonian time.

Using relation $q_t = q_\tau - 1$ we can estimate the deceleration parameter in physical time corresponding to observations of supernovae: $q_{\tau e} = q_{te} + 1 = (-0.56 \pm 0.11) + 1 = +0.44 \pm 0.11$. Hence, in physical time, which is actually governs the real astrophysical observations, the "expansion" of the Universe is not accelerating, but rather decelerating.

Hence, the illusion of "accelerating expansion" of the Universe aroused from the fact that for the interpretation of the observations of astrophysical processes developing in decelerating physical time, researchers used the cosmological model with invariable uniform scale of Newtonian time.

The cause of discovered "accelerating expansion" of the Universe, some theorists associate with non-zero Einstein's cosmological constant, which, in turn, is explained by assumption of an existence of the mysterious "dark energy". Dark energy is a hypothetical form of energy that invisible fills space and is responsible for the accelerating expansion of our Universe. In the "standard" ΛCDM–model of GRT cosmology, this mysterious dark energy composes nearly three-quarters of the mass–energy of the Universe! Since the "dark energy" is included in the "standard" model of classical cosmology only to explain the accelerating expansion of the Universe, this gloom ghost will not be slow to disappear as soon as the illusory nature of the "accelerating expansion" of the Universe will be recognized.

In formulae of this presentation the following fundamental constants are used: gravitational constant $G = 6.674 \cdot 10^{-8}\,\mathrm{cm^3\,g^{-1}\,s^{-2}}$; Planck constant $\hbar = h/2\pi = 1.055 \cdot 10^{-27}\,\mathrm{erg\,s}$; the speed of light in vacuum $c = 2.998 \cdot 10^{10}\,\mathrm{cm\,s^{-1}}$; elementary electrical charge $e (e^2 = 2.307 \cdot 10^{-19}\,\mathrm{g\,cm^3\,s^{-2}})$; classical radius of electron $r_e = e^2/m_e c^2 = 2.818 \cdot 10^{-13}\,\mathrm{cm}$; mass of electron $m_e = 9.110 \cdot 10^{-28}\,\mathrm{g}$, mass of proton $m_p = 1.673 \cdot 10^{-24}\,\mathrm{g}$; the Stefan–Boltzmann constant $\sigma = 7.566 \cdot 10^{-15}\,\mathrm{erg\,cm^{-3}\,K^{-4}}$.

References

[1] Ignatowsky, W. von.: Einige allgemeine Bemerkungen zum Relativittsprinzip. Verh. d. Deutsch. Phys. Ges. **12** (1910), 788796. Translation (Rus) - `http://synset.com`.

[2] Milne, E. A.: World-structure and the expansion of the Universe. Zeitschrift für Astrophysik **6** (1933), 195. Also in: Walker, A. G., *Proc. Lond. Math. Soc.* vol. 42, 1937, p. 90; vol. 46, 1940, pp. 113–154; vol. 48, 1943, 161–179. Walker, A. G., J. Lond. Math. Soc. **19** (1944), 219–229.

[3] Taganov, I. N.: Quantum cosmology. Deceleration of Time. Staint Petersburg: TIN, 2008. ISBN 978-902632-05-4.

[4] Taganov, I. N.: Irreversible-Time Physics. Saint Petersburg: TIN, 2013. ISBN 978-5-902632-12-2.

[5] Taganov, I. N., Saari, V.-V. E.: Ancient riddles of Solar eclipses. Asymmetric Astronomy. Saint Petersburg: TIN, 2014. ISBN 978-5-902632-15-3.

[6] Taganov, I. N., Babenko, Y. I.: Antitime and antispace. Second Edition. Saint Petersburg: TIN, 2016. ISBN 978-5-902632-18-4.

The electronic editions of books [4, 5, 6] can be downloaded free from the web-site `www.timepace.net` from the section "Books and Articles".

Conference *Cosmology on Small Scales 2016*
Michal Křížek and Yurii Dumin (Eds.)
Institute of Mathematics CAS, Prague

DO RECENT OBSERVATIONS OF GIANT MOLECULAR CLOUDS SUGGEST MODIFICATION OF GRAVITY?

Itzhak Goldman[1,2]

[1] Afeka Engineering College
Tel Aviv, Israel
[2] Department of Astrophysics Tel Aviv University
Tel Aviv, Israel
goldman@afeka.ac.il

Abstract: The Larson scaling relations of Giant Molecular Clouds (GMC) in the Galaxy (Larson 1981 [9]) were re-examined in a seminal paper by Heyer et al. (2009) [6]. They have used the more accurate data of Galactic Ring Survey (GRS) [7] and found that the scaling relations *actually depend* on the cloud surface mass density.
Here we take a step further and examine the observed velocity dispersion, normalized by virial value of the velocity dispersion, as function of the surface mass density. The data does suggest that the above ratio is a function the surface mass density. For low surface mass densities the ratio is about twice the value corresponding to large surface mass densities. The transition surface mass density corresponds to a self acceleration of the cloud being $\sim 10^{-8}\,\mathrm{cm/s^2}$. This is the value which characterizes within the modified Newtonian Dynamics (MOND) the transition from the Newtonian to the MOND regime.
Next, we test the normalized velocity dispersion as function of the volume mass density. We find a transition from a value of ~ 1 to a value of ~ 2 when the mass density decreases below a value of $\rho = 2.22 \times 10^{-22}\,\mathrm{g\,cm^{-3}}$. Such a behaviour is in accord with Chameleon gravity models.
We note that within both the MOND and Chameleon frameworks, all GMC are *gravitationally bound*, in contrast with Newtonian gravity for which only the high mass density GMCs are bound. Thus, in the modified gravity frameworks one expects a higher efficiency of star formation.

Keywords: Giant molecular clouds, modified gravity, astronomy

PACS: 95.55.Jz, 95.30.Sf, 98.58.Db, 95.85.Bh, 95.85.-e

1. Introduction

Giant molecular clouds (GMC) are the largest structures in the Galaxy. They are the sites of star formation and therefore attracted observational and theoretical attention. More than thirty years ago Larson (1981) [9] published the famous relations

between parameters of the GMC. Among them was the relation between the velocity dispersion and the cloud size $\sigma_v \propto R^{0.38}$. Subsequent observation (e.g. Solomon et al. 1987 [12] (SRBY)) pointed to a relation of the form $\sigma_v \propto R^m$ with $m \approx 0.5$. The velocity dispersions are supersonic. There were various attempts to explain the scaling relations as resulting from supersonic turbulence and/or from quasi-static configuration involving magnetic fields in addition to gravity (see e.g. Fleck 1983 [3], Canuto and Battaglia 1985 [1], Heyer et al. 2001 [4], Heyer & Brunt 2004 [5]).

Heyer et al. (2009) [6] employed the more accurate data of the Boston University Galactic Ring Survey (GRS) [7] and found that the velocity dispersion-radius scaling relation depends on the cloud surface mass density. The GRS data span almost 3 orders of magnitude in the value of the the surface mass density: a substantial improvement on the previous data span which allowed them to quantify the above dependence via

$$\sigma_v \propto R^{0.5}\Sigma^{0.5} \tag{1}$$

with Σ the surface mass density

$$\Sigma = \frac{M}{\pi R^2}. \tag{2}$$

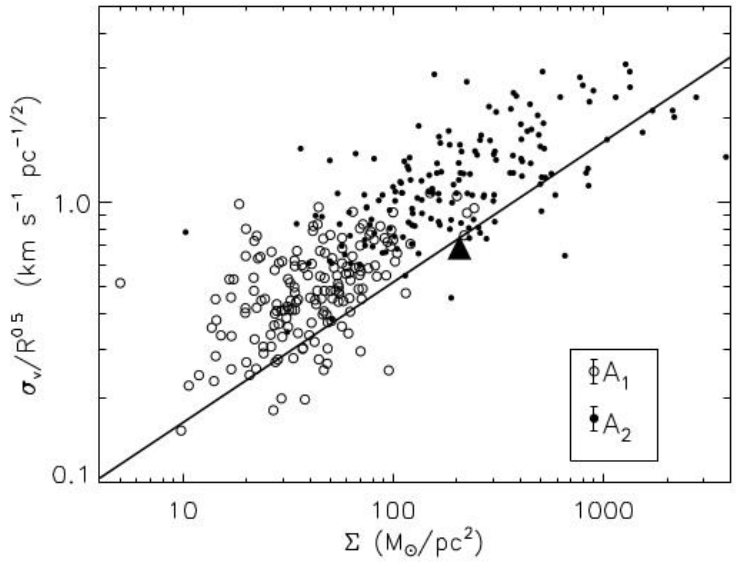

Figure 7. Variation of the scaling coefficient, $v_\circ = \sigma_v/R^{1/2}$, with mass surface density derived within the SRBY cloud boundaries (open circles) and the 1/2 maximum isophote of H_2 column density (filled circles). The filled triangle denotes the value derived by SRBY. The solid line shows the loci of points corresponding to gravitationally bound clouds. There is a dependence of the coefficient with mass surface density in contrast to Larson's velocity scaling relationship. The error bars in the legend reflect a 20% uncertainty of the distance to each cloud.

Figure 1: Figure 7 of Heyer et al. (2009)

Figure 1 displays Figure 7 of Heyer et al. (2009) [6]. For each cloud they have used two separate approaches: in the first A_1, they used the criteria of SRBY to determine the cloud radius. In the second A_2, they used the *better* defined radius of the half-power isophot of the peak column density value within the cloud. The figure presents both data sets (derived from one observational data set).

In effect (2) implies that

$$\sigma_v \approx \sqrt{\frac{GM}{R}} \tag{3}$$

suggesting that the clouds are in a self gravitating equilibrium rather than a manifestation of turbulent hierarchical structure.

2. The normalized velocity dispersion dependence on the surface mass density and MOND

The results of Heyer et al. (2009) [6] imply that the normalized velocity dispersion

$$\sigma_n = \frac{\sigma_v}{\sqrt{\frac{GM}{5R}}} \tag{4}$$

is constant regardless of the value of the surface mass density was made. In this paper we use the *same* data in order to examine whether σ_n is *indeed constant.* Figure 2 displays σ_n versus Σ. The second data set A_2 of Heyer et al. (2009) [6], was used because of its higher precision.

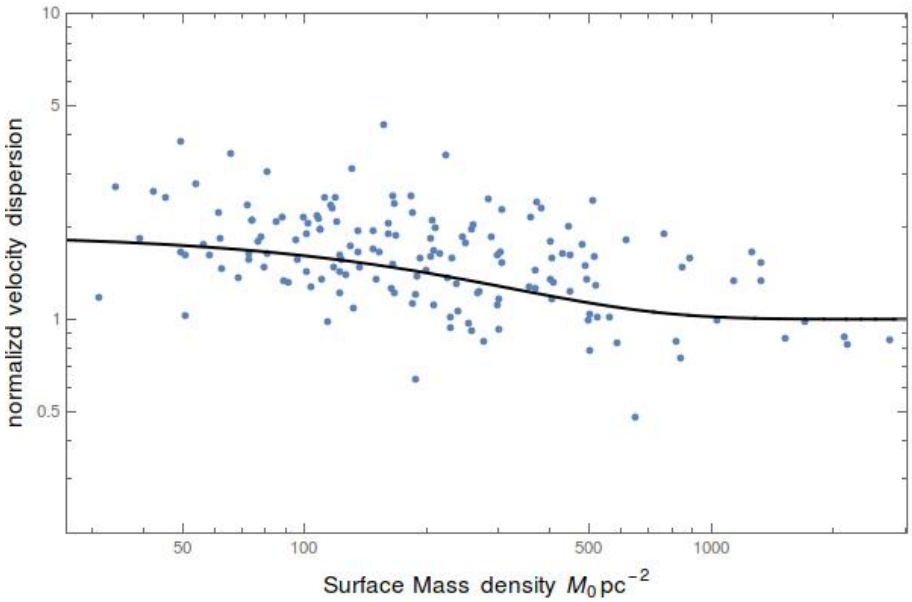

Figure 2: The normalized velocity dispersion as function of the surface mass density

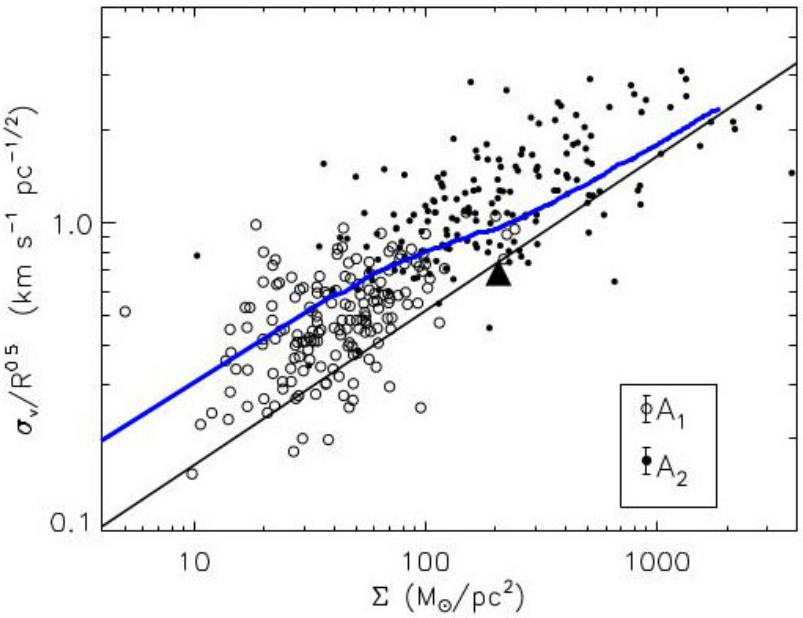

Figure 3: Figure 1 corrected by the present results

The scatter in the data is quite large but the general trend is obvious: for small surface mass densities the mean value of the ratio is ~ 2 while for large values it is ~ 1. The fit function:

$$\sigma_n = \frac{\sigma_v}{\sigma_{\rm vir}} = 1 + 0.9 \times {\rm e}^{-\Sigma/260} \tag{5}$$

has a value of $\chi^2 = 2.52$; implying a good fit to the data. To reach this value a rather conservative assumption (Heyer et al. (2009) [6]) that

$$\Delta\sigma_n = 0.2\sigma_n \tag{6}$$

was made.

The self gravitational acceleration of the cloud is related to the surface mass density by

$$a_{\rm self} = \frac{GM}{R^2} = \pi G\Sigma. \tag{7}$$

The value of $\Sigma = 260 M_\odot\,{\rm pc}^{-2}$ corresponds to $a_{\rm self} = 1.19 \times 10^8\,{\rm cm\,s}^{-2}$. This is very close to a_0 of MOND – Milgrom's Modified Newtonian Dynamics [10]. Interestingly Milgrom (1989) [11] noted that the then available GMC data were centered on a Σ of the order of a_0. Here, we show *the transition* between the Newtonian and the MOND regimes.

Figure 3 shows how would Figure 1 have looked with the present results taken into account.

3. The normalized velocity dispersion dependence on the volume mass density and Chameleon gravity

The previous result provides a motivation to check whether the data can be relevant with regard to Chameleon gravity models (see review by Khoury 2013 [8]). In these models a massive scalar or vector field of gravity strength acts in addition to gravity. The mass of the field (or the inverse of the field screening range) are proportional to a positive power of the environment volume mass density. So the field is effective in low density environments and is screened out in high density environments, hence the name of the models. We use here an example where $m \propto \rho^{1/2}$. The best fit function to the data is

$$\sigma_n = 1 + 1.2\mathrm{e}^{-\sqrt{\rho/30}}, \quad \rho = \frac{4\pi M}{3R^3}. \tag{8}$$

The value of $30 M_\odot\,\mathrm{pc}^{-3}$ corresponds to $2.22 \times 10^{-22}\,\mathrm{g\,cm}^{-3}$ or an equivalent value of hydrogen atoms of $n_H = 133\,\mathrm{cm}^{-3}$. We see indeed a transition of the normalized velocity dispersion from a value close to 2 to a value close to 1, as the mass density increases. This is in line with the Chameleon models.

The fit function (8) yields a value $\chi^2 = 2.95$ implying a good fit but slightly worse than that of (5).

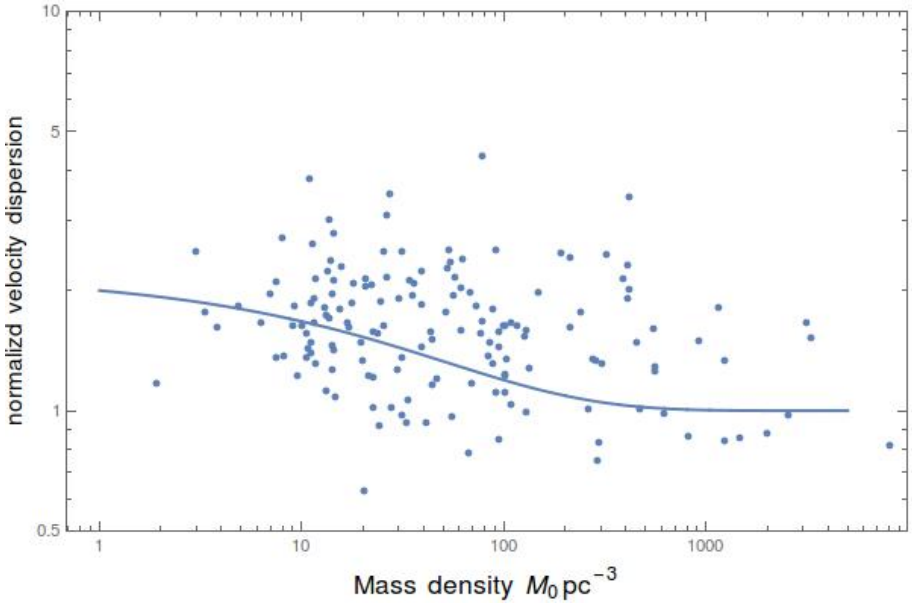

Figure 4: The normalized velocity dispersion as function of the volume mass density. The curve is the fit function of (8).

4. Discussion

We obtained the normalized velocity dispersion as function of the surface mass density and as a function of the volume mass density. The data shows a transition of the normalized velocity dispersion from ~ 1 to ~ 2 for surface mass densities much larger/smaller than $260 M_{\odot}\,\mathrm{pc}^{-2}$ corresponding to an acceleration equal the MOND acceleration. The values of the normalized velocity dispersion for the lowest surface mass density observational value is equal to that predicted by MOND.

The normalized velocity dispersion changes from ~ 1 to ~ 2 for mass densities much larger/smaller than $2.2 \times 10^{-22}\,\mathrm{g\,cm}^{-3}$. This is in accord with what is expected from Chameleon gravity.

Dobbs et al. (2011) [2] showed that most GMC are not bound gravitationally, since for many clouds $\sigma_n > 1$. They explained the higher velocity dispersion as due to stellar feedback and cloud-cloud collisions. However, both in MOND and the Chameleon approaches, the clouds are gravitationally bound even for the low surface mass densities and volume mass densities. The implication is that within these frameworks star formation should be more efficient than in Newtonian gravity, since the clouds are bound even when the mass density is low.

Acknowledgements

Thanks are due to Idit Goldman for encouragement in preparation of the manuscript. This work has been supported by an Afeka College Research Grant.

References

[1] Canuto, V. M. and Battaglia, A.: ApJL **294** (1985), L125.

[2] Dobbs, C. L., Burkert, A., and Pringle, J. E.: MNRAS **413** (2011), 2935.

[3] Fleck, R. C., Jr.: ApJL **272** (1983), L45.

[4] Heyer, M. H., Carpenter, J. M., and Snell, R. L.: ApJ **551** (2001), 852.

[5] Heyer, M. H. and Brunt, C. M.: ApJL **615** (2004), L45.

[6] Heyer M., Krawczyk C., Duval J., and Jackson J. M.: ApJ **699** (2009), 1092.

[7] Jackson, J. M., Rathborne, J. M., Shah, R. Y. et al.: ApJS **163** (2006), 145.

[8] Khoury, J.: Classical and Quantum Gravity **30** (2013), 214004.

[9] Larson, R. B.: MNRAS **194** (1981), 809L.

[10] Milgrom, M.: ApJ **270** (1983), 365.

[11] Milgrom, M.: A&A **211** (1989), 37.

[12] Solomon, P. M., Rivolo, A. R., Barrett, J., and Yahil, A.: ApJ **319** (1987), 730.

Conference *Cosmology on Small Scales 2016*
Michal Křížek and Yurii Dumin (Eds.)
Institute of Mathematics CAS, Prague

THE OBSERVED SPATIAL DISTRIBUTION OF MATTER ON SCALES RANGING FROM 100 KPC TO 1 GPC IS INCONSISTENT WITH THE STANDARD DARK-MATTER- BASED COSMOLOGICAL MODELS

Pavel Kroupa[1,2]

[1] Helmholtz Institut für Strahlen und Kernphysik
Universität Bonn, Nussallee 14–16, 53115 Bonn, Germany
[2] Charles University in Prague, Faculty of Mathematics and Physics
Astronomical Institute, V Holešovičkách 2, CZ-180 00 Praha 8, Czech Republic
pavel@astro.uni-bonn.de

Abstract: The spatial arrangement of galaxies (of satellites on a scale of 100 kpc) as well as their three-dimensional distribution in galaxy groups such as the Local Group (on a scale of 1 Mpc), the distribution of galaxies in the nearby volume of galaxies (on a scale of 8 Mpc) and in the nearby Universe (on a scale of 1 Gpc) is considered. There is further evidence that the CMB shows irregularities and anisotropic cosmic expansion. The overall impression one obtains, given the best data we have, is matter to be arranged as not expected in the dark-matter based standard model of cosmology (SMoC). There appears to be too much structure, regularity and organisation. Dynamical friction on the dark matter halos is a strong direct test for the presence of dark matter particles, but this process does not appear to be operative in the real Universe. This evidence suggests strongly that dynamically relevant dark matter does not exist and therefore cosmology remains largely not understood theoretically. More-accepted awareness of this case would by itself constitute a major advance in research providing fabulous opportunities for bright minds, and the observational data strongly suggest that gravitation must be effectively Milgromian, corresponding to a generalized Poisson equation in the classical limit. Thus, physical cosmology offers a significant historically relevant opportunity for ground-breaking work, at least for those daring to do so.

Keywords: Dark matter, cosmology, Milky Way, CMB

PACS: 98.35.-a, 98.52.Wz, 98.56.-p, 98.62.Ai, 98.62.Py, 98.65.At, 98.80.-k

1. Introduction

The direct searches for dark matter particles, which the vast majority of researchers believe dominate the matter density of the Universe, have been coming up

empty handed despite a huge effort to find these particles with various elaborate, large and expensive experiments on Earth and in space. But the astronomical evidence has already been showing that dark matter particles cannot be there. This seems to be a contradictory statement, because astronomical evidence has been used to argue for the existence of dark matter particles which must be new particles not contained in the standard model of particle physics (SMoPP), which is otherwise a well tested theory.

The argument is as follows: If it is assumed that the Universe is described by Einstein's field equation[1] such that Newtonian gravitation is valid in the classical regime and if all the matter was produced in the Big Bang, then the rate with which structures form as cosmic time progresses, and also the motions of stars and gas in the emerging galaxies when compared to observations, shows conclusively that gravity must be stronger than provided by the matter we know. One hypothesis is that much more gravitating matter, that is dark matter which cannot interact electromagnetically with normal matter and which is not described by the standard model of particle physics (SMoPP), is required to yield, roughly, the observed effects. Given this result, the researcher can now assume this model (Einstein plus dark matter, lets call it the null hypothesis) to be valid and perform detailed calculations of galactic systems to further test the hypothesis. Additional assumptions (inflation and dark energy) are also needed and together comprise the dark-matter-based standard model of cosmology (SMoC). A discussion of the current status of the SMoC can be found in [12] and a critical discussion is also provided by [32].

This model can then be tested on various astronomical data, as outlined below. The argument followed here is to proceed testing the SMoC using the relative spatial distribution and, when available, the relative motions of galaxies. The tests then become very robust, that is, do not depend on the details of baryonic physics, since the tests apply largely to the presence of galaxies within their dark matter halos. Thus, if dark matter halos exist, their spatial arrangements relative to each other and their motions relative to each other are being tested, rather than the detailed "sub-grid" properties of individual galaxies. Baryonic processes then only play a role in determining if a dark matter halo hosts a galaxy or not, and arguably, dark matter halos more massive than $10^9\,M_\odot$ are understood to host galaxies with initial mass $> 10^7\,M_\odot$. This text is a short summary pointing to the relevant literature, rather than providing the detailed analysis of each problem. More detailed discussions of these issues, which this text is also based on, are available in [34, 35, 36, 37, 38].

The analysis of the distribution of galaxies in the Local Group can be split into two parts: the distribution of satellite galaxies (Section 2), the distribution of non-satellite galaxies (Section 3). The distribution of galaxies in the Local Volume (Section 4) and the variation of the mean matter density in the Local Universe provide

[1] As emphasized in [35, 38] this is an extrapolation by many orders of magnitude in scale and gradient of the potential of an empirically derived law, strictly valid *only* on the scale of the Solar-system. See footnote 2 for an analogy.

further tests, in particular also of the Cosmological Principle. This question is addressed independently by probing evidence for isotropic cosmic expansion (Section 7). A direct test for the presence of dynamically relevant dark matter particles is provided by observable consequences of dynamical friction (Section 6).

2. The 100 kpc scale

It is by now well established that the satellite galaxies around the Milky Way are highly significantly distributed anisotropically in a rotational disk-like structure with radius of about 250 kpc and thickness of about 30 kpc [33, 46, 47, 55, 63]. The Andromeda galaxy has a richer population of satellite galaxies with perhaps a number of planar structures [45], but one planar structure which contains 50 per cent of all satellites is even more pronounced and thinner than that of the Milky Way [21]. Both disks-of-satellites are correlated [57]. Other major galaxies show significant evidence that such satellite planes are common [22, 24]. The dwarf spheroidal galaxies in the M81 group, which is the nearest Local-Group analogue (distance about 3.6 Mpc), are in a flattened distribution [15] and the satellite galaxies of Cen A (distance about 3.66 Mpc) are likewise in a plane, which is perpendicular to the dust lane of Cen A [52]. The observational results are thus rather clear: disks of satellites are common, and in fact they seem to be the rule rather than the exception. This is impossible to be the case in the SMoC.

It has been shown that just to find the one Milky Way satellite system in a dark-matter universe is very unlikely. To have such structures around many hosts, let alone that the Milky Way and Andromeda systems are correlated, essentially leads to a combined probability of zero, assuming the SMoC to be valid and the dwarf galaxies in the Local Group to be in their own dark matter halos [35, 59]. Basically, this single observational result falsifies the SMoC, as has been realized early-on already [33].

Claims that the disks of satellites can be accounted for readily within the SMoC such that they do not constitute a serious problem have been found to be flawed [23, 59, 61, 24]. SMoC simulations show that rotating disks of satellites are as unlikely within pairs of dark matter halos (resembling the pair Milky Way–Andromeda) as in isolated halos [60].

The physical reason for this discrepancy between observation and the SMoC is that the SMoC necessitates *all* Milky-Way-type dark matter halos to form from numerous stochastic mergers of smaller halos such that the result is that the distribution of dark-matter-dominated satellite galaxies is spheroidal. Although the dark matter sub-halos fall-in from cosmic filaments, these have widths larger than the virial radii of the dark matter halos, such that the infall of satellite galaxies, even if being anisotropic to some degree, remains in significant disagreement with the thin disks-of-satellites, since the Rosetta-orbits phase-mix and shrink through dynamical friction [48, 56]. Indeed, the observed positions and velocities of those satellite galaxies for which such data exist show that infall-solutions do not exist, because dynamical friction on the extended dark matter halos is too efficient [1].

The only known physical process which can lead to such rotating disk of satellites is that the dSph satellite galaxies are ancient tidal dwarf galaxies (TDGs). How such populations can form has been demonstrated [74, 54]. Such low-mass dwarf galaxies cannot capture significant amounts of dark matter and their putative dark matter content would then be explainable by Milgromian gravitation [43, 44, 16].

For future tests, [58, 62] predict the proper motions of the Milky Way satellite galaxies based on the argument that they need to orbit within the disk-of satellites as otherwise the chance of having such a vast polar structure for randomly moving satellites would be negligibly small. And, if dSph satellites are ancient TDGs, then their number is expected to correlate with other indicators for past galaxy–galaxy encounters, such as the bulge mass [34, 42]. This opens a possibility for further testing this notion (i.e. that dSph satellite galaxies are mostly if not exclusively old TDGs) through observational campaigns using small (also amateur) telescopes [26].

3. The 1 Mpc scale

The dwarf galaxies in the Local Group which are not satellites are distributed in a very organized manner, namely in two ≈ 50 kpc thin planes of about 1.5 Mpc extension, whereby each is nearly equidistant from the line joining the Milky Way and Andromeda [57]. These structures suggest the Milky Way and Andromeda to be causally connected, and this poses an important constraint on models of the formation of the Local Group. The physically best-motivated cause for this entire structure, including the correlated disks of satellite systems around the Milky Way and Andromeda, is for the two major galaxies to have had an encounter about 9–11 Gyr ago [78, 2]. This is only possible if they do not have dark matter halos, as they would otherwise have merged by now (e.g. [3] for similar cases). The structure of the Local Group is indeed not explainable within the dark matter framework.

The next group of galaxies beyond the Local Group is the M81 system at a distance of about 3.6 Mpc. Here we already do not have such good three-dimensional coordinate information, but the system of dwarf galaxies in it is known to be highly anisotropic [15] as noted in Section 2. The highly significant anisotropy in the Cen A group [52] at a distance of approximately 3.66 Mpc has been noted above.

Furthermore, the major galaxies in the M81 group have been encountering each other at least once, because the system is filled with tidal HI gas. This provides crucial information on the existence of dark matter halos because solutions do not seem to exist which explain the matter distribution as well as the present-day positions and line-of-sight velocities [71, 77]. Essentially, if dark matter halos exist, then this system ought to have already merged. The probability that all three major inner galaxies of the M81 system have just met in the very recent (less than 1 Gyr) past after forming independently is remotely small [53].

The same argument applies to compact groups of galaxies [69]. Too many compact groups are observed with a constancy in number density with redshift such that they appear to be largely non-merging in contradiction to the expectation in

the SMoC. That the compact groups have just assembled in the past 1 Gyr of their observation with the member galaxies having formed independently of each other constitutes a negligible physical possibility, especially given the large number of such systems. The only viable physical explanation for the existence of so many compact groups is that the galaxies in them interact for many Gyr without merging. This is not possible in a dark-matter-based cosmological model.

4. The 8Mpc scale

Cosmological structure is evident in the galaxy distribution within the Local Volume which is a sphere with a radius of about 8 Mpc around the Local Group. This volume contains galaxies within the local sheet and also the local void. At least two fundamental problems with the observed distribution of galaxies have been emphasized [64]: (i) the local void is too empty and (ii) massive galaxies are too far from the sheet within the outer regions of the void. Each problem individually they describe as being about 1 per cent or less probable within the SMoC, such that the combined probability that the observed distribution can arise in the SMoC approaches zero. Consequently, structure formation appears to have proceeded differently to the SMoC.

5. The 1Gpc scale

The Local Universe on a scale of about 1 Gpc around the Local Group should have small fluctuations in the density of galaxy counts, but within about 300 Mpc of us the density decreases significantly with decreasing distance to about 50 per cent its global cosmological value posing serious tension with the SMoC [28, 29, 10, 75]. The under-density on a sale of 300 Mpc and less is significantly more pronounced than allowed by the SMoC (Fig. 1 in [38]). This has bearing on the deduced acceleration of cosmic expansion, because photons arriving from larger distances are redshifted more than in a homogenous universe. This may be partially or entirely responsible for the dark-energy effect [76, 11], and this needs to be studied further.

6. The lack-of-dynamical friction and lack-of-merging problems

It has been noted by [68] that the observed galaxy population does not support the profusion of mergers that are expected in the SMoC such that these authors argue that dynamical friction must be less efficient. This is consistent with the deficit of galaxies with bulges compared to SMoC predictions and the survival of pure disk galaxies since 8 Gyr [73, 31, 19, 67] and with the absence of the evolution of the ratio of the co-moving number density of the most massive galaxies relative to less-massive galaxies [14]. The absence of an evolution of the number density of elliptical galaxies [17] and the lack of recoiled super-massive black holes [39] are furthermore also consistent with this general lack of evidence for mergers being an important process in the evolution of galaxies, in contrast to the expectations from the SMoC.

But this is only possible if the dynamical influence of dark matter is much below that in the SMoC (which would by itself be a violation of the SMoC), or if dark matter does not exist, as otherwise the massive and expansive dark matter halos around each galaxy are dictated by the theory. That is, it is not possible to arbitrarily reduce the process of dynamical friction to fit the data but keeping the dark matter halos as obtained from the SMoC. Consistent with this problem is the lack of merging already observed in the M81 group of galaxies and in the compact galaxy groups (Section 3).

7. Discussion

Given the statements in the Introduction, it is apparent that in order to save the model we have two possibilities:

1. We can shrug the problems away by arguing that we *simply know the model to be right anyway.* Such a statement is rather popular and is based on the main-stream understanding that the CMB is extremely well represented by the SMoC as evident with the Planck results. Any irregularities in the non-linear structure-formation regime (galaxy clusters, galaxies) are then not to be taken too seriously. But there are tensions between the CMB and the SMoC (see Section 17.3.1 in [35] and also [25] and e.g. [20]). For example, there is tentative evidence for an unexpected alignment of various independent measures of anisotropy in the CMB, SN1a-based cosmological expansion and galaxy morphology possibly raising questions concerning the Cosmological Principle [25, 27]. There is also tension between the locally-measured Hubble constant and the Hubble constant as derived from the CMB [66, 4]. Ignoring such tensions and claiming excellent fits of the SMoC to the CMB as proving the dark-matter models to be correct may serve the short-term aims of a famous-few but undermines the very principle of natural scientific research, as such claims are based on belief rather than comprehensive evidence, remembering that no theory can ever be proven, but merely tested and if necessary discarded.

   Thus, this avenue of thinking is not convincing.

2. It may be speculated that baryonic physics, which is described by perhaps the best model of physics we have (the SMoPP), conspires on every studied scale to annul the discrepancies in the sense that what we observed does not seem to match, but what we cannot see is an excellent account of reality.

   Such an argument rests on speculation of unverifiable processes and needs to be discarded.

3. The more scientific approach is to accept the failures and to seek an entirely different model. Such a model would need to be dark-matter free in order to test if baryonic structures alone, which are described by the best model of physics we currently have (the SMoPP), may be able to account for the observations, but in a different gravitational framework. Gravitation remains

the least well understood force, if it is a force at all, and thus this ansatz appears to be the most promising avenue. Our work in Bonn and Strasbourg, using the Phantom of Ramses (PoR) computer code ([41], see also [13]), developed with sparse funding from Bonn, is now allowing us to perform exactly this work in the Milgromian-gravitational framework [49, 51, 18]. The results so far appear highly promising [65, 70].

8. Conclusion

The above discussion suggests that the real Universe appears to produce more structure, which is at least partially more ordered and organized than the SMoC, and that the observed galaxy population neither matches nor does it evolve as expected by the SMoC. The explicit tests for the presence of dark matter via dynamical friction suggest this process not to be acting. All of this is consistent with the null results in the searches for dark matter particles. Here I would wish to emphasize the incredible *consistency* of the tests amongst each other: none of the tests performed yield positive results concerning the SMoC, and all appear to suggest more structure and organisation. This is important to note, because we do not have the situation where a test yields excellent agreement while another one does not. They are all consistently problematical for the SMoC. In [35, 37, 38] the *theory confidence graph* lists the many individual tests performed such that, if each failed test decreases the confidence by 50 per cent then the remaining confidence in the SMoC remains today at less than 10^{-5} per cent.

We are left with inferring that the important hypothesis that dark matter particles exist needs to be rejected by astronomical data. Gravitation must therefore be effectively[2] stronger on scales relevant for galaxies. Mordehai Milgrom [49] has conceptualized a generalized gravity known as MOND, or as Milgromian gravitation. This finding can be seen as constituting the greatest advance in gravitational physics since Newton and Einstein and it is based on a generalized Poisson equation and a Lagrangian [8] and can also be embedded in a general-relativistic theory, as discovered by Jacob Bekenstein [5] with notable reviews [6, 7] with alternatives [9, 72, 30]. The observed deviations from Newtonian gravitation at the very weak accelerations, which are described by Milgromian gravity, may be a result of vacuum processes, perhaps as discussed for Minkowski space by Milgrom [50]. Milgromian dynamics has proven to be extraordinarily successful [18] and is now being used in numerical experiments to study galaxy formation and evolution [41, 70, 65]. These numerical experiments appear to be showing an incredible amount of success in reproducing all major issues in the astrophysics of galaxies, as our work at the Universities of Stras-

[2] *Effectively*, because it may still be Einsteinian but with additional but non-exotic physics possibly playing a role in Minkowski space [50]. This is nicely visualized by an analogy by Indranil Banik: consider a trampoline. One can measure its depth-extension $s = s(w)$ as a function of weight w. These measurements can be fitted by an empirical law for macroscopic weights (e.g. $w > 1\,\mathrm{kg}$). We would then not expect this same law $s = s(w)$ to hold in an extrapolation to $w < 10^{-5}\,\mathrm{g}$, for instance, because molecular forces will begin to play a role for very small w.

bourg and Bonn is demonstrating. Further work will be published in due course, subject to the availability of funding.

As to the issue of a more structured universe which may also be more organized [40], it appears that a Milgromian universe may provide the former, and self-regulatory growth processes may provide the latter which may be related to the fundamental assumption of conservation of matter.

Closing this critical discussion, one of the currently most fundamental problems in theoretical physics is the origin of Milgromian dynamics rather the nature of (non-existing) dark matter particles. This is likely to be an immense opportunity for talented young researchers. Concerning the theory of galactic astrophysics, understanding the formation and evolution of galaxies in Milgromian gravity provides a great opportunity for talented young researchers interested in performing numerical astrophysics experiments.

Acknowledgements

I thank the organizers of this conference in the ancient and scientifically highly relevant city of Prague in September 2016 for inviting me to provide this lecture.

References

[1] Angus, G. W., Diaferio, A., and Kroupa, P.: Using dwarf satellite proper motions to determine their origin. Mon. Not. R. Astron. Soc. **416** (2011), 1401–1409.

[2] Banik, I. and Zhao, H.: Dynamical history of the Local Group in ΛCDM. Mon. Not. R. Astron. Soc. **459** (2016), 2237–2261.

[3] Barnes, J. E.: Dynamics of Galaxy Interactions. In: R. C. Kennicutt, Jr. F. Schweizer, J. E. Barnes, D. Friedli, L. Martinet, and D. Pfenniger (Eds.), *Galaxies: Interactions and Induced Star Formation, Saas-Fee Advanced Course 26. Lecture Notes 1996. Swiss Society for Astrophysics and Astronomy, XIV*, Springer-Verlag Berlin/Heidelberg; ISBN: 3-540-63569-6, 1998, p. 275.

[4] Beaton, R. L., Freedman, W. L., Madore, B. F. et al.: The Carnegie-Chicago Hubble Program. I. A new approach to the distance ladder using only distance indicators of population II. Astron. Journal, submitted in 2016, arXiv:1604.01788.

[5] Bekenstein, J. D.: Relativistic gravitation theory for the modified Newtonian dynamics paradigm. Phys. Rev. D **70** (2004), 083509.

[6] Bekenstein, J.: The modified Newtonian dynamics – MOND and its implications for new physics. Contem. Phys. **47** (2006), 387–403.

[7] Bekenstein, J. D.: Relativistic MOND as an alternative to the dark matter paradigm. Nuclear Phys. A **827** (2009), 555–560.

[8] Bekenstein, J. and Milgrom, M.: Does the missing mass problem signal the breakdown of Newtonian gravity? Astrophys. J. **286** (1984), 7–14.

[9] Blanchet, L. and Heisenberg, L.: Dipolar dark matter with massive bigravity. J. Cosmol. Astroparticle Phys. **12** (2015), 026.

[10] Böhringer, H., Chon, G., Bristow, M., and Collins, C. A.: The extended ROSAT-ESO Flux-Limited X-ray Galaxy Cluster Survey (REFLEX II). V. Exploring a local underdensity in the southern sky. Astron. Astrophys. **574** (2015), 26–34.

[11] Buchert, T.: Dark energy from structure: a status report. Gen. Rel. Grav. **40** (2008), 467–527.

[12] Bull, P., Akrami, Y., Adamek, J. et al.: Beyond ΛCDM: Problems, solutions, and the road ahead. Physics of the Dark Universe **12** (2016), 56–99.

[13] Candlish, G. N., Smith, R., and Fellhauer, M.: RAyMOND: an N-body and hydrodynamics code for MOND. Mon. Not. R. Astron. Soc. **446** (2015), 1060–1070.

[14] Conselice, C. J.: Galaxy Formation: Where do we stand? In: VIII. International Workshop on the Dark Side of the Universe, 2012, arXiv:1212.5641.

[15] Chiboucas, K., Jacobs, B. A., Tully, R. B., and Karachentsev, I. D.: Confirmation of faint dwarf galaxies in the M81 group. Astron. J. **146** (2013), 126–160.

[16] Dabringhausen, J., Kroupa, P., Famaey, B., Fellhauer M.: Understanding the internal dynamics of elliptical galaxies without non-baryonic dark matter. Mon. Not. R. Astron. Soc. (2016), accepted.

[17] Delgado-Serrano, R., Hammer, F., Yang, Y. B. et al.: How was the Hubble sequence 6 Gyr ago? Astron. Astrophys. **509** (2010), 78.

[18] Famaey, B. and McGaugh, S. S.: Modified Newtonian Dynamics (MOND): Observational phenomenology and relativistic extensions. Living Reviews in Relativity **15** (2012).

[19] Fernández Lorenzo, M., Sulentic, J., Verdes-Montenegro, L. et al.: Are (pseudo)bulges in isolated galaxies actually primordial relics? Astrophys. J. Lett. **788** (2014), L39–L45.

[20] Grandis, S., Rapetti, D., Saro, A., Mohr, J. J., and Dietrich, J. P.: Quantifying tensions between CMB and distance datasets in models with free curvature or lensing amplitude (2016), arXiv:1604.06463.

[21] Ibata, R. A., Lewis, G. F., Conn, A. R. et al.: A vast, thin plane of corotating dwarf galaxies orbiting the Andromeda galaxy. Nature **493** (2013), 62–65.

[22] Ibata, N. G., Ibata, R. A., Famaey, B., and Lewis, G. F.: Velocity anti-correlation of diametrically opposed galaxy satellites in the low-redshift Universe. Nature **511** (2014), 563–566.

[23] Ibata, R. A., Ibata, N. G., Lewis, G. F. et al.: A thousand shadows of Andromeda: Rotating planes of satellites in the Millennium-II Cosmological Simulation. Astrophys. J. Lett. **784** (2014), L6–L11.

[24] Ibata, R. A., Famaey, B., Lewis, G. F., Ibata, N. G., and Martin, N.: Eppur si Muove: Positional and kinematic correlations of satellite pairs in the low z universe. Astrophys. J. **805** (2015), 67–77.

[25] Javanmardi, B., Porciani, C., Kroupa, P., and Pflamm-Altenburg, J.: Probing the isotropy of cosmic acceleration traced by Type Ia Supernovae. Astrophys. J. **810** (2015), 47–57.

[26] Javanmardi, B., Martinez-Delgado, D., Kroupa, P. et al.: DGSAT: Dwarf galaxy survey with amateur telescopes. I. Discovery of low surface brightness systems around nearby spiral galaxies. Astron. Astrophys. **588** (2016), 89–101.

[27] Javanmardi, B. and Kroupa, P.: Anisotropy in the all-sky distribution of galaxy morphologies. Astron. Astrophys., submitted.

[28] Karachentsev, I. D.: Missing dark matter in the local universe. Astrophys. Bull. **67** (2012), 123–134.

[29] Keenan, R. C., Barger, A. J., and Cowie, L. L.: Evidence for a 300 Megaparsec scale under-density in the local galaxy distribution. Astrophys. J. **775** (2013), 62–78.

[30] Khoury, J.: Another path for the emergence of modified galactic dynamics from dark matter superfluidity. Phys. Rev. D **93** (2016), 103533.

[31] Kormendy, J., Drory, N., Bender, R., and Cornell, M. E.: Bulgeless giant galaxies challenge our picture of galaxy formation by hierarchical clustering. Astrophys. J. **723** (2010), 54–80.

[32] Křížek, M. and Somer, L.: A critique of the standard cosmological model. Neural Netw. World **24** (2014), 435–461.

[33] Kroupa, P., Theis, C., and Boily, C. M.: The great disk of Milky-Way satellites and cosmological sub-structures. Astron. Astrophys. **431** (2005), 517–521.

[34] Kroupa, P., Famaey, B., de Boer, K. S. et al.: Local-Group tests of dark-matter concordance cosmology. Towards a new paradigm for structure formation. Astron. Astrophys. **523** (2010), 32–54.

[35] Kroupa, P.: The Dark Matter Crisis: Falsification of the current standard model of cosmology. Publ. Astron. Soc. Australia **29** (2012), 395–433.

[36] Kroupa, P., Pawlowski, M., and Milgrom, M.: The failures of the standard model of cosmology require a new paradigm. Internat. J. Modern Phys. D **21** (2012), 1230003.

[37] Lessons from the Local Group (and beyond) on dark matter. In: K. C. Freeman, B. G. Elmegreen, D. L. Block, and M. Woolway (Eds.), *Lessons from the Local Group*, Dordrecht: Springer, 2015.

[38] Kroupa, P.: Galaxies as simple dynamical systems: observational data disfavor dark matter and stochastic star formation. Canad. J. Phys. **93** (2015), 169–202.

[39] Lena, D., Robinson, A., Marconi, A. et al.: Recoiling supermassive black holes: A search in the nearby universe. Astrophys. J. **795** (2014), 146–177.

[40] Llinares, C., Knebe, A., and Zhao, H.: Cosmological structure formation under MOND: a new numerical solver for Poisson's equation. Mon. Not. R. Astron. Soc. **391** (2008), 1778–1790.

[41] Lüghausen, F., Famaey, B., and Kroupa, P.: Phantom of RAMSES (POR): A new Milgromian dynamics N-body code. Canad. J. Phys. **93** (2015), 232–241.

[42] López-Corredoira, M. and Kroupa, P.: The number of tidal dwarf satellite galaxies in dependence of bulge index. Astrophys. J. **817** (2016), 75–82.

[43] McGaugh, S. and Milgrom, M.: Andromeda dwarfs in light of Modified Newtonian Dynamics. Astrophys. J. **766** (2013), 22–29.

[44] McGaugh, S. and Milgrom, M.: Andromeda dwarfs in light of Modified Newtonian Dynamics. Astrophys. J. **775** (2013), 139–145.

[45] Metz, M., Kroupa, P., and Jerjen, H.: The spatial distribution of the Milky Way and Andromeda satellite galaxies. Mon. Not. R. Astron. Soc. **374** (2007), 1125–1145.

[46] Metz, M., Kroupa, P., and Libeskind, N. I.: The orbital poles of Milky Way satellite galaxies: A rotationally supported disk of satellites. Astrophys. J. **680** (2008), 287–294.

[47] Metz, M., Kroupa, P., and Jerjen, H.: Discs of satellites: the new dwarf spheroidals. Mon. Not. R. Astron. Soc. **394** (2009), 2223–2228.

[48] Metz, M., Kroupa, P., Theis, C., Hensler, G., and Jerjen, H.: Did the Milky Way dwarf satellites enter the halo as a group? Astrophys. J. **697** (2009), 269–274.

[49] Milgrom, M.: A modification of the Newtonian dynamics as a possible alternative to the hidden mass hypothesis. Astrophys. J. **270** (1983), 365–370.

[50] Milgrom, M.: The modified dynamics as a vacuum effect. Phys. Lett. A **253** (1999), 273–279.

[51] Milgrom, M.: The Mond limit from spacetime scale invariance. Astrophys. J. **698** (2009), 1630–1638.

[52] Müller, O., Jerjen, H., Pawlowski, M. S., and Binggeli, B.: Testing the two planes of satellites in the Centaurus group. Astron. Astrophys. (2016), submitted, arXiv:1607.04024.

[53] Oehm, W., Thies, I., and Kroupa, P.: Constraints on the existence of dark matter halos by the galaxy group M81. Mon. Not. R. Astron. Soc. (2016), submitted.

[54] Pawlowski, M. S., Kroupa, P., and de Boer, K. S.: Making counter-orbiting tidal debris. The origin of the Milky Way disc of satellites? Astron. Astrophys. **532** (2011), 118–143.

[55] Pawlowski, M. S., Pflamm-Altenburg, J., and Kroupa, P.: The VPOS: a vast polar structure of satellite galaxies, globular clusters and streams around the Milky Way. Mon. Not. R. Astron. Soc. **423** (2012), 1109–1126.

[56] Pawlowski, M. S., Kroupa, P., Angus, G. et al.: Filamentary accretion cannot explain the orbital poles of the Milky Way satellites. Mon. Not. R. Astron. Soc. **424** (2012), 80–92.

[57] Pawlowski, M. S., Kroupa, P., and Jerjen, H.: Dwarf galaxy planes: the discovery of symmetric structures in the Local Group. Mon. Not. R. Astron. Soc. **435** (2013), 1928–1957.

[58] Pawlowski, M. S. and Kroupa, P.: The rotationally stabilized VPOS and predicted proper motions of the Milky Way satellite galaxies. Mon. Not. R. Astron. Soc. **435** (2013), 2116–2131.

[59] Pawlowski, M. S., Famaey, B., Jerjen, H. et al.: Co-orbiting satellite galaxy structures are still in conflict with the distribution of primordial dwarf galaxies. Mon. Not. R. Astron. Soc. **442** (2014), 2362–2380.

[60] Pawlowski, M. S. and McGaugh, S. S.: Co-orbiting planes of sub-halos are similarly unlikely around paired and isolated hosts. Astrophys. J. Lett. **789** (2014), L24–L31.

[61] Pawlowski, M. S., Famaey, B., Merritt, D., and Kroupa, P.: On the persistence of two small-scale problems in CDM. Astrophys. J. **815** (2015), 19–31.

[62] Pawlowski, M. S., McGaugh, S. S., and Jerjen, H.: The new Milky Way satellites: alignment with the VPOS and predictions for proper motions and velocity dispersions. Mon. Not. R. Astron. Soc. **453** (2015), 1047–1061.

[63] Pawlowski, M. S.: The alignment of SDSS satellites with the VPOS: effects of the survey footprint shape. Mon. Not. R. Astron. Soc. **456** (2016), 448–458.

[64] Peebles, P. J. E. and Nusser, A.: Nearby galaxies as pointers to a better theory of cosmic evolution. Nature **465** (2010), 565–569.

[65] Renaud, F., Famaey, B., and Kroupa P.: Star formation triggered by galaxy interactions in Milgromian gravity. Mon. Not. R. Astron. Soc., submitted.

[66] Riess, A. G., Macri, L. M., Hoffmann, S. L. et al.: A 2.4% determination of the local value of the Hubble constant. Astrophys. J. **826** (2016), 56.

[67] Sachdeva, S. and Saha, K.: Survival of pure disk galaxies over the last 8 billion years. Astrophys. J. Lett. **820** (2016), L4–L9.

[68] Shankar, F., Mei, S., Huertas-Company, M. et al.: Environmental dependence of bulge-dominated galaxy sizes in hierarchical models of galaxy formation. Comparison with the local universe. Mon. Not. R. Astron. Soc. **439** (2014), 3189–3212.

[69] Sohn, J., Hwang, H. S., Geller, M. J. et al.: Compact groups of galaxies with complete spectroscopic redshifts in the local universe. Korean Astron. Soc. **48** (2015), 381–398.

[70] Thies, I., Kroupa, P., and Famaey, B.: Simulating disk galaxies and interactions in Milgromian dynamics. In: Second BELISSIMA Workshop, arXiv:1606.04942, 2016.

[71] Thomson, R. C., Laine, S., and Turnbull, A.: Towards an interaction model of M81, M82 and NGC 3077. In: J. E. Barnes and D. B. Sanders (Eds.), *Galaxy Interactions at Low and High Redshift*, IAU Symposium Nr. 186, p. 135, 1999.

[72] Trippe, S.: Milgrom's law and 's shadow: How massive gravity connects galactic and cosmic dynamics. Korean Astron. Soc. **48** (2015), 191–194.

[73] Weinzirl, T., Jogee, S., Khochfar, S., Burkert, A., and Kormendy, J.: Bulge n and B/T in high-mass galaxies: Constraints on the origin of bulges in hierarchical models. Astrophys. J. **696** (2009), 411–447.

[74] Wetzstein, M., Naab, T., and Burkert, A.: Do dwarf galaxies form in tidal tails? Mon. Not. R. Astron. Soc. **375** (2007), 805–820.

[75] Whitbourn, J. R. and Shanks, T.: The galaxy luminosity function and the local hole. Mon. Not. R. Astron. Soc. **459** (2016), 496–507.

[76] Wiltshire, D. L.: Cosmic clocks, cosmic variance and cosmic averages. New J. Phys. **9** (2007), 377.

[77] Yun, M. S.: Tidal interactions in M81 Group. In: J. E. Barnes, and D. B. Sanders (Eds), *Galaxy Interactions at Low and High Redshift*, IAU Symposium Nr. 186, p. 81, 1999.

[78] Zhao, H., Famaey, B., Lüghausen, F., and Kroupa, P.: Local group timing in Milgromian dynamics. A past Milky Way-Andromeda encounter at $z > 0.8$. Astron. Astrophys. **557** (2013), L3–L7.

Conference *Cosmology on Small Scales 2016*
Michal Křížek and Yurii Dumin (Eds.)
Institute of Mathematics CAS, Prague

ON THE FRIEDMANN EQUATION FOR THE THREE-DIMENSIONAL HYPERSPHERE

Michal Křížek[1], Attila Mészáros[2]

[1]Institute of Mathematics, Czech Academy of Sciences
Žitná 25, CZ-115 67 Prague 1, Czech Republic
krizek@cesnet.cz
[2]Astronomical Institute of Charles University, Faculty of Mathematics and Physics
V Holešovičkách 2, CZ-180 00 Prague 8, Czech Republic,
meszaros@cesnet.cz

Abstract: The present standard cosmological model of the evolution of our universe, is based on the Friedmann equation, which was published by Alexander Friedmann in 1922. He applied Einstein's equations to an expanding three-dimensional sphere which enabled him to avoid boundary conditions. However, his description was very brief. Therefore, the main objective of this article is to detailed a derivation of the Friedmann equation for an unknown expansion function $a = a(t)$ representing the radius of the universe. Furthermore, we present serious arguments showing why the validity of Einstein's equations should not be extrapolated to the entire universe.

Keywords: Einstein's equations, standard cosmological model, dark matter, dark energy, cosmological parameters

PACS: 04.20-q, 95.35+d, 95.36+x, 98.80-k

1. How to imagine the sphere $\mathbb{S}^3$?

In accordance with the original article [5] by Friedmann, we assume that for each fixed time t, the universe[1] can be modeled by a three-dimensional sphere (hypersphere)[2]

$$\mathbb{S}^3_a = \{(x, y, z, w) \in \mathbb{E}^4 \,|\, x^2 + y^2 + z^2 + w^2 = a^2\}$$

with radius $a = a(t) > 0$, where $\mathbb{E}^4$ is the Euclidean space. It is actually a three-dimensional surface of a four-dimensional ball. The manifold $\mathbb{S}^3_a$ is maximally sym-

[1]The universe will be an isochrone in spacetime for constant t. It is often called the space.

[2]In 1900 Karl Schwarzschild already conjectured [25] that the universe can be described as a huge three-dimensional hypersphere. Albert Einstein also assumed that the gravitational interaction of mass causes a positive curvature and that the universe can be modeled by a three-dimensional hypersphere with unchanging radius, see [4, p. 152].

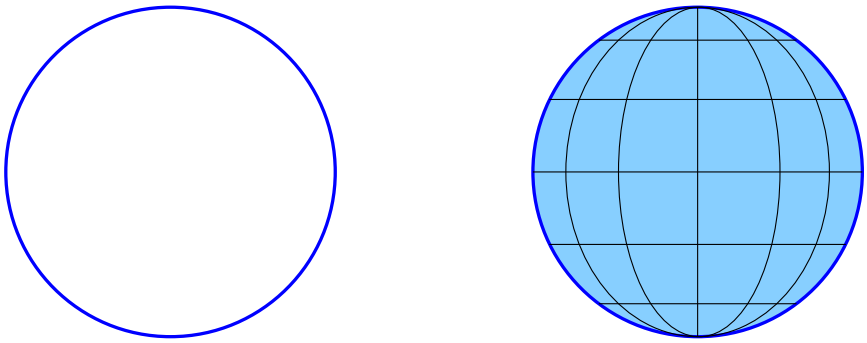

Figure 1: The unit circle on the left is the sphere $\mathbb{S}^1 = \{(x, y) \in \mathbb{E}^2 \,|\, x^2+y^2 = 1\}$. The surface of the unit ball on the right is the sphere $\mathbb{S}^2 = \{(x, y, z) \in \mathbb{E}^3 \,|\, x^2+y^2+z^2 = 1\}$. It can be expressed using the polar coordinates as follows: $x = r\cos\phi$, $y = r\sin\phi$, and the remaining third coordinate will be, by the Pythagoras theorem, equal to $z = \pm\sqrt{1-r^2}$, where $r \in [0, 1]$ and $\phi \in [0, 2\pi)$.

metric[3] which expresses the fact that our universe is homogeneous and isotropic on large scales. If $a = 1$ we will, for simplicity, omit the subscript a.

Contrary to e.g. a cylindrical surface, a two-dimensional sphere (see the right part of Fig. 1)

$$\mathbb{S}^2 = \{(x, y, z) \in \mathbb{E}^3 \,|\, x^2 + y^2 + z^2 = 1\}$$

cannot be isometrically unrolled into the Euclidean plane $\mathbb{E}^2$. Therefore, all maps of the Earth's surface are more or less distorted. Similarly, the curved hypersphere $\mathbb{S}^3$ cannot be mapped into the flat space $\mathbb{E}^3$ without any distortion of distances. Therefore, we will further present five independent manners of how to imagine the unit hypersphere $\mathbb{S}^3$.

1. The first manner uses parallel cuts. In the Euclidean space $\mathbb{E}^4$ consider a point with coordinates

$$\begin{aligned} x &= r\sin\theta\cos\phi, \\ y &= r\sin\theta\sin\phi, \\ z &= r\cos\theta, \\ w &= \pm\sqrt{1-r^2}, \end{aligned} \tag{1}$$

where $r \in [0, 1]$, $\theta \in [0, \pi]$, and $\phi \in [0, 2\pi)$. Then we easily find that

$$x^2 + y^2 + z^2 + w^2 = 1, \tag{2}$$

and thus $(x, y, z, w) \in \mathbb{S}^3$. For clarity, we now cut[4] the hypersphere $\mathbb{S}^3$ by parallel planes $w = \text{const.}$ for $|w| < 1$. This yields two-dimensional spheres with radii

[3] The corresponding group of symmetries is the orthogonal group $O(4)$.

[4] If we similarly cut the unit sphere $\mathbb{S}^2$ by parallel planes $z = \text{const.}$ for $|z| < 1$, we get circles with radii $r = \sqrt{1-z^2}$ and centers $(0, 0, z)$, see the parallels in the right part of Fig. 1.

$r = \sqrt{1-w^2}$ and centers $(0,0,0,w)$. Their union[5] is the hypersphere $\mathbb{S}^3$. The points $(x,y,z) \in \mathbb{S}^2_r$ are then expressed in standard spherical coordinates defined by the first three equations of (1). The angle $\theta = 0$ corresponds to the North Pole[6] and to the degenerated radius $r = 0$ (cf. Figs. 1 and 3).

2. The second manner uses the following *hyperspherical coordinates*

$$\begin{aligned} x &= \sin\chi \sin\theta \cos\phi, \\ y &= \sin\chi \sin\theta \sin\phi, \\ z &= \sin\chi \cos\theta, \\ w &= \cos\chi, \end{aligned}$$

where $\chi, \theta \in [0,\pi]$ and $\phi \in [0, 2\pi)$. We observe that these coordinates are a natural generalization of the standard spherical coordinates for the unit sphere $\mathbb{S}^2$ (cf. (1)) and that the equality (2) holds again.

Note that the manifold $\mathbb{S}^3$ with radius 1 can be divided into infinitely many spherical shells with radii $\sin\chi$ for $\chi \in [0,\pi]$. The corresponding surface areas are $4\pi \sin^2\chi$. Using the hyperspherical coordinates, we find that

$$\mathrm{vol}(\mathbb{S}^3) = 4\pi \int_0^\pi \sin^2\chi \,\mathrm{d}\chi = 2\pi[\chi - \frac{1}{2}\sin 2\chi]_0^\pi = 2\pi^2,$$

which leads to $\mathrm{vol}(\mathbb{S}^3_a) = 2\pi^2 a^3$ for an arbitrary radius $a > 0$ (cf. [4, p. 152]).

3. The third manner relies on local orthogonal projections. For simplicity, we first investigate the sphere $\mathbb{S}^2$. On $\mathbb{S}^2$ consider a small curved "square neighborhood" whose center is at the point $(0,1,0)$ and its sides are parts of great circles passing through the poles $(0,0,\pm 1)$ and the points $(\pm 1,0,0)$ on the equator. The left part of Fig. 2 shows the orthogonal projection of this neighborhood to the tangent plane $y = 1$. E.g. meridians are projected to converging vertical arcs.

Similarly, on the sphere $\mathbb{S}^3$ we may consider a small curved cube, whose edges are parts of great circles. The right part of Fig. 2 shows the orthogonal projection of this cube to the hyperplane $\mathbb{E}^3$ tangent to $\mathbb{S}^3$ at the center of the curved cube.

4. The fourth manner is the well-known stereographic projection. First, we again consider only the sphere $\mathbb{S}^2$. We will project from the North Pole $N = (0,0,1)$ all the remaining points of $\mathbb{S}^2$ onto the plane tangential to the South Pole $S = (0,0,-1)$. Then the meridians of the sphere (see Fig. 1 right) are mapped to lines passing through S and the parallels are mapped on circles.[7] This projection is a one-to-one mapping from $\mathbb{S}^2 \setminus N$ onto $\mathbb{E}^2$.

[5] Similarly, the union of all parallels (circles) from the right part of Fig. 1 is the sphere $\mathbb{S}^2$.

[6] For $r \in [0,1]$, $\theta \in [-\pi/2, \pi/2]$, and $\phi \in [0, 2\pi)$ we may also consider the coordinates $x = r\cos\theta\cos\phi$, $y = r\cos\theta\sin\phi$, and $z = r\sin\theta$, where $\theta = 0$ corresponds to the equator.

[7] Such a stereographic projection was used in the construction of the astronomical dial representing the celestial sphere at the Prague Astronomical Clock (Horologe).

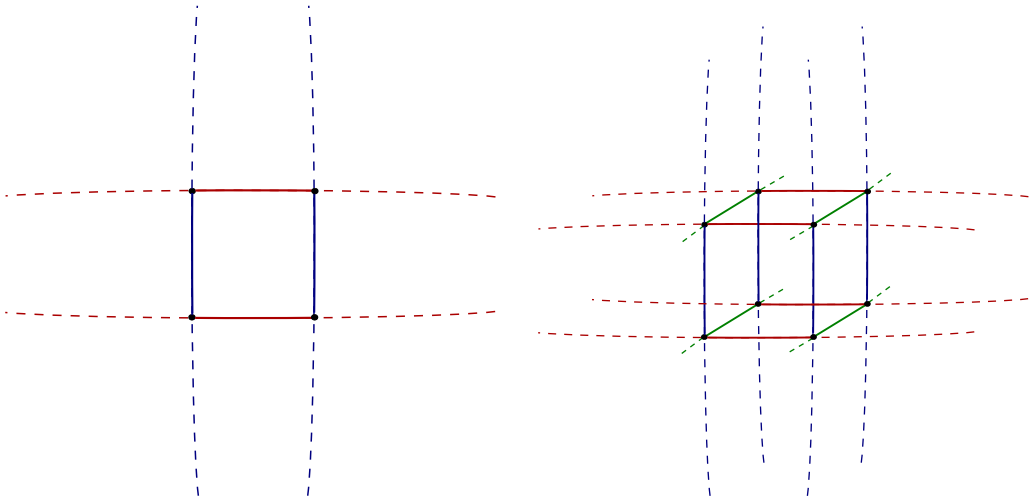

Figure 2: Local orthogonal projection of a part of the sphere $\mathbb{S}^n$ into the tangent hyperplane $\mathbb{E}^n$ for $n = 2$ and $n = 3$. All broken lines are parts of ellipses whose semimajor axes are equal to 1.

Similarly, for the hypersphere $\mathbb{S}^3$ we select two opposite poles $N = (0, 0, 0, 1)$ and $S = (0, 0, 0, -1)$. Then all points from $\mathbb{S}^3 \setminus N$ are projected from the North Pole N into a three-dimensional hyperplane tangent to $\mathbb{S}^3$ at the South Pole S. Great circles passing through N and S will be again mapped on lines passing through S, etc.

5. Finally, the best of all. The last manner uses the Gaussian plane of complex numbers $\mathbb{C}$. Setting

$$\boldsymbol{x} = x + \mathrm{i}y, \;\; \boldsymbol{z} = z + \mathrm{i}w \in \mathbb{C},$$

the hypersphere

$$\mathbb{S}^3 = \{(x, y, z, w) \in \mathbb{E}^4 \mid |x|^2 + |y|^2 + |z|^2 + |w|^2 = 1\}$$

can be expressed as a manifold resembling the unit circle in complex variables

$$\mathbb{S}^3 \cong \{(\boldsymbol{x}, \boldsymbol{z}) \in \mathbb{C}^2 \mid |\boldsymbol{x}|^2 + |\boldsymbol{z}|^2 = 1\}.$$

Moreover, we clearly have $|\boldsymbol{x}|^2 = |\boldsymbol{x}^2|$ and $|\boldsymbol{z}|^2 = |\boldsymbol{z}^2|$.

2. Metric tensor for a positive curvature index

The metric tensor of the spacetime has in general 10 independent entries. It is the solution of Einstein's equations of general relativity (see (20) below). Now we show that due to the high symmetry of the hypersphere $\mathbb{S}^3_a$ all the non-diagonal entries of the metric tensor vanish.

The unit hypersphere $\mathbb{S}^3$ is actually a three-dimensional hypersurface in four-dimensional Euclidean space $\mathbb{E}^4$. Therefore, according to (1) and [21, p. 253], the components of local coordinate vectors for $r < 1$ are

$$\begin{aligned}
p_1(r,\theta,\phi) &= \frac{\partial}{\partial r}p(r,\theta,\phi) = (\sin\theta\cos\phi, \sin\theta\sin\phi, \cos\theta, -r(1-r^2)^{-1/2}),\\
p_2(r,\theta,\phi) &= \frac{\partial}{\partial \theta}p(r,\theta,\phi) = (r\cos\theta\cos\phi, r\cos\theta\sin\phi, -r\sin\theta, 0),\\
p_3(r,\theta,\phi) &= \frac{\partial}{\partial \phi}p(r,\theta,\phi) = (-r\sin\theta\sin\phi, r\sin\theta\cos\phi, 0, 0),
\end{aligned}$$

where the vector p with components p_1, p_2, p_3 lies in the hyperplane tangent at the point $(x, y, z, w) \in \mathbb{S}^3$ (cf. Fig. 3 for a two-dimensional sphere).

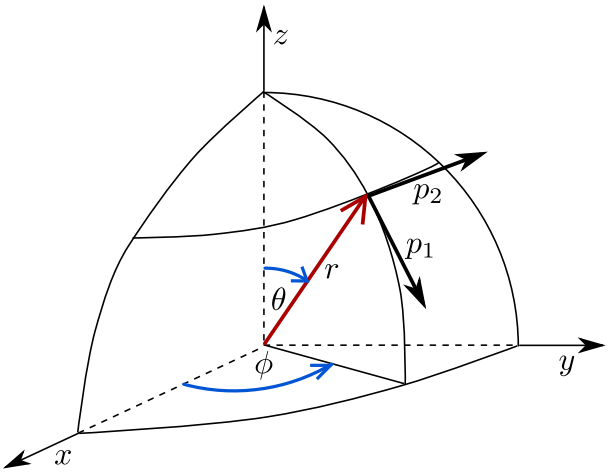

Figure 3: Local coordinate orthogonal vectors p_1 and p_2 in the plane tangent at the point $(x, y, z) \in \mathbb{S}^2$ given in the standard spherical coordinates (r, ϕ, θ), cf. (1).

The covariant coordinates of the symmetric metric tensor corresponding to the unit hypersphere $\mathbb{S}^3$ are given by the relations

$$\tilde{g}_{\alpha\beta} = p_\alpha \cdot p_\beta \quad \text{for} \quad \alpha, \beta = 1, 2, 3,$$

where $\cdot$ denotes the scalar product. Hence, it follows that

$$\begin{aligned}
\tilde{g}_{11} &= \sin^2\theta\cos^2\phi + \sin^2\theta\sin^2\phi + \cos^2\theta + \frac{r^2}{1-r^2} = 1 + \frac{r^2}{1-r^2} = \frac{1}{1-r^2},\\
\tilde{g}_{22} &= r^2\cos^2\theta\cos^2\phi + r^2\cos^2\theta\sin^2\phi + r^2\sin^2\theta = r^2,\\
\tilde{g}_{33} &= r^2\sin^2\theta\sin^2\phi + r^2\sin^2\theta\cos^2\phi = r^2\sin^2\theta,
\end{aligned}$$

and the other entries vanish, because $p_1 \cdot p_2 = p_1 \cdot p_3 = p_2 \cdot p_3 = 0$ due to the symmetry of $\mathbb{S}^3$. The metric tensor corresponding to the unit sphere $\mathbb{S}^3$ is therefore given by the diagonal matrix

$$\tilde{g}_{\alpha\beta} = \begin{pmatrix} \dfrac{1}{1-r^2} & 0 & 0 \\ 0 & r^2 & 0 \\ 0 & 0 & r^2 \sin^2\theta \end{pmatrix}, \quad \alpha, \beta = 1, 2, 3, \tag{3}$$

where $r \in [0, 1)$, $\theta \in [0, \pi]$, and $\phi \in [0, 2\pi)$.

The metric tensor associated to the the whole space-time manifold is then also given by the diagonal matrix

$$g_{ij} = \begin{pmatrix} 1 & 0 & 0 & 0 \\ 0 & \dfrac{-a^2}{1-r^2} & 0 & 0 \\ 0 & 0 & -a^2 r^2 & 0 \\ 0 & 0 & 0 & -a^2 r^2 \sin^2\theta \end{pmatrix}, \quad i, j = 0, 1, 2, 3. \tag{4}$$

The zero index corresponds to the time coordinate and the remaining three indices correspond to spatial coordinates. In the sequel, the Greek indices will run through the set $\{1, 2, 3\}$, while the Latin indices through the set $\{0, 1, 2, 3\}$.

A historical note. In the theory of relativity, the metric associated to (4) is usually written using infinitesimally small quantities[8] as follows:

$$\mathrm{d}s^2 = c^2 \mathrm{d}t^2 - a^2(t)\Big[\frac{\mathrm{d}r^2}{1-r^2} + r^2(\mathrm{d}\theta^2 + \sin^2\theta\, \mathrm{d}\phi^2)\Big], \tag{5}$$

where the time coordinate fulfills

$$x_0 = ct$$

and $r \in [0, 1)$ is dimensionless. The metric (5) of the space-time manifold modeling the evolution of the universe for a special expansion function $a = a(t)$ first appeared in the article by Howard Percy Robertson [23, p. 826] in 1929. The same formula was also published by Arthur Geoffrey Walker [28, p. 121] in 1936. Therefore, the metric (5) is called the *Robertson-Walker* metric.[9] However, Walker does not cite Robertson's article [23], but only some Robertson's later works from Astrophys. J. 82 (1935), 284–301; 83 (1936), 187–201, 257–271. Consequently, the priority definitely belongs to Robertson.

For the entries of the covariant metric tensor (4) we thus have

$$g_{00} = 1, \quad g_{0\alpha} = 0, \quad g_{\alpha\beta} = -a^2(t)\tilde{g}_{\alpha\beta} \quad \text{for } \alpha, \beta = 1, 2, 3, \tag{6}$$

[8] Throughout this text, we will deliberately avoid the use of ill-defined infinitesimally small quantities $\mathrm{d}s$, $\mathrm{d}t$, $\mathrm{d}r$, etc.

[9] The metric (5) is sometimes also called the Friedmann-Lemaître-Robertson-Walker metric or just FLRW-metric due to the pioneering papers [5] and [16].

where $\tilde{g}_{\alpha\beta}$ is the metric tensor of the unit sphere $\mathbb{S}^3$,

$$\tilde{g}_{11} = \frac{1}{1-r^2}, \quad \tilde{g}_{22} = r^2, \quad \tilde{g}_{33} = r^2 \sin^2\theta, \quad \text{and} \quad \tilde{g}_{\alpha\beta} = 0 \quad \text{for} \quad \alpha \neq \beta$$

(i.e. the tilde actually corresponds only to the expression in brackets in relation (5)).

Since the inverse matrix to (4) is also diagonal, for the entries of the contravariant symmetric metric tensor we have

$$g^{00} = 1, \quad g^{0\alpha} = 0, \quad g^{\alpha\beta} = -\frac{1}{a^2}\tilde{g}^{\alpha\beta}, \tag{7}$$

where

$$\tilde{g}^{11} = 1 - r^2, \quad \tilde{g}^{22} = \frac{1}{r^2}, \quad \tilde{g}^{33} = \frac{1}{r^2 \sin^2\theta}, \quad \tilde{g}^{\alpha\beta} = 0 \quad \text{for} \quad \alpha \neq \beta,$$

$r \neq 0$, and $\theta \neq 0$.

3. Calculation of the Christoffel symbols

Entries of the Ricci tensor which appears in Einstein's equations (20) are defined by means of the Christoffel symbols (cf. (17) below). In the covariant form (i.e. only with lower indices) the *Christoffel symbols* are defined as follows

$$\Gamma_{ijk} = \frac{1}{2}(g_{ij,k} + g_{ki,j} - g_{jk,i}), \tag{8}$$

where the index after the comma indicates, for simplicity, the ordered number of a variable according to which we differentiate. From this and the symmetry of the metric tensor g_{ij} we immediately obtain also the symmetry of the Christoffel symbols in the second and third index,

$$\Gamma_{ijk} = \Gamma_{ikj} \quad \text{for } i, j, k = 0, 1, 2, 3. \tag{9}$$

Therefore, there are not $4 \times 4 \times 4 = 64$ different Christoffel symbols, but generally only $4 \times (1 + 2 + 3 + 4) = 40$. Now let us calculate all of them.

From (8) and (4) we see that

$$\Gamma_{000} = \frac{1}{2} g_{00,0} = 0.$$

Since the off-diagonal entries in (4) vanish and the derivative of a constant function is zero, we obtain by (8) for $\alpha = 1, 2, 3$

$$\Gamma_{0\alpha0} = \Gamma_{00\alpha} = \frac{1}{2}(g_{0\alpha,0} + g_{00,\alpha} - g_{\alpha0,0}) = 0.$$

Similarly, we get

$$\Gamma_{\alpha 00} = \frac{1}{2}(g_{\alpha 0,0} + g_{0\alpha,0} - g_{00,\alpha}) = 0. \tag{10}$$

All 7 Christoffel symbols, in which at least two indices are zeros, and thus equal to 0.

Next, assume that just one index is zero. Then, according to (6) for $\alpha, \beta = 1, 2, 3$ we get only 6 Christoffel symbols due to the symmetry (9),

$$\Gamma_{0\alpha\beta} = \frac{1}{2}(g_{0\alpha,\beta} + g_{\beta 0,\alpha} - g_{\alpha\beta,0}) = -\frac{1}{2}g_{\alpha\beta,0} = aa_{,0}\tilde{g}_{\alpha\beta},$$

where

$$a_{,0} = \frac{\partial a}{\partial x_0} = \frac{1}{c}\frac{\partial a}{\partial t} \tag{11}$$

is a dimensionless quantity. For the additional $3 \times 3 = 9$ Christoffel symbols we have by (6)

$$\Gamma_{\alpha 0\beta} = \Gamma_{\alpha\beta 0} = \frac{1}{2}(g_{\alpha\beta,0} + g_{0\alpha,\beta} - g_{\beta 0,\alpha}) = \frac{1}{2}g_{\alpha\beta,0} = -aa_{,0}\tilde{g}_{\alpha\beta}, \tag{12}$$

since we again differentiate with respect to the time variable.

Finally, assume that all indices are nonzero, i.e., we will differentiate only with respect to spatial coordinates. Then by (8) and (6), we have

$$\Gamma_{\alpha\beta\gamma} = \frac{1}{2}(g_{\alpha\beta,\gamma} + g_{\gamma\alpha,\beta} - g_{\beta\gamma,\alpha}) = -\frac{a^2}{2}(\tilde{g}_{\alpha\beta,\gamma} + \tilde{g}_{\gamma\alpha,\beta} - \tilde{g}_{\beta\gamma,\alpha}) = -a^2\tilde{\Gamma}_{\alpha\beta\gamma}$$

and the number of these remaining Christoffel symbols is $3 \times 6 = 18$. Hence, we have established in total $7 + (6 + 9) + 18 = 40$ values of the Christoffel symbols (which are generally different).

Next we'll use the familiar *Einstein's summation convention* for summation over repeating upper and lower index. To get once contravariant and twice covariant Christoffel symbol (i.e. with one upper and two lower indices) that appears in the definition of the Ricci tensor (17), we use the following relation[10] [17, p. 340]

$$\Gamma^i{}_{jk} = g^{i\ell}\Gamma_{\ell jk}$$

with summation over $\ell = 0, 1, 2, 3$, i.e. $g^{i\ell}\Gamma_{\ell jk} = \sum_{\ell=0}^{3} g^{i\ell}\Gamma_{\ell jk}$. In particular, we find that

$$\Gamma^0{}_{jk} = g^{0\ell}\Gamma_{\ell jk} = g^{00}\Gamma_{0jk} = \Gamma_{0jk},$$

since by (7) the off-diagonal entries of the contravariant metric tensor vanish and $g^{00} = 1$. Similarly for $\alpha, \beta = 1, 2, 3$ we have by (6)

$$\Gamma^\alpha{}_{jk} = g^{\alpha i}\Gamma_{ijk} = g^{\alpha\beta}\Gamma_{\beta jk} = -\frac{1}{a^2}\tilde{g}^{\alpha\beta}\Gamma_{\beta jk},$$

[10] Using (8), we get $\Gamma^i{}_{jk} = \frac{1}{2}g^{i\ell}(g_{\ell j,k} + g_{k\ell,j} - g_{jk,\ell})$.

as $g^{\alpha 0} = 0$. Furthermore, from the equality (10) we have

$$\Gamma^{\alpha}_{\ 00} = 0$$

and by (12) we obtain

$$\Gamma^{\alpha}_{\ 0\beta} = -\frac{1}{a^2}\tilde{g}^{\alpha\gamma}\Gamma_{\gamma 0\beta} = -\frac{1}{a^2}\tilde{g}^{\alpha\gamma}(-aa_{,0})\tilde{g}_{\beta\gamma} = \delta^{\alpha}_{\ \beta}\frac{a_{,0}}{a}, \tag{13}$$

where $\delta^{\alpha}_{\ \gamma}$ is the well-known *Kronecker delta* (i.e. $\delta^1_{\ 1} = \delta^2_{\ 2} = \delta^3_{\ 3} = 1$ and $\delta^{\alpha}_{\ \beta} = 0$ for $\alpha \neq \beta$). From relations (7) it follows that

$$\Gamma^{0}_{\ 00} = 0, \quad \Gamma^{0}_{\ 0\alpha} = 0, \quad \Gamma^{\alpha}_{\ 00} = g^{\alpha i}\Gamma_{i00} = 0, \quad \Gamma^{0}_{\ \alpha\beta} = aa_{,0}\tilde{g}_{\alpha\beta} \tag{14}$$

and

$$\Gamma^{\alpha}_{\ \beta\gamma} = g^{\alpha j}\Gamma_{j\beta\gamma} = g^{\alpha\varepsilon}\Gamma_{\varepsilon\beta\gamma} = -\frac{1}{a^2}\tilde{g}^{\alpha\varepsilon}(-a^2\tilde{G}_{\varepsilon\beta\gamma}) = \tilde{g}^{\alpha\varepsilon}\tilde{\Gamma}_{\varepsilon\beta\gamma} = \tilde{\Gamma}^{\alpha}_{\ \beta\gamma}. \tag{15}$$

We see that in calculating the mixed Christoffel symbol, the expansion function a is cancelled out.

4. Calculation of the Ricci tensor

First note that

$$\tilde{g}^{\alpha\beta}\tilde{g}_{\beta\gamma} = \delta^{\alpha}_{\ \gamma} \quad \text{for} \quad \alpha, \beta, \gamma = 1, 2, 3.$$

Using Einstein's summation convention, we thus have

$$\delta^{\alpha}_{\ \alpha} = 3 \qquad \text{and} \qquad \delta^{\alpha}_{\ \beta}\delta^{\beta}_{\ \alpha} = 3, \tag{16}$$

which can be seen by a step-by-step substitution for $\alpha, \beta = 1, 2, 3$.

Further recall the definition of *the Ricci tensor*

$$R_{ij} = R_{ji} = R^{k}_{\ ikj} = \Gamma^{k}_{\ ij,k} - \Gamma^{k}_{\ ik,j} + \Gamma^{\ell}_{\ ij}\Gamma^{k}_{\ \ell k} - \Gamma^{\ell}_{\ ik}\Gamma^{k}_{\ j\ell}\,, \tag{17}$$

where $R^{k}_{\ i\ell j}$ is the Riemann tensor[11]. From this and (13)–(16) we come to

$$\begin{aligned} R_{00} &= \Gamma^{k}_{\ 00,k} - \Gamma^{k}_{\ 0k,0} + \Gamma^{\ell}_{\ 00}\Gamma^{k}_{\ \ell k} - \Gamma^{\ell}_{\ 0k}\Gamma^{k}_{\ 0\ell} = -\Gamma^{\alpha}_{\ 0\alpha,0} - \Gamma^{\alpha}_{\ 0\beta}\Gamma^{\beta}_{\ 0\alpha} \\ &= -\Big(\frac{a_{,0}}{a}\delta^{\alpha}_{\ \alpha}\Big)_{,0} - \Big(\frac{a_{,0}}{a}\delta^{\alpha}_{\ \beta}\Big)\Big(\frac{a_{,0}}{a}\delta^{\beta}_{\ \alpha}\Big) \\ &= -3(a_{,0}/a)_{,0} - 3(a_{,0}/a)^2 = -3\frac{a_{,00}}{a}, \end{aligned} \tag{18}$$

where $a_{,00}$ denotes the second derivative with respect to time variable x_0, and

$$\begin{aligned} R_{0\alpha} &= \Gamma^{k}_{\ 0\alpha,k} - \Gamma^{k}_{\ 0k,\alpha} + \Gamma^{\ell}_{\ 0\alpha}\Gamma^{k}_{\ \ell k} - \Gamma^{\ell}_{\ 0k}\Gamma^{k}_{\ \alpha\ell} \\ &= \Gamma^{\beta}_{\ 0\alpha,\beta} - \Gamma^{\beta}_{\ 0\beta,\alpha} + \Gamma^{\beta}_{\ 0\alpha}\Gamma^{\gamma}_{\ \beta\gamma} - \Gamma^{\beta}_{\ 0\gamma}\Gamma^{\gamma}_{\ \alpha\beta} \\ &= \Gamma^{\beta}_{\ 0\alpha}\Gamma^{\gamma}_{\ \beta\gamma} - \Gamma^{\beta}_{\ 0\gamma}\Gamma^{\gamma}_{\ \alpha\beta} = \frac{a_{,0}}{a}\delta^{\beta}_{\ \gamma}\tilde{\Gamma}^{\gamma}_{\ \beta\gamma} - \frac{a_{,0}}{a}\delta^{\beta}_{\ \gamma}\tilde{\Gamma}^{\gamma}_{\ \alpha\beta} \\ &= \frac{a_{,0}}{a}\big(\tilde{\Gamma}^{\gamma}_{\ \alpha\gamma} - \tilde{\Gamma}^{\beta}_{\ \alpha\beta}\big) = 0, \end{aligned}$$

[11]The *Riemann tensor* is defined by $R^{k}_{\ imj} = \Gamma^{k}_{\ ij,m} - \Gamma^{k}_{\ im,j} + \Gamma^{\ell}_{\ ij}\Gamma^{k}_{\ \ell m} - \Gamma^{\ell}_{\ im}\Gamma^{k}_{\ j\ell}$.

where we used the fact that $\Gamma^{\beta}_{0\alpha,\beta} = \Gamma^{\beta}_{0\beta,\alpha} = 0$, because derivatives with respect to spatial coordinates vanish due to (13). However, we will not employ the equality of $R_{0\alpha} = 0$ to derive the Friedmann equations.

Finally, according to (13)–(17) for $\alpha, \beta = 1, 2, 3$ we have

$$\begin{aligned} R_{\alpha\beta} &= \Gamma^{k}_{\alpha\beta,k} - \Gamma^{k}_{\alpha k,\beta} + \Gamma^{\ell}_{\alpha\beta}\Gamma^{k}_{\ell k} - \Gamma^{\ell}_{\alpha k}\Gamma^{k}_{\beta\ell} \\ &= \Gamma^{0}_{\alpha\beta,0} + \underline{\tilde{\Gamma}^{\gamma}_{\alpha\beta,\gamma}} - \underline{\tilde{\Gamma}^{\gamma}_{\alpha\gamma,\beta}} + \Gamma^{0}_{\alpha\beta}\Gamma^{\gamma}_{0\gamma} \\ &\quad + \underline{\tilde{\Gamma}^{\gamma}_{\alpha\beta}\tilde{\Gamma}^{\varepsilon}_{\gamma\varepsilon}} - \Gamma^{0}_{\alpha\gamma}\Gamma^{\gamma}_{\beta 0} - \Gamma^{\gamma}_{\alpha 0}\Gamma^{0}_{\beta\gamma} - \underline{\tilde{\Gamma}^{\gamma}_{\alpha\varepsilon}\tilde{\Gamma}^{\varepsilon}_{\beta\gamma}} \\ &= \tilde{R}_{\alpha\beta} + (a_{,00}a + a_{,0}^2)\tilde{g}_{0\beta} + 3a_{,0}^2\tilde{g}_{\alpha\beta} - a_{,0}^2\tilde{g}_{\alpha\beta} - a_{,0}^2\tilde{g}_{\alpha\beta} \\ &= \tilde{R}_{\alpha\beta} + (a_{,00}a + 2a_{,0}^2)\tilde{g}_{\alpha\beta} = (a_{,00}a + 2a_{,0}^2 + 2)\tilde{g}_{\alpha\beta}, \end{aligned} \tag{19}$$

where the sum of the underlined terms defines the Ricci tensor $\tilde{R}_{\alpha\beta} = 2\tilde{g}_{\alpha\beta}$ (see [29, p. 383]), which has nonzero entries only on the diagonal due to the maximal symmetry of the manifold $\mathbb{S}^3$, see (3).

Remark. We see that the Ricci tensor contains no spatial derivatives of the metric tensor, although according to (17) it is defined by the first derivatives of the Christoffel symbols and these are by (8) defined by the first derivatives of the metric tensor. The reason is a very high symmetry of the sphere $\mathbb{S}^3$ (see [29]).

5. Derivation of the Friedmann equations from Einstein's equations

For simplicity, suppose first that the cosmological constant in Einstein's equations is $\Lambda = 0$. Then *Einstein's equations* have the form

$$R_{ij} - \frac{1}{2}Rg_{ij} = \frac{8\pi G}{c^4}T_{ij}, \tag{20}$$

where the left-hand side is called the *Einstein tensor*, $R = g^{ij}R_{ij}$ is the *Ricci scalar*, the entries of the metric tensor g_{ij} are unknown gravitational potentials, which are via relations (8) and (17) contained also in the Ricci tensor, and T_{ij} is the *tensor of density of energy and momentum*. Since $\mathbb{S}^3_a$ is maximally symmetric, all the tensors in (20) are diagonal and

$$T_{00} = T^{0}_{0} = T^{00} = \rho c^2, \quad T^{1}_{1} = T^{2}_{2} = T^{3}_{3} = -p,$$

where the mass density $\rho = \rho(t)$ and the pressure $p = p(t)$ are independent of the space coordinates [17, p. 728]. From this we have (see [29, pp. 342, 472])

$$R_{ij} = \frac{8\pi G}{c^4}\big(T_{ij} - \frac{1}{2}Tg_{ij}\big), \tag{21}$$

where

$$T = T^{0}_{0} + T^{\alpha}_{\alpha} = \rho c^2 - 3p$$

is the trace and $R=-8\pi GT/c^4$. The 00-entry of these specially modified Einstein's equations (21) takes by (18) and (6) the form

$$-3\frac{a_{,00}}{a}=\frac{8\pi G}{c^4}\Big(\rho c^2-\frac{1}{2}g_{00}(\rho c^2-3p)\Big)=\frac{4\pi G}{c^2}\Big(\rho+\frac{3p}{c^2}\Big).$$

From this and (20), we get the linear differential equation of the 2nd order[12]

$$\frac{\ddot a}{a}=-\frac{4\pi G}{3}\Big(\rho+\frac{3p}{c^2}\Big), \tag{22}$$

where the dot denotes the time derivative. Einstein's equations (20) are nonlinear, in general, due to (17). Notice how the nonlinearity elegantly disappears in (18) for the hypersphere $\mathbb{S}^3_a$.

Note that the other three equations $R_{0\alpha}=8\pi Gc^{-4}\big(T_{0\alpha}-\frac{1}{2}Tg_{0\alpha}\big)=0$ for $\alpha=1,2,3$ do not give us any useful relationship for the unknown functions a,ρ,p.

Finally, according to (19), (7), and (21), we have

$$\begin{aligned}(a_{,00}a+2a_{,0}^2+2)\tilde g_{\alpha\beta}=R_{\alpha\beta}&=\frac{8\pi G}{c^4}\Big(-pg_{\alpha\beta}-\frac{1}{2}g_{\alpha\beta}(\rho c^2-3p)\Big)\\&=\frac{4\pi G}{c^4}g_{\alpha\beta}(p-\rho c^2)=\frac{4\pi G}{c^4}(-a^2\tilde g_{\alpha\beta})(p-\rho c^2).\end{aligned}$$

Thus from (11) we obtain

$$(a\ddot a+2\dot a^2+2c^2)\tilde g_{\alpha\beta}=\frac{4\pi Ga^2}{c^2}(\rho c^2-p)\tilde g_{\alpha\beta}.$$

This is altogether six equations, but the three corresponding to the diagonal entries are the same and the remaining three non-diagonal entries vanish and lead to the unusable identity $0=0$. So we obtain only one equation

$$a\ddot a+2\dot a^2+2c^2=4\pi Ga^2\Big(\rho-\frac{p}{c^2}\Big). \tag{23}$$

Hence, together with (22), we get two equations for three unknowns a,ρ,p. As the third equation we may consider, e.g., the state equation $p=p(\rho)$.

Now multiply the equation (22) by the function a^2 and subtract it from (23). Then we find that

$$2\dot a^2+2c^2=4\pi Ga^2\Big(\rho-\frac{p}{c^2}\Big)+\frac{4\pi Ga^2}{3}\Big(\rho+\frac{3p}{c^2}\Big),$$

which after a simple adjustment leads to the sought nonlinear *Friedmann equation* of the first order

$$\boxed{\frac{\dot a^2}{a^2}+\frac{c^2}{a^2}=\frac{8\pi G\rho}{3}.} \tag{24}$$

[12]This equation is sometimes called the linear Friedmann equation, even though it does not appear in the original paper [5] by Friedmann.

Note that (22)–(24) are three equations, but only two of them are independent.

Alan Guth [7, p. 348] calls the Friedmann equations (22) and (24) the Einstein equations, since they in fact arose by applying (20) to the very special manifold $\mathbb{S}^3_a$.

Remark. The case of a nonzero cosmological constant $\Lambda \neq 0$ can be formally rewritten by appropriate transformations (25) to the case $\Lambda = 0$. For $\Lambda \neq 0$ let us set

$$\overline{p} := p - \frac{\Lambda c^4}{8\pi G} \quad \text{and} \quad \overline{\rho} := \rho + \frac{\Lambda c^2}{8\pi G}, \tag{25}$$

i.e., the pressure $\overline{p}$ can also attain negative values. We see that $\overline{p} + \overline{\rho}c^2 = p + \rho c^2$ and that the equation

$$R_{ij} - \frac{1}{2}Rg_{ij} - \Lambda g_{ij} = \frac{8\pi G}{c^4}T_{ij} = \frac{8\pi G}{c^4}((p + \rho c^2)U_iU_j - pg_{ij}),$$

where $U_i = (1, 0, 0, 0)$, changes into the form (20) without the cosmological constant

$$R_{ij} - \frac{1}{2}Rg_{ij} = \frac{8\pi G}{c^4}((\overline{p} + \overline{\rho}c^2)U_iU_j - \overline{p}g_{ij}).$$

Then we obtain like in (22)

$$\frac{\ddot{a}}{a} = -\frac{4\pi G}{3}\Big(\overline{\rho} + \frac{3\overline{p}}{c^2}\Big) = -\frac{4\pi G}{3}\Big(\rho + \frac{3p}{c^2} - \frac{\Lambda c^2}{4\pi G}\Big)$$

and instead of the Friedmann equation (24) we get

$$\frac{\dot{a}^2}{a^2} + \frac{c^2}{a^2} = \frac{8\pi G\overline{\rho}}{3} = \frac{8\pi G\rho}{3} + \frac{\Lambda c^2}{3}. \tag{26}$$

The corresponding graph of the expansion function $a = a(t)$ is given in [14, p. 70].

6. Cosmological parameters

First, recall the definition of the *Hubble parameter*

$$H(t) := \frac{\dot{a}(t)}{a(t)} \tag{27}$$

and divide the Friedmann equation (26) by the square $H^2 \geq 0$ as it is usually done in the literature on cosmology, i.e., without a preliminary warning that we may possibly divide by zero, which can lead to various paradoxes (see [13], [15]). Then we get the so-called *normalized Friedmann equation*

$$1 = \Omega_{\mathrm{M}}(t) + \Omega_{\Lambda}(t) + \Omega_{\mathrm{K}}(t) \tag{28}$$

for three cosmological parameters, which are defined as follows

$$\Omega_{\mathrm{M}}(t) := \frac{8\pi G\rho(t)}{3H^2(t)} > 0, \quad \Omega_{\Lambda}(t) := \frac{\Lambda c^2}{3H^2(t)}, \quad \Omega_{\mathrm{K}}(t) := -\frac{c^2}{\dot{a}^2(t)}. \tag{29}$$

Saul Perlmutter calls the parameter Ω_{M} the *mass density* and Ω_{Λ} the *vacuum energy density* (see [20]). The parameter Ω_{K} is called the *curvature parameter* in [19].

Notice that for Einstein's stationary universe[13] with $\dot{a}(t) \equiv 0$ the mass density parameter Ω_{M} attains by (27) and (29) an infinite value, even though nothing unusual happens. We should properly say that this parameter is not well defined as its denominator is zero. We divide by zero also in the case of the other two parameters from (29).

Similarly, we divide by zero in the case of the so-called oscillating universe, where the expansion function repeatedly increases and then decreases [27]. The reason is that the derivative $\dot{a}$ vanishes at the point of maximum.

Let us emphasize that the measured density of baryonic matter is always finite. This shows that the Friedmann model is strange, since the ratio between dark and baryonic matter may attain arbitrarily large values. Cosmological parameters have a strange behavior also in other cases [13].

At present there is a large number of papers on the so-called *precise cosmology* that categorically state (see Fig. 4):

The universe is composed of 26.8 % of dark matter, 4.9 % of baryonic matter, and 68.3 % of dark energy.

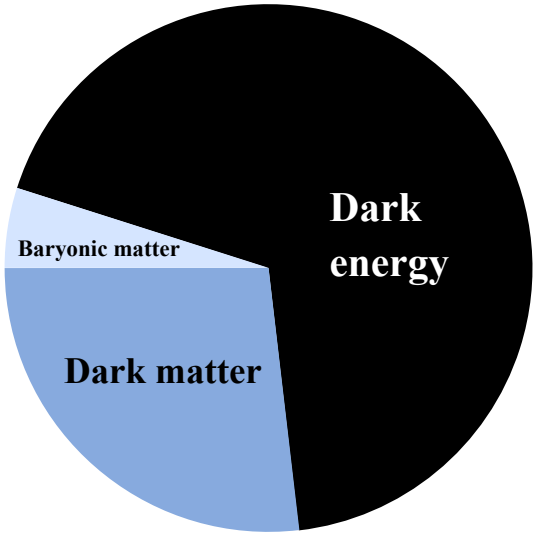

Figure 4: Results of the Planck satellite [19] are interpreted in such a way that our universe consists of about 26.8 % of dark matter, 4.9 % of baryonic matter, and 68.3 % of dark energy. However, they are based on the normalized Friedmann equation (28), which was derived using excessive extrapolations by many orders of magnitude. Cosmological parameters are searched so that the solution of (28) is as close as possible to the measured data. The amount of baryonic matter is estimated by a luminous matter [30, p. 74].

[13]The value of the corresponding radius a follows directly from the Friedmann equation (26).

Rightly they should claim:

According to the standard FLRW cosmological model based on the Friedmann equation, the universe could consist of about 27 % of dark matter, 5 % of baryonic matter, and 68 % of dark energy.[14]

It is important to realize the fundamental difference between these two statements. Therefore, we will now look in more detail how the above percentages were obtained.

The current values of cosmological parameters are determined, for example, by very distant explosions of type Ia supernovae, which are treated as the so-called standard candles (for details see [20], [22]). Type Ia supernovae have about 10–15 % less luminosity[15] than if the expansion of the universe would decelerate only by gravity. From this it can be concluded that the supernova light spreads into a larger volume, and therefore the expansion of the universe accelerates. To determine the distances of supernovae (see [8], [22, p. 1021]) the following formula from [3, p. 511] derived from the Friedmann equation for the so-called *luminosity distance* is used

$$d_{\mathrm{L}} = \frac{c(1+z)}{H_0\sqrt{|\Omega_{\mathrm{K}}|}}\sin\Big(\sqrt{|\Omega_{\mathrm{K}}|}\int_0^z \frac{\mathrm{d}\overline{z}}{\sqrt{(1+\overline{z})^2(1+\Omega_{\mathrm{M}}\overline{z}) - \overline{z}(2+\overline{z})\Omega_\Lambda}}\Big). \tag{30}$$

Here $H_0 = H(t_0) \approx 70\,\mathrm{km\,s^{-1}Mpc^{-1}}$ is the current value of the Hubble parameter [26] at time $t = t_0$ which corresponds to the present, and $\Omega_{\mathrm{K}} = 1 - \Omega_{\mathrm{M}} - \Omega_\Lambda$ by (28), where for brevity the actual values of the cosmological parameters are denoted by

$$\Omega_{\mathrm{M}} = \Omega_{\mathrm{M}}(t_0), \quad \Omega_\Lambda = \Omega_\Lambda(t_0), \quad \text{and} \quad \Omega_{\mathrm{K}} = \Omega_{\mathrm{K}}(t_0).$$

From this, the measured values of the redshift z of absorption spectral lines of silicon, and the luminosity of type Ia supernovae we can determine particular values of cosmological parameters (29) by χ^2 test [22, p. 1021]. In the case of an oscillating (or stationary) universe, the Hubble parameter vanishes and in (30) we again divide by zero. The resulting set of admissible values of cosmological parameters is marked by SNe in Fig. 5.

For admissible values of cosmological parameters $\Omega_{\mathrm{M}} = 0.01$, $\Omega_\Lambda = 1.1$ (cf. Fig. 5), and $\overline{z} = 3$, the expression under the square root in (30) is negative, because

$$(1+\overline{z})^2(1+\Omega_{\mathrm{M}}\overline{z}) - \overline{z}(2+\overline{z})\Omega_\Lambda = 4^2(1+0.03) - 3\cdot 5\cdot 1.1 = -0.02.$$

[14] By Jan Maršák, the terms dark matter and dark energy from Fig. 4 are inconsistent, i.e., they are not on the same meaning level. Energy is consistent with the term mass through the relation $E = mc^2$. In this case, the physical quantities energy and mass are real numbers with appropriate physical dimensions, while matter is neither a real number nor a physical quantity. Energy is not a particular substance as material objects. The statement that dark energy is a part of our universe is therefore confusing.

[15] According to [1] and [24], it is necessary to consider the extinction of light by host galaxies. The measured luminosity depends considerably on whether the supernova lies inside or on the edge of the galaxy, what direction has its rotation axis, etc. Hence, type Ia supernovae are standard candles only roughly.

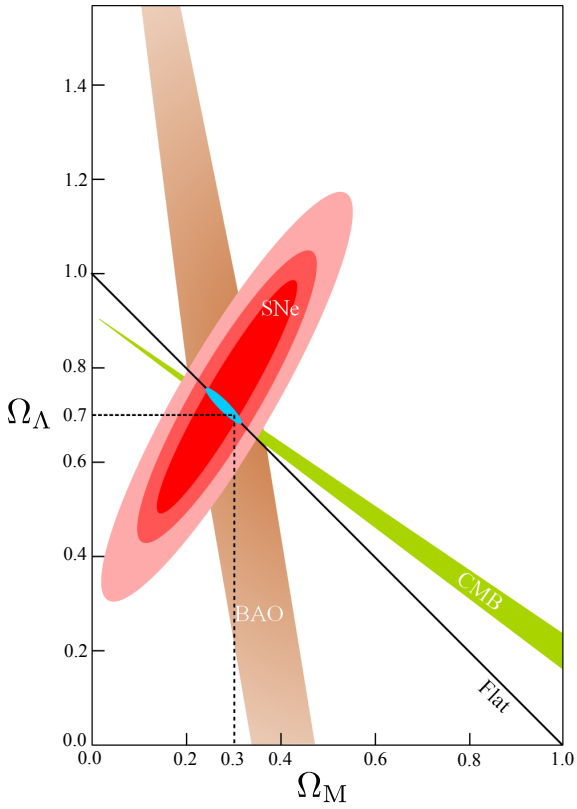

Figure 5: Admissible values of the cosmological parameters Ω_M and Ω_Λ, obtained by three different methods BAO (Baryonic Acoustic Oscillations), CMB (Cosmic Microwave Background), and SNe (Supernova explosions). However, these methods are not independent, because they are all based on the Friedmann equation (26) derived by questionable extrapolations. Moreover, the measured data were taken from the observable universe which is modeled by a completely different manifold than the universe described by the hypersphere $\mathbb{S}^3_a$, where the expansion function satisfies (26).

In spite of that, the standard cosmological calculator (Ned Wright's Cosmological Calculator) gives a quite acceptable value $d_L = 164.1$ Gly.

The sum of the measured values Ω_M and Ω_Λ is approximately equal to 1 (see (28) and Fig. 4). However, this does not allow us to claim that the true space is flat (i.e. infinite Euclidean) as it is often stated at present. Even if the sum were to be

$$\Omega_M + \Omega_\Lambda = 1.0000000000001,$$

we would still have a bounded hyperspherical (i.e. elliptic Riemannian) universe that can be described by the sphere $\mathbb{S}^3_r$ with an incredibly large radius r. Such a space is locally almost Euclidean, but finite. There is a big difference between a bounded and unbounded space. Moreover, the sphere $\mathbb{S}^3_r$ has an entirely **different topology**

than the flat space $\mathbb{E}^3$ which is promulgated by cosmologists at present. Testing the equatity $\Omega_{\mathrm{M}} + \Omega_\Lambda = 1$ remainds an inconvenient and incorrect computer test $X = Y$ in single-precision arithmetic (4 bytes), where X and Y are declared to be real (not integer).

Generally speaking, the prevailing conviction says that dark energy is some mysterious substance which is responsible for the accelerated expansion of the universe and this is attributed to the cosmological constant Λ. Its physical dimension is m^{-2}, since the left-hand side of (26) has dimension s^{-2}. In spite of that, cosmologists describe it as the density of energy which has another physical dimension in the SI units (International System of Units), namely $\mathrm{kg\,m^{-1}s^{-2}}$. From the relation (29) defining the parameter $\Omega_\Lambda(t)$ it is obvious that the kilogram (kg) does not appear there. Can we thus talk about density of energy?

In the system $c = 1$, meters and seconds can be arbitrarily exchanged using a suitable multiplicative constant. However, the physical dimension of Λ again does not correspond to the density of energy, since kilograms still do not appear there.

We can easily verify that the physical dimension of the fraction $(c^4/G)\cdot\mathrm{m}^{-2}$ is the same as the density of energy (cf. the right-hand side of (20)) in the units $\mathrm{kg\,m^{-1}s^{-2}}$. In the system $c = 1$ and $G = 1$ this is the same physical dimension as Λ has, since we may arbitrarily exchange kilograms, seconds, and meters using some appropriate multiplicative constants. In such a system, force, velocity, and power are dimensionless and we may evaluate energy and also time in kilograms or meters. It is true that many relations will be much simpler in these restricted units, but the constants c and G in equation (26) are not actually equal to unity. Therefore, we should not allow c and G to disappear in equation (26), and thus Λ should not be interpreted as density of energy in the system SI.

7. Excessive extrapolations

From Sections 2–5 we observe that the Friedmann equation (26) for a positive curvature of the universe was derived by a completely rigorous mathematical manner. However, the contemporary cosmological model based on the equation (26) does not give acceptable results not even for a nonpositive curvature (see [6], [11]). For instance, it admits a division by zero in (29). It also leads to a wide range of paradoxes and has other serious problems (e.g. the problem of the existence of a mysterious invisible dark matter and even more mysterious dark energy, the horizon problem, the problem of homogeneity and isotropy of the universe, the flatness problem, the problem of setting up accurate initial conditions, the problem of hierarchical structures, the problem of the existence of giant black holes in the early universe, and the Big Bang problem itself). Why this is so? The main reason is that the reality is identified with a mathematical model ignoring the modeling error.

Now let us look at this fact in detail. Consider a unit cube with edge $e = 1\,\mathrm{m}$ (see Fig. 6) and solve a steady-state heat conduction problem

$$-\Delta u = f$$

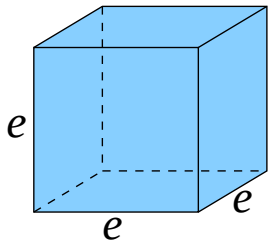

Figure 6: A homogeneous isotropic cube with edge of length e

with some boundary conditions, where $\Delta = \partial^2/\partial x^2 + \partial^2/\partial y^2 + \partial^2/\partial z^2$ is the Laplace operator, u is the temperature, and f is proportional to the density of heat forces. This elliptic problem approximates very well the true temperature in homogeneous isotropic solids which can be verified by direct measurements. However, in applying the heat equation on the atomic level in the cube with edge $e = 10^{-10}\,\mathrm{m}$, we get nonsensical numbers, since it is not clear how to define the temperature on such a small scale. We also obtain nonsensical numbers for $e = 10^{10}\,\mathrm{m}$. Such a large cube would immediately collapse into a back hole, since the diameter of this cube is about ten times larger than the diameter of the Sun. We can, of course, solve the above steady-state heat conduction problem on an arbitrarily large cube. However, the question is for which e do we still get acceptable results, and when the resulting temperatures have nothing to do with reality.

Other equations of mathematical physics (such as supraconductivity equations, Navier–Stokes equations for fluids, Korteweg-de Vries equations, linear elasticity equations, Maxwell's equations, semiconductor equations, magneto-hydro-dynamic equations, and so on) are subjected to analogous restrictions.

In 1922, cosmologists had no idea about the real size of the universe, since other galaxies were discovered later by Edwin Hubble. In spite of that, Alexander Friedmann [5] silently assumed that Einstein's equations describe absolutely exactly the behavior of gravity on cosmological scales. However, this assumption is highly unrealistic, since Einstein's equations[16] "are tested" on the scales of astronomical units and excessive extrapolations are made to the whole universe that is at least $1\,000\,000\,000\,000\,000 = 10^{15}$ times larger than 1 au. Einstein's equations are not scale-invariant[17] on a bounded expanding hypersphere $\mathbb{S}^3_{a(t)}$, since they do not trustworthily describe phenomena at atomic level or an extreme state just after the Big Bang [7] when matter and antimatter collided, highly energetic photons appeared, and the temperature thus shortly increased [2, p. 113]. Additionally, they are nonlinear and contain fixed fundamental physical constants c and G. The present state

[16] More precisely only the parametrized post-Newtonian (PPN) formalism is tested. The reason is that Einstein's equations are so complicated that their exact solution for two mutually orbiting bodies is not known.

[17] In spite of that, the well-known relationship $s = vt$ from Newtonian mechanics is scale-invariant in the Euclidean space.

of our universe depends on its history, whereas the Friedmann equation is reversible, i.e., its solution depends only on the value of the expansion function at the present time t_0 and not on the history [11]. Since the terminal condition $\dot{a}(t_0)/a(t_0) = H_0$ is known, we may evaluate $a(t_0)$ from equation (26) and then integrate (26) backward. From this we get $t_0 = 13.82$ Gyr, see [15, p. 274]. Nevertheless, from such a simple calculation we should not make any categorical conclusions about the age of the universe as is often done.

Therefore, we have to study models that are independent of the Friedmann equation (see e.g. [10], [11], [12], [18, p. 299]) to check whether dark matter exists or not. If it does not exist, then the relation (30) derived from the Friedmann equation can hardly yield some reliable distance. The FLRW cosmological model thus resembles the situation of the article *Lemma 1*, see [9], which can be characterized as follows:

Suppose that Lemma 1 implies Lemma 2, from which we further derive Lemma 3. These auxiliary results imply a certain important mathematical theorem, which is a basis of a new fascinating and beautiful theory. But after some time we find that Lemma 1 is wrong, and therefore the theorem need not hold.

In contemporary cosmology such Lemma 1 is the statement that Einstein's equations are valid for the whole universe. This assertion is just a hypothesis which has not been verified by an experiment and was obtained by excessive extrapolations by many orders of magnitude in pioneering articles [4] and [5]. Since the twenties, this fault stretches through the entire cosmology.

Acknowledgements

The authors would like to thank Antonín Dvořák, Jan Chleboun, Jan Maršák, and Vladimír Novotný for valuable comments, and to Hana Bílková for technical assistance. The preparation of this article was supported by RVO 67985840.

References

[1] Balázs, L. G., et al.: A possible interrelation between the estimated luminosity distances and the internal extinctions of type Ia supernovae. Astronom. Nachr. **327** (2006), 917–924.

[2] Börner, G.: *The early universe. Facts and fiction*. Springer, Berlin, 1993.

[3] Carroll, S. M., Press, W. H., and Turner, E. L.: The cosmological constant. Annu. Rev. Astron. Astrophys. **30** (1992), 499–542.

[4] Einstein, A.: *Kosmologische Betrachtungen zur allgemeinen Relativitätstheorie*. Königlich-Preuss. Akad. Wiss. Berlin (1917), 142–152.

[5] Friedman, A.: Über die Krümmung des Raumes. Z. Phys. **10** (1922), 377–386. English translation: On the curvature of space. General Relativity and Gravitation **31** (1999), 1991–2000.

[6] Friedmann, A.: Über die Möglichkeit einer Welt mit konstanter negativer Krümmung des Raumes. Z. Phys. **21** (1924), 326–332. English translation: On the possibility of a world with constant negative curvature of space. General Relativity and Gravitation **31** (1999), 2001–2008.

[7] Guth, A. H.: Inflationary universe: A possible solution to the horizon and flatness problems. Phys. Rev. D **23** (1981), 347–356.

[8] Kim, A. G., et al.: Implications for the Hubble constant from the first seven supernovae. Astrophys. J. Lett. **476** (1997), L63–L66.

[9] Königsdorf, H.: Lemma 1. In: Meine ungehörigen Träume, Geschichten, Berlin, Aufbau-Verlag, Edition Neue Texte, 1978; Pokroky Mat. Fyz. Astronom. **27** (1982), 101–106.

[10] Křížek, M., Křížek, F., and Somer, L.: Which effects of galactic clusters can reduce the amount of dark matter. Bulg. Astron. J. **21** (2014), 43–65.

[11] Křížek, M., Křížek, F., and Somer, L.: *Antigravity — Its origin and manifestations*. Lambert Acad. Publ., Saarbrücken, 2015.

[12] Křížek, M., Křížek, F., and Somer, L.: Dark matter and rotation curves of spiral galaxies. Bulg. Astron. J. **25** (2016), 64–77.

[13] Křížek, M. and Somer, L.: A critique of the standard cosmological model. Neural Netw. World **24** (2014), 435–461.

[14] Křížek, M. and Somer, L.: Manifestations of dark energy in the Solar system. Grav. Cosmol. **21** (2015), 58–71.

[15] Křížek, M. and Somer, L.: Excessive extrapolations in cosmology. Grav. Cosmol. **22** (2016), 270–280.

[16] Lemaître, G. E.: Un Univers homogène de masse constante et de rayon croissant rendant compte de la vitesse radiale des nébuleuses extragalactiques. Ann. Soc. Sci. de Bruxelles (1927), April, 49–59.

[17] Misner, C. W., Thorne, K. S., and Wheeler, J. A.: *Gravitation*. 20th edition, W. H. Freeman, New York, 1997.

[18] Peacock, J. A.: *Cosmological physics*. Cambridge Univ. Press, 1999.

[19] Planck Collaboration, Planck 2013 results, I. Overview of products and scientific results. Astron. Astrophys. **571** (2014), A1, 48 pp.

[20] Perlmutter, S.: Supernovae, dark energy, and the accelerating universe. Physics Today **56** (2003), April, 53–60.

[21] Rektorys, K.: *Survey of applicable mathematics I.* Kluwer Acad. Publ., Dordrecht, 1994.

[22] Riess, A. G., et al.: Observational evidence from supernovae for an accelerating universe and a cosmological constant. Astronom. J. **116** (1998), 1009–1038.

[23] Robertson, H. P.: On the foundation of relativistic cosmology. Proc. Nat. Acad. Sci. **15** (1929), 822–829.

[24] Rowan-Robinson, M.: Do type Ia supernovae prove $\Lambda > 0$? Mon. Not. R. Astron. Soc. **332** (2002), 352–360.

[25] Schwarzschild, K.: Über das zulässige Krümmungsmaaß des Raumes. Vierteljahrsschift der Astronomischen Gesellschaft **35** (1900), 337–347; English translation: On the permissible numerical value of the curvature of space. Abraham Zelmanov J. **1** (2008), 64–73.

[26] Tammann, G. A. and Reindl, B.: The ups and downs of the Hubble constant. Rev. Modern Astron. **19** (2006), 1–29.

[27] Tolman, R. C.: *Relativity, thermodynamics, and cosmology.* Clarendon Press, Oxford, 1934; Dover, New York, 1987.

[28] Walker, A. G.: On Milne's theory of world-structure. Proc. London Math. Soc. **42** (1936), 90–127.

[29] Weinberg, S.: *Gravitation and cosmology: Principles and applications of the general theory of relativity.* John Wiley, New York, London, 1972.

[30] Weinberg, S.: *Cosmology.* Oxford Univ. Press, 2008.

Conference *Cosmology on Small Scales 2016*
Michal Křížek and Yurii Dumin (Eds.)
Institute of Mathematics CAS, Prague

COSMOLOGICAL CONSEQUENCES OF THE MODEL OF LOW-ENERGY QUANTUM GRAVITY

Michael A. Ivanov

Physics Department
Belarus State University of Informatics and Radioelectronics
6 P. Brovka Street, BY 220027, Minsk, Republic of Belarus
ivanovma@tut.by

Abstract: The model of low-energy quantum gravity by the author is based on the conjecture on the existence of the graviton background. An interaction of photons and moving bodies with this background leads to small additional effects having essential cosmological consequences. In the model, redshifts of remote objects and the dimming of supernovae Ia may be interpreted without any expansion of the Universe and without dark energy. Some of these consequences are discussed and confronted with supernovae Ia, long GRBs, and quasars observations in this paper. It is shown that the two-parametric theoretical luminosity distance of the model fits observations with high confidence levels (100 % for the SCP Union 2.1, 43 % for JLA compilations, 99.81 % for long GRBs, and 13.73 % for quasars), if all data sets are corrected for no time dilation. These two parameters are computable in the model.

Keywords: Gravitation, distances and redshifts, observations and theory

PACS: 98.80.Es, 4.50.Kd, 04.60.Bc

1. Introduction

In contrast with classical electrodynamics in the XIX century or quantum electrodynamics in the XX century, at present we have a complete lack of experimental evidence to construct a theory of quantum gravity. From dimensional reasons only, if one assumes that the Newton constant is universal for any scales, the effects of quantum gravity are expected to be measurable over extremely small distances or very high energies. There are proposals how to detect some effects in a laboratory — for example, [21, 5], — or to observe a possible small violation of the Lorentz invariance for remote sources, but we have not any results in a frame of current paradigms which may pave us to the goal. Another constrain is, as I think, the common expectation that the future theory should be some symbiosis of the geometrical theory of general relativity and quantum mechanics. Geometry is useful for a description of

the average motion of big bodies due to the universality of gravitation, but it is not the fact that quantum effects may be described geometrically. It is also necessary to keep in mind that the nature of gravity as well as the nature of quantum behavior of microparticles are unknown — we have remarkable descriptions in different languages but not understanding in both cases.

I describe here briefly some consequences of my approach to quantum gravity [12, 13], in which the phenomenon is a very-low-energy one and is caused by the background of super-strong interacting gravitons. The main quantum effect of this approach is the Newtonian attraction; its small effects enforce us to look at the known results of astrophysical observations from another point of view and give us the reasons to doubt in the validity of the current standard cosmological model. This paper contains the alternative ideas in cosmology, which differ essentially from the mainstream paradigm based on the Big Bang conjecture.

2. The model of low-energy quantum gravity

The geometrical description of gravity in general relativity does not involve any mechanism of interaction. It is similar to the Newtonian model: we don't know how it works. In my model of low-energy quantum gravity [12, 13], gravity is considered as the screening effect. It is suggested that the background of super-strong interacting gravitons exists in the universe. Its temperature should be equal to the one of CMB. Screening this background creates for any pair of bodies both attraction and repulsion forces due to pressure of gravitons. For single gravitons, these forces are approximately balanced, but each of them is much bigger than a force of Newtonian attraction. If single gravitons are pairing, an attraction force due to pressure of such graviton pairs is twice exceeding a corresponding repulsion force if graviton pairs are destructed by collisions with a body. This peculiarity of the quantum mechanism of gravity leads to the difference of inertial and gravitational masses of a black hole. In such the model, the Newton constant is connected with the Hubble constant that gives a possibility to obtain a theoretical estimate of the last. We deal here with a flat non-expanding universe fulfilled with super-strong interacting gravitons; it changes the meaning of the Hubble constant which describes magnitudes of three small effects of quantum gravity but not any expansion or an age of the universe.

3. Small effects of the model due to its quantum nature

There are two small effects for photons in the sea of super-strong interacting gravitons [12]: average energy losses of a photon due to forehead collisions with gravitons and an additional relaxation of a photonic flux due to non-forehead collisions of photons with gravitons. The first effect leads to the geometrical distance/redshift relation:

$$r(z) = \ln(1+z) \cdot c/H_0, \tag{1}$$

where H_0 is the Hubble constant and c is the velocity of light. The both effects lead to the luminosity distance/redshift relation:

$$D_L(z) = c/H_0 \cdot \ln(1+z) \cdot (1+z)^{(1+b)/2} \equiv c/H_0 \cdot f_1(z), \tag{2}$$

where $f_1(z) \equiv \ln(1+z) \cdot (1+z)^{(1+b)/2}$; the "constant" b belongs to the range $0 - 2.137$ [14] ($b = 2.137$ for very soft radiation, and $b \to 0$ for very hard one). For an arbitrary source spectrum, a value of the factor b should be still computed. It is clear that in a general case it should depend on a rest-frame spectrum and on a redshift. Because of this, the Hubble diagram should be a multivalued function of a redshift: for a given z, b may have different values for different kinds of sources. Furthermore, the Hubble diagram may depend on the used procedure of observations: different parts of rest-frame spectrum will be characterized with different values of the parameter b.

Actually, the factor b describes an analog of the blurring effect of tired-light models. Due to the quantum nature of this effect in the model, non-forehead collisions of photons with gravitons should lead to relatively big average angles of deviations of photons of visible range:

$$\Delta\varphi \sim \frac{10^{-3}\ \text{eV}}{2.5\ \text{eV}} = 4 \cdot 10^{-4}\ \text{rad},$$

where $10^{-3}\,\text{eV}$ and $2.5\,\text{eV}$ are average graviton and photon energies. By multiple collisions, deviated photons will not be recognized as emitted by a small-angle remote object. But images of high-z objects may be partly blurred due to a fraction of low-energy gravitons.

The third small effect of this model is the constant deceleration of massive bodies due to forehead collisions with gravitons. It is an analog of the redshift in this model. We get for the body acceleration w_0 by a non-zero velocity v:

$$w_0 = -ac^2(1 - v^2/c^2). \tag{3}$$

For small velocities we have for it: $w_0 \simeq -H_0 c$. If the Hubble constant H_0 is equal to $2.14 \cdot 10^{-18}\,\text{s}^{-1}$ (it is the theoretical estimate of H_0 in this approach), a modulus of the acceleration will be equal to $|w_0| \simeq H_0 c = 6.419 \cdot 10^{-10}\,\text{m/s}^2$, that is of the same order of magnitude as a value of the observed additional acceleration $(8.74 \pm 1.33) \cdot 10^{-10}\,\text{m/s}^2$ for NASA probes Pioneer 10/11, see [3].

4. Advanced LIGO technologies may be partly used to verify the redshift mechanism

The main conjecture of this approach about the quantum gravitational nature of redshifts may be verified in a ground-based laser experiment. To do it, one should compare spectra of laser radiation before and after passing some distance l in a high-vacuum tube [11]. The temperature T of the graviton background coincides in the model with the one of CMB. Assuming $T = 2.7\,\text{K}$, we have for the

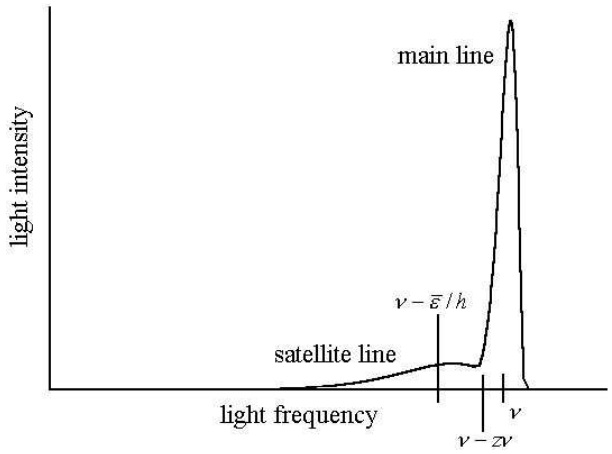

Figure 1: The main line and the expected red-shifted satellite line of a stable laser radiation spectrum after a delay line. Satellite's position should be fixed near $\nu - \bar{\epsilon}/h$, and its intensity should linear rise with a path of photons in a delay line, l. A center-of-mass of both lines is expected to be approximately near $\nu - z\nu$.

average graviton energy: $\bar{\epsilon} = 8.98\,\mathrm{eV}$. Because of the quantum nature of redshift, the satellite of main laser line of frequency ν would appear after passing the tube with a redshift of $10^{-3}\,\mathrm{eV}/h$, where h is the Planck constant, and its position should be fixed (see Fig. 1, z is the redshift). It will be caused by the fact that on a very small way in the tube only a small part of photons may collide with gravitons of the background. The rest of them will have unchanged energies. The center-of-mass of laser radiation spectrum should be shifted proportionally to a photon path. Due to the quantum nature of shifting process, the ratio of satellite's intensity to main line's intensity should have the order: $\sim \frac{h\nu}{\bar{\epsilon}} \frac{H_0}{c} l$. The theoretical value of H_0 in the model is: $H_0 = 2.14 \cdot 10^{-18}\,\mathrm{s}^{-1}$. An instability of a laser must be only much smaller than 10^{-3} if a photon energy is equal to ~ 1 eV. Given a very low signal photon number frequency, one could use a single photon counter to measure the intensity of the satellite line after a narrow-band filter with filter transmittance k. If q is a quantum output of a photomultiplier cathode, f_n is a frequency of its noise pulses, and n is a desired signal-to-noise ratio, then an evaluated time duration t of data acquisition would be equal to:

$$t = \frac{(\bar{\epsilon} c n)^2 f_n}{(H_0 q k P l)^2},$$

where P is a laser power. Assuming for example: $n = 10$, $f_n = 10^3\,\mathrm{s}^{-1}$, $q = 0.3$, $k = 0.1$, $P = 200\,\mathrm{W}$, $l = 300\,\mathrm{km}$, we have the estimate: $t \approx 3 \cdot 10^3\,\mathrm{s}$. Such the value of l may be achieved if one forces a laser beam to whipsaw many times between mirrors in the vacuum tube with the length of a few kilometers.

The advanced LIGO detectors [1], which were used to observe the gravitational-wave event GW150914, have many technological achievements needed to do the de-

scribed experiment: stable powerful lasers and input optics, high-vacuum tubes with optical resonator that multiplies the physical length by the number of round-trips of the light, mirror suspension systems with actuators. Some parameters of LIGO systems are of the same order as in the considered example. If one constructs the future LIGO detector with some additional equipment, the verification of the redshift mechanism may be performed in parallel with the main task or during a calibration stage of the detector.

5. Cosmological consequences of the model

There are the two circumstances introduced in the model to rich the needed strength of gravitational attraction: 1) gravitons should be super-strongly interacting, and 2) a part of gravitons should be paired and the pairs must be destructed by interaction with bodies. It leads to the very unexpected consequence: in the model, a black hole should have different gravitational and inertial masses, i.e., its possible existence contradicts to general relativity. Another unexpected feature of this approach is a necessity of "an atomic structure" of matter, because the considered mechanism does not work without it.

The property of asymptotic freedom of this model at very short distances leads to the important consequences, too. First, a black hole mass threshold should exist. A full mass of black hole should be restricted from the bottom with m_0; the rough estimate for it is: $m_0 \sim 10^7 M_\odot$. The range of transition to gravitational asymptotic freedom for a pair of protons is between 10^{-11}–10^{-13} m, and for a pair of electrons it is between 10^{-13}–10^{-15} m. This transition is non-universal; it means, second, that a geometrical description of gravity on this or smaller scales, for example on the Planck one, is not valid.

Any massive body moving relative to the graviton background should suffer in the model the constant deceleration of the order of $\sim H_0 c$, i.e. of the same order as an anomalous acceleration of the NASA's deep space probes (the Pioneer anomaly) [3]. Recently, it was shown by S. Turyshev et al. [26], that the thermal origin of the Pioneer anomaly is very possible. From another side, the mass discrepancy in spiral galaxies appears at very low accelerations less than some a_0 and not much above a_0 (see [9]), where the boundary acceleration a_0 has the same order. The need for dark matter in spiral galaxies appears at very low accelerations. A simple alternative to dark matter is MOND by M. Milgrom [19], in which such the boundary acceleration is introduced by hand. The main feature of MOND is the strengthening of gravitational attraction in a case of low accelerations; I do not think that an exact form of this strengthening has been guessed in MOND. But MOND gives us a clear hint that general relativity may be not valid on galactic or bigger scales of distances, and its application in cosmology is in doubt. In my model, the universal deceleration of bodies should lead in any bound system to an additional acceleration of them relative to the system's center of inertia. Some additional strengthening of gravitation on a periphery of galaxies may be caused in the model by the destruction of

graviton pairs flying through their central parts whereas pairs flying to the center are destructed in a less degree. The problem is open in this model.

The standard cosmological model is based on the assumption that redshifts of remote objects arise due to an expansion of the Universe. The model was re-builded a few times to save this base, the last innovation of it is an introduction of dark energy. Many researchers are searching for dark energy now or plan to do it, for example, with the help of large colliders. This basic cosmological assumption is considered by the community as a dogma, an invioalable sanctuary of present cosmology. For example, all observations of remote objects in the time domain are corrected for time dilation — but this effect is an attribute only of the standard model. In my model this assumption does not seem to be absolutely necessary. There exists a possibility in the model to interpret observations in another manner, without any expansion of the Universe.

5.1. The Hubble diagram of this model

In this model, the luminosity distance is given by equation (2). The theoretical value of relaxation factor b for a soft radiation is $b = 2.137$. Let us begin with this value of b, considering the Hubble constant as a single free parameter to fit observations. The theoretical Hubble diagram of this model is compared with Supernovae Ia observational data by Riess et al. [22] (corrected for no time dilation as: $\mu(z) \to \mu(z) + 2.5 \cdot \lg(1+z)$, where $\lg x \equiv \log_{10} x$) in Fig. 2. As you can see, the theoretical diagram fits observations very well without any dark energy.

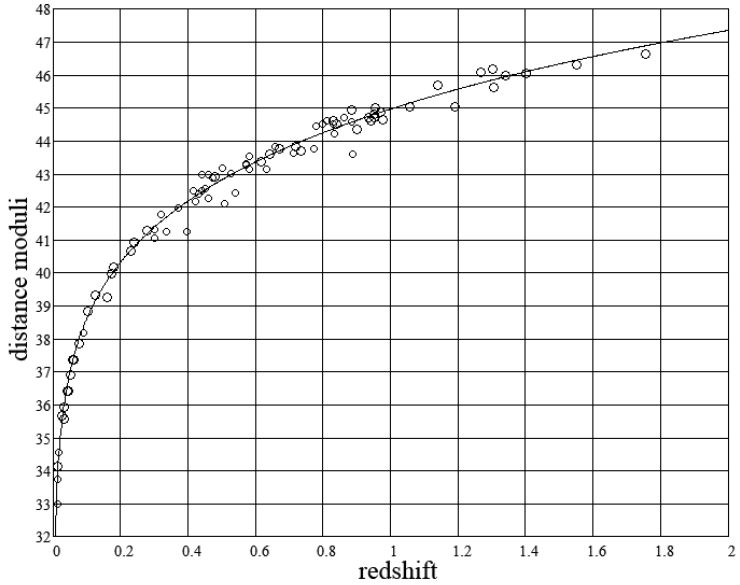

Figure 2: The theoretical Hubble diagram $\mu_0(z)$ of this model (solid); Supernovae Ia observational data (circles, 82 points) are taken from Table 5 of [22] and corrected for no time dilation.

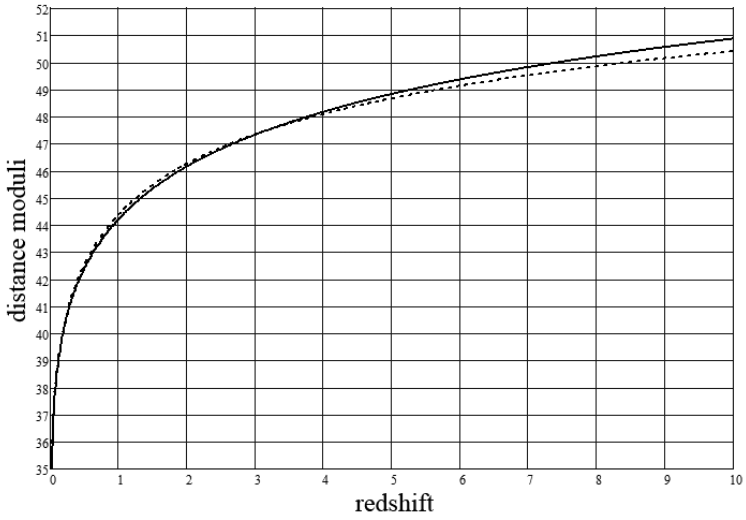

Figure 3: The two theoretical Hubble diagrams: $\mu_0(z)$ of this model with $b = 1.137$ taking into account the effect of time dilation of the standard model (solid); $\mu_c(z)$ for a flat Universe with the concordance cosmology by $\Omega_M = 0.27$ and $w = -1$ (dash).

The luminosity distance in the concordance cosmology by $w = -1$ is:

$$D_L(z) = c/H_0 \cdot (1+z) \int_0^z [(1+x)^3\Omega_M + (1-\Omega_M)]^{-0.5} dx \equiv c/H_0 \cdot f_2(z), \qquad (4)$$

where $f_2(z) \equiv (1+z) \int_0^z [(1+x)^3\Omega_M + (1-\Omega_M)]^{-0.5}$, Ω_M is the normalized matter density. To demonstrate how similar are predictions about distance moduli as a function of redshift of this model and of the concordance cosmology, the two theoretical Hubble diagrams are shown in Fig. 3: $\mu_0(z)$ of this model with $b = 1.137$ taking into account the effect of time dilation of the standard model (solid); and $\mu_c(z)$ for a flat Universe with the concordance cosmology by $\Omega_M = 0.27$ and $w = -1$ (dash). You can see a good accordance of this diagrams up to $z \approx 4$.

At present, two big compilations of SN Ia observations are available: the SCP Union 2.1 compilation (580 supernovae) [25] and the JLA compilation (740 supernovae) [6]. These compilations may be used to evaluate the Hubble constant in this approach. Using the definition of distance modulus: $\mu(z) = 5 \lg D_L(z)(\text{Mpc}) + 25$, we get from equation (2) for the theoretical distance modulus $\mu_0(z)$: $\mu_0(z) = 5 \lg f_1(z) + k$, where the constant k is equal to:

$$k \equiv 5 \lg(c/H_0) + 25.$$

If the model fits observations, then we shall have for $k(z)$:

$$k(z) = \mu(z) - 5 \lg f_1(z), \qquad (5)$$

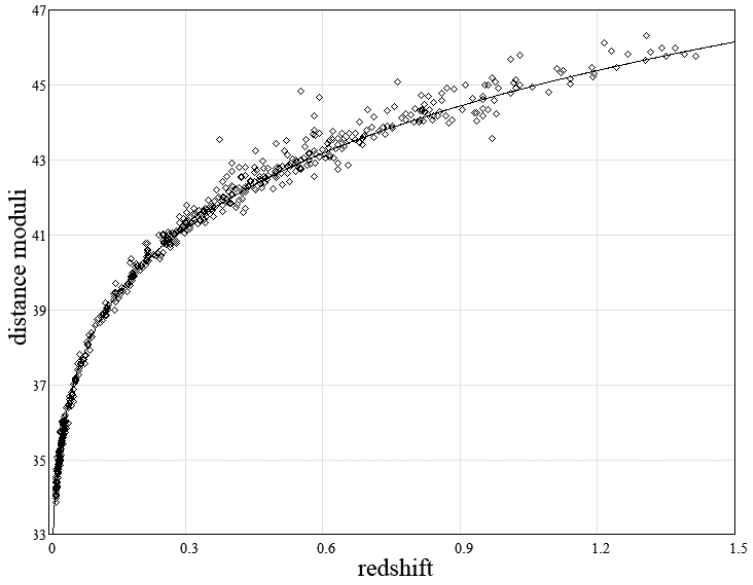

Figure 4: The theoretical Hubble diagram $\mu_0(z)$ of this model (solid); Supernovae Ia observational data (580 points of the SCP Union 2.1 compilation) are taken from [25] and corrected for no time dilation.

where $\mu(z)$ is an observational value of distance modulus. The weighted average value of $k(z)$:

$$\langle k(z)\rangle = \frac{\sum k(z_i)/\sigma_i^2}{\sum 1/\sigma_i^2}, \tag{6}$$

where σ_i^2 is a dispersion of $\mu(z_i)$, will be the best estimate of k. Here, σ_i^2 is defined as: $\sigma_i^2 = \sigma_{i\,\mathrm{stat}}^2 + \sigma_{i\,\mathrm{sys}}^2$. The average value of the Hubble constant may be found as:

$$\langle H_0\rangle = \frac{c\cdot 10^5}{10^{\langle k(z)\rangle/5}\cdot \mathrm{Mpc}}. \tag{7}$$

For a standard deviation of the Hubble constant we have:

$$\sigma_0 = \frac{\ln 10\cdot\langle H_0\rangle}{5}\cdot\sigma_k, \tag{8}$$

where σ_k^2 is a weighted dispersion of k, which is calculated with the same weights as $\langle k(z)\rangle$.

The theoretical Hubble diagram $\mu_0(z)$ of this model with $\langle k(z)\rangle$ which is calculated using the SCP Union 2.1 compilation [25] is shown in Fig. 4 together with observational points corrected for no time dilation. Values of $k(z)$ (580 points) and $\langle k(z)\rangle$, $\langle k(z)\rangle + \sigma_k$, $\langle k(z)\rangle - \sigma_k$ (lines) are shown in Fig. 5. For this compilation we have: $\langle k\rangle \pm \sigma_k = 43.216 \pm 0.194$. Calculating the χ^2 value as:

$$\chi^2 = \sum \frac{(k(z_i) - \langle H_0\rangle)^2}{\sigma_i^2}, \tag{9}$$

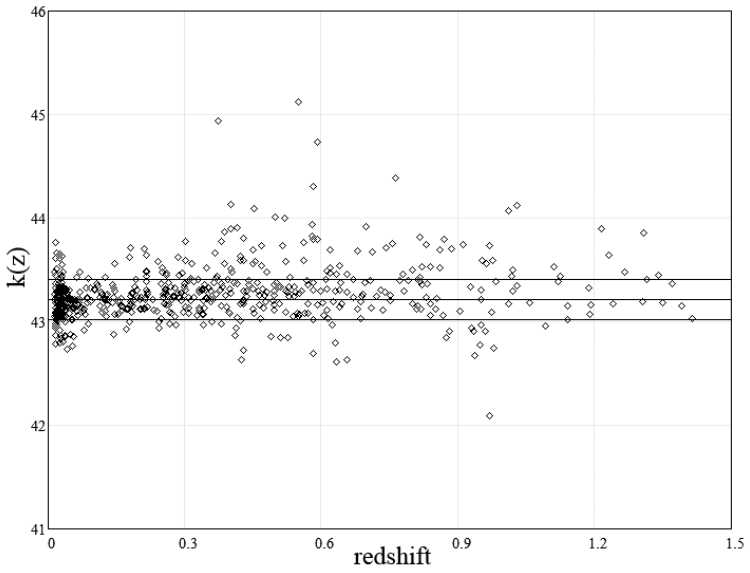

Figure 5: Values of $k(z)$ (580 points) and $\langle k(z)\rangle$, $\langle k(z)\rangle + \sigma_k$, $\langle k(z)\rangle - \sigma_k$ (lines) for the SCP Union 2.1 compilation.

we get $\chi^2 = 239.635$. By 579 degrees of freedom of this data set, it means that the hypothesis that $k(z) = \text{const.}$ cannot be rejected with 100 % C.L. Using equations (6) and (7), we get for the Hubble constant from the fitting:

$$\langle H_0\rangle \pm \sigma_0 = (2.211 \pm 0.198)\cdot 10^{-18}\,\mathrm{s}^{-1} = (68.223 \pm 6.097)\,\frac{\mathrm{km}}{\mathrm{s}\cdot\mathrm{Mpc}}.$$

The theoretical value of the Hubble constant in the model: $H_0 = 2.14\cdot 10^{-18}\,\mathrm{s}^{-1} = 66.875\ \mathrm{km}\cdot\mathrm{s}^{-1}\cdot\mathrm{Mpc}^{-1}$ belongs to this range. The traditional physical dimension $\mathrm{km}\cdot\mathrm{s}^{-1}\cdot\ \mathrm{Mpc}^{-1}$ is not connected here with any expansion.

To repeat the above calculations for the JLA compilation, I have used 31 binned points from Tables F.1 and F.2 of [6] (diagonal elements of the correlation matrix in Table F.2 are dispersions of distance moduli). We have for this compilation by $b = 2.137$: $\langle k\rangle \pm \sigma_k = 43.174 \pm 0.049$ with $\chi^2 = 51.66$. By 30 degrees of freedom of this data set, it means that the hypothesis that $k(z) = \text{const.}$ cannot be rejected only with 0.83 % C.L. Varying the value of b, we find the best fitting value of this parameter: $b = 2.365$ with $\chi^2 = 30.71$. It means that the hypothesis that $k(z) = \text{const.}$ cannot be rejected now with 43.03 % C.L. This value of b is 1.107 times greater than the theoretical one. For the Hubble constant we have in this case:

$$\langle H_0\rangle \pm \sigma_0 = (2.254 \pm 0.051)\cdot 10^{-18}\,\mathrm{s}^{-1} = (69.54 \pm 1.58)\,\frac{\mathrm{km}}{\mathrm{s}\cdot\mathrm{Mpc}}\,.$$

Results of the best fitting are shown in Figs. 6, 7.

If observations of long Gamma-Ray Bursts (GRBs) for small z are calibrated using SNe Ia, observational points are fitted with this theoretical Hubble diagram,

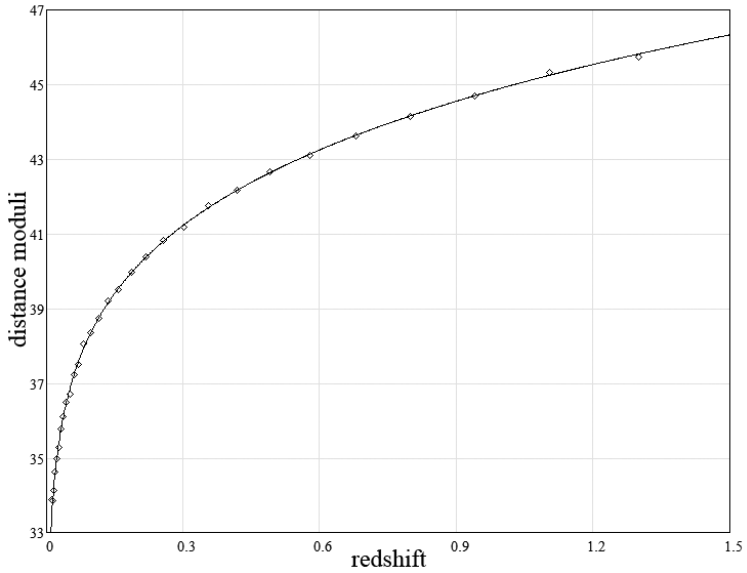

Figure 6: The theoretical Hubble diagram $\mu_0(z)$ of this model with $b = 2.365$ (solid); Supernovae Ia observational data (31 binned points of the JLA compilation) are taken from Tables F.1 and F.2 of [6] and corrected for no time dilation.

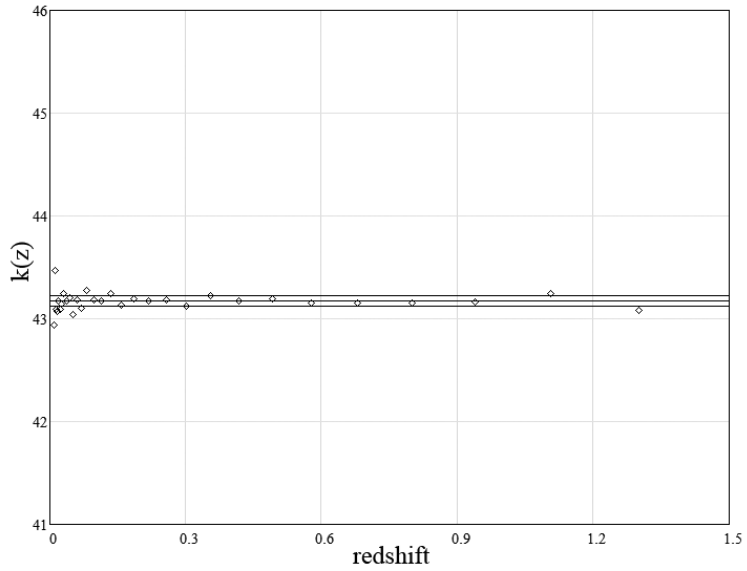

Figure 7: Values of $k(z)$ (31 binned points) and $\langle k(z)\rangle$, $\langle k(z)\rangle + \sigma_k$, $\langle k(z)\rangle - \sigma_k$ (lines) for the JLA compilation.

too [13]. But for hard radiation of GRBs, the factor b may be smaller, and the real diagram for them may differ from the one for SNe Ia. With this limitation, the long GRBs observational data (109 points) are taken from Tables 1, 2 of [27] and fitted in the same manner with $b = 2.137$. In this case we have: $\langle k\rangle \pm \sigma_k = 43.262 \pm 8.447$

with $\chi^2 = 70.39$. By 108 degrees of freedom of this data set, it means that the hypothesis that $k(z) = \text{const.}$ cannot be rejected with 99.81 % C.L. For the Hubble constant we have in this case:

$$\langle H_0 \rangle \pm \sigma_0 = (2.162 \pm 0.274) \cdot 10^{-18}\,\text{s}^{-1} = (66.71 \pm 8.45)\,\frac{\text{km}}{\text{s} \cdot \text{Mpc}}\,.$$

Results of the fitting are shown in Figs. 8 and 9.

Very recently, a new data set of 44 long Gamma-Ray Bursts was compiled with the redshift range of $[0.347; 9.4]$, see [16], in which two empirical luminosity correlations (the Amati relation and Yonetoku relation) were used to calibrate observations. Because the GRB Hubble diagram calibrated using luminosity correlations is almost independent on the GRB spectra, as it has been shown by the authors, I use here values of $\mu(z_i) \pm \sigma_i$ from columns 7 of Tables 2 and 3 of [16], based on the Band function, but with both calibrations. If this data set is fitted in the same manner with $b = 2.137$, we have for the Amati calibration: $\langle k \rangle \pm \sigma_k = 43.168 \pm 1.159$ with $\chi^2 = 40.585$. By 43 degrees of freedom of this data set, it means that the hypothesis that $k(z) = \text{const.}$ cannot be rejected with 57.66 % C.L. For the Hubble constant we have in this case:

$$\langle H_0 \rangle \pm \sigma_0 = (2.26 \pm 1.206) \cdot 10^{-18}\,\text{s}^{-1} = (69.732 \pm 37.226)\,\frac{\text{km}}{\text{s} \cdot \text{Mpc}}\,.$$

By $b = 2.137$, we have for the Yonetoku calibration: $\langle k \rangle \pm \sigma_k = 43.148 \pm 1.197$ with

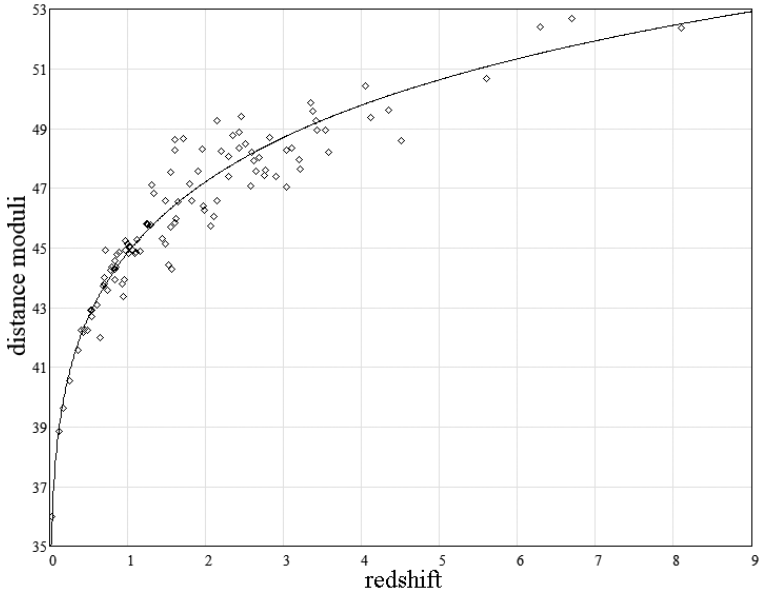

Figure 8: The theoretical Hubble diagram $\mu_0(z)$ of this model (solid); long GRBs observational data (109 points) are taken from Tables 1, 2 of [27] and corrected for no time dilation.

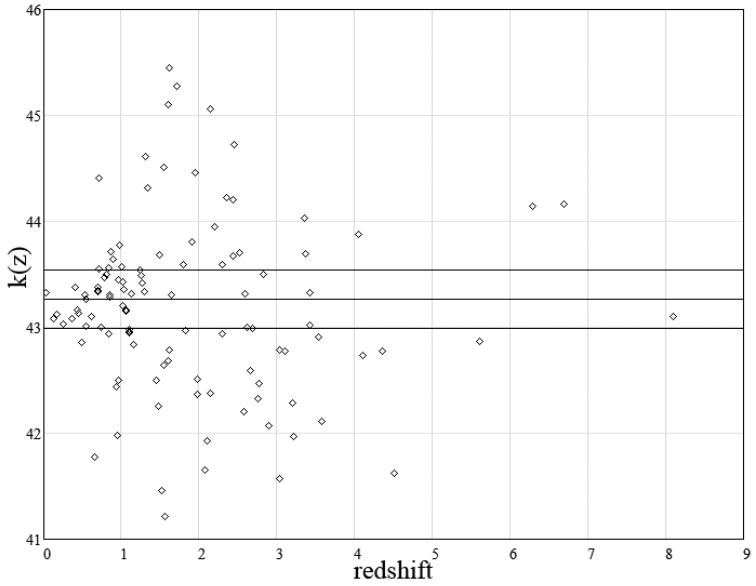

Figure 9: Values of $k(z)$ (109 points) and $\langle k(z)\rangle$, $\langle k(z)\rangle + \sigma_k$, $\langle k(z)\rangle - \sigma_k$ (lines) for long GRBs.

$\chi^2 = 43.148$. It means that the hypothesis that $k(z) =$ const. cannot be rejected with 46.5 % C.L. For the Hubble constant we have in this case:

$$\langle H_0\rangle \pm \sigma_0 = (2.281 \pm 1.257)\cdot 10^{-18}\,\mathrm{s}^{-1} = (70.386 \pm 38.793)\frac{\mathrm{km}}{\mathrm{s}\cdot\mathrm{Mpc}}.$$

But best fitting values of b are less than 2.137 in both cases: $b = 1.885$ for the Amati calibration ($\langle k\rangle \pm \sigma_k = 43.484 \pm 1.15$, $\chi^2 = 39.92$, with 60.57 % C.L. and $\langle H_0\rangle \pm \sigma_0 = (1.954 \pm 1.035)\cdot 10^{-18}\,\mathrm{s}^{-1} = (60.309 \pm 31.932)\,\mathrm{km/s/Mpc}$), and $b = 1.11$ for the Yonetoku one ($\langle k\rangle \pm \sigma_k = 44.439 \pm 1.037$, $\chi^2 = 32.58$, with 87.62 % C.L. and $\langle H_0\rangle \pm \sigma_0 = (1.259 \pm 0.601)\cdot 10^{-18}\,\mathrm{s}^{-1} = (38.841 \pm 18.546)\,\mathrm{km/s/Mpc}$). Namely smaller values of this parameter for bigger photon energies are expected in the model. For best fitting values of b, values of distance moduli are overestimated in both calibrations: on ~ 0.225 for the Amati calibration, and on ~ 1.18 for the Yonetoku calibration, if we compare values of $\langle k\rangle$ with its theoretical value of 43.259. It leads to the corresponding underestimation of the Hubble constant. Results of the best fitting for the Yonetoku calibration are shown in Fig. 10.

Recently, a new method to test cosmological models was introduced, based on the Hubble diagram for quasars [24]. The authors built a data set of 1 138 quasars for this purpose. Some later, this method and the data set were used to compare different models [17]. I have used here the binned quasar data set (18 binned points) of the paper [17] to verify my model in the described above manner. This data set contains the sum of observed distance modulus and an arbitrary constant A. To find this unknown constant for the calibration of QSO observations, I have computed

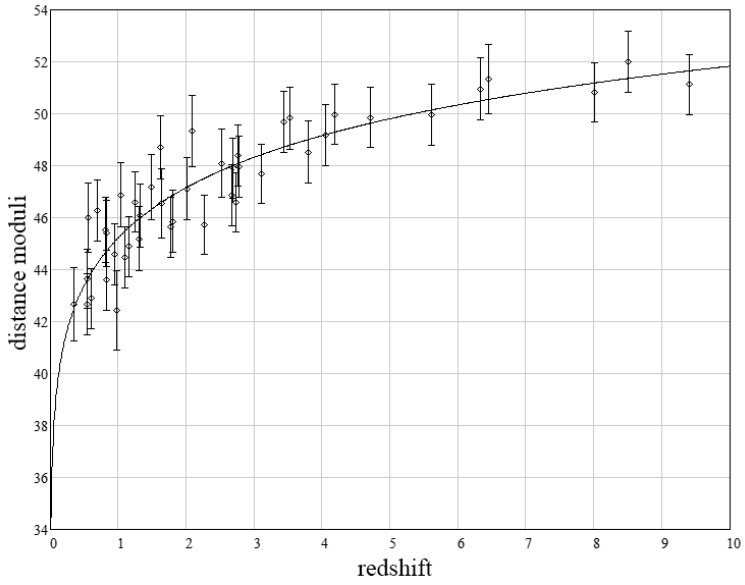

Figure 10: The theoretical Hubble diagram $\mu_0(z)$ of this model with $b = 1.11$ (solid); GRB observational data with the Yonetoku calibration (44 points) are taken from Table 3 of [16] and corrected for no time dilation.

$\langle k'(z)\rangle = \langle k(z)\rangle + A$ and replaced $\langle k(z)\rangle$ by its value for the JLA compilation; it gave: $A = 50.248$. This linking means that the average values of the Hubble constant should be identical for the two data sets. Subtracting this value of A, we get from the fitting of the quasar data by $b = 2.137$: $\langle k\rangle \pm \sigma_k = 43.175 \pm 0.340$ with $\chi^2 = 23.378$. By 17 degrees of freedom of this data set, it means that the hypothesis that $k(z) = \text{const.}$ cannot be rejected now with 13.73 % C.L. For the Hubble constant we have:

$$\langle H_0\rangle \pm \sigma_0 = (2.253 \pm 0.340) \cdot 10^{-18}\,\mathrm{s}^{-1} = (69.534 \pm 10.873)\,\frac{\mathrm{km}}{\mathrm{s}\cdot\mathrm{Mpc}}\,.$$

Results of the fitting are shown in Fig. 11.

5.2. Comparison with the LCDM cosmological model

To compare the above results of fitting with results for the LCDM cosmology, let us replace $f_1(z) \to f_2(z)$ (see equation (4)) and repeat the calculations. Of course, all data sets should remain now corrected for time dilation. The results of fitting are presented in Table 1; for convenience, the main above results for the model of low-energy quantum gravity are collected in the table, too. It is obvious, that confidence levels for both models do not allow to reject any of them.

For me, it was a big surprise that the Einstein–de Sitter model (equation (4) with $\Omega_M = 1$) cannot be rejected on a base of the full SCP Union 2.1 data set and the χ^2-criterion. We get $\chi^2 = 428.579$ and 99.9999 % C.L. The cause is in a big

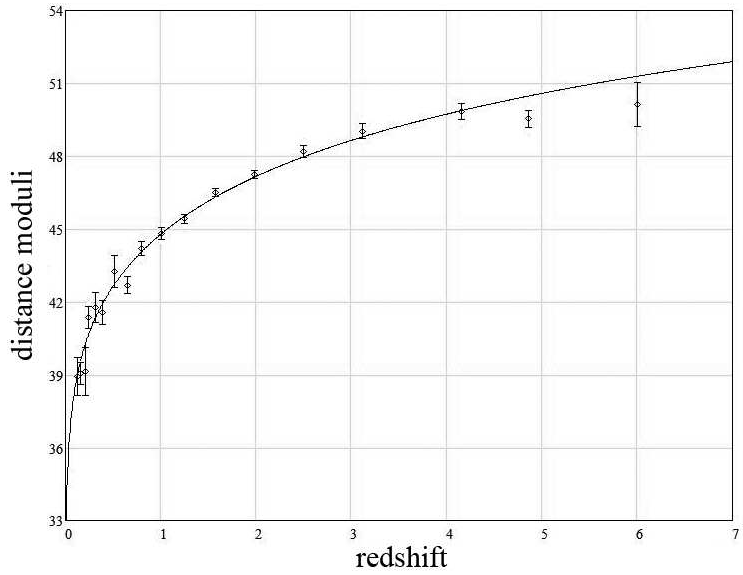

Figure 11: The theoretical Hubble diagram $\mu_0(z)$ of this model (solid); quasar observational data (18 binned points) [17] are corrected for no time dilation.

number of small-z supernovae Ia in this set; it leads to a big number of degrees of freedom, but to small differences of χ^2 for models with similar values of $D_L(z)$ in this range of z. But if one splits the data set in two subsets, for example with $z \leq 0.5$ and $z > 0.5$, and uses the first subset to evaluate $\langle H_0 \rangle$, then using this $\langle H_0 \rangle$ and the second subset to compute χ^2 by much smaller number of degrees of freedom, one can reject this model with high probability (when $z > 0.5$, we get $\chi^2 = 247.551$ by 166 observations and 0.004 % C.L.). Results for the model of low-energy quantum gravity and the LCDM cosmological model are not essentially changed by the splitting. But the Einstein–de Sitter model with $\Omega_M = 1$ bests the LCDM cosmological model with any amount of dark energy for the 44 long GRBs data set with the Yonetoku calibration.

5.3. The Hubble parameter $H(z)$ of this model

If the geometrical distance is described by equation (1), for a remote region of the universe we may introduce the Hubble parameter $H(z)$ in the following manner:

$$dz = H(z) \cdot \frac{dr}{c}, \tag{10}$$

to imitate the local Hubble law. Taking a derivative $\frac{dr}{dz}$, we get in this model for $H(z)$:

$$H(z) = H_0 \cdot (1 + z). \tag{11}$$

It means that in the model:

$$\frac{H(z)}{(1+z)} = H_0. \tag{12}$$

the model of low-energy quantum gravity				
Data set	b	χ^2	C.L., %	$< H_0 > \pm\sigma_0$
SCP Union 2.1 [25]	2.137	239.635	100	68.22 ± 6.10
JLA [6]	2.365	30.71	43.03	69.54 ± 1.58
109 long GRBs [27]	2.137	70.39	99.81	66.71 ± 8.45
44 long GRBs [16],	2.137	40.585	57.66	69.73 ± 37.23
the Amati calibration	**1.885**	39.92	60.57	60.31 ± 31.93
44 long GRBs [16],	2.137	43.148	46.5	70.39 ± 38.79
the Yonetoku calibration	**1.11**	32.58	87.62	38.84 ± 18.55
quasars [17]	2.137	23.378	13.73	69.53 ± 10.87
the LCDM cosmological model				
Data set	Ω_M	χ^2	C.L., %	$< H_0 > \pm\sigma_0$
SCP Union 2.1 [25]	0.30	217.954	100	69.68 ± 5.94
JLA [6]	0.30	29.548	48.90	70.08 ± 1.56
109 long GRBs [27]	0.30	66.457	99.94	70.04 ± 8.62
44 long GRBs [16],	0.30	40.777	56.81	68.99 ± 36.92
the Amati calibration	**0.49**	40.596	57.61	60.75 ± 32.44
44 long GRBs [16],	0.30	38.456	66.85	69.59 ± 36.10
the Yonetoku calibration	**1.0**	34.556	81.72	49.51 ± 24.35
quasars [17]	0.30	21.368	21.03	69.68 ± 10.42

Table 1: Results of fitting the Hubble diagram with the model of low-energy quantum gravity and the LCDM cosmological model. The best fitting values of b and Ω_M for 44 long GRBs are marked by the bold typeface.

The last formula gives us a possibility to evaluate the Hubble constant using observed values of the Hubble parameter $H(z)$. To do it, I use here 28 points of $H(z)$ from [10] and one point for $z < 0.1$ from [23]. The last point is the result of HST measurement of the Hubble constant obtained from observations of 256 low-z supernovae Ia. Here I refer this point to the average redshift $z = 0.05$. Observed values of the ratio $H(z)/(1+z)$ with $\pm\sigma$ error bars are shown in Fig. 12 (points). The weighted average value of the Hubble constant is calculated by the formula:

$$\langle H_0 \rangle = \frac{\sum \frac{H(z_i)}{1+z_i}/\sigma_i^2}{\sum 1/\sigma_i^2}. \tag{13}$$

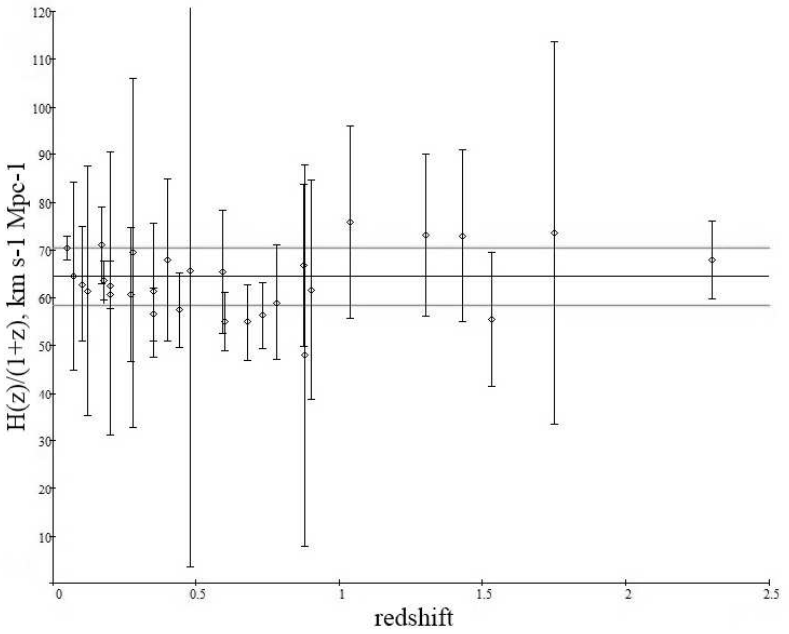

Figure 12: The ratio $H(z)/(1+z) \pm \sigma$ and the weighted value of the Hubble constant $\langle H_0 \rangle \pm \sigma_0$ (horizontal lines). Observed values of the Hubble parameter $H(z)$ are taken from Table 1 of [10] and one point for $z < 0.1$ is taken from [23].

The weighted dispersion of the Hubble constant is found with the same weights:

$$\sigma_0^2 = \frac{\sum \left(\frac{H(z_i)}{1+z_i} - \langle H_0 \rangle \right)^2 / \sigma_i^2}{\sum 1/\sigma_i^2}. \tag{14}$$

Calculations give for these quantities:

$$\langle H_0 \rangle \pm \sigma_0 = (64.40 \pm 5.95)\,\mathrm{km\,s^{-1}\,Mpc^{-1}}. \tag{15}$$

The weighted average value of the Hubble constant with $\pm\sigma_0$ error bars are shown in Fig. 12 as horizontal lines.

Calculating the χ^2 value as:

$$\chi^2 = \sum \frac{\left(\frac{H(z_i)}{1+z_i} - \langle H_0 \rangle \right)^2}{\sigma_i^2}, \tag{16}$$

we get $\chi^2 = 16.491$. By 28 degrees of freedom of our data set, it means that the hypothesis described by equation (11) cannot be rejected with 95 % C.L.

If we use another set of 21 cosmological model-independent measurements of $H(z)$ based on the differential age method [20], we get (see Fig. 13):

$$\langle H_0 \rangle \pm \sigma_0 = (63.37 \pm 4.56)\,\mathrm{km\,s^{-1}\,Mpc^{-1}}. \tag{17}$$

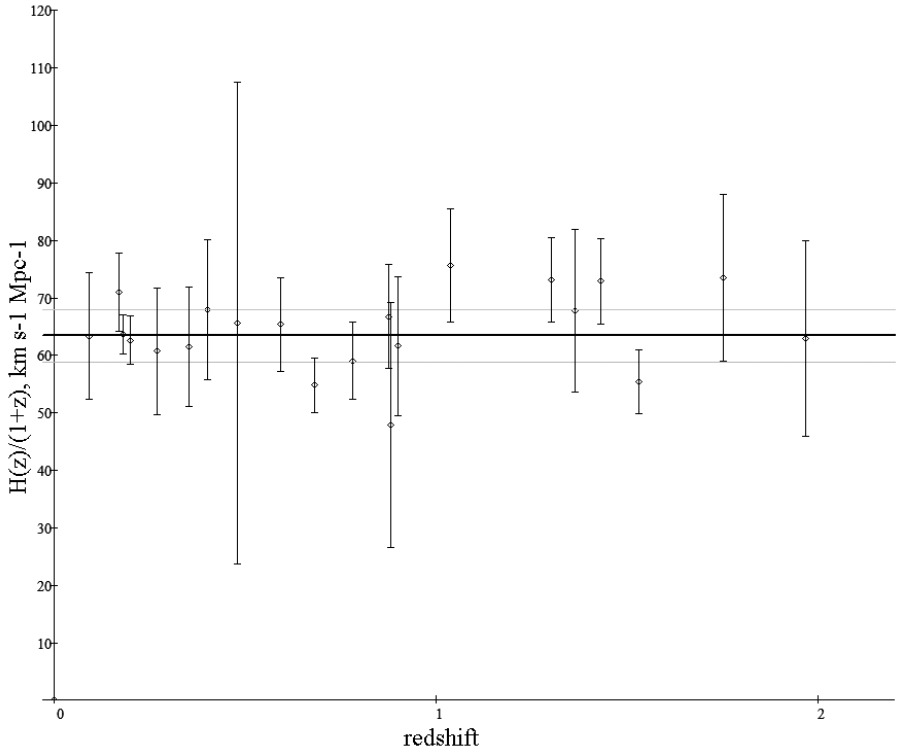

Figure 13: The ratio $H(z)/(1+z) \pm \sigma$ and the weighted value of the Hubble constant $\langle H_0 \rangle \pm \sigma_0$ (horizontal lines). Observed values of the Hubble parameter $H(z)$ are taken from [20].

The value of χ^2 in this case is smaller and equal to 3.948. By 21 degrees of freedom of this new data set, it means that the hypothesis described by equation (11) cannot be rejected with 99.998 % C.L.

Some authors try in a frame of models of expanding universe to find deceleration-acceleration transition redshifts using the same data set (for example, [10]). The above conclusion that the ratio $H(z)/(1+z)$ remains statistically constant in the available range of redshifts is model-independent. For the considered model, it is an additional fact against dark energy as an admissible alternative to the graviton background.

5.4. The Alcock-Paczynski test of this model

The Alcock-Paczynski cosmological test consists in an evaluation of the ratio of observed angular size to radial/redshift size [2]. Recently, this test has been carried out for a few cosmological models by Fulvio Melia and Martin Lopez-Corredoira [18]. They used new model-independent data on BAO peak positions from [4] and [8]. For two mean values of z ($\langle z \rangle = 0.57$ and $\langle z \rangle = 2.34$), the measured angular-diameter distance $d_A(z)$ and Hubble parameter $H(z)$ give for the observed charac-

teristic ratio $y_{\rm obs}(z)$ of this test the values: $y_{\rm obs}(0.57) = 1.264 \pm 0.056$ and $y_{\rm obs}(2.34) = 1.706 \pm 0.076$. In this model we have: $d_{\rm com}(z) = d_A(z) = r(z)$, where $d_{\rm com}(z)$ is the cosmological comoving distance. Because the Universe is static here, the ratio $y(z)$ for this model is defined as:

$$y(z) = \frac{r(z)}{z \cdot \frac{d}{dz} r(z)} = \frac{r(z) \cdot H(z)}{cz} = \left(1 + \frac{1}{z}\right) \cdot \ln(1+z), \tag{18}$$

where $H(z)$ is defined by equation (10). This function without free parameters characterizes any tired light model (model 6 in [18]). We have only two observational points to fit them with this function. Calculating the χ^2 value as:

$$\chi^2 = \sum \frac{(y_{\rm obs}(z_i) - y(z_i))^2}{\sigma_i^2}, \tag{19}$$

we get $\chi^2 = 0.189$, that corresponds to the confidence level of 91 % for two degrees of freedom.

6. Conclusion

As it is shown above, the Hubble diagram of supernovae Ia, GRBs and quasars being corrected for no time dilation, the Hubble parameter $H(z)$ and the ratio of observed angular size to radial/redshift size are well fitted in this model. The Hubble diagram for GRBs may differ in the model from the diagram for SNe Ia, and some signs of this difference are seen, perhaps, in the case of the 44 long GRBs data set. In the model, space-time is flat, and the geometrical distance as a function of the redshift coincides with the angular diameter distance. Given that a galaxy number density is constant in the no-evolution scenario, theoretical predictions for galaxy number counts in this model have been found using only the luminosity and geometrical distances defined by equations (1) and (2), see [15]. The geometrical distance $r(z)$ of this model is very different from the one of the standard model; for example, GRB 090429B with $z = 9.4$, see [7] took place 24.6 Gyr ago in a frame of this model; the age of the Universe of the standard model: ~ 13.5 Gyr corresponds here to $z \simeq 2.6$.

At present this model is not a full cosmological one; it is necessary to develop many open problems to bring it closer to the pursuable completeness. But even now it has interesting advantages: the model's parameters H_0 and b are computable; there is not any need in dark energy (and in the Bing Bang, inflation, expansion).

I am grateful to the authors of the paper [17] for the binned quasar data set which I have received by my request.

References

[1] Abbott, B. P. et al.: *GW150914: The advanced LIGO detectors in the era of first discoveries*. Phys. Rev. Lett. **116** (2016), 131103; arXiv:1602.03838 [gr-qc].

[2] Alcock, C. and Paczynski, B.: *An evolution free test for non-zero cosmological constant*. Nature **281** (1979), 358.

[3] Anderson, J. D. et al.: *Indication, from Pioneer 10/11, Galileo, and Ulysses data, of an apparent anomalous, weak, long-range acceleration*. Phys. Rev. Lett. **81** (1998), 2858; *Study of the anomalous acceleration of Pioneer 10 and 11*. Phys. Rev. **D65** (2002), 082004; gr-qc/0104064 v4.

[4] Anderson, L. et al.: *The clustering of galaxies in the SDSS-III baryon oscillation spectroscopic survey: baryon acoustic oscillations in the data releases 10 and 11 galaxy samples*. MNRAS **441** (2014), 24.

[5] Bekenstein, J. D.: *Is a tabletop search for Planck scale signals feasible?* Phys. Rev. **D86** (2012), 124040 arXiv:1211.3816 [gr-qc].

[6] Betoule, M. et al.: *Improved cosmological constraints from a joint analysis of the SDSS-II and SNLS supernova samples*; arXiv:1401.4064v2 [astro-ph.CO].

[7] Cucchiara, A. et al.: *A photometric redshift of $z \sim 9.4$ for GRB 090429B*. ApJ **736** (2011), 7; arXiv:1105.4915 [astro-ph.CO].

[8] Delubac, T. et al.: *Baryon acoustic oscillations in the Ly? forest of BOSS DR11 quasars*. AA **574** (2015), A59; arXiv:1404.1801 [astro-ph.CO].

[9] Famaey, B. and McGaugh, S.: *Modified Newtonian dynamics (MOND): observational phenomenology and relativistic extensions*. arXiv:1112.3960v2 [astro-ph.CO].

[10] Farooq, O., and Ratra, B.: *Hubble parameter measurement constraints on the cosmological deceleration-acceleration transition redshift*. arXiv:1301.5243 [astro-ph.CO].

[11] Ivanov, M. A.: May gravitons be super-strong interacting particles? In: W. Hikida et al. (Eds.), *Proc. 14th Workshop on General Relativity and Gravitation*. Kyoto, 2004, 305–308. [gr-qc/0410076].

[12] Ivanov, M. A.: Gravitons as supper-strong interacting particles, and low-energy quantum gravity. In: *Focus on quantum gravity research*, D. C. Moore (Ed.), Nova Science, NY, 2006, 89–120; [`hep-th/0506189`], [`http://ivanovma.narod.ru/nova04.pdf`].

[13] Ivanov, M. A.: *Selected papers on low-energy quantum gravity*. [`http://ivanovma.narod.ru/selected-papers-Ivanov11.pdf`].

[14] Ivanov, M. A.: *Hubble diagrams of soft and hard radiation sources in the graviton background: to an apparent contradiction between supernova Ia and gamma-ray burst observations*; astro-ph/0609518.

[15] Ivanov, M. A.: *Galaxy number counts in a presence of the graviton background*; astro-ph/0606223v3.

[16] Lin, H.-N., Li, X., and Chang, Z.: *Effect of GRB spectra on the empirical luminosity correlations and the GRB Hubble diagram.* arXiv:1604.02285 [astro-ph.HE].

[17] Lopez-Corredoira, M., Melia, F., Lusso, E. and Risaliti, G.: *Cosmological test with the QSO Hubble diagram*; arXiv:1602.06743 [astro-ph.CO].

[18] Melia, F., and Lopez-Corredoira, M.: *Alcock-Paczynski test with model-independent BAO data.* arXiv:1503.05052v1 [astro-ph.CO].

[19] Milgrom, M.: *A modification of the Newtonian dynamics as a possible alternative to the hidden mass hypothesis.* ApJ **270** (1983), 365-370; *A modification of the Newtonian dynamics — implications for galaxies.* ApJ **270** (1983),371-383.

[20] Moresco, M.: *Raising the bar: new constraints on the Hubble parameter with cosmic chronometers at* $z \sim 2$; arXiv:1503.01116v1 [astro-ph.CO].

[21] Pikovski, I. et al.: *Probing Planck-scale physics with quantum optics.* Nature Physics **8** (2012), 393.

[22] Riess, A. G. et al.: *Type Ia Supernova discoveries at* $z > 1$ *from the Hubble space telescope: evidence for past deceleration and constraints on dark energy evolution.* ApJ **607** (2004), 665; astro-ph/0402512.

[23] Riess, A. G., et al.: *A 3% solution: determination of the Hubble constant with the Hubble space telescope and wide field camera 3.* ApJ **730** (2011), 119. arXiv:1103.2976 [astro-ph.CO].

[24] Risaliti, G. and Lusso, E.: *A Hubble diagram for quasars.* ApJ **815** (2015), 33; arXiv:1505.07118 [astro-ph.CO].

[25] Suzuki, N. et al.: *The Hubble space telescope cluster supernova survey: V. Improving the dark energy constraints above* $z > 1$ *and building an early-type-hosted supernova sample.* ApJ **746** (2012), 85; arXiv:1105.3470v1 [astro-ph.CO].

[26] Turyshev, S. et al.: *Support for the thermal origin of the Pioneer anomaly.* Phys. Rev. Lett. **108** (2012), 241101; arXiv:1204.2507 [gr-qc].

[27] Wei, H.: *Observational constraints on cosmological models with the updated long Gamma-ray bursts.* arXiv:1004.4951v3 [astro-ph.CO].

LIST OF PARTICIPANTS

Alexander Borisovich Balakin
Department of General Relativity and Gravitation, Institute of Physics,
Kazan Federal University, Kremlevskaya 18, 420008 Kazan, Russia
alexander.balakin2011(at)yandex.ru

Yurij Viktorovich Baryshev
Astronomical Department, Mathematics and Mechanics Faculty of the Saint-Petersburg State University, Universitetskij prospekt 28, Staryj Peterhoff, Saint-Petersburg 198504 Russia
yubaryshev(at)mail.ru

Michal Bílek
Astronomical Institute, Czech Academy of Sciences, Boční II, CZ-141 31 Prague 4, Czech Republic
bilek(at)asu.cas.cz

Hana Bílková
Institute of Computer Science, Czech Academy of Sciences, Pod Vodárenskou věží 2, CZ-182 07 Prague 8, Czech Republic
hanka(at)cs.cas.cz

Sergio Hernandez Cuenca
Imperial College London, W6 9SX, London, Great Britain
Sergio.hernaddez13(at)imperial.ac.uk

František Dinnbier
Astronomical Institute, Czech Academy of Sciences, Boční II, CZ-141 31 Prague 4, Czech Republic
Fr.Dinnbier(at)seznam.cz

Yurii V. Dumin
P. K. Sternberg Astronomical Institute of M. V. Lomonosov Moscow State University Universitetskii pr. 13, 119992 Moscow, Russia
Space Research Institute, Russian Academy of Sciences, Profsoyznaya str. 84/32, 117997 Moscow, Russia
dumin(at)sai.msu.ru, dumin(at)yahoo.com

Antonín Dvořák
Kovoprojekta Brno a.s., Poznaňská 22, CZ-616 00 Brno, Czech Republic
antonin.dvorak(at)centrum.cz, advorak(at)kovoprojekta.cz

Maxim Dvornikov
Pushkov Institute of Terrestrial Magnetism, Ionosphere and Radiowave Propagation, IZMIRAN, Kaluzhskoe HWY 4, 142190 Troitsk, Moscow, Russia
maxdvo(at)izmiran.ru

Georg Feulner
Potsdam Institute for Climate Impact Research, Building A62, Telegrafenberg, D-14412, Potsdam, Germany
feulner(at)pik-potsdam.de

Itzhak Goldman
Afeka Engineering College and Tel Aviv University, Mivtza Kadesh 38, Tel Aviv, Israel
goldman(at)afeka.ac.il

Michail A. Ivanov
Belarus State University of Informatics and Radioelectronics, 6 P. Brovka Street, BY 220027 Minsk, Republic of Belarus
ivanovma(at)tut.by

David Kaftan
Nad Soutokem 1418/9, CZ-143 00 Prague 4, Czech Republic
david.kaftan(at)post.cz

Igor Dmitrievich Karachentsev
Special Astrophysical Observatory, Russian Academy of Sciences, Nizhnij Arkhyz, Zelenchukski region, Karachai-Cherkessian Republic, R-369 167 Russia
ikar(at)sao.ru

Jaroslav Klokočník
Astronomical Institute, Czech Academy of Sciences, CZ-251 65 Ondřejov, Czech Republic
jklokocn(at)asu.cas.cz

Sergei Kopeikin
Department of Physics and Astronomy, University of Missouri in Columbia, U.S.A.
kopeikinS(at)missouri.ru

Sergey Korotov
Department of Computing, Mathematics and Physics, Bergen University College, Inndalsveien 28, 5020 Bergen, Norway
sergey.korotov(at)hib.no

Filip Křížek
Nuclear Physics Institute, Czech Academy of Sciences, Hlavní 130, CZ-250 68 Řež, Czech Republic
filip.krizek(at)cern.ch

Michal Křížek
Institute of Mathematics, Czech Academy of Sciences, Žitná 25,
CZ-115 67 Prague 1, Czech Republic
krizek(at)cesnet.cz, krizek(at)math.cas.cz

Pavel Kroupa
University of Bonn, Helmholtz-Institut für Strahlen- und Kemphysik,
Nussallee 14–16, D-53115 Bonn, Germany
pavel(at)astro.uni-bonn.de

František Lomoz
Sedlčany Astronomical Observatory, CZ-115 67 Sedlčany, Czech Republic
F.Lomoz(at)seznam.cz

André Maeder
Geneva Observatory, 19, chemin des Marais, CH-1234 Vessy, Switzerland
Andre.Maeder(at)unige.ch

Dmitry Makarov
Special Astrophysical Observatory, Russian Academy of Sciences, Nizhnij Arkhyz, Zelenchukski region, Karachai-Cherkessian Republic, R-369 167 Russia
dim(at)sao.ru

Lidia Makarova
Special Astrophysical Observatory, Russian Academy of Sciences, Nizhnij Arkhyz, Zelenchukski region, Karachai-Cherkessian Republic, R-369 167 Russia
lidia(at)sao.ru

Tomáš Málek
Institute of Mathematics, Czech Academy of Sciences, Žitná 25,
CZ-115 67 Prague 1, Czech Republic
malek(at)cesnet.cz

Alexandr Mikhailovich Malinovskiy
Astro Space Center of Lebedev Physical Institute, Profsoyznaya str., 84/32,
117997 Moscow, Russia
Alexandr.M.Malinovsky(at)gmail.com

Jan Maršák
Pedagogical Institute, Prague, Czech Republic
jmarsak(at)seznam.cz

Attila Mészáros
Astronomical Institute of Charles University, V Holešovičkách 2, CZ-180 00 Prague 8, Czech Republic
meszaros(at)cesnet.cz

Bivudutta Mishra
Department of Mathematics, Birla Institute of Technology and Science-Pilani, Hyderabad Campus, Jawahar Nagar, Shameerpet Mandal, Ranga Reddy Dist., Telangana-500078, India
bivu(at)hyderabad.bits-pilani.ac.in

Jaroslav Mlýnek
Department of Mathematics, Technical University of Liberec, Studentská 2, Liberec, Czech Republic
Jaroslav.Mlynek(at)tul.cz

Jan Novák
Institute of Computer Science, Czech Academy of Sciences, Pod Vodárenskou věží 2, CZ-182 07 Prague 8, Czech Republic
jan.jano.novak(at)gmail.com

Vladimír Novotný
Cosmological Section of the Czech Astronomical Society, Jašíkova 1533/4, CZ-149 00 Prague 4, Czech Republic
nasa(at)seznam.cz

Marek Nowakovski
Departamento de Fisica, Universidad de los Andes, Cra 1E, 18A-10, Bogota, Colombia
mnowakos(at)uniandes.edu.co

Rahul Prasad Nigam
A-204, Birla Institute of Technology and Science-Pilani, Hyderabad Campus, Shameerpet, Hyderabad, India
rahul.nigam(at)hyderabad.bits-pilani.ac.in

Marcello Ortaggio
Institute of Mathematics, Czech Academy of Sciences, Žitná 25, CZ-115 67 Prague 1, Czech Republic
ortaggio(at)math.cas.cz

Soňa Peková
Vemodia a.s., V Hůrkách 3, CZ-158 00 Prague 5, Czech Republic
sona.pekova(at)vemodia.cz

Vladimir A. Popov
Department of General Relativity and Gravitation, Institute of Physics,
Kazan Federal University, Kremlevskaya 18, 420008 Kazan, Russia
vladipopov(at)mail.ru

Milan Práger
Institute of Mathematics, Czech Academy of Sciences, Žitná 25,
CZ-115 67 Prague 1, Czech Republic
prager(at)math.cas.cz

Karel Segeth
Institute of Mathematics, Czech Academy of Sciences, Žitná 25,
CZ-115 67 Prague 1, Czech Republic
segeth(at)math.cas.cz

Vladimír Skalský
Faculty of Materials Science and Technology, Slovak University of Technology,
SK-917 24 Trnava, Slovakia
vladimir.skalsky(at)slovanet.sk

Ilia Vladimirovich Sokolov
Institute of Astronomy, Russian Academy of Sciences, 48 Pyatnitskaya st., 119017
Moscow, Russia
ilia.v.sokolov(at)gmail.com

Lawrence Somer
Department of Mathematics, Catholic University of America,
Washington, D.C. 20064, U.S.A.
somer(at)cua.cz

Alessandro D. A. M. Spallicci
Université d'Orléans, Observatoire des Sciences de l'Univers, Campus CNRS,
3A Av. de la Recherche Scientifique, F-45071 Orléans, France
spallicci(at)cnrs-orleans.fr

Igor N. Taganov
Russian Geographical Society, Serebristy bulv. 37, apt. 175, Saint Petersburg,
197341 Russia
taganov.igor(at)mail.ru

Konstantin A. Tomilin
S. I. Vavilov Institute for the History of Science and Technology,
Begovaya str., 11, 123, Moscow, 125284 Russia
ktomilin(at)mail.ru

Tomáš Vejchodský
Institute of Mathematics, Czech Academy of Sciences, Žitná 25,
CZ-115 67 Prague 1, Czech Republic
vejchod(at)math.cas.cz

Vladimír Wagner
Nuclear Physics Institute, Czech Academy of Sciences, Hlavní 130, CZ-250 68 Řež,
Czech Republic
wagner(at)ujf.cas.cz

Richard Wunsch
Astronomical Institute, Czech Academy of Sciences, Boční II, CZ-141 31 Prague 4,
Czech Republic
richard(at)wunsch.cz

Suk-Jin Yoon
Department of Astronomy, Yonsei University, Seoul, South Korea
sjyoon0691(at)yonsei.ac.kr

Aleksei Zaiats
Department of General Relativity and Gravitation, Institute of Physics,
Kazan Federal University, Kremlevskaya 18, 420008 Kazan, Russia
Zayats.ae(at)gmail.com

Jana Žd'árská
K Panskému poli 274, CZ-251 01 Světice, Czech Republic
jazdar(at)seznam.cz

David Žd'árský
K Panskému poli 274, CZ-251 01 Světice, Czech Republic
d.zdarsky(at)seznam.cz

Jan Zítko
Department of Numerical Analysis, Faculty of Mathematics and Physics,
Charles University, Sokolovská 83, CZ-186 75 Prague 8, Czech Republic
zitko(at)karlin.mff.cuni.cz

Weijia Zhang
Clarendon Laboratory, University of Oxford, Parks Road, Oxford, OX1 3PU,
United Kingdom
Weijia.Zhang(at)physics.ox.ac.uk

PROGRAM OF THE CONFERENCE

Wednesday, September 21

13:00–13:30 Registration

13:30–13:40 Opening

Chair: Yurii V. Dumin

13:40–14:30 **Igor Karachentsev**, Cosmography of the local universe

14:30–15:20 **André Maeder**, Scale invariance: Its cosmological and local effects

15:20–15:50 Coffee Break

Chair: Lawrence Somer

15:50–16:40 **Yurii V. Dumin**, Local Hubble expansion: Current state of the problem

16:40–17:30 **Georg Feulner**, The faint young Sun paradox

17:30–18:00 **Michal Křížek**, Anthropic principle and the local Hubble expansion

Thursday, September 22

Chair: André Maeder

9:00–9:50 **Pavel Kroupa**, The observed spatial distribution of matter on scales ranging from 100 kpc to 1Gpc is inconsistent with the standard dark-matter-based cosmological models

9:50–10:40 **Marek Nowakovski**, A local portrait of the cosmological constant

10:40–11:10 Coffee Break

Chair: Igor Karachentsev

11:10–11:40 **Lidia Makarova**, Dwarf galaxies in the local volume of the Universe

11:40–12:10 **Dmitry Makarov**, Tully-Fisher relation of flat galaxies

12:10–14:00 Lunch Break

Chair: Pavel Kroupa

14:00–14:30 **Itzhak Goldman**, Do recent observations of giant molecular clouds suggest modification of gravity?

14:30–15:00 **Ilia V. Sokolov**, Clustering of galaxies around the GBR 021004 sight-line at $z \sim 0.5$

15:00–15:30 Coffee Break

Chair: Yurii V. Dumin

15:30–16:00 **Konstantin A. Tomilin**, Gravitational constant: history and modern status

16:00–16:50 **Igor N. Taganov**, Theoretical estimation of the Hubble constant

16:50–17:40 **Yurij V. Baryshev**, Two fundamental cosmological laws of the local universe (remote presentation)

Friday, September 23

Chair: Itzhak Goldman

9:00–9:30 **Attila Mészáros**, Anisotropies in the sky distributions of the gamma-ray bursts and the cosmological principle

9:30–10:00 **Rahul Prasad Nigam**, Role of magnetic field in structure formation

10:00–10:30 **Alessandro D. A. M. Spallicci**, Non-Maxwellian electromagnetism implications on astrophysical and cosmological scales

10:30–11:00 Coffee Break

Chair: Attila Mészáros

11:00–11:30 **Alexander B. Balakin**, Non-minimal coupling and a new small scale in the cosmological landscape around a magnetic monopole

11:30–12:00 **Aleksei Zaiats**, Non-minimal coupling and a new small scale in the cosmological landscape around an electric monopole

12:00–14:00 Lunch Break

Chair: Marek Nowakovski

14:00–14:30 **Vladimir A. Popov**, Perturbations in the superfluid Chaplygin gas cosmology

14:30–15:00 **Bivudutta Mishra**, Anisotropic Bianchi type VI_h cosmological models in modified gravity

15:00–15:30 **Michal Křížek, Attila Mészáros**, On the Friedmann equation for the three-dimensional hypersphere

15:30–16:00 **Discussion**

Saturday, September 24

9:00–12:00 Excursion to the astronomical and cosmological sights of Prague

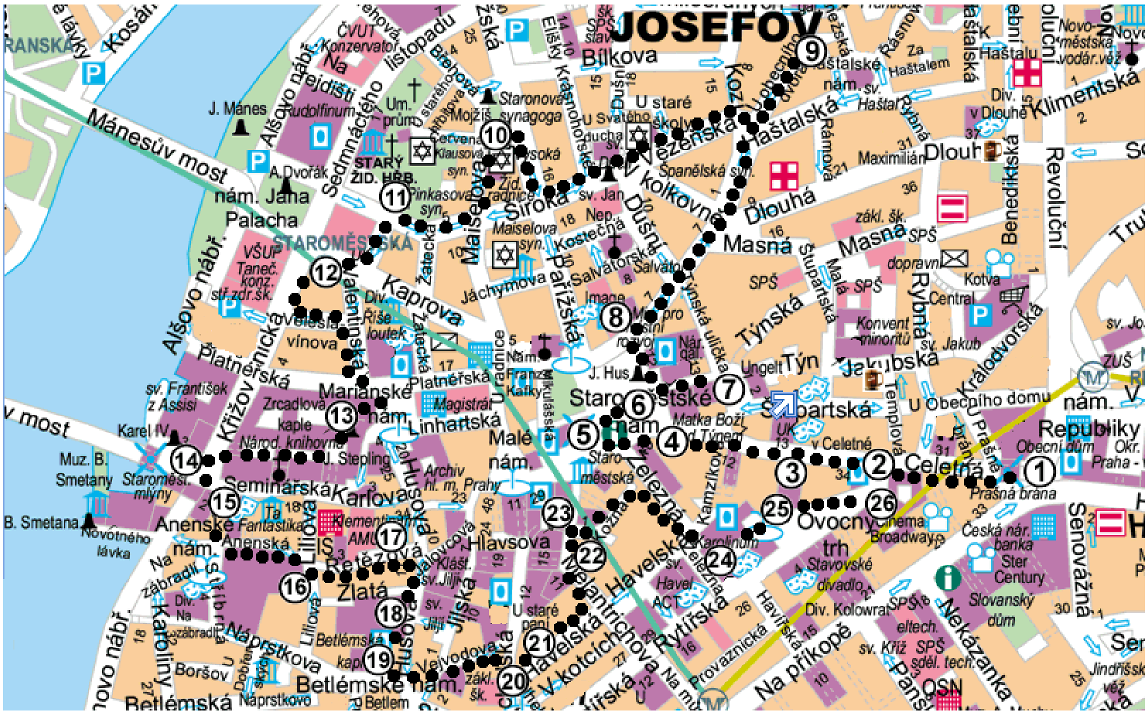

Map of the proposed walk through the astronomical and cosmological sightseeings of the Old Town:

1. Powder Tower (Prašná brána) — King's entrance to the Old Town
2. Memorial plaque of Bernard Bolzano
3. Vlastenecký sál, where Ch. Doppler presented his groundbreaking lecture
4. Painting of Giordano Bruno and the memorial plaque of Albert Einstein
5. Old Town City Hall with the Astronomical Clock — Prague's Horologe
6. Prague's Meridian
7. Tomb of Tycho Brahe
8. House no. 7/930, where the grandfather of Wolfgang Pauli lived
9. Memorial plaque of Christian Doppler
10. Jewish Clock
11. Jewish Cemetery
12. Bust of Jaroslav Heyrovský, the first Czech Nobel Prize Winner
13. Astronomical Tower – on its top there is a statue of Atlas supporting the Universe which is represented by an armillary sphere (see the back cover of these Proceedings).

14. Cosmological model on the Old Town Tower of the Charles Bridge[1]
15. Kepler's Museum
16. Original building of the Union of Czech Mathematicians and Physicists
17. Café Montmartre often visited by Albert Einstein
18. Memorial plaque of the Czech Technical University in Husova no. 5/240
19. Bethlehem Chapel
20. Bust of Jan Amos Komenský
21. Ancient astronomical instruments were constructed in Havelská no. 3/511
22. Memorial plaque of Jan Marek Marci
23. St. Michal Church, where Křišťan z Prachatic was a priest
24. Main building of Charles University founded in 1348
25. Bust of Ernst Mach
26. College of King Václav IV, where Johannes Kepler lived, no. 12/573

For more details see A. Šolcová and M. Křížek: Pokroky Mat. Fyz. Astronom. **51** (2006), 217–230, **52** (2007), 127–141, and **55** (2010), 215–230, available at `www.dml.cz`.

Stop 2. Memorial plaque of Bernard Bolzano (1781–1848). He wrote the monograph *Paradoxes of infinity* which has important consequences in cosmology.

[1]**Stop 14.** The Tower is divided into three parts that represent Aristotle's Cosmological model of the Universe. Above is the fixed celestial sphere with stars, in the middle there is the supralunar sphere, and below is the sublunar sphere. The foundation stone for the Charles Bridge was laid down in 1357 on 9^{th} July at 5 a.m. and 31 minutes. This date is connected with the palindrome 135797531 recommended by astrologers.

A memorial plaque dedicated to G. Bruno is placed at the entrance of the Prague Planetarium (Královská obora no. 233).

Stop 4. Painting of the Italian astronomer Giordano Bruno (1548–1600) on the house in the Old Town Square no. 16/552. In 1588, Bruno visited Prague. In his treatise *De l'Infinito, universo e mondi* (1584) he conjectured that the universe is infinite and that each star is similar to the Sun. Therefore, he is often considered to be the founder of modern cosmology.

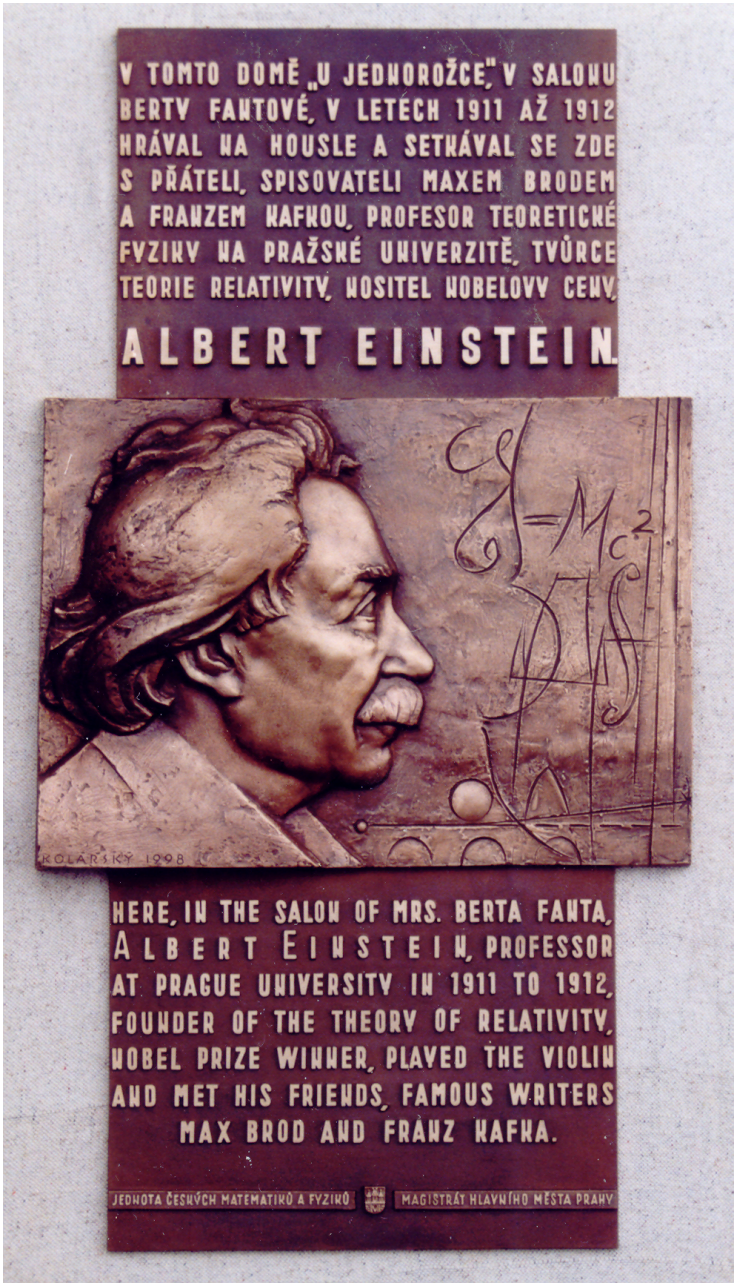

Stop 4. Memorial plaque of Albert Einstein (1879–1955) in the Old Town Square no. 17/551. Einstein taught physics at Prague University from 1911 to 1912 and learned the tensor calculus from Georg Pick. This helped him to develop the main ideas of the general theory of relativity. During his stay in Prague, Einstein published seven articles. He explained, e.g., why photons change the frequency in a gravitational field and why their trajectories are bent. Another memorial plaque of A. Einstein is at the entrance of the Faculty of Science of Charles University in Viničná 7/1594, where he worked. He lived in Lesnická 7/1215, where his bust is situated at present.

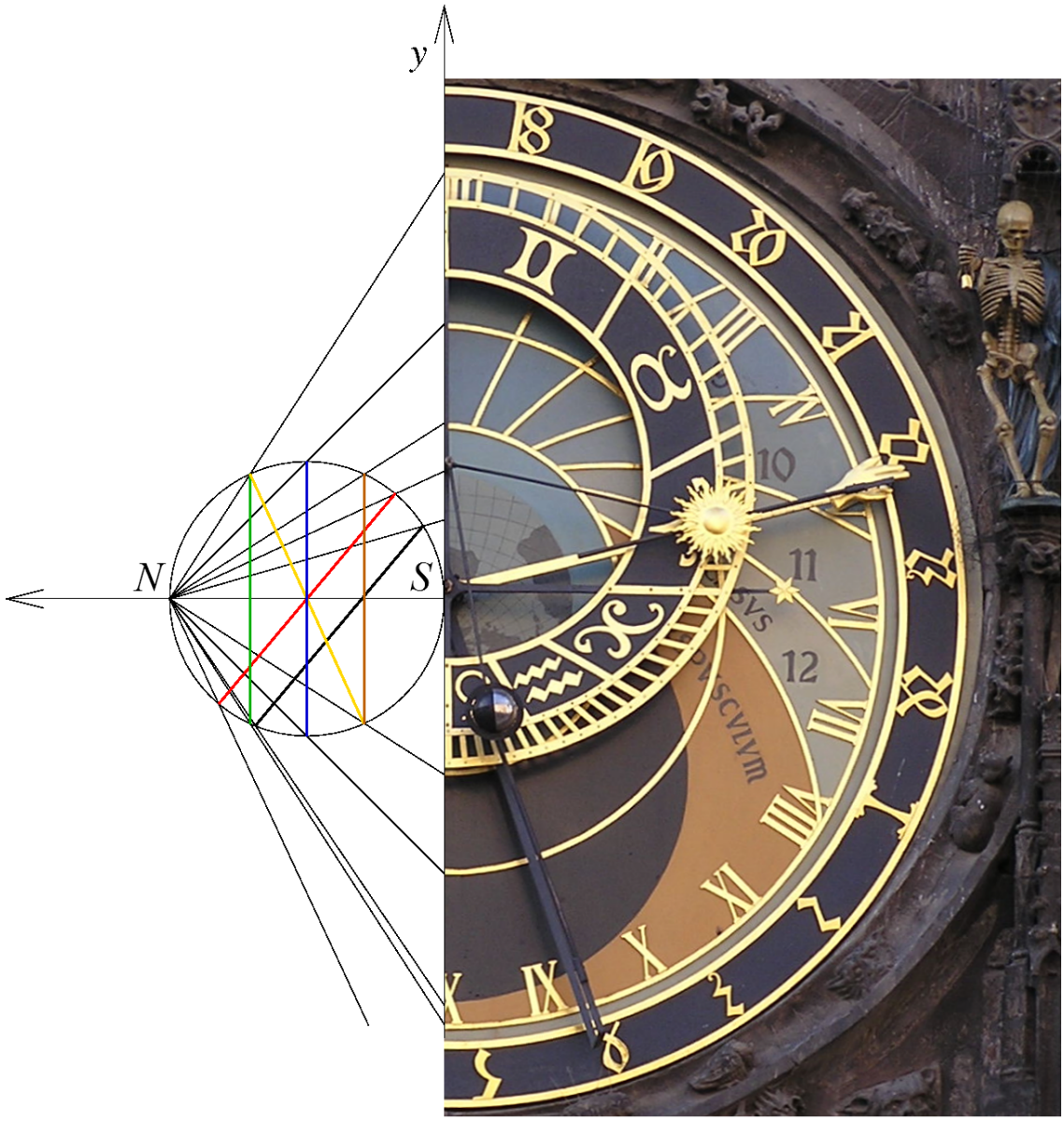

Stop 5. Astronomical dial of the Prague horologe in the Old Town Square. It represents a geocentric model of the Universe. The astronomical clock shows the position of the Sun on the ecliptic, the motion of the Moon and its phases, culmination and setting of the Sun, the Moon, and zodiac signs. The gilded solar hand shows the Central-European Time (CET) in the ring of Roman numerals. The difference between CET and the original Prague local time (see **Stop 6**) is only 138 seconds. The black circular area at the bottom of the dial-plate corresponds to astronomical night, when the Sun is lower than 18° below horizon.

The mathematical model of the astronomical clock was invented by Jan Ondřejův, called *Šindel*, and the clock was realized by the skilled clockmaker Mikuláš (Nicholas) from Kadaň around 1410. The horologe uses the stereographic projection of the celestial sphere from its North Pole N onto the tangent plane passing through the South Pole S which is at the center of the astronomical dial. The smallest interior circle around the South Pole illustrates the Tropic of Capricorn, while the exterior circle illustrates to the Tropic of Cancer. The concentric circle between them corresponds to the equator of the celestial sphere. An important theorem on stereographic projection (known already to Ptolemy) states:

Any circle on the sphere which does not pass through the North Pole is mapped onto a circle as well.

Therefore, six important circles of the celestial sphere: equator, ecliptic, Prague's horizon, Tropic of Cancer, Tropic of Capricorn, and the circle of astronomical night are mapped onto circles on the astronomical dial.

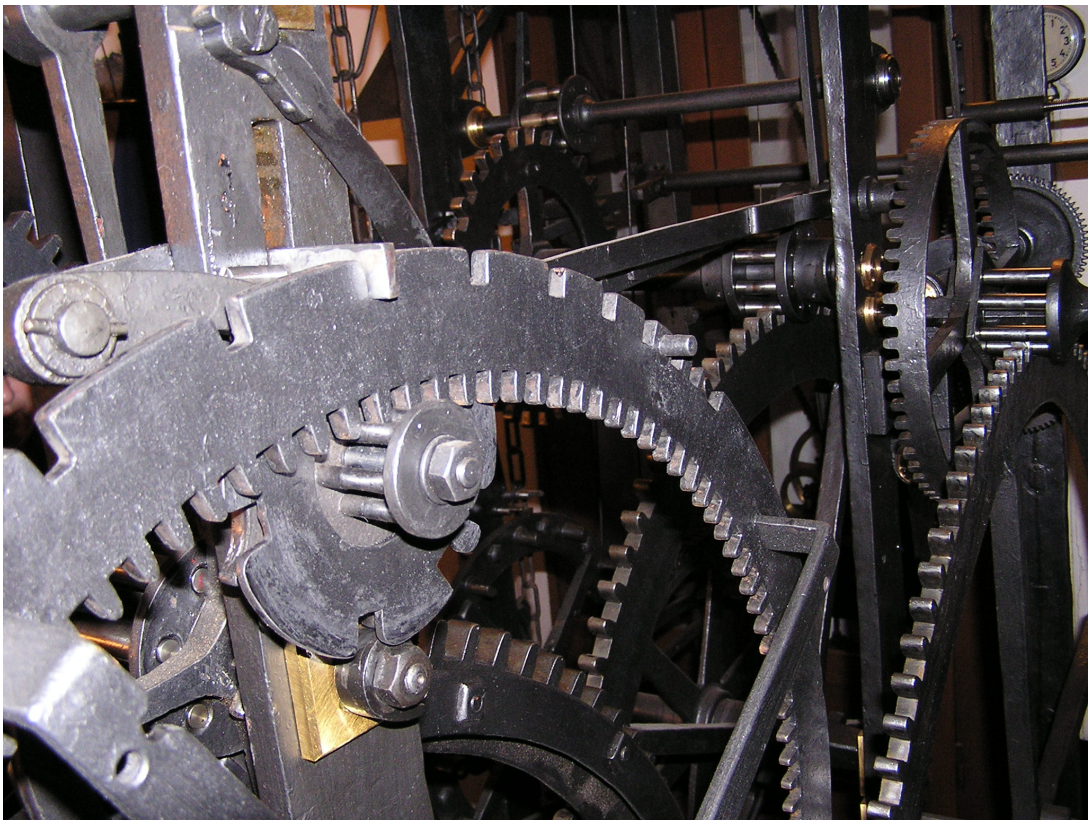

The astronomical clock is an astrolabe controlled by a sophisticated mechanism. For more details see M. Křížek, A. Šolcová, and L. Somer: The mathematics behind Prague's horologe, Math. Culture **1** (2010), no. 2, 69–77, or Comment. Math. Univ. Carolin. **48** (2007), 373–388, available at `www.dml.cz`.

Memorial plaque of T. Brahe in Nový svět no. 1/76 (photo J. Žd'árská)

Stop 7. Marble tomb of Tycho Brahe (1546–1601) in the Týn Church. Brahe's precise measurements of Mars' positions helped Johannes Kepler to discover the three Kepler's laws.

Stop 9. Memorial plaque of Christian Doppler (1803–1853) in the street U Obecního dvora no. 7/799, where he lived. In 1842, Doppler gave a groundbreaking lecture *On the color light of binary stars* in Vlastenecký sál (= Patriotic Hall) of Charles University in Ovocný trh no. 3/541 (**Stop 24** and also **Stop 3**), where he first introduced the effect later called the *Doppler phenomenon*. This phenomenon is the basis of the so-called *redshift* frequently used in the current cosmology. Another memorial plaque of Ch. Doppler is placed in the Charles Square (Karlovo náměstí) no. 20.

Stop 15. Kepler's Museum is located in Karlova street no. 4/177, where Johannes Kepler (1571–1630) lived from 1607 to 1612. During this period he discovered the first two of his three laws about elliptic orbits of planets around the Sun. They were published in *Astronomia nova* (1609). J. Kepler was already living in the city since 1600.

Stop 25. Bust of Ernst Mach (1838–1916) in Ovocný trh no. 7/562 who worked in this building from 1867 to 1879 as Director of the University Physics Institute. Here he started his groundbreaking research on shock waves. They are characterized by the *Mach number* which is a dimensionless quatity representing the ratio of flow velocity past a boundary to the local speed of sound. Einstein cited the so-called *Mach's principle* as one of the three principles underlying general relativity.

Group of statues of Tycho Brahe and Johannes Kepler at the crossing of the streets Keplerova and Parléřova

SUBJECT INDEX